



Sulfur Cycling in *Prymnesium parvum* on the Norfolk Broads

by

Peter Paolo Lanzarote Rivera

This thesis is submitted in fulfilment of the requirements of the degree of
Doctor of Philosophy at the University of East Anglia

School of Biological Sciences
University of East Anglia
Norwich

December 2020

This copy of the thesis has been supplied on condition that anyone who consults it is understood to recognise that its copyright rests with the author and that use of any information derived there from must be in accordance with current UK Copyright Law. In addition, any quotation or extract must include full attribution.

DECLARATION

I, Peter Paolo Lanzarote Rivera, declare that this thesis is a record of my own work and that I composed it. It has not been submitted in any previous application for a degree in any other university. All quotations have been distinguished by quotation marks and all sources of information are specifically acknowledged.

ABSTRACT

The Norfolk Broads, Britain's largest protected wetland, has been plagued by series of harmful algal blooms (HABs) of *Prymnesium parvum* (haptophyceae) causing serious fish-kill events. I show that Hickling Broads *P. parvum* strains produce novel prymnesin toxins, more closely related to northern European strains than to those identified in the UK, potentially indicating recent invasion and colonisation event/s. *P. parvum* also produces the important organosulfur osmolyte dimethylsulfoniopropionate (DMSP), which is the major precursor for the climate-active gas dimethylsulfide (DMS) and an abundant marine nutrient. There have been no molecular studies investigating the natural cycling of DMSP by *P. parvum* nor of its effects on the microbial community structure. Despite the brackish nature of Broads water, *P. parvum* and DMSP, at levels up to 60 nM, were ever-present over a season. There was a strong correlation between the abundance of *P. parvum*, its *DSYB* DMSP synthesis gene transcripts and DMSP, suggesting this HAB alga as the major DMSP producer. *P. parvum* strains did not produce DMS itself, and despite significant DMSP levels in Broads water, bacteria with the potential to catabolise DMSP through the DddP DMSP lyase or DmdA DMSP demethylase were rare or undetected in Broads water, respectively. This is consistent with DMSP having an important role in these organisms and these catabolic systems being marine. *P. parvum* strains of diverse origin (freshwater, brackish and marine) all produced DMSP at similar levels throughout their life cycle, which was upregulated during late exponential to early stationary phase and by raised salinity, consistent with stress response and osmoregulatory functions. This case study provides novel insights to the role of brackish water HAB in DMSP dynamics of lake systems, their role in local biogenic sulfur cycling, and the prymnesin toxins they produce.

Access Condition and Agreement

Each deposit in UEA Digital Repository is protected by copyright and other intellectual property rights, and duplication or sale of all or part of any of the Data Collections is not permitted, except that material may be duplicated by you for your research use or for educational purposes in electronic or print form. You must obtain permission from the copyright holder, usually the author, for any other use. Exceptions only apply where a deposit may be explicitly provided under a stated licence, such as a Creative Commons licence or Open Government licence.

Electronic or print copies may not be offered, whether for sale or otherwise to anyone, unless explicitly stated under a Creative Commons or Open Government license. Unauthorised reproduction, editing or reformatting for resale purposes is explicitly prohibited (except where approved by the copyright holder themselves) and UEA reserves the right to take immediate 'take down' action on behalf of the copyright and/or rights holder if this Access condition of the UEA Digital Repository is breached. Any material in this database has been supplied on the understanding that it is copyright material and that no quotation from the material may be published without proper acknowledgement.

ACKNOWLEDGMENTS

Foremost, I would like to thank my supervisor, Professor Jonathan Todd, for his unwavering support and invaluable guidance throughout my PhD journey. I am really grateful to him for giving me the opportunity to be part of his brilliant research team – the ‘Todd Tigers’ and exposed me to the wonderful world of DMSP. His encouragement, patience, and trust in my ability to carry out this study have helped me a lot and inspired me to continue to do more research and do better science. I have learned a lot from him of which I am truly grateful.

I would like to thank lovely Andy, who was very patient with me and always there to answer all my questions. I was very lucky to have him as my secondary supervisor, guiding me through my experiments. To Ana and Beth, for their friendship and laughter we shared. They were always there to cheer me up when times were rough. Thanks to Ornella for the guidance and advice when I needed it most. Much appreciation to Ji, Jingli, Carla, YanFen, Shun and Mando for being awesome buddies and helping me with my experiments. Thanks to Kasha, Ocean, Keanu, Melliela and Libby for being a unique bunch of labbies. Thanks to Pam for morning company and technical support. She is a true gem in the lab. To the past and present members of Todd’s and Murrel’s lab, thank you so much for the friendship and support.

For Prymnesium project collaborators, I would like to thank Rob Field, Martin Rejzek, Ben Wagstaff and Gerhard Saalbach of the John Innes Center (JIC) who welcomed me to do the toxin analysis. Thank you to Colin Murrell, Jenny Pratscher, and Elliot Brooks for the help, guidance and support when I first started my PhD. Many thanks to Gavin Devaney, Hannah Southon and the people from the Broads Authority (BA) for the logistics and the assistance provided throughout the field sampling especially during harsh weather conditions. I really appreciate all your help.

I would also like to thank CHED-Newton Fund from the British Council for the funding.

Thanks to Nicky and Deb for the company and friendship and always making me feel at home in Norwich. I really appreciate the care, support and kindness you’ve provided me through the years. Thank you to my friends here in Norwich especially Chris who was there all the time whenever I needed him. I am thankful to my family, even though we are thousands of miles apart, I can feel the love, care, and support. To my beautiful wife Baru, thank you for giving me the love and support especially during the write-up process in Covid pandemic time. You always give me strength when I faltered. I am really thankful and blessed to have you around and keeping me sane.

Finally, I would like to thank God almighty for giving me strength and guiding me all throughout my PhD study.

CONTENTS

ABSTRACT.....	3
1 INTRODUCTION.....	21
1.1 Harmful Algal Blooms (HABs) and Fish Kills.....	21
1.2 <i>Prymnesium parvum</i> Carter.....	22
1.2.1 Taxonomic and phylogenetic classification.....	23
1.2.2 Morphology and physiology.....	24
1.2.3 Life cycle (proposed).....	27
1.2.4 Growth requirements	28
1.2.5 Toxicity.....	29
1.2.6 Geographic occurrence/distribution	31
1.3 The Broads and <i>Prymnesium parvum</i>.....	33
1.4 <i>P. parvum</i> and β-dimethylsulfoniopropionate (DMSP).....	36
1.5 Biological functions of DMSP.....	38
1.6 DMSP synthesis.....	38
1.7 DMSP breakdown.....	41
1.8 Study aims and objectives.....	45
2 MATERIALS AND METHODS.....	48
2.1 Field study on the Broads.....	49
2.1.1 Study site – Hickling Broad.....	49
2.1.2 Sample collection.....	50
2.1.3 Processing of field samples.....	52
2.1.4 Optical microscopy (Phytoplankton Community).....	52
2.1.5 Isolation of <i>Prymnesium</i> strains.....	53
2.1.6 Isolation of bacterial strains.....	54
2.2 Media and growth conditions.....	54
2.2.1 Strains and laboratory growth conditions.....	54
2.2.2 <i>Prymnesium</i> non-standard growth conditions.....	58
2.2.3 Sample preparation from cultures.....	58
2.2.4 Algal cell counting and PAM fluorometry.....	59
2.3 Nucleic acid extraction.....	59
2.3.1 Environmental DNA and RNA extraction and purification.....	59
2.3.2 Bacterial DNA extraction and purification.....	60

2.3.3 <i>Prymnesium</i> RNA extraction and purification.....	61
2.4 <i>Prymnesium</i> whole transcriptome sequencing.....	61
2.5 16S rRNA amplicon sequencing (environmental samples).....	62
2.6 <i>In silico</i> sequence analysis.....	62
2.6.1 Identification of <i>DSYB</i> and <i>Alma</i> -like genes in <i>P. parvum</i>	62
2.6.2 Sequence optimization and gene synthesis.....	62
2.6.3 Primer design for PCR, qPCR and RT-PCR.....	63
2.7 Quantitative polymerase chain reaction (qPCR).....	64
2.7.1 <i>Prymnesium</i> ITS2 copy numbers in field samples.....	64
2.7.2 Reverse transcription reaction.....	64
2.7.3 <i>DSYB</i> abundance (qPCR) and transcription (RT-qPCR).....	65
2.7.4 qPCR and RT-qPCR analyses.....	65
2.7.5 Post-run analysis.....	65
2.8 Genetic manipulations.....	66
2.8.1 <i>In vitro</i> genetic manipulation.....	66
2.8.1.1 Polymerase chain reaction (PCR).....	66
2.8.1.2 Agarose gel electrophoresis).....	66
2.8.1.3 PCR purification protocol.....	66
2.8.1.4 Gel extraction protocol.....	67
2.8.1.5 Cloning into pRK415 and pLMB509.....	67
2.8.1.6 pGEM-T Easy cloning.....	67
2.8.2 <i>In vivo</i> genetic manipulation.....	68
2.8.2.1 Polymerase chain reaction (PCR).....	68
2.8.2.2 Heat shock transformations.....	68
2.8.2.3 Conjugation by triparental mating.....	69
2.8.2.4 Plasmid extractions from Minipreps/Midipreps.....	69
2.8.2.5 Restriction digests (FastDigest Enzymes).....	70
2.9 Metabolite analysis.....	70
2.9.1 Quantification of DMSP.....	70
2.9.2 LC-MS detection of toxins.....	71
2.10 Protein quantification.....	72
2.11 Catalysed reporter deposition - fluorescence <i>in situ</i> hybridization	
(CARD- FISH).....	73
2.12 Statistical significance and standard deviation	73

3	<i>Prymnesium parvum</i> ASSOCIATED MICROBIOMES.....	75
3.1	Introduction.....	76
3.2	Methods.....	77
3.2.1	Hickling broad sampling.....	77
3.2.2	Phytoplankton community analysis by microscopy.....	78
3.2.3	DNA and RNA extraction and purification.....	78
3.2.4	16S rRNA gene amplicon sequencing.....	79
3.2.5	Isolation of bacterial strains.....	79
3.2.6	Screening for DMSP-producing and -catabolizing bacteria.....	80
3.2.7	Gas chromatography (GC) analysis.....	81
3.2.8	Bacterial DNA extraction and purification.....	81
3.2.9	PCR amplification of bacterial 16S rRNA genes.....	82
3.2.10	Catalysed reporter deposition – fluorescence <i>in situ</i> hybridisation (CARD-FISH).....	82
3.3	Results.....	83
3.3.1	Phytoplankton community.....	83
3.3.2	Bacterial community profiling.....	86
3.3.3	Isolation of <i>P. parvum</i> bloom-associated bacteria.....	88
3.3.4	CARD-FISH.....	89
3.4	Discussion.....	92
3.4.1	Phytoplankton community change.....	92
3.4.2	<i>P. parvum</i> bloom-associated microbial communities.....	94
3.4.3	Bacterial isolation and screening for DMSP/DMS production.....	96
3.3.4	CARD-FISH on <i>P. parvum</i>	97
3.5	Conclusion.....	97
4	ROLE of DMSP on HARMFUL ALGAL BLOOMS (HABs).....	99
4.1	Introduction.....	100
4.2	Methods.....	103
4.2.1	Sampling site, sample collection and processing.....	103
4.2.2	Isolation of <i>Prymnesium</i> strains.....	104
4.2.3	Algal and bacterial growth media.....	104
4.2.4	Algal cell counting and PAM fluorometry.....	105
4.2.5	Nucleic acid extraction.....	105

4.2.6 Whole transcriptome sequencing.....	106
4.2.7 <i>DSYB</i> and <i>Alma</i> -like in <i>P. parvum</i>	107
4.2.8 Primer design, real-time qPCR, and RT-qPCR.....	108
4.2.9 Genetic manipulations.....	109
4.2.10 MTHB S-methyltransferase assays.....	109
4.2.11 <i>Alma</i> DMSP <i>in vitro</i> and <i>in vivo</i> cleavage assays.....	110
4.2.12 <i>Prymnesium</i> DMSP lyase activity.....	111
4.2.13 Quantification of DMSP and DMS by GC.....	111
4.3 Results.....	112
4.3.1 Seasonal abundance of <i>Prymnesium</i>	112
4.3.2 Is <i>Prymnesium</i> a significant source of DMSP in the Broads?.....	118
4.3.3 <i>P. parvum</i> DMSP production in the Broads.....	120
4.3.4 Does <i>P. parvum</i> cleave DMSP?.....	125
4.3.5 Broads bacterial DMSP catabolism (temporal change).....	125
4.4 Discussion.....	127
4.4.1 <i>P. parvum</i> and DMSP.....	127
4.4.2 <i>P. parvum</i> DMSP synthesis and breakdown.....	128
4.5 Conclusion.....	128
5 EFFECTS OF BIOTIC AND ABIOTIC FACTORS ON <i>P. parvum</i> DMSP PRODUCTION.....	129
5.1 Introduction.....	130
5.2 Methods.....	133
5.2.1 Strains of <i>Prymnesium</i> tested.....	133
5.2.2 Biomass sampling and preparation.....	133
5.2.3 Growth measurements.....	134
5.2.4 Intracellular DMSP measurements.....	134
5.2.5 <i>P. Parvum</i> growth phases.....	134
5.2.6 Different salinity treatments.....	137
5.2.7 Varying nitrogen conditions.....	137
5.2.8 Oxidative stress (H ₂ O ₂) treatments.....	138
5.2.9 Viral-like particles (VLP) exposure experiment.....	138
5.2.10 <i>DSYB</i> transcription at varying salinity and nitrogen conditions.....	140
5.3 Results.....	141
5.3.1 <i>Prymnesium</i> DMSP in various studies.....	141
5.3.2 DMSP production at different growth stages.....	143

5.3.3 Effect of varying salinity.....	146
5.3.4 Effect of varying nitrogen.....	147
5.3.5 Effect of oxidative stress.....	148
5.3.6 Effect of viral-like particles (VLPs).....	149
5.4 Discussion.....	151
5.4.1 Production at different growth phases.....	151
5.4.2 Effect of varying salinity and nitrogen.....	152
5.4.3 Other tested variables: ROS and VLPs.....	154
5.5 Conclusion.....	157
5.6 Supplementary figures.....	158
6 DETECTION AND CHARACTERIZATION OF <i>Prymnesium</i> TOXINS.....	161
6.1 Introduction.....	162
6.2 Methods.....	166
6.2.1 Isolation of <i>P. parvum</i> broad strains.....	166
6.2.2 Culture conditions and extraction of toxins.....	166
6.2.3 LC-MS detection of prymnesin toxins.....	166
6.2.4 HIK PR1A ITS sequence and phylogenetic inference.....	167
6.2.5 Effect of Varying P and low salinity on prymnesins.....	167
6.3 Results.....	168
6.3.1 Prymnesin profiles of the Broads isolates.....	168
6.3.2 Distribution of <i>P. parvum</i> producing A-, B-, C-type prymnesins.....	171
6.3.3 Effect of varying P and low salinity on prymnesins.....	173
6.4 Discussion.....	176
6.4.1 Hickling broad <i>P. parvum</i> produce B-type prymnesins.....	176
6.4.2 First B-type prymnesin producing <i>P. parvum</i> in the UK.....	177
6.4.3 Phylogeny of <i>P. parvum</i>	178
6.4.4 Effect of low phosphorus and low salinity on prymnesin production.....	178
6.5 Conclusion.....	179
6.6 Supplementary data.....	181
7 GENERAL DISCUSSION AND CONCLUDING REMARKS.....	197
7.1 Research gaps and goals.....	198
7.2 Key findings described in this Thesis.....	200
7.2.1 <i>Prymnesium parvum</i> blooms affect Hickling Broads prokaryotic and eukaryotic communities.....	200

7.2.2 Seasonal dynamics of <i>Prymnesium parvum</i> in Hickling Broad.....	202
7.2.3 <i>Prymnesium parvum</i> as major source of DMSP in the Broads.....	203
7.2.4 Hickling <i>P. parvum</i> DSYB abundance and transcription.....	204
7.2.5 Does <i>P. parvum</i> cleave DMSP? and who cleaves DMSP on the Broads?.....	204
7.2.6 Factors affecting <i>P. parvum</i> DMSP production.....	206
7.2.7 Ichthyotoxins produced by Broads <i>P. parvum</i>	208
7.3 Limitations of the study.....	209
7.3.1 <i>P. parvum</i> effects on eukaryotic and prokaryotic communities.....	209
7.3.2 DMSP turnover.....	210
7.3.3 Quantitation of prymnesins in the broads.....	210
7.4 Recommendations for future research.....	210
7.4.1 Further work on broad/lake systems DMSP/DMS production.....	210
7.4.2 Fate of algal-derived DMSP on the Broads.....	211
7.4.3 <i>Prymnesium</i> -bacterial interactions.....	211
7.4.4 Field measurements of prymnesins.....	212
7.5 Concluding remarks.....	212
REFERENCES.....	213
RESEARCH ARTICLES.....	237

LIST OF FIGURES

Figure 1.1: Bayesian tree of members of the Prymnesiales.....	24
Figure 1.2: Details of the morphology of <i>Prymnesium parvum</i>	26
Figure 1.3: Proposed life cycle of <i>P. parvum</i> / <i>P. patelliferum</i>	28
Figure 1.4: Structures of prymnesin-1 and prymnesin-2.....	30
Figure 1.5: Worldwide occurrences and distribution of <i>P. parvum</i> populations.....	31
Figure 1.6: Geographical distribution of the Broads.....	35
Figure 1.7: Dead fish on the waterways on the Upper Thurne area of the Norfolk Broads.....	36
Figure 1.8: Mechanisms of DMSP and DMS cycling in the marine/aquatic environment and atmosphere.....	37
Figure 1.9: The three DMSP biosynthetic pathways used by higher plants, macroalgae, microalgae, diatoms, dinoflagellates, and bacteria.....	39
Figure 1.10: DMSP biodegradation pathways.....	43
Figure 2.1: Map of upper Thurne area of the Norfolk Broads, Norfolk, UK.....	49
Figure 2.2: Map showing the five sampling stations where environmental samples were taken.....	50
Figure 2.3: The fabrication of glass micropipette and the method of isolating individual cells of <i>P. parvum</i>	53
Figure 2.4: Calibration curve used to calculate DMSP concentrations in samples.....	71
Figure 2.5: Calibration curve used to calculate protein concentration in Bradford Reagent.....	72
Figure 3.1: Example of purified bacterial isolates from Hickling Broad.....	80
Figure 3.2: Phytoplankton community change through time on Hickling Broad as expressed in percent abundance of 4 major phytoplankton groups.....	84
Figure 3.3: Phytoplankton community composition in bloom and non-bloom samples.....	85
Figure 3.4: Microbial community composition in bloom and non-bloom samples.....	87
Figure 3.5: DMS production of bacterial isolates incubated in MBM media with 0.5 mM DMSP as measured by GC-FPD.....	89
Figure 3.6: Confocal laser scanning micrographs of bacterial cells attached to	

<i>P. parvum</i> cells visualized by CARD–FISH using Cy3-labelled probes.....	91
Figure 4.1: High quality algal RNA on well number 2 from 6 RNA isolations made from <i>P. parvum</i> cells HIK PR1A.....	107
Figure 4.2: Hickling broad water biogeochemical properties and algal biomass.....	113
Figure 4.3: Monitoring of <i>P. parvum</i> cells by basic microscopy (bar) and <i>P. parvum</i> ITS copies via qPCR (line) in the broad water samples.....	116
Figure 4.4: <i>P. parvum</i> cell counts by microscopy (bar) and <i>P. parvum</i> ITS copies via qPCR (line) in the broad water samples from Hickling Broad at four sampling stations.....	118
Figure 4.5: Comparison of <i>P. parvum</i> abundance estimates obtained via microscopy (bar) and DMSP concentrations (blue line) at station 5.....	119
Figure 4.6: Light microscopy images of <i>P. parvum</i> HIK PR1A (a), HIK PR6H (b) and axenic culture of HIK PR1A at exponential phase (c).....	120
Figure 4.7: Comparison of DMSP produced (DMSP per cell volume) by different strains of <i>P. parvum</i> from culture collections as well as the newly isolated strains from Hickling Broad, Norfolk and Woodbridge Fen Fisheries, Suffolk.....	121
Figure 4.8: Gel electrophoresis image showing the optimised PCR amplification of <i>DSYB</i> using qPCR primers on 10 different <i>P. parvum</i> strains.....	123
Figure 4.9: Comparison of DMSP concentrations (bar) as measured by GC and <i>DSYB</i> abundance via qPCR (dash line) (a) and <i>DSYB</i> transcript copies via RT-qPCR (b) at station 5 in Hickling broad.....	124
Figure 4.10: Comparison of DMSP concentrations (bar) as measured by GC and bacterial <i>dddP</i> transcription copies thru RT-qPCR at station 5 in Hickling broad.....	126
Figure 5.1: Growth curves of different <i>P. parvum</i> strains obtained from culture collections (a) and newly isolated <i>P. parvum</i> strains from Hickling Broad and Woodbridge Fen Fisheries (b).....	135
Figure 5.2: Light micrograph of intact resting ‘cysts’ of <i>Prymnesium parvum</i> CCAP 946/6 formed on the surface of solid f/2 agar plate.....	136
Figure 5.3: Concentrations of H ₂ O ₂ in the culture replicates monitored at the start and at the end of the exposure experiment using Quantofix test strips.....	138
Figure 5.4: Initial VLP treatments on <i>P. parvum</i> CCAP 946/6 cultures. (Left) is the set of cultures at the start of infection; (Right) is the set of cultures at 48-h post-infection.....	140

Figure 5.5: Variation in Fv/Fm Ratio <i>P. parvum</i> strains grown under controlled culture conditions during the 52-day monitoring.....	143
Figure 5.6: DMSP concentrations of different <i>P. parvum</i> strains, including two of the newly isolated strains, at different growth phases.....	144
Figure 5.7: DMSP concentration of <i>P. parvum</i> CCAP 946/6 strain at different growth phases including dormant cyst phase.....	145
Figure 5.8: DMSP concentrations of different <i>P. parvum</i> strains at different salinity regimes (5, 10, 35, and 50 PSU) (a) and <i>P. parvum</i> HIK PR1A <i>DSYB</i> transcription at three salinity conditions (b).....	146
Figure 5.9: DMSP concentrations of different <i>P. parvum</i> strains grown at different nitrogen concentrations (LN - Low N or N - deplete, NN - Normal N, and HN - High N or N - replete) (a) and <i>P. parvum</i> HIK PR1A <i>DSYB</i> transcription at these conditions (b).....	148
Figure 5.10: Intracellular DMSP concentration (mMolL^{-1}) of <i>P. parvum</i> CCAP 946/6 treated with H_2O_2 (ROS).....	149
Figure 5.11: Intracellular DMSP concentration (mMolL^{-1}) of <i>P. parvum</i> CCAP 946/6 infected with VLP.....	150
Figure 6.1: The structures of A-type and B-type prymnesins.....	163
Figure 6.2: Relative abundance of Prymnesin types found in <i>P. parvum</i> strains isolated from Hickling broad.....	169
Figure 6.3: MS-based identification of B-type prymnesins from Hickling broad <i>P. parvum</i> isolates.....	170
Figure 6.4: Relative abundance of Prymnesin types found in <i>P. parvum</i> strains isolated from Woodbridge Fen Fisheries.....	171
Figure 6.5: Geographical distribution of <i>Prymnesium parvum</i> producing A-, B-, and C-type prymnesins.....	172
Figure 6.6: Phylogeny of 26 widely distributed strains of <i>Prymnesium parvum</i> inferred from Bayesian analysis.....	173
Figure 6.7: Relative ratios of the individual prymnesin peak areas as a function of the sum of all prymnesin peak areas present in the sample.....	174
Figure 6.8: Relative abundances of the individual Prymnesin-B analogs/sub-types present in the sample grown at low, normal and high phosphate conditions.....	175

LIST OF TABLES

Table 2.1: Coordinates of sampling locations on Hickling Broad, Norfolk.....	51
Table 2.2: List of strains and plasmids used in this study.....	55
Table 2.3: List of oligonucleotide primers used in this study.....	63
Table 4.1: Physical and chemical parameters in water samples from Hickling broad (station 5) during the course of the study period.....	115
Table 4.2: DMSP production by <i>Rhizobium leguminosarum</i> and <i>Labrenzia aggregata</i> expressing cloned <i>P. parvum</i> <i>DSYB</i> gene and DMS production of <i>Escherichia coli</i> and <i>Labrenzia aggregata</i> mutant with cloned <i>Alma</i> gene.....	122
Table 5.1: Intracellular concentration of DMSP in different cultures of <i>Prymnesium</i> from various studies.....	141

LIST OF SUPPLEMENTARY MATERIALS

Supplementary Figure 5.1: Preliminary determination of growth curves of <i>P. parvum</i> strains obtained from culture collections.....	158
Supplementary Figure 5.2: Initial VLP treatments on <i>P. parvum</i> HIK PR1A cultures at 72-h post-infection.....	158
Supplementary Figure 5.3: Concentration of DMSP particulate (mMOL ⁻¹) on two model diatoms (A) <i>T. pseudonana</i> CCMP 1335 and (B) <i>P. tricornutum</i> CCAP 1055/1.....	159
Supplementary Figure 5.4: Virus-like Particle (VLP) infection cycle propagated on <i>P. parvum</i> CCAP 946/6.....	160
Supplementary Table 6.1: All proposed systematic names of A-, B-, C-type prymnesins.....	181
Supplementary Table 6.2: List of <i>Prymnesium parvum</i> strains, salinity and the type of prymnesin produced.....	184
Supplementary Figure 6.1: MS-based identification of B-type prymnesins from environmental samples taken from Hickling Broad.....	186
Supplementary Data: 696 base pairs (including introduced gaps) of internal transcribed spacers (ITS-1 and ITS-2) and the 5.8S rDNA gene of <i>P. parvum</i> strains.....	187

ABBREVIATIONS

·OH	hydroxyl radical
μM	micromolar
μmol m ⁻² s ⁻¹	photon flux
16S rRNA	16S ribosomal RNA
18S rRNA	18S ribosomal RNA
28S rRNA	28S ribosomal RNA
3-HP	3-hydroxypropionate
aa	amino acid
APS	adenosine phosphosulfate
BLAST	basic local alignment search tool
Bp	base pairs
BSA	bovine serum albumin
C	carbon
CARD-FISH	catalyzed reporter deposition - fluorescence <i>in situ</i> hybridization
CCAP	culture collection of algae and protozoa
CCN	cloud condensation nuclei
cDNA	complementary DNA
CLAW	R. Charlson, J. Lovelock, M. Andreae and S. Watson hypothesis
CoA	Coenzyme A
CO ₂	carbon dioxide
DMS	dimethyl sulfide
DMSHB	4-dimethylsulfonio-2-hydroxybutyrate
DMSO	dimethylsulfoxide
DMSOP	dimethylsulfoxonium propionate
DMSP	dimethylsulfoniopropionate
DMSP-a	3-dimethylsulfoniopropylamine
DMSP-ald	3-dimethylsulfoniopropionaldehyde
DNA	deoxyribonucleic acid
dNTPs	deoxyribonucleotide triphosphate
DO	dissolved oxygen
DOM	dissolved organic matter

EDTA	ethylenediametetraacetic acid
EhV	<i>Emiliana huxleyi</i> virus
ESI	electrospray ionization
FAA	fatty acid amide
Fe	iron
FH ₄	tetrahydrofolate
Fm	maximum fluorescence
fmol	femtomole
Fv	variable fluorescence
g	gram
GB	glycine betaine
GC	gas chromatography
H ₂	hydrogen
H ₂ O ₂	hydrogen peroxide
H ₂ S	hydrogen sulfide
h	hour
HAB	Harmful Algal Bloom
HCl	hydrochloric acid
HEPES	2-[4-(2-hydroxyethyl)piperazin-1-yl]ethanesulfonic acid
HGT	horizontal gene transfer
HPLC	high-performance liquid chromatography
HRMS	high resolution mass spectrometry
IPTG	isopropyl β-D-1-thiogalactopyranoside
ITS	internal transcribed spacer
L	litre
LB	Luria Broth
LC-MS	liquid chromatography-mass spectrometry
m	meter
M	molar (concentration)
m/z	mass to charge ratio
MBM	minimal basal media
MeOH	methanol
MeSH	methanethiol
Met	methionine

MgCl ₂	magnesium chloride
mM	millimolar
MMETSP	Marine Microbial Eukaryote Transcriptome Sequencing Project
MMPA	methyl mercaptopropionate
MS	mass spectrometry
MTA	methylthioacryloyl
MTHB	4-methylthio-2-hydroxybutyrate
MTOB	4-methylthio-2-oxobutyrate
MTPA	3-methylthiopropylamine
MPA	3-mercaptopropionate
MW	molecular weight
N	nitrogen
NaCl	sodium chloride
NaNO ₃	sodium nitrate
NaOH	sodium hydroxide
NCBI	National Center for Biotechnology Information
nm	nanometers (wavelength)
nM	nanomolar
NMR	nuclear magnetic resonance
NO ₃	nitrate
NTC	no template control
<i>n</i> -PrOH	<i>n</i> -propanol
O ₂	oxygen
OD	optical density
OTUs	operational taxonomic units
P	phosphate/phosphorus
PBS	phosphate-buffered saline
PEG	polyethylene glycol
PCR	polymerase chain reaction
PO ₄ ³⁻	phosphate
PpDNAV	<i>Prymnesium parvum</i> DNA virus
PRM1	prymnesin-1
PRM2	prymnesin-2
PSU	practical salinity units

pmol	picomole
qPCR	quantitative polymerase chain reaction
R2A	Reasoner's 2A agar
Rbs	ribosome binding site
RT	reverse transcription
RT-qPCR	reverse transcription - quantitative polymerase chain reaction
ROS	reactive oxygen species
RPM	revolutions per minute
S	sulfur
Si	silicate
SAM	S-adenosyl methionine
SDS	sodium dodecyl sulfate
SMM	S-methylmethionine
SO ₂	sulfur dioxide
SO ₄ ²⁻	sulfate
TEM	transmission electron microscopy
Tris-HCL	tris(hydroxymethyl)aminomethane hydrochloride
TY	tryptone yeast
UV	ultraviolet
V	voltage
VLP	virus-like particle
YTSS	yeast extract, tryptone, sea salts

Chapter 1

Introduction

1 Introduction

1.1 Harmful Algal Blooms (HABs) and Fish Kills

Harmful algal blooms (HABs) are the rapid proliferation of phytoplankton/algae that can cause negative impacts to animals, humans, and the aquatic/marine environment (GEOHAB, 2001; Moestrup et al., 2009). Normally, HABs involve a single or small group of phytoplankton species that can co-occur in certain environment. Their blooms wreak havoc on the surrounding ecosystem either through dissolved oxygen (DO) depletion or water anoxia/hypoxia, production of algal toxins or biotoxins, mechanical damage to gill-breathing organisms, and/or by any other means (Smayda, 1997). While there are several known factors, e.g. eutrophication, climate change, wind, and current flow etc., that may contribute to the formation of HABs, how these factors come together to form a 'bloom' is not fully understood (NOAA, 2017). And even though HAB-forming species only comprise a small subset of the algal community, their blooms have fairly huge impacts. They cause deleterious effects on human and animal health, reduce tourism, beach and shellfish bed closures, decrease catch for both recreational and commercial fisheries, and ecosystem disruption and degradation – all these lead to enormous losses for the local/regional economy (Smayda, 2008; Berdalet et al., 2015). HAB frequency and severity appears to have grown in recent years, and in turn, there have been increased efforts from scientists, stakeholders, and regulatory authorities to prevent and combat its negative effects. Governing bodies have focused their efforts on prevention, mitigation and management, while scientists have sought to investigate the primary causes of HABs and characterize the natural compounds/metabolites (including toxins) associated with their blooms (Anderson et al., 2012). Science-based approaches have helped various stakeholders in alleviating the harmful effects of these HABs.

HABs can be classified into two main groups of organisms: the toxin producers, which can contaminate seafood and these toxins can be bioaccumulated or magnified as it moves up through the food web (trophic transfer) or can cause 'Fish Kills' (ichthyotoxicity), and the high-biomass producers, which can cause anoxia/hypoxia and indiscriminate kills of marine organisms after reaching super high concentrations. Some have characteristics of both (UNESCO, 2011). HAB-associated fish kills (fish-die off) are the sudden death of a large number of fishes or other aquatic animals over a short period of time and often within a particular area (US-EPA, 2000). A densely concentrated algal bloom can deplete oxygen in the water due to the high respiration

rate of the algae, or by bacterial respiration during bloom collapse or decay (Paerl et al., 2018). In effect, the fish suffocate due to lack of oxygen. Some fish-killing algae can cause physical/mechanical damage to the gill membranes, with a similar result that they are unable to take in enough oxygen (Mardones et al., 2018). One of the most notorious fish killers is the haptophyte algae *Prymnesium parvum*, which is the main focus of this study and will be discussed throughout the text.

1.2 *Prymnesium parvum* Carter

Prymnesium parvum (Carter, 1937), is a unicellular, cosmopolitan, invasive toxin-producing microalga. Colloquially known as the 'golden algae' due to the abundance of its natural pigments and the water discoloration it forms during large-scale bloom events. It is a member of the Haptophyta family (prymnesiophytes), a fundamental group of marine phytoplankton involved in many important biogeochemical cycles (Medlin & Cembella, 2013; Eikrim et al., 2017). Toxigenic prymnesiophytes, especially *P. parvum*, can easily form dense blooms in marine, brackish, and even inland freshwater systems once growth conditions are favorable (Liu et al., 2015). *P. parvum* is also considered as mixotrophic algae and is capable of heterotrophic growth through consumption of smaller organisms like bacteria (Nygaard & Tobiesen, 1993) and protists (Kawachi et al., 1991; Tillmann, 2004) or ingesting dissolved organic matter (DOM) (Carvalho et al., 2010). Some studies have shown that *P. parvum* cells can also gang up and kill their predator (Tillmann, 2003). Mixotrophy enables *P. parvum* to thrive in low light and nutrient conditions, thus outcompeting other (strictly) autotrophic microalgae (Brutemark & Garneli, 2011).

P. parvum has been associated with causing devastating fish kills around the world every year through the formation of HABs and the eventual release of a myriad of natural products including toxins (ichthyotoxins) and other metabolites that have led to severe ecological and economic damages (Wagstaff et al., 2018). Its global spread and distribution success is also partly due to its eurythermal and euryhaline nature (Baker et al., 2007), having been shown to tolerate water temperatures between 5°C to 30°C and salinity levels ranging from 1 (just above freshwater) to 100 (hypersaline strength) practical salinity units (PSU) (Larsen & Bryant, 1998; Sabour et al., 2000; Watson, 2001).

1.2.1 Taxonomic and Phylogenetic Classification

The taxonomy and phylogeny of protists are constantly changing. *P. parvum* is currently classified as a member of the kingdom Chromista, phylum Haptophyta, class Prymnesiophyceae, order Prymnesiales and family Prymnesiaceae (Caron et al., 2017). Being a member of the phylum Haptophyta, *P. parvum* is a close relative of the large-scale bloom-forming coccolithophorid, *Emiliana huxleyi*, whose oceanic blooms are often so large, spanning several tens of thousands of square kilometers, that they can be seen from the outer space (Moore et al., 2012). Other members of the Prymnesiales, including *Chrysochromulina*, have previously been shown to form independent clades, with the genus *Prymnesium* occupying a single clade. Members of *Haptolina* forms a sister group with *Prymnesium* and *Imantonia* plus *Pseudohaptolina* (Fig. 1.1). The genus *Prymnesium* currently comprises of ten species, four of which are known to be toxic and *P. parvum* is one of them. This latest analysis originally published by Edvardsen et al. (2011) and redrawn by Medlin and Cembella (2013) was based on a combination of nuclear 18S rRNA and partial 28S rRNA gene sequences, as well as plastid 16S rRNA ribosomal encoding DNA sequences.

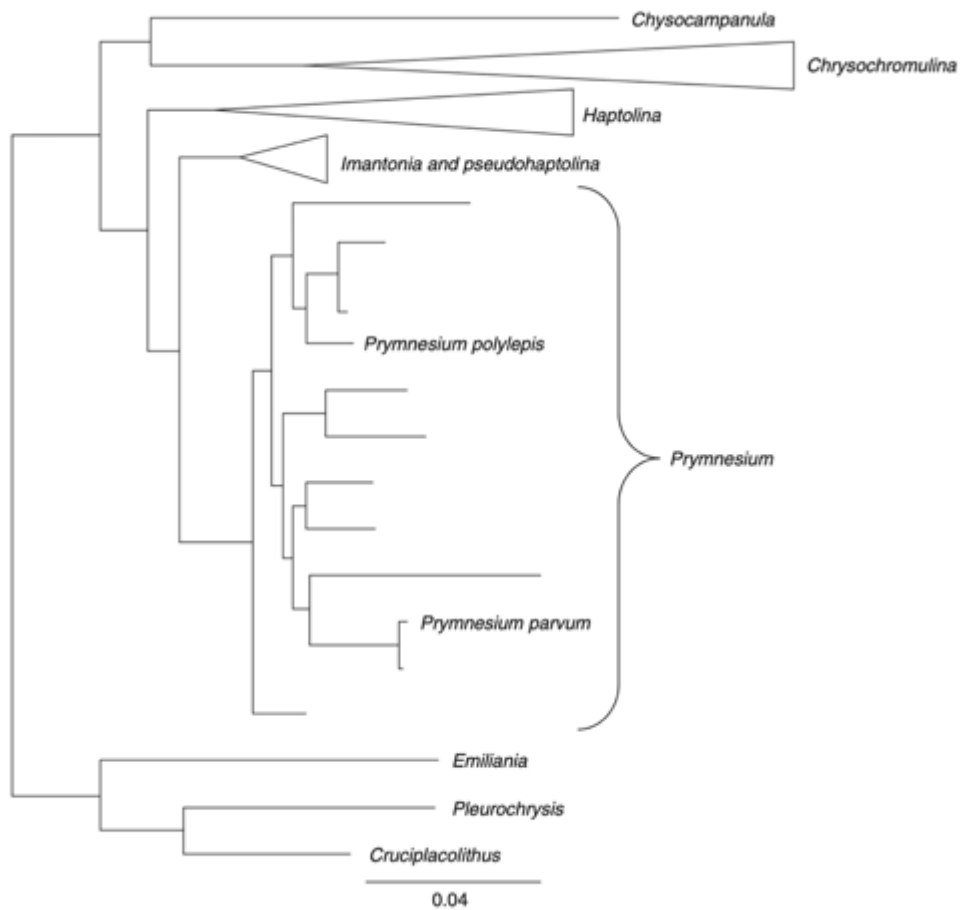


Figure 1.1. Bayesian tree based on concatenated nuclear 18S and partial 28S and plastid 16S ribosomal encoding DNA sequences of members of the Prymniales. *Cruciplacolithus neohelis*, *Emiliana huxleyii*, and *Pleurochrysis carterae* were used as outgroups. Adapted from Edvardsen B, Eikrem W, Throndsen J, Saez A, Probert I, and Medlin LK (2011) Ribosomal DNA phylogenies and a morphological revision set the basis for a new taxonomy of the Prymniales (Haptophyta). *European Journal of Phycology* 46: 202–228.

1.2.2 Morphology and Physiology

P. parvum is a planktonic, uninucleate, single-cell flagellated microalga normally with an ellipsoid, narrowly ovoid or irregular cell shape (Manton & Leedale, 1963; Prescott, 1968; Lee, 1980). The nucleus of the organism is centrally situated between two chloroplasts, one being lateral and the other parietal, that are usually yellow-green to olive in color. A two-membrane chloroplast endoplasmic reticulum is present with the outer membrane of the chloroplast ER being continuous with the outer membrane of the nuclear envelope (Green et al., 1982; Lee, 1980). A single polarized Golgi apparatus, located at the anterior part of the cell between the

bases of the two flagella and the nucleus (Bold & Wynne, 1985; Watson, 2001). A contractile vacuole is also sometimes found at the anterior end of *P. parvum* cells (Lee, 1980). Peripheral muciferous bodies and lipoidal globules may also be present (Fig. 1.2A). The cellular length and width of *P. parvum* can range from 8-16 micrometers and 4-10 micrometers, respectively. The cells can be slightly compressed sometimes with the posterior end rounded or tapered and the anterior end obliquely truncated (Green et al., 1982). A single *P. parvum* cell has two equal flagella subapically inserted from a groove and a well-developed haptonema that emerged in between the flagella (Fig. 1.2B)(Green & Jordan, 1994; Lee, 1980). The flagellae are used mainly for motility and the haptonema are involved in surface attachment and/or phagotrophy, aiding the organisms mixotrophic lifestyle (McLaughin, 1958; Prescott, 1978; Moss, 2001). The flagellar length can range between 12-15 micrometers and the length of flexible, non-coiling haptonema ranges between 3-5 micrometers. Each cell has two types of body scales arranged in two layers. The outer layer scales have narrow inflexed rims and those of the inner layer have wide, strongly inflexed rims (Fig. 1.2C)(Green et al., 1982). The scales are the primary important diagnostic feature used in distinguishing *P. parvum* from closely related algal species, and the flagella-to-cell length ratio and the haptonema-to-cell length ratio are also important diagnostic features that aid in identifying this organism, especially when collected in the environment during mixed algal blooms (Chang & Ryan 1985). Temporary and/or resting cysts formed by *P. parvum* are very rare and lack documentary proof/evidence. They have been reported to have an oval or circular shape (Green et al., 1982; Wang & Wang, 1992). While HABs are frequently referred to as “red-tide” blooms because of the orange to red discoloration of the water when they bloom, *P. parvum* blooms produce bright gold coloration due to the abundance of its accessory pigments such as fucoxanthin, b-carotene and other xanthophylls, collectively known as carotenoids), concentrated in its chloroplasts (Wilhelm & Manns, 1991) (Fig. 1.2 D).

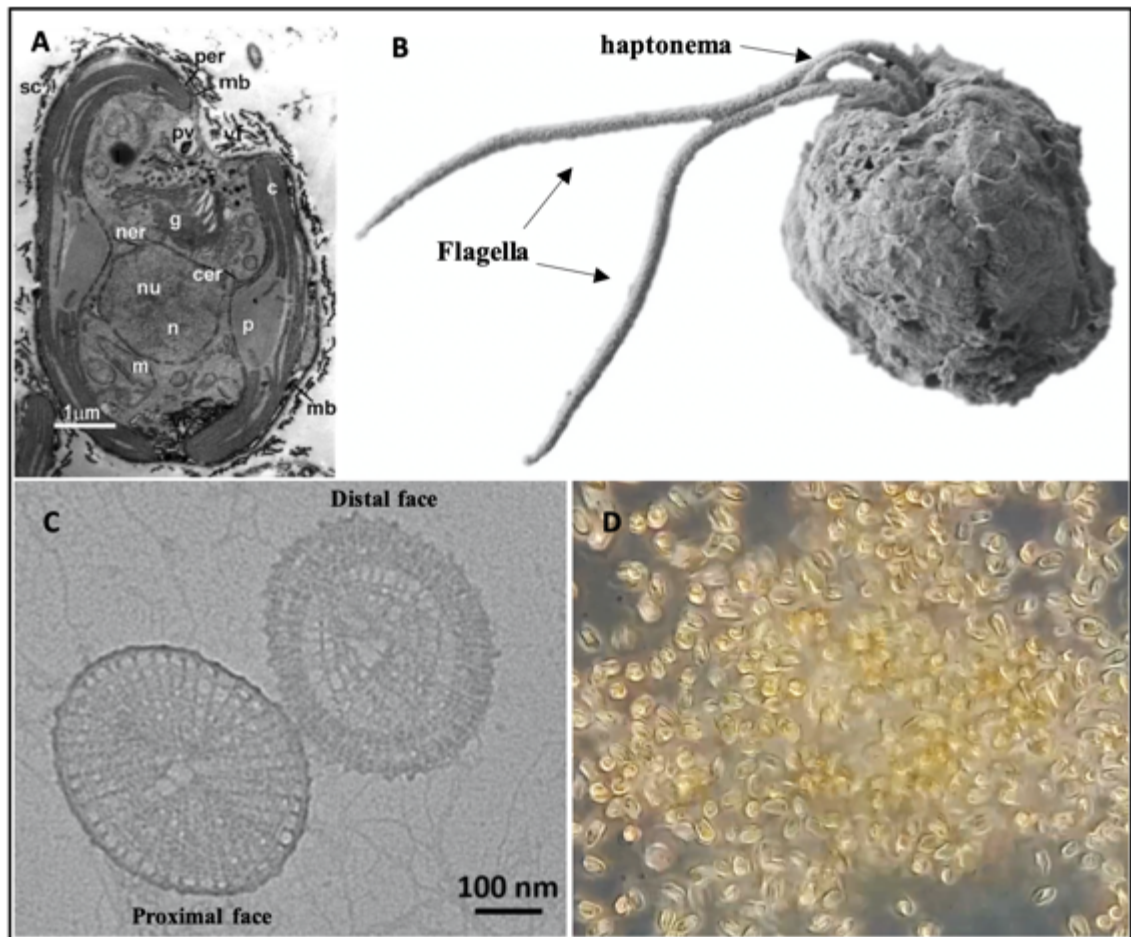


Figure 1.2. Details of the morphology of *Prymnesium parvum* as observed by (A) transmission electron microscopy showing longitudinal section: c: chloroplasts, cer: chloroplasts endoplasmic reticulum, vf: vestibular fossa, per: periplastidial endoplasmic reticulum, n: nucleus, nu: nucleolus, ner: nuclear endoplasmic reticulum, m: mitochondria, p: pyrenoids, g: Golgi body, mb: muciferous body, pv: pulsatill vacuole, sc: scales. (B) scanning electron microscopy showing whole surface of the cell. Note the presence of short haptonema in between the 2 long flagellae. (C) Scales of *P. parvum* observed by transmission electron microscopy (TEM) showing distal (outside) and proximal (inside) faces (scale bar represents 100 nm). (D) light micrograph of the *P. parvum* cells showing intense golden color when in high abundance or density. (Figure 1.2 A-C Adapted from Wagstaff et al., 2018).

1.2.3 Life cycle (proposed)

Studies on the reproductive cycle have suggested that *P. parvum* has an alternating life cycle (haplodiplontic) in nature (Bold & Wynn, 1985; Larsen et al., 1993; Larsen, 1999). It has been proposed that *P. parvum* life cycle consists of two morphologically different flagellated haploid cell types (*P. parvum* and *P. parvum* f. *patelliferum*), one flagellated diploid cell type (*P. parvum*), and a non-motile form considered to be a resting stage or cyst (Fig. 1.3) (Edvardsen & Medlin, 2007). This life cycle is very similar to the members of genus *Chrysochromulina*, e.g. *Chrysochromulina polylepis*, which are known to be closely related to *Prymnesium* as shown previously in Fig. 1.1 (Larsen & Bryant, 1998). The two morphologically different haploid cell types are so different that they have been previously assigned or separated as two distinct species (Larsen & Edvardsen, 1998). One possible reason for the existence of these haploid forms is for energy conservation. The smaller DNA quantity in haploid cells, the lower the nutrients they require. It is also thought that sexual reproduction is a part of the *P. parvum* life cycle under favorable environmental conditions (Freitag et al., 2011) but this has not been proven in a laboratory setting. Reproductive studies in the lab (Larsen & Edvarsen, 1998) on *P. parvum* and *P. patelliferum* showed that when two haploid *P. patelliferum* were mixed they were not able to produce *P. parvum* offspring (either diploid or haploid) but combinations of *P. parvum* unexpectedly produced both haploid *P. parvum* and *P. patelliferum* (Larsen & Medlin, 1997). Therefore, a heteromorphic life cycle has been proposed for *P. parvum*, with both haploid and diploid stages (Fig. 1.3). Furthermore, this life cycle shows the formation of haploid *P. parvum* and *P. patelliferum* through meiosis of diploid *P. parvum* cells, and the formation of diploid *P. parvum* through syngamy (the merging of two haploid cells) (Larsen & Edvarsen, 1998) as shown in Fig. 1.3.

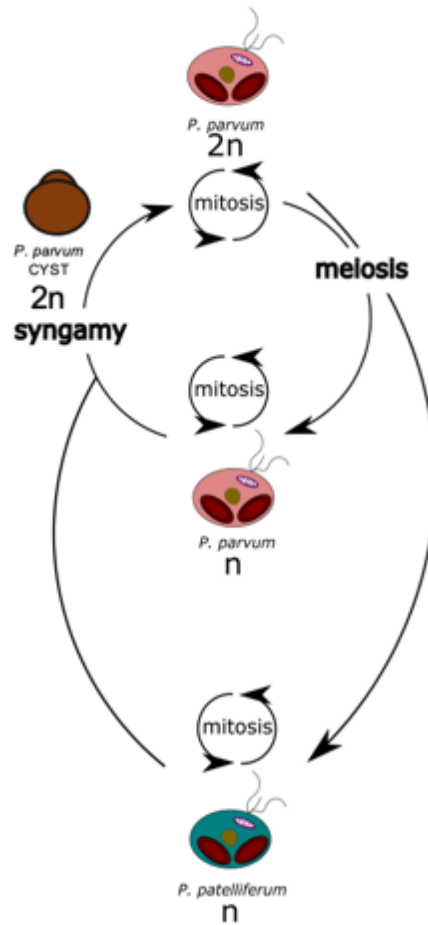


Figure 1.3. Proposed life cycle of *P. parvum*/*P. patelliferum*. Adapted from Larsen and Edvardsen (1998).

1.2.4 Growth Requirements

Salinity. Studies have found that *P. parvum* can thrive in a wide range of salinities (euryhaline organism). McLaughlin (1958) showed that optimal NaCl concentrations for the growth of one Scottish and two Israeli strains of *P. parvum* occurred at 0.3% - 6% with growth possible at 0.1% - 10%. Padilla (1970) observed that low salinities (less than 10%) increased the doubling time of *P. parvum* cells and induced high levels of protein and nucleic acid production. Larsen and Bryant (1998) reported that the Norwegian, Danish and English strains of *P. parvum* they tested grew over a wide range of salinities each with different optimum growth concentrations, and that all three strains survived salinities from 3 to 30 PSU (or 0.3% - 3%).

Temperature. In a study by Shilo and Aschner (1953), they showed that temperatures greater than 30°C were inhibitory to the growth of *P. parvum* cells, and 35°C resulted in cell rupture/lysis. Larsen, Eikrem and Paasche (1993) found that the *P. parvum* strain from Denmark had an optimal growth temperature of 26 °C but was limited when the temperature was brought down to 10 °C. Larsen and Bryant (1998) reported that the Danish, Norwegian, and English strains of *P. parvum* exhibited a maximum growth rate at 15°C with strains tolerating a wide temperature range of 5°C to 30°C. This supports the notion that *P. parvum* is a eurythermal organism.

Light. Wynne and Rhee (1988) observed that the activity of alkaline phosphatase was higher at high light intensities. They noted that an increase in light intensities allows *P. parvum* to increase the speed at which it is able to take up phosphate from its environment, and thus abrupt changes in light intensities have a profound effect on competition. However, Padan et al. (1967) found that excessive light inhibits the growth of *P. parvum*.

Nutrients. *P. parvum* can satisfy its phosphate requirements from a wide range of compounds probably due to the presence of many phosphatases (McLaughlin, 1958). As an obligate phototroph, *P. parvum* was found to graze on bacteria, especially when phosphate is limited, and this might be the only source of phosphate for this microalga when phosphate is scarce (Nygaard & Tobiesen, 1993). For nitrogen source, ammonia other compounds such as ammonium salts, the amino acids aspartic and glutamic acid, alanine, methionine, histidine, proline, glycine, tyrosine, serine, leucine, and isoleucine were found to be utilized by *P. parvum* at low pH (McLaughlin, 1958). In alkaline conditions, nitrate, creatine, asparagine, arginine, alanine, histidine, methionine and acetyl-urea were also found to be good sources of nitrogen (McLaughlin, 1958; Watson, 2001).

1.2.5 Toxicity

Prymnesium parvum and other members of the genus *Prymnesium* are known to produce and excrete numerous compounds and secondary metabolites (e.g. prymnesins toxins) whose function and biosynthesis are not entirely understood. There are innumerable possibilities that might explain the specific functions of these compounds. Some of these compounds may give the organism a competitive advantage over other phytoplankton in the environment (i.e., allelopathy) (Smayda, 2008). As such, these chemicals inhibit growth or kill other phytoplankton species. Allelochemicals produced and secreted by *P. parvum* have been shown to kill both

competing algal species and their grazers (Tillmann, 2003; Granéli, 2006). Closely related to this “killing capacity” is the mixotrophic tendencies of *Prymnesium*, i.e. the ability to ingest immobilized competitors and grazers (Tillmann, 2003; Skovgaard & Hansen, 2003). This strategy to ‘kill and eat your enemies’ by means of toxic compounds is thought to significantly contribute to the ability of *P. parvum* to form dense, persistent, and recurring blooms.

Prymnesium parvum is believed to produce numerous mixture of toxins. These toxins have hemolytic, cytotoxic, ichthyotoxic and possibly neurotoxic activities. However, toxins produced by the alga likely constitute a suite of compounds with diverse cellular origins and biological activities (Manning & La Claire, 2001). Igarashi et al. (1996) successfully characterized the first two types of these toxins: the prymnesin-1 and -2 (PRM1 & PRM2), which are now known as A-type Prymnesins (Fig. 1.4). Both prymnesins have potent hemolytic and ichthyotoxic properties. More recent studies have found two additional types of prymnesins in different strains of *Prymnesium* and these are the B- and C-type prymnesins (Rasmussen et al., 2016; Binzer et al., 2019). The configuration of these huge cyclic polyethers has led researchers to postulate that, like the dinoflagellate toxins brevetoxin and okadaic acid, the synthesis of these molecules might involve polyketide synthase genes (Manning & La Claire, 2013). Unfortunately, quantification of these toxins remains difficult until today.

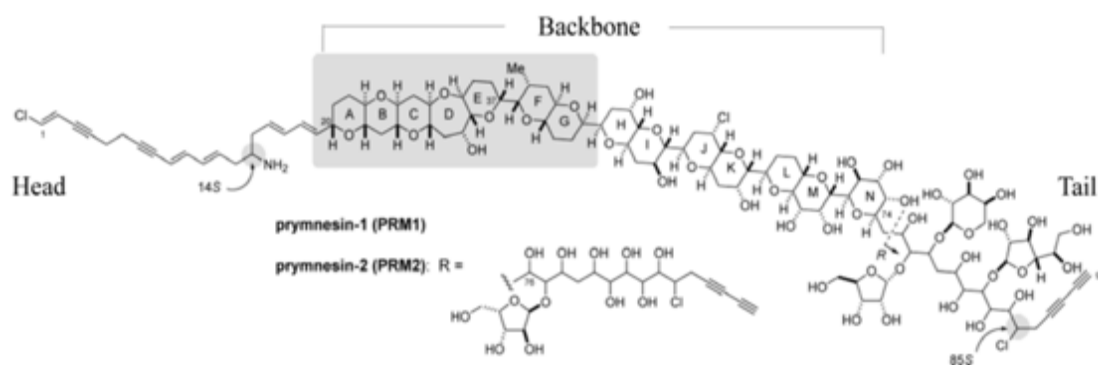


Figure 1.4. Structures of prymnesin-1 and prymnesin-2 (Manning & La Claire, 2010).

Other toxic compounds that have been extracted from *P. parvum* include lipopolysaccharide-like compounds (Paster, 1973), proteolipid (Dafni et al., 1972), galactoglycerolipids (Kozakai et al., 1982), fatty acid amides [Bertin et al., 2012], and fatty acids (Henrikson et al., 2010). It is worth noting that some of these have been dismissed by Blossom et al. (2014).

1.2.6 Geographic occurrence/distribution

In 1911, J. Büttner originally described and identified *P. parvum* as *Wysotzkiella gladiociliata* in his paper 'Die farbigen Flagellaten des Kieler Hafens' and referred it as 'another flagellate with three flagella.' It was a milestone discovery during that time albeit the incorrect description regarding the third flagella (Larsen, 1998). Later on Liebert and Deens (1920) identified *Prymnesium parvum* as the causative organism for mass fish mortalities in Denmark and Holland. This alga was later confirmed with more devastating toxic blooms in the same area (Otterstrøm & Steemann-Nielsen, 1940). It is still not known when was the first ever fish kill due to *P. parvum* blooms but this was the first confirmed record of fish kill associated with it. In 1938, mass mortalities of pike, perch, roach, eels, bream, and trench were recorded in the Ketting Nor off the coast of Jutland, and again in 1939 in the Selso So located on a peninsula of Sjaelland Island, Denmark (Reichenbach-Klinke, 1973). After this, the alga has since been extensively documented as being associated with seasonal toxic blooms and mass mortality events in aquaculture ponds and native populations of gill-breathing animals (Collins, 1978; Green et al., 1982) and shellfish (Chang et al., 1985) in marine coasts, estuaries, brackish water and freshwater lakes. This implies that HABs of *P. parvum* are nuisance on a global scale (Fig. 1.5) (Manning & La Claire, 2010).



Figure 1.5. Worldwide occurrences and distribution of *P. parvum* populations based on countries where reported. Red dots indicate areas with records of large scale *P. parvum* blooms and Fish Kills while the green dots indicate presence. Most of the blooms tend to occur in temperate and subtropical zones. Adapted and compiled from Edvarsen & Larsen (2003) and Manning and La Claire (2010).

Most *P. parvum* blooms tend to be restricted to cooler waters located in the subtropical and temperate zones between the Tropic of Cancer and Arctic Circle and between the Tropic of Capricorn and Antarctic Circle (Fig. 1.5). In Israel, *P. parvum* was first recorded in 1947. It quickly spread throughout the country, and as the fish-breeding industry (African tilapia) was threatened, this alga was investigated extensively for several decades in Israel (Reich & Aschner, 1947; Shilo & Shilo, 1953; Ulitzur, 1969). In the United Kingdom, the first confirmed record of devastating fish kill due to *Prymnesium* was in 1969 on the Norfolk Broads that led to the demise of approximately 200,000-300,000 fish (Holdway et al., 1978; Bales et al., 1993). It has been argued that these events may have happened in the past, for archival records from the area showed consequential mass fish kills with similar water discoloration and fish phenotypes. Local folks referred it as the 'Norfolk Tea' (Holdway et al., 1978). In 1989, Atlantic salmon (*Salmo salar*) and rainbow trout (*Oncorhynchus mykiss*) died in aquaculture enclosures in the Sandsfjord system (southwest Norway) with fewer of the free-living fish in the brackish water fjord system affected (Kaartvedt et al., 1991). *P. parvum* blooms have been related to recurrent fish kills in Vasse-Wonnerup estuary (W.A.) of Australia with kills most common in January-March since 1970s (Hallegraeff, 1992). These fish kills, like those of the Sandsfjord system in Norway, showed that wild fish stocks are less vulnerable to the *P. parvum* toxins than caged fish since they can swim away from affected or toxic areas. *P. parvum* fish kills in Oued Mellah Reservoir in Morocco occurred in November-December 1998 and again in September-October 1999 (Sabour et al., 2000). Recurrent kills in carp ponds due to *P. parvum* in the People's Republic of China have also been reported since 1963 (Guo et al., 1996). The first confirmed fish kill due to *P. parvum* in Texas, USA occurred in 1985 on the Pecos River with approximately 110,000 fish dying (Rhodes & Hubbs, 1992). Since then, Texas Parks and Wildlife Department (TPWD) has estimated approximately 34 million fish deaths due to blooms of the alga, a loss economically estimated at 13 million dollars (Southard et al., 2010). Reports of mass fish kills were also recorded in other parts of the world like Scotland (rock pools) (Comin & Ferrer, 1978), Germany (Dietrich & Hesse, 1990), Finland (Lindholm et al., 1999), Spain (Comin & Ferrer, 1978), Bulgaria, Palestine (Green et al., 1982), South Africa (Töbe et al., 2006), India (Thomas, 2014), New Zealand (Chang et al., 1985) and even Brazil (Bergesch et al., 2008).

P. parvum blooms were once thought to be restricted only in marine or brackish estuarine environments but more recent blooms are slowly gaining its notoriety to invade/disrupt inland freshwater reservoirs/systems (Dickson & Kirst, 1987; Guo et al., 1996). Highlighting the ability of what was once considered a marine organism to thrive in a range of climates (Manning & La

Claire, 2010). Proposed vectors of transfer include contaminated ballast/bilge water, bird guano and encystment/excystment cycle (Green et al., 1982; Hallegraeff, 1993).

1.3 The Broads and *Prymnesium parvum*

The term Broadland or simply the "Broads", is used to describe a series of mostly small, shallow features or lakes formed by the flooding of medieval peat diggings, that lie in the valleys of the major rivers draining the eastern part of Norfolk and Suffolk (Davies, 1980; George, 1992; Moss, 2001). More than 60 broads have been recognized, varying in size from small pools to the largest of 120 ha (Fig. 1.6) (Broads Authority, 2017). In the late 1800s the total area of broads was approximately 1200 ha but this has been reduced to about 700 ha, largely due to marginal overgrowth of vegetation. The broads are part of an extensive system of fens, marshes and interconnecting waterways in the catchment of the Rivers Bure, Yare and Waveney; this system is collectively known as Broadland (Davies, 1980).

The Broadland is essentially freshwater, but because the rivers have such low gradients the lower reaches are brackish and saline. The influence of tide is particularly apparent on the River Yare. In Norwich, 40 km from the sea, there is a vertical movement of half a meter at spring tide. Hickling Broad and Horsey Mere and other waterways associated with the River Thurne, a tributary of the River Bure, are brackish, not as the result of tidal excursion but because a saline water table underlies this part of Broadland (Davies, 1980). Most the broads are in the northern part of Broadland. There are few broads or unreclaimed fen within the valleys of the Rivers Yare and Waveney.

The Broads, their channels, and the surrounding marshlands have immense national significance, both as a resource for tourism, recreational boating and other water-based pursuits. They act as a haven for rare wildlife (home to a quarter of Britain's rarest flora and fauna), a hotspot of aquatic and wetland biodiversity, and results in the Norfolk Broads being Britain's largest protected wetland, recently classified as a national park. However, intensification of agriculture and increases in human population density over the last 200 years have greatly increased pressures on the aquatic environment through eutrophication (Broads Authority, 2015).

Considerable reclamation of the highly fertile alluvial land of Broadland has occurred over the centuries. Of the 23,500 ha in Broadland 20,500 ha have been embanked and partially drained for grazing and arable cultivation. The remaining 3,000 ha of unreclaimed fen provides some

storage of floodwater impounded as a result of North Sea surges and high tides. These 'washes' are also utilized for reed and sedge crops (George, 1992). The change from grassland to arable farming and the extensive use of fertilizers, a proportion of which are lost to the drainage entering the Broadland, are contributory factors to the declining water quality and increasing eutrophication problem of the Broadland waters (Broads Authority, 2015).

More recently the Broads has been afflicted with several environmental issues such as saline incursions/surges and eutrophication, but of particular concern is the frequent recurrence of *P. parvum* blooms that leads to massive losses in wild fish stocks. Fish mortalities since the 1960s have been associated with *P. parvum* blooms. From then on, blooms have occurred almost every year, with no apparent seasonality. Bales et al. (1993) discussed large fish kills that have occurred in 1969 and 1970, and smaller kills in 1973 and 1975 particularly in the Hickling Broad area and its surrounding area in the River Thurne (Fig. 1.6). The ecosystem of the area changed from largely charophyte-dominated to phytoplankton-dominated in the mid-1970s. They suggested that this was due to the sudden influx and nesting of black-headed gulls (*Larus ridibundus*) and the resultant eutrophication brought about by gull guano. The gull guano was thought to have provided the necessary organic nutrients in the water for microalgal species such as *P. parvum* to bloom. This theory was later supported by the observation that as the gull records declined, *P. parvum* incidents also decreased.

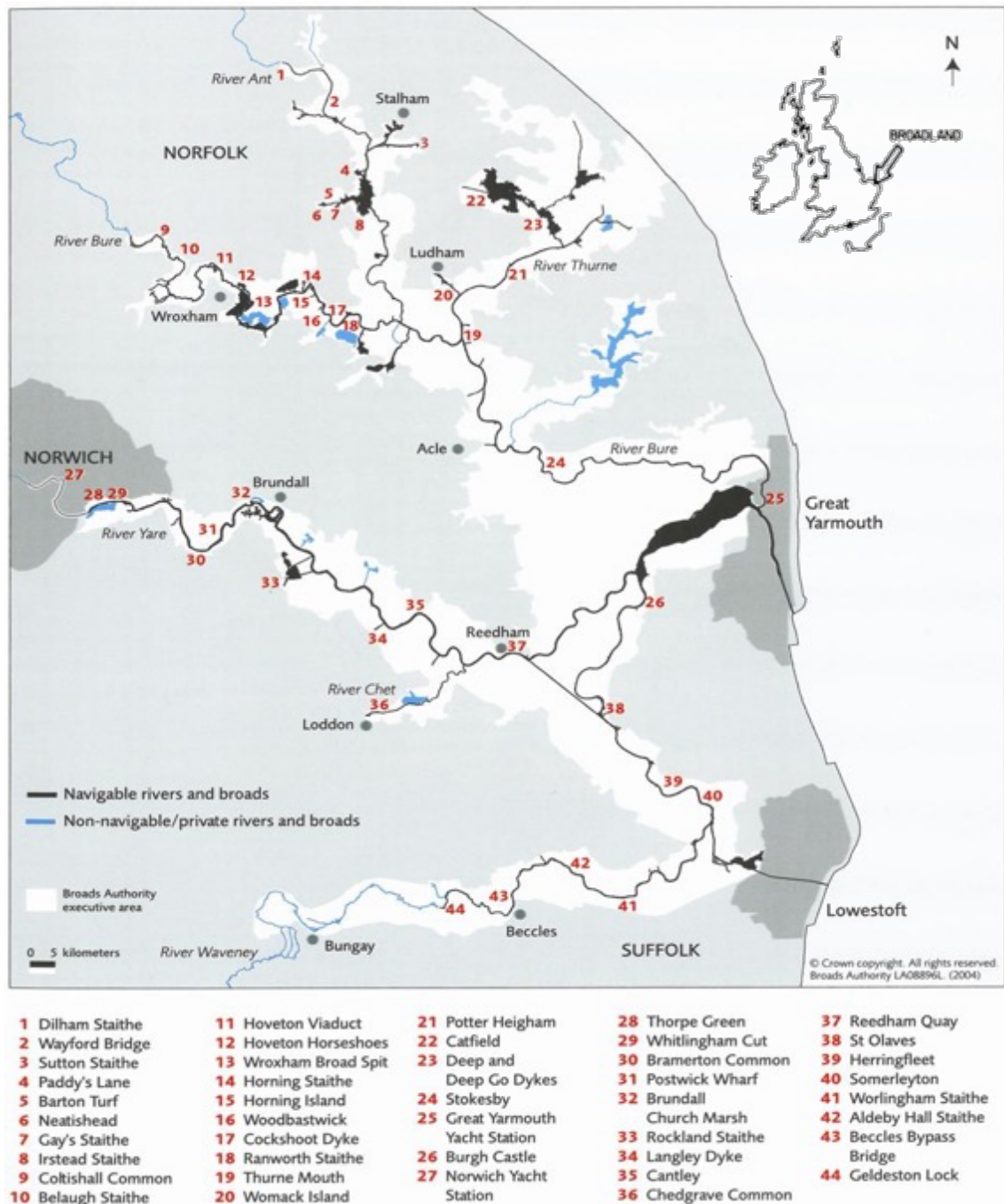


Figure 1.6. Geographical distribution of the broads (Broads Authority, 2015).

P. parvum blooms can wipe out an entire fish population if no immediate intervention is placed. The mass fish die-off affects angling, tourism, and other recreational activities thereby affecting the local economy. The Broads Authority estimated that the tourism industry of the Broads contributes around £550 million every year to the local economy (Broads Authority, 2017). The loss of fish stocks due to toxic *P. parvum* blooms threatens this revenue as what has happened in Spring to Summer of 2015 when multiple blooms of *P. parvum* across the Upper Thurne system

left waterways littered with extremely unpleasant sightings and foul smell of dead rotting fishes (Fig. 1.7).



Figure 1.7. Dead fish on the waterways on the Upper Thurne area of the Norfolk Broads. Image captured by Martin Rejzek during a toxic *P. parvum* bloom in April 2015.

1.4 *P. parvum* and β -dimethylsulfoniopropionate (DMSP)

Dickson and Kirst (1987) speculated that the persistence of *P. parvum* blooms in variable saline environments may be due to its ability to synthesize compatible solutes. They showed that the osmotic adjustment in the marine algae through increased production of a tertiary sulphonium compound: β -dimethylsulfoniopropionate (DMSP) and an unknown polyol. Later on haptophytes, like *P. parvum*, were found to be relatively high producers of DMSP compared to other phytoplankton groups, i.e. diatoms and green algae (Keller et al., 1989). DMSP is a zwitterionic tertiary sulfonium compound ($C_5H_{10}O_2S$) that is virtually present throughout the euphotic zone of the ocean because it constitutes major intracellular osmolyte/metabolite of most marine phytoplankton (Keller et al., 1989). It was first isolated in a red macroalga, *Polysiphonia fastigiata* (Challenger & Simpson, 1948). Since then, DMSP has received increasing interdisciplinary interest, because it is the principal precursor of dimethylsulfide (DMS) gas, which dominates the oceanic emission of volatile organic sulfur to the atmosphere (Andreae,

1990) and this gas is responsible for the main transfer of reduced sulfur from the ocean to the atmosphere (Andreae, 1990; Ayers & Gras 1991) (Fig. 1.8).

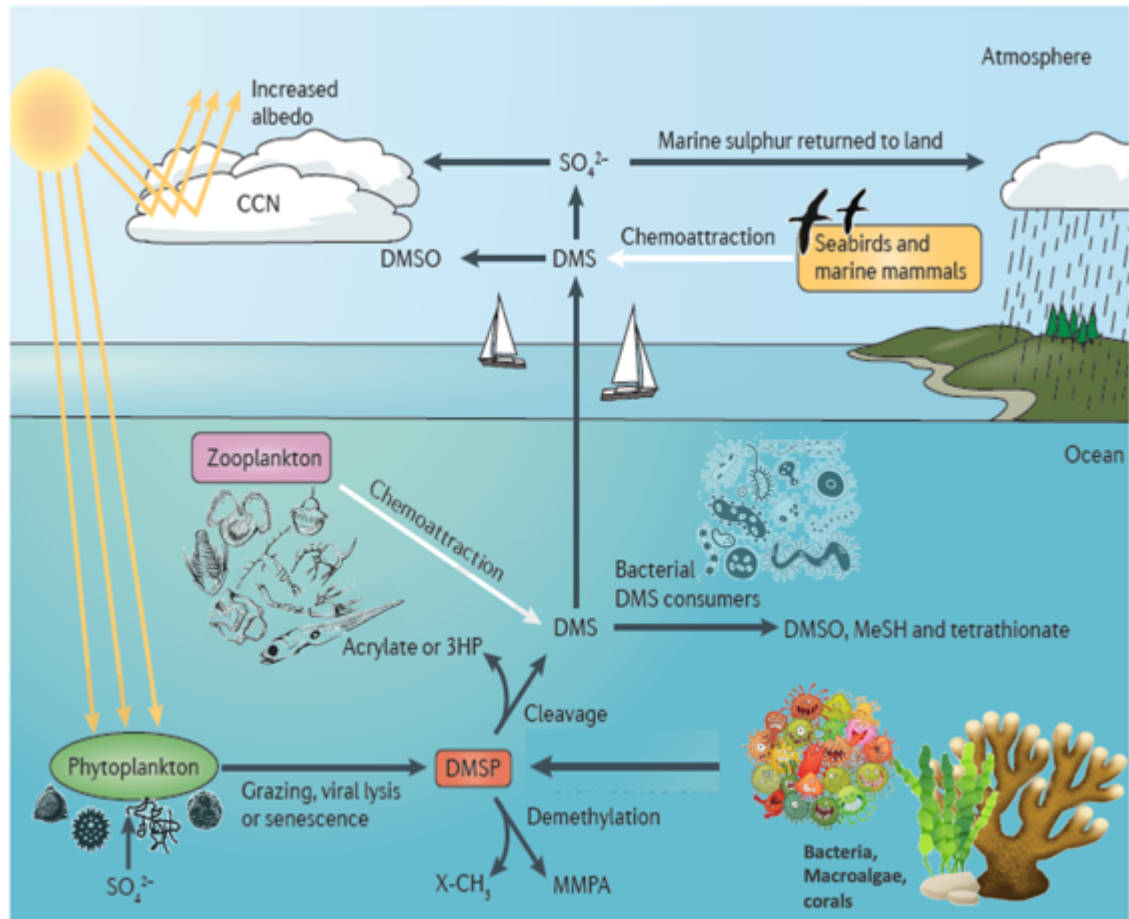


Figure 1.8. Mechanisms of DMSP and DMS cycling in the marine/aquatic environment and atmosphere. DMSO, dimethyl sulfoxide; CCN, cloud-condensing nuclei; MMPA, 3-methiolpropionate; 3HP, β -hydroxypropionate; MeSH, methanethiol; $X-CH_3$, unidentified molecule with a terminal methyl group. Adapted from Curson et al. (2011).

DMS is estimated to represent 21 % of the global sulfur flux (Simó et al., 2002), it is the major natural sulfur input. This DMS flux represents a significant input in the global sulfur cycle of 15×10^{12} to 33×10^{12} g S/yr (Kettle et al., 1999) and accounts for more than 38 % of the global sulfate burden of the atmosphere (Simó et al., 2002). DMS is the most important biogenic sulfur source for the formation of aerosols and condensation nuclei (CCN) in the troposphere and the global sulfur cycle it is responsible for most of the sulfur transport from the ocean to land (Andreae, 1990; Brimblecombe & Lein 1989) (Fig. 1.8). The density of the sulfur aerosols formed in the atmosphere during the DMS oxidation is an important factor in the global radiation budget, as it

influences both the scattering of short-wave light in the troposphere and the condensation and radiation properties of clouds (Charlson et al., 1987; Andreae & Crutzen, 1997). The atmospheric oxidation of the DMS through the conversion of nitrate and hydroxyl radicals is also closely related to the formation of ozone in the marine Boundary layer (Platt & Le Bras, 1997). These properties of the DMS offer great potential for interactions between biological production in the ocean and climate change.

1.5 Biological functions of DMSP

DMSP has multiple physiological functions in marine phytoplankton, plants, and bacteria. It is one of the major compatible solutes that stabilizes enzymatic processes, and regulates osmotic pressure and serves as a methyl donor in cell metabolism (Kirst, 1996; Randal et al., 1996; Stefels, 2000; Lyon, 2011). This molecule has been shown to provide osmoprotection to bacteria (Pichereau et al., 1998; Cosquer et al., 1999; Sun et al., 2012), and proposed to have the same role in phytoplankton, and nearshore plants (Ghoul et al., 1995; Yang et al., 2011). It was also reported to have cryoprotection (Karsten, 1991) properties. DMSP production in phytoplankton was hypothesized to be the result of an overflow mechanism of reduced substances and excess energy (Stefels, 2000). Furthermore, it was found to have a grazing repellent function (Wolfe et al., 1997; Strom et al., 2003) and might have an ecological side effect as an info-chemical (Steinke et al., 2002). Furthermore, DMSP and most of its breakdown products are strong antioxidants that can efficiently scavenge toxic intracellular hydroxyl and oxygen radicals (Sunda et al., 2002; Husband et al., 2012). Within marine microbial food webs dissolved DMSP can be a major source of reduced sulfur and carbon for bacterial production (Simó et al., 2002; Kiene et al., 2000). Many marine bacteria can use DMSP as carbon and sulfur source, some are completely dependent on it, i.e. *Candidatus 'Pelagibacter ubique'*, a member of the widely distributed SAR11 clade which is devoid of assimilatory sulphate reduction genes (Tripp et al., 2008). However, despite progress in the understanding of the physiological significance of DMSP for marine phytoplankton and bacteria, there are considerable uncertainties in predicting both the variability of its production and the oceanic emissions of DMS to the atmosphere (Kettle et al., 1999).

1.6 DMSP synthesis

The biosynthetic pathways of DMSP production have been established for coastal plants (Hanson et al., 1994), green and red algae (Challenger & Simpson, 1948; Green, 1962), phytoplankton

(diatoms (Kettles et al., 2014), haptophytes (Malin & Steinke, 2004) and dinoflagellates (Stefels, 2000) and corals (Raina et al., 2013). However, a more recent study had found that DMSP synthesis/production is not only limited to eukaryotes but also prokaryotes like many marine bacteria (Curson et al., 2017) and these DMSP producing bacteria are important and abundant in coastal sediments (Williams et al., 2019) as well as in deep ocean surfaces (Zheng et al., 2020). The three pathways for DMSP biosynthesis from methionine have been described in plants, green algae, dinoflagellates, and bacteria (Gage et al., 1997; Uchida et al., 1996; Rhodes et al., 1997; Curson et al., 2017) (Fig. 1.9).

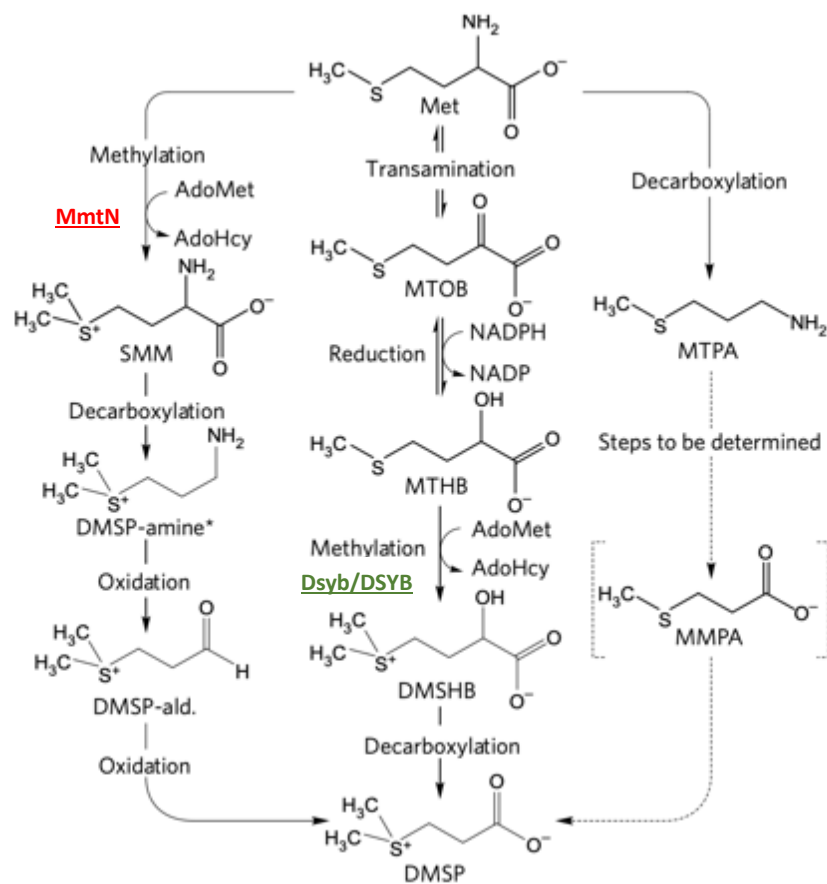


Figure 1.9. The three DMSP biosynthetic pathways used by higher plants, macroalgae, microalgae, diatoms, dinoflagellates, and bacteria. Named after their first step, after L-methionine, the first pathway is the methylation pathway which is found to be utilized mostly by higher plants and some bacteria. In bacteria, the methylation of L-Met to SMM is carried out by MmtN. Second, is the transamination pathway, which is widely distributed, utilized by macroalgae, microalgae, corals, and bacteria. In eukaryotes, the committed step of the MTHB methylation is carried out by DSYB, and in prokaryotes by

dsyB. The third and last is the decarboxylation pathway and so far, utilised by only one dinoflagellate (Adapted from Curson et al., 2017).

Nearshore plants *Wollastonia biflora* (L.) DC. [syn. *Wedelia biflora* (L.) DC., *Melanthera biflora* (L.) Wild Sea Aster, Asteraceae] (Hanson et al., 1994) and *Spartina alterniflora* (Smooth Cordgrass, Poaceae) (Kocsis et al., 1998) have been found to synthesise DMSP *de novo* through the methylation pathway (Fig. 1.9, Left). The initial precursor in both plants is L-methionine. L-methionine (Met) is methylated to S-methyl-L-methionine (SMM) by the enzyme S-adenosyl-L-methionine:L-methionine S-methyltransferase (James et al., 1995). The two plants differ in their central intermediate step in the biosynthetic pathway. For *W. biflora* the central step consists a pyridoxal 5'-phosphate (PLP) dependent transamination-decarboxylation sequence obtaining 3-(dimethylsulfonio)propionaldehyde (DMSP-ald) (Rhodes et al., 1997). While in *S. alterniflora*, SMM is decarboxylated to 3-dimethylsulfoniopropylamine (DMSP-amine) and further converted into DMSP-ald by oxidative deamination (Kocsis et al., 1998; Kocsis et al., 2000). The last step, which is the same for both plants, involves the oxidation of DMSP-ald to DMSP (Kocsis et al., 1998; James et al., 1995). More recently, Williams et al., (2019) discovered that some DMSP producing bacteria, including *alphaproteobacteria*, *gammaproteobacteria* and *actinobacteria*, are capable of synthesising SMM from L-Met, an ability previously thought to be limited to higher plants. They have shown that the methionine methyltransferase MmtN (Fig. 1.9, Orange Highlight), identified from the model bacterium *Novosphingobium* sp. BW1, was responsible for the conversion of L-Met to SMM in this type of bacteria synthesising DMSP.

In macro algal DMSP synthesis DMSP is derived from the amino acid L-methionine (Greene, 1962) via the transamination pathway (Fig. 1.9, middle). For a green seaweed *Ulva intestinalis* (previously *Enteromorpha intestinalis*), Met is transformed to 4-(methylthio)-2-oxobutanoic acid (MTOB) (Gage et al., 1997) via a 2-oxoglutarate-dependent transamination reaction (Summers et al., 1998). Then MTOB is reduced to 4-methylthio-2-hydroxybutyrate (MTHB) (Gage et al., 1997) requiring NAD(P)H. MTHB is then S-methylated, with S-Adenosyl-L-methionine as the methyl group donor (SAM) to produce 4-dimethylsulphonio-2-hydroxybutyrate (DMSHB), and finally DMSHB is oxidatively decarboxylated to yield DMSP (Greene, 1962; Gage et al., 1997). The S-methylation from MTHB to DMSHB catalysed by the MTHB S-methyltransferase enzyme (DsyB for bacteria, DSYB for phytoplankton) is specific to DMSP producers (Fig. 1.9, Green Highlight). The same pathway is also utilised in several groups of microalgae like the prasinophyte *Tetraselmis*, the prymnesiophyte *Emiliana huxleyii*, the diatom *Melosira nummuloides* (Summers

et al., 1998), and animals like the corals *Acropora millepora* and *Acropora tenuis* (Raina et al., 2013), and several marine bacteria (Curson et al., 2017) making it the most widespread DMSP biosynthetic pathway.

A third known DMSP synthesis pathway is known as the decarboxylation pathway, proposed for one heterotrophic dinoflagellate *Cryptothecodinium cohnii* (Fig. 1.9, right). First, Met is decarboxylated to form 3-(methylthio)propylamine (MTPA) by L-methionine decarboxylase. Then is proposed to be generated methylmercaptopropionic acid (MMPA) by an undetermined enzyme prior to the formation of DMSP. The complete steps of the pathway are yet to be determined (Uchida et al., 1996).

Candidate genes involved in the biosynthesis of DMSP were proposed from studies in the sea-ice diatom *Fragilariopsis cylindrus* (Summers et al., 1998), but these genes were not characterized. The first characterized gene proved to be key in the biosynthesis of DMSP is the MTHB methyltransferase, *dsyB*, from the Alphaproteobacterium *Labrenzia aggregata* LZB033 (Curson et al., 2017) and the subsequent discovery of its homologous counterpart in many phytoplankton, *DSYB* (Curson et al., 2018). We found that the *DSYB* methylthiohydroxybutyrate (MTHB) methyltransferase enzyme was localized mostly in the chloroplasts and mitochondria of the haptophyte algae *Prymnesium parvum*, and stable isotope tracking experiments support these organelles as the sites of DMSP synthesis (Curson et al., 2018). This was the first cellular colocalization and compartmentalization of DMSP biosynthesis in the haptophyte algae. Recently, an isoform MTHB S-methyltransferase isoform, termed TpMMT, was identified in the centric diatom *Thalassiosira pseudonana* (Kageyama et al., 2018) but it was not functionally ratified outside of this diatom.

1.7 DMSP breakdown

When DMSP is released into the surrounding waters from DMSP-producing organisms, either through cell autolysis following senescence (Stefels & van Boekel, 1993), viral/bacterial attack and cell breakage (Bratbak, 1996), or as a result of grazing (Kiene et al., 2000) and microzooplankton (Wolfe & Steinke, 1996), it becomes an available resource for marine bacteria and phytoplankton that are able to take it up and utilize it (Dickschat et al., 2015).

Currently there are two main pathways (demethylation and cleavage) known to degrade DMSP (Fig. 1.10) and both provide carbon and energy to the bacterial cell (Curson et al., 2011; Varaljay

et al., 2015). The most common route of DMSP degradation is through demethylation (also known as demethylation/demethiolation), a series of reactions starting with initial demethylation of DMSP, that breaks it down into other useful compounds and allow nutrients (carbon and sulfur) to be taken up or assimilated into bacterial biomass (Kiene et al., 2000). About 50-90 % of the DMSP taken up by the bacterial cells is thought to undergo this degradation process (Kiene et al., 2000). This in turn can release gaseous methanethiol (MeSH), enabling the assimilation of biogenic sulfur from DMSP that can be used for the biosynthesis of amino acids (Dickschat et al., 2015), or used by other planktonic groups. This DMSP degradation pathway was known to exist for many years but only recently have the complete steps been fully elucidated. The demethylation pathway involved two steps: First, the initial demethylation of DMSP and second, by the demethiolation of methyl mercaptopropionate (MMPA) (Reisch et al., 2011). The first gene associated with demethylation of DMSP, designated *dmdA*, was discovered by Howard et al. (2006) and the DmdA enzyme catalysing DMSP has strict substrate specificity, suggesting that this role is its sole purpose (Reisch et al., 2011). It also requires the presence of FH₄ (tetrahydrofolate), which acts as the methyl group acceptor, becoming Me-FH₄ (Howard et al., 2006). Me-FH₄ can then become the methyl donor in both methionine and S-adenosyl-methionine synthesis, or can be oxidised to become Formyl-FH₄, a carbon donor in the synthesis of cysteine from glycine (Reisch et al., 2011). The resulting MMPA from this demethylation is then demethiolated. This demethiolation step result in the release of MeSH, CO₂, and acetaldehyde (Fig. 8b). The MMPA-CoA thioester intermediate was discovered in *Ruegeria pomeroyi*, and its formation is catalysed by a methylmercaptopyrionyl-CoA ligase, termed DmdB that requires one molecule of ATP (Reisch et al., 2011). The MMPA moiety of this thioester is dehydrogenated, forming a double bond and the loss of two electrons to FAD, becoming FADH₂. This reaction results in a methylthioacryloyl-CoA (MTA-CoA) intermediate, and is catalysed by DmdC, a dehydrogenase (Reisch et al., 2011). The final enzyme involved in this pathway is DmdD, which belongs to the crotonase family (Tan et al., 2013). This enzyme catalyses multiple steps in this final reaction, starting with hydration that incorporates a molecule of H₂O, and liberates MeSH immediately. This forms a malonate semialdehyde-CoA (MaS-CoA) intermediate, which undergoes hydrolysis with a second H₂O molecule that releases the CoA group from the rest of the molecule (Tan et al., 2013). It is thought that MaS-CoA spontaneously decomposes to acetaldehyde, releasing CO₂. This acetaldehyde can then be converted to acetate via an acetaldehyde dehydrogenase (Reisch et al., 2011).

The second DMSP degradation pathway is the catalytic lyase pathway (cleavage), where DMSP is broken down to release DMS and either 3-hydroxypropionate (3-HP) (Todd et al., 2009) or acrylate through the action of DMSP lyase enzymes (Curson et al., 2011). The breakdown of DMSP to DMS is catalysed by enzymes termed Ddd enzymes in marine bacteria and *Alma1* in microalgae (Fig. 1.10b) (Dickschat et al., 2015; Alcolombri et al., 2015). Such isozymes can also be found in micro- and macro-algae, bacteria, and fungi (Steinke et al., 1996; Yoch, 2002; Todd et al., 2009). There are currently seven known *ddd* genes and one *Alma1*, with organisms often containing a selection of them. Although all the Ddd⁺ enzymes result in the release of DMS, they comprise a varied group of peptides with distinct mechanisms which suggest that there is no single comprehensive system for DMS production (Curson et al., 2008). There is one DMS-producing enzyme identified that does not lead to acrylate production, instead it releases 3-HP, that is the DddD enzyme. The inferred pathway involved the modification of DMSP with acyl coenzyme-A (Todd et al., 2009) for the DddD enzyme is from the family of type III acyl-coenzyme A (CoA) transferases (Todd et al., 2007).

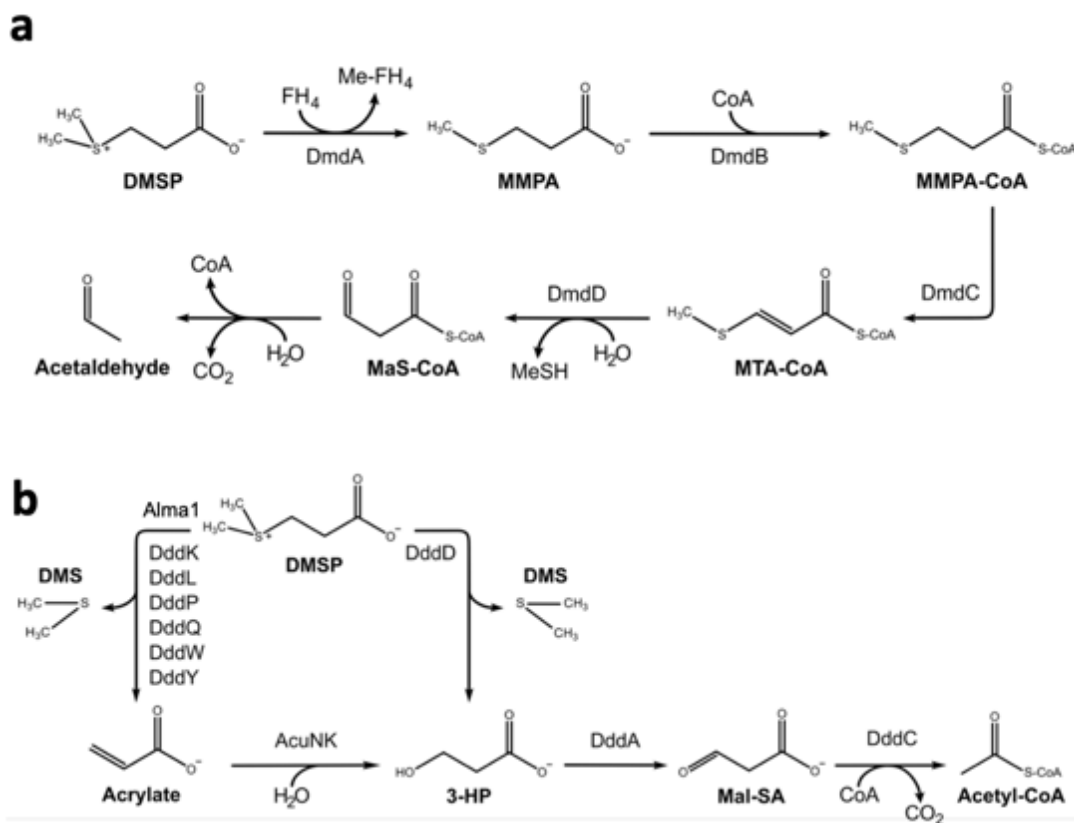


Figure 1.10. DMSP biodegradation pathways (a). The DmdA enzyme via the demethylation (and demethiolation) pathway removes a methyl group from DMSP generating 3-methylmercapto-

propionate (MMPA). DmdB then catalyses the conversion of MMPA to MMPA-CoA, followed by the oxidation to MTA-CoA via DmdC. MTA-CoA is transformed via DmdD, and the immediate release of MeSH to form MaS-CoA. This is finally converted to acetaldehyde and the release of CoA and a CO₂ molecule. The DMSP cleavage pathway (b), resulting in the production of DMS through one or two ways. These reactions are controlled by various *ddd* (bacteria) and *Alma* (microalgae) genes. The atypical direct lysis of DMSP to 3-HP is catalysed by DddD, whereas the DddL, DddP, DddQ, DddW, DddY, and Alma1 lyse it to acrylate first, which is then converted into 3-HP via AcuNK. DddA catalyses the oxidation of 3-HP to Mal-SA, and DddC enables the addition of coenzyme A to form acetyl-CoA. (Adapted from Brumett et al., 2015).

Some bacteria that catabolise DMSP have been found to utilise both demethylation and cleavage pathways, switching between the two when most appropriate (Kiene & Linn, 2000; Simo et al., 2001). The environmental factors that govern the switch favouring one pathway over the other have remained elusive, marking a major gap in the mechanistic link between microbial processes and global-scale carbon and sulfur biogeochemical cycling. There were several factors have been proposed to regulate this switch, including nutrient supply, light, and temperature (Levine et al., 2012; Varaljay et al., 2015) but these remained inconclusive. More recently, Gao et al. (2020) through microfluidic studies, reported that cleavage gene have higher expression than demethylation gene near the surface of a DMSP-producing phytoplankton cell, but demethylation gene remained expressed throughout the entire algal phycosphere, indicating that the ambient DMSP concentrations regulate the switching/expression of these two pathways.

While DMSP cleavage is commonly linked to marine bacteria, past studies have reported several marine microalgae capable of lysing DMSP into DMS. Significant DMSP lyase activity (DLA) was reported in the field and in cultures of phytoplankton such as *Phaeocystis spp.*, *Lingulodinium polyedrum*, *Alexandrium fundyense*, *Scrippsiella trochoidea*, *Heterocapsa triquetra*, *Symbiodium microadriaticum*, etc. (Stefels et al., 1995, 2007; Niki et al., 2000; Yoch et al., 2002; Yost & Mitchelmore, 2009; Caruana & Malin, 2014). DLA in these phytoplankton have been widely known for several decades, but the genes responsible for this activity have not been fully identified. In 2015, Alcolombri and colleagues identified the first algal gene, named *Alma1*, responsible for DMSP cleavage to DMS in coccolithophore *Emiliana huxleyi*. The *Alma1* gene shares no homology to any of the known bacterial DMSP lyase families. It is a member of the aspartate racemase superfamily. Based on sequence similarity, *Alma1* and its paralogs from *E. huxleyi* are present in a wide range of phytoplankton as well as certain bacteria, highlighting the

diversity of this protein (Yost and Mitchelmore, 2009; Alcolombri et al., 2015). There are seven *Alma1* paralogs within the *E. huxleyi* genome (*Alma1-7*) and divided into four clades. Clade A (*Alma3/6* and *Alma7*) is closest to *Alma* genes from *Phaeocystis antarctica*, a bloom-forming algal species that possesses high DLA and huge DMS production (Stefels, 1996). Clade A includes dinoflagellates (e.g., *Symbiodinium* sp.) and other haptophytes (e.g., *Prymnesium parvum*), and coral orthologs (from *Acropora millepora*). Clade B includes *E. huxleyi Alma4/5* and the *Chrysochromulina polylepis* gene. Clade C includes *E. huxleyi Alma1* and *Alma2* that is the closely related *Isochrysis*. The more distant clade D comprises bacterial genes with ~ 30 % identity to *Alma1*, but its relevance is yet to be determined. *Alma1* paralogs from *E. huxleyi*, *Phaeocystis Antarctica*, *A. millepora* (coral), and *Symbiodinium* sp. were synthesized and tested for lyase activity toward DMSP. Of those tested, however, only one *E. huxleyi* paralog, *Alma1*, and *Symbiodinium* A1 paralog had DMSP lyase activity, indicating that there is still much to learn about the phytoplankton DMSP lyases (Alcolombri et al., 2015).

1.8 Study aims and objectives

The over-arching goal of this study was to obtain a more developed understanding of the cellular processes involved in the production of DMSP and its by-product DMS, the factors affecting it, and their roles in the toxic bloom-forming haptophyte *Prymnesium parvum*, using combined quantitative chromatography and functional genomic approaches. This phytoplankton has been implicated in the recurring fish kills which have proven to be real problem on the Norfolk Broads over the years. Examining DMSP/DMS importance to the algae will shed light on understanding its invasiveness and persistence.

Therefore, to accomplish this goal, I divided this study into four aims addressing the following specific objectives:

1. **To determine bacterial groups associated with *P. parvum* and the impacts of *P. parvum* blooms on the Hickling Broad microbial community.** Bacterial-algal interaction or symbioses are not uncommon and have been observed between a number of organisms, but studies done on *P. parvum* remain elusive. In this chapter, I determined the effects of *P. parvum* blooms on the phytoplankton and bacterial community and compared it to non-bloom period using combined microscopy and *in situ* assessment of community diversity in samples by 16s rRNA gene amplicon

sequencing. Culture dependent techniques were employed to identify bacterial groups/species that may produce DMSP or rely on it. DNA and RNA were extracted from microbial communities in the environmental samples. I used Catalyzed Reporter Deposition - Fluorescence in situ Hybridization (CARD-FISH) to identify and characterize bacterial groups associated with *P. parvum* cells that may play important role in the formation of the algal blooms.

2. **To isolate model strains of *P. parvum* from Hickling Broad and characterize its DMSP synthesizing gene, *DSYB*, and determine *P. parvum*'s DMSP production at different life stages as influenced by different environmental factors.** Relevant strains of *P. parvum* from the broads were isolated using single-cell isolation techniques and monoclonal cultures were grown and subjected to a broad range of variables known to affect DMSP synthesis. High quality cDNA was sequenced to identify the DMSP synthesizing gene, *DSYB*, specific for Broad's *P. parvum*. *DSYB* gene probes were designed to monitor abundance and expression in environmental samples as well as in cultured samples. Algal growth by cell counting, photosynthetic efficiency and DMS production by gas chromatography (GC) were also measured. Key genes involved in the production and breakdown of DMSP were cloned from *P. parvum* cDNA into *Escherichia coli* expression vectors, expressed, and functionally ratified. There are some physiological or environmental conditions known to affect DMSP production and regulation in *P. parvum*. Here, I measured DMSP concentrations at different growth stages and under different salinity and nutrient regimes with the aim of elucidating the importance of these abiotic factors in DMSP production and regulation.
3. **To determine the temporal change in DMSP production and *DSYB* abundance in *P. parvum* on the Hickling Broad and investigate the potential biological roles that DMSP and DMS play in *P. parvum*'s persistent blooms.** Surface broad waters from the Norfolk Broad were sampled and particulate DMSP concentrations were measured by Gas Chromatography assays and correlated to the environmental parameters and *P. parvum* cell density. Community DNA and cDNA were used as template for PCR and RT-qPCR with gene probes designed for DMSP synthesis gene (*DSYB*) and bacterial catabolic genes (*dddP* and *DmdA*) to assess the diversity and abundance of these genes. This is the first report using *DSYB* abundance and

expression as a proxy in monitoring the environmental DMSP production associated with Harmful Algal Blooms.

- 4. To characterize toxins produced by Hickling Broad *P. parvum* strains.** Toxic algal blooms across the Norfolk Broads in 2015 prompted various stakeholders to take immediate action in monitoring and identifying the toxin present in the water samples. Through a combination of genetic analysis and metabolite analysis, *P. parvum* was implicated and prymnesins were detected in the environmental and biological samples for the first time. Here, I isolated and characterize the prymnesin type produced by Hickling Broad *P. parvum* strains and compared it to other *P. parvum* strains from culture collections.

Chapter 2

Materials and Methods

2.1 Field study on the Broads

2.1.1 Study site – Hickling Broad

The Hickling broad (52°44'N, 1°34'E) was chosen as the study site due to the frequency and severity of *P. parvum* blooms and a major hotspot for fish-killing events. It represents an area of 122 hectares with average water depths just above 1 meter. It is part of the larger Broadland system (the 'Broads') that is divided into two major groups, the Norfolk and Suffolk broads. Currently, there are 63 recognized shallow navigable lakes ('broads'), connected by the three major rivers, Waveney, Yare, and Bure and Bure's two tributaries, the Ant and Thurne (Fig. 2.1).

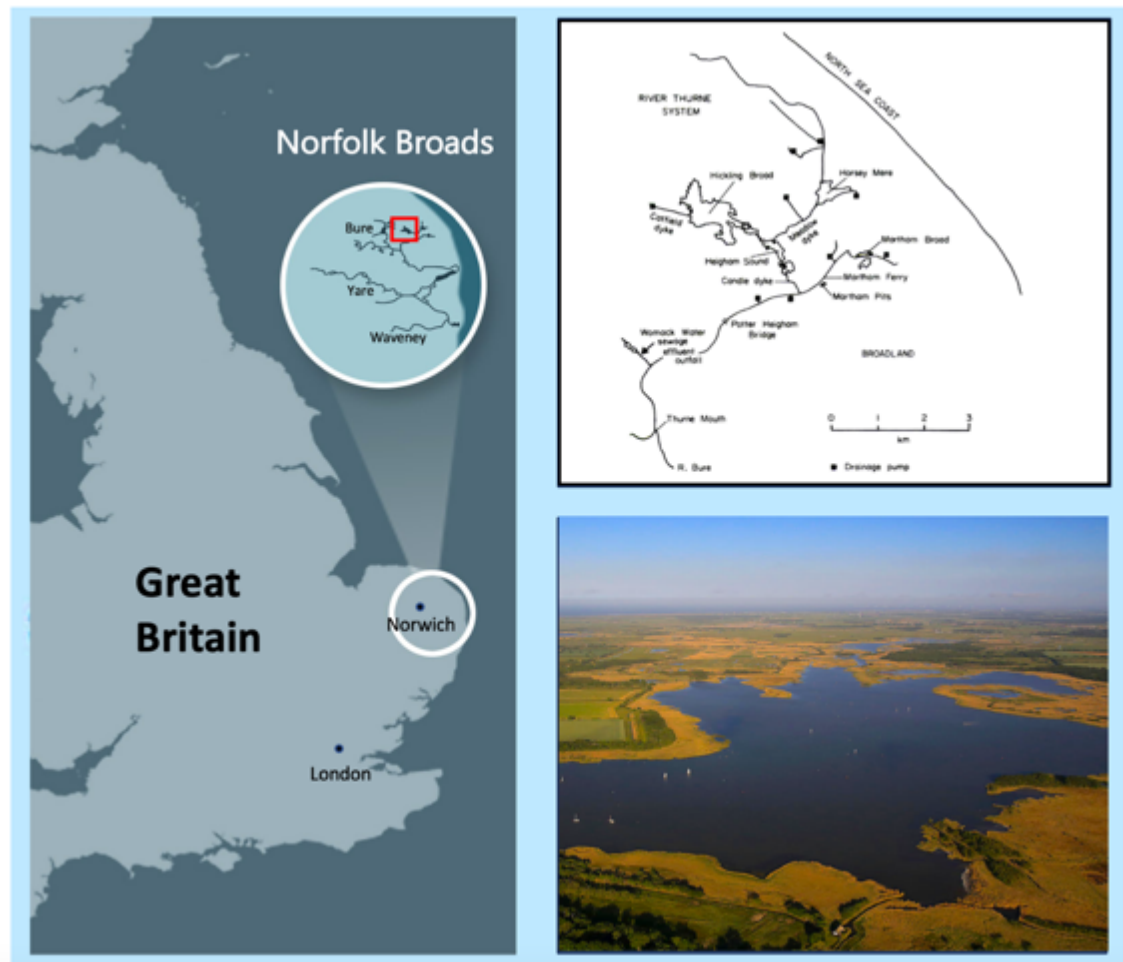


Figure 2.1. Map of upper Thurne area of the Norfolk Broads, Norfolk, UK. Left – Map of Great Britain and the Broadland systems highlighted by white circle. Top Right - Location of Hickling broad is denoted by the arrow. Adapted from Holdway et al. (1978). Bottom Right – Map showing the aerial view of the Hickling Broad © Broads Authority.

Anecdotal records have revealed the presence of *P. parvum* in some of these broads but majority of HAB events were somewhat confined to the upper Thurne river system, frequently posing issues to the largest broad – the Hickling Broad and its surrounding area.

2.1.2 Sample collection

In March 2015, hundreds of dead fish were found by the members of the public floating on the banks of Hickling Broad and surrounding waters. Concerned citizens immediately notified the Environment Agency (EA) and the Broads Authority (BA) for more fish appeared to be in distress and dying. This fish kill event was due to a sudden bloom of ichthyotoxic *Prymnesium parvum* in the area. Since then, regular fortnightly sampling and monitoring were implemented by the Broads Authority and sampling sites were set up to cover the majority of the Broad. I utilised 5 of these (12-point) sampling points for my study (Fig. 2.2, Table 2.1)

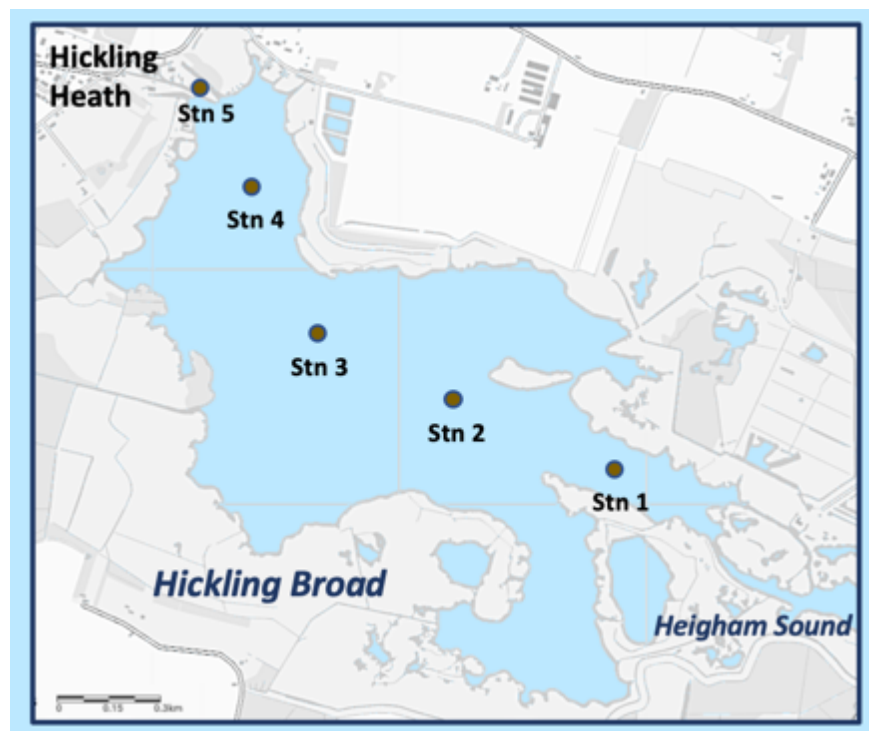


Figure 2.2. Map showing the five sampling stations where environmental samples were taken following a transect from the broad mouth to head of Hickling Broad. Previous fish kills were observed on the Northwest area of the Broad typically concentrated on station 5. Hickling Broad, Norfolk, Norwich, United Kingdom. 52°44'12.76" N, 1°35'07.96" E. Map was generated using ARCGIS. Scale bar (top right) – 0.3 km ©Broads Authority.

A batch of water samples was taken from Hickling Broad during a fish-killing bloom of *P. parvum* in April 2015 and another sampling was done in a non-bloom condition in September 2016. On two occasions, samples were taken by Dr. Jennifer Pratscher and Mr. Elliot Brooks, and collaborators from the John Innes Center (JIC) on the 'Prymnesium Project' with aid from the Broads Authority. Apart from these two sampling periods, I did subsequent water sampling on Hickling Broad every two weeks from April 2017 until March 2018. A set of 4 x 50 ml and 1 x 250 ml water samples were taken from each of the 5 sampling points (Table 2.1), following a transect across Hickling Broad and in concordant sampling points set up by the Broads Authority (Fig. 2.2). Additional 2L Nunc bottles filled with Broad water were taken for phytoplankton identification and community monitoring, and these were immediately fixed onboard with Lugol's iodine solution. All samples were collected at approximately 20 cm depth, making sure to exclude the surface layer.

Table 2.1 Coordinates of sampling locations on Hickling Broad, Norfolk.

Sampling Stations	Latitude	Longitude
Station 1	52°44'04.66"N	1°35'23.75"E
Station 2	52°44'19.12"N	1°34'39.49"E
Station 3	52°44'29.04"N	1°34'17.54"E
Station 4	52°44'44.90"N	1°34'19.10"E
Station 5	52°44'47.62"N	1°34'12.55"E

During each sampling event, water physicochemical parameters were recorded. *In situ* measurements of salinity (thru specific conductivity), pH, DO, and temperature were collected using YSI Professional Pro Meter (YSI Instruments, United States). Another set of samples were also collected by the Broads Authority (BA) for Chl-a, Ammonium (NH₄⁺), nitrate (NO₃⁻), and phosphate (PO₄³⁻) measurements. These were sent out to the Environmental Agency (EA) for further processing. The rest of the samples were returned immediately (within 3h of sampling) to the Department of Biological Sciences, UEA for microscopy, DNA and RNA extraction, and metabolite processing.

2.1.3 Processing of field samples

In preparing samples for DNA isolation, two 50mL plastic tubes containing algal biomass were immediately pelleted by centrifugation (6000 rpm, 4°C) for 10 min. Pellets were resuspended in 1 ml nuclease-free water (Ambion, Thermo Fisher Scientific). Suspensions from the same sampling point were pooled yielding pooled tubes of spun-down 100 ml broad-water. Cell suspensions were subsequently pelleted (10,000 rpm, 4°C) in 2 mL centrifuge tubes for 1 min, the supernatant was discarded, and cell pellets were flash-frozen with liquid nitrogen and stored at -80°C until further processing.

To obtain samples for RNA isolation, 50 ml of algal biomass was filtered onto 47 mm 1.2 µm RTTP polycarbonate filters (Fisher Scientific, UK) and filters were stored in 2 mL centrifuge tubes, immediately flash-frozen with liquid nitrogen, and stored at -80 °C until further processing.

For DMSP quantification by Gas Chromatography (GC), 50-100 ml of broad water samples from sampling sites were filtered onto 47 mm GF/F glass microfiber filters (Fisher Scientific, UK) using a Welch WOB-L 2534 vacuum pump, and filters were then blotted on paper towel to remove excess liquid and stored at -80 °C in 2ml centrifuge tubes for particulate DMSP (DMSP_p) measurement. All processes were done in triplicates.

In preparing samples for microscopy, Lugol's fixed water samples were allowed to settle following an improvised Utermöhl technique (Utermöhl, 1958). Between 50 and 100 mL of the sample were dispensed into settling chambers and cells were allowed to settle for at least 15 and up to 30 h. The overlying water was removed using pipetting, and then stored in 20 ml vials in the dark until further analysis using direct microscopic technique.

2.1.4 Optical microscopy (phytoplankton community)

Lugol's fixed water samples were allowed to settle following an improvised Utermöhl technique (Utermöhl, 1958). Between 50 and 100 mL of the sample were dispensed into settling chambers and cells were allowed to settle for at least 15 and up to 30 h. The overlying water was removed using pipetting and kept in 20 ml vials. Microalgal community cell counts were measured by adding 1 ml of fixed sample into Sedgewick rafter chamber and counting the number of algal cells using bright field microscopy (Serfling, 1949). Cells were counted with 100x, 200x and 400x magnifications using a Carl Zeiss inverted microscope. Phytoplankton were identified to the

lowest possible taxonomic level using appropriate literature (CEN, 2004) and keys for marine and freshwater environments (Tomas, 1997; Cox, 1996; Botes, 2003; Huynh & Serediak, 2006; John et al., 2003; Karlson et al., 2010). A minimum of 500 individual units were counted, leading to a counting error not exceeding 10% (Lund, 1958). Identification was limited to 14 dominant genera in >100 samples analysed.

2.1.5 Isolation of *Prymnesium* strains

P. parvum strains HIK PR1A, HIK PR6H, and HIK PR12D were isolated from the Hickling Broad during a *P. parvum* bloom in June 2017 and *P. parvum* strains WBF PRC1 and WBF PRD2 were isolated from the Woodbridge Fen Fisheries, Suffolk Broads during a suspected *P. parvum* bloom in February 2018. To do this, broad water samples (50 ml) from Hickling broad and Woodbridge Fen Fisheries were inoculated into f/2 medium-Si (100 ml, 5 PSU). Several *P. parvum* strains were picked and made monoclonal by micropipetting single cells using a fabricated glass micropipette (Fig. 2.3) and subjected through several rinses of sterile medium (Andersen, 2005) and transferred into 96 -well plates.

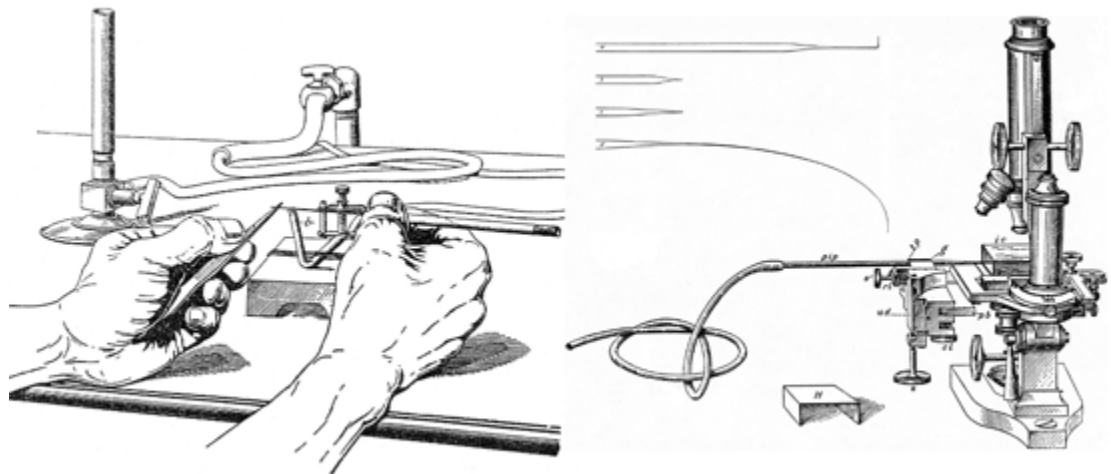


Figure 2.3. The fabrication of glass micropipette and the method of isolating individual cells of *P. parvum* from mixed algal community samples. The isolation process was carried out under a modern inverted microscope (not shown). Image adapted from Barber (1914).

Isolates were then allowed to grow for 2-3 weeks with the growth conditions detailed in 'Strains and Growth Conditions' Section 2.2.1. Isolates from enriched cultures were further made free from other contaminating picoplankton by serial dilution. Semi-axenic strains were transferred to 42-well plates and allowed to grow for approximately 2-3 weeks. Cultures were then made

axenic by treatment with multiple rounds of antibiotics (Section 2.2.1). The absence of any contaminating bacteria was confirmed by epifluorescence microscopy of culture samples stained with DAPI (Porter & Feig, 1980). Clonal cultures were then carefully transferred and up-scaled to 75 cm³ cell culture flasks (Nunc™ EasyFLASK with Filter Caps, ThermoFisher Scientific) containing 20-40 ml modified F/2 medium-Si. New *P. parvum* strains used in this study are listed in Table 2.2.

2.1.6 Isolation of bacterial strains

At the height of *P. parvum* bloom in June 2017, sampling for bacterial isolation was done to look at *P. parvum* bloom associated bacterial community. Water samples were collected into 250 ml wide mouth sterile reagent bottles obtained from station 5 (high *P. parvum* cell counts) and brought back to the laboratory for processing. 4 x 50 mL aliquots of the sample were spun down to 1 mL concentrate and a serial dilution was performed to a dilution factor of 10⁻⁵, then 100 µl of serially diluted samples were added to previously prepared agar plates. Four types of growing medium were used - LB, MB, YTSS and R2A containing mixed carbon sources, with no selective pressure other than selection for heterotrophic bacteria. Spread plates were incubated at a lower temperature of 20 °C to approximate that of the waters sampled and colonies of different morphologies were purified to single colonies.

2.2 Media and growth conditions

2.2.1 Strains and laboratory growth conditions

Non-axenic and axenic cultures of *P. parvum* CCAP 946/1B, *P. parvum* CCAP 946/6, *P. parvum* CCAP 946/1D, *P. parvum* CCAP 941/1A, *P. parvum* f. *patelliferum* CCAP 946/4, and *P. parvum* CCAP 941/6 acquired from the Culture Collection of Algae and Protozoa (CCAP) (Scottish Association for Marine Science, SAMS, Scotland) and newly isolated strains, *P. parvum* HIK PR1A, *P. parvum* HIK PR6H, *P. parvum* HIK PR12D, *P. parvum* WBF PRC1 and *P. parvum* WBF PRD2, were used in this the study (Table 2.2). All Algal cultures were grown in f/2 medium (Guillard, 1975) made with enriched seawater artificial water (ESAW) (Berges et al., 2001) or sterilised/autoclaved broad-water without adding Na₂SiO₃ at 22 °C with a light intensity of 120 µEm⁻² s⁻¹ and a light/dark cycle of 16h light/8h dark. Algal growth media were modified according to the requirements of the experimental conditions being tested. For xenic strains, cultures were

treated with multiple rounds of antibiotic treatment (streptomycin (400 µgml⁻¹), chloramphenicol (50 µgml⁻¹), gentamicin (20 µgml⁻¹) and ampicillin (100 µgml⁻¹) were added) prior to experiments.

Escherichia coli was grown in Luria-Bertani (LB) (Sambrook et al., 1989) complete medium at 37 °C. *Rhizobium leguminosarum* J391 was grown in tryptone yeast (TY) (Beringer, 1974) complete medium or RM minimal medium (with 10 mM succinate as carbon source and 10 mM NH₄Cl as nitrogen source) at 28 °C. *Labrenzia aggregata* J571 (Curson et al., 2017) was grown in YTSS (Gonzalez et al., 1996) complete medium or MBM (Baumann & Baumann, 1981) minimal medium (with 10 mM succinate as carbon source and 10 mM NH₄Cl as nitrogen source) at 30 °C. Where necessary, antibiotics were added to bacterial cultures at the following concentration: streptomycin (400 µg ml⁻¹), kanamycin (20 µg ml⁻¹), spectinomycin (200 µg ml⁻¹), gentamicin (20 µg ml⁻¹), ampicillin (100 µg ml⁻¹). Strains used in this study are listed in Table 2.2.

Table 2.2. List of strains and plasmids used in this study.

Strain/Plasmid	Description	Reference
<i>Prymnesium parvum</i> CCAP946/1B	<i>Prymnesium</i> strain used for growth experiments to determine intracellular DMSP concentration and <i>DSYB</i> expression under standard conditions and different environmental conditions	CCAP Culture Collection; Isolated at River Blackwater, Essex, United Kingdom by Butcher (1952)
<i>Prymnesium parvum</i> CCAP946/6	<i>Prymnesium</i> strain used for growth experiments to determine intracellular DMSP concentration and <i>DSYB</i> expression under standard conditions and different environmental conditions	CCAP Culture Collection; Isolated at Millport, Isle of Cumbrae, United Kingdom by Droop (1953)
<i>Prymnesium parvum</i> CCAP946/1D	<i>Prymnesium</i> strain used for growth experiments to determine intracellular DMSP concentration and <i>DSYB</i> expression under standard conditions and different environmental conditions	CCAP Culture Collection; Isolated at Nir-David, North District, Israel by Reich (1953)
<i>Prymnesium parvum</i> CCAP941/1A	<i>Prymnesium</i> strain used for growth experiments to determine intracellular DMSP concentration and <i>DSYB</i> expression under standard conditions and different environmental conditions	CCAP Culture Collection; Isolated at River Stour, Essex, United Kingdom by Butcher (no date specified)

<i>Prymnesium parvum</i> f. <i>patelliferum</i> CCAP946/4	<i>Prymnesium</i> strain used for growth experiments to determine intracellular DMSP concentration and <i>DSYB</i> expression under standard conditions and different environmental conditions	CCAP Culture Collection; Isolated at West End of Fleet, Dorset, England by Hibberd (1976)
<i>Prymnesium parvum</i> CCAP941/6	<i>Prymnesium</i> strain used for growth experiments to determine intracellular DMSP concentration and <i>DSYB</i> expression under standard conditions and different environmental conditions	CCAP Culture Collection; Isolated at River Stour, Essex, United Kingdom by Butcher (no date specified)
<i>Prymnesium parvum</i> HIK PR1A (New Strain)	<i>Prymnesium</i> strain used for RNA sequencing, growth experiments to determine intracellular DMSP concentration and <i>DSYB</i> expression under standard conditions and different environmental conditions, Toxin Profiling	This Study; Isolated at Hickling Broad, Norfolk, United Kingdom by Rivera (2017)
<i>Prymnesium parvum</i> HIK PR6H (New Strain)	<i>Prymnesium</i> strain used for growth experiments to determine intracellular DMSP concentration and <i>DSYB</i> expression under standard conditions and different environmental conditions and Toxin Profiling	This Study; Isolated at Hickling Broad, Norfolk, United Kingdom by Rivera (2017)
<i>Prymnesium parvum</i> HIK PR12D (New Strain)	<i>Prymnesium</i> strain used for growth experiments to determine intracellular DMSP concentration and Toxin Profiling	This Study; Isolated at Hickling Broad, Norfolk, United Kingdom by Rivera (2017)
<i>Prymnesium parvum</i> WBF PRC1 (New Strain)	<i>Prymnesium</i> strain used for growth experiments to determine intracellular DMSP concentration and Toxin Profiling	This Study; Isolated at Woodbridge Fisheries, Suffolk, United Kingdom by Rivera (2018)
<i>Prymnesium parvum</i> WBF PRC2 (New Strain)	<i>Prymnesium</i> strain used for growth experiments to determine intracellular DMSP concentration and Toxin Profiling	This Study; Isolated at Woodbridge Fisheries, Suffolk, United Kingdom by Rivera (2018)
<i>Prymnesium parvum</i> PLY 94A	<i>Prymnesium</i> strain used for growth experiments to determine intracellular DMSP concentration under standard conditions and different environmental conditions and toxin profiling	MBACC; Isolated at English Bay, British Columbia, Canada (no specified date)
<i>Prymnesium parvum</i> f. <i>patelliferum</i> PLY 527D	<i>Prymnesium</i> strain used for growth experiments to determine intracellular DMSP concentration under standard conditions and	MBACC; Isolated at North of Büsum, North Sea, Germany (no specified date)

	different environmental conditions and toxin profiling	
<i>Escherichia coli</i> 803	Strain used for routine transformations	Wood (1966)
<i>Escherichia coli</i> JM101	Strain for expression of <i>lacZ</i> gene in blue-white screen	Yanisch-Perron <i>et al.</i> (1985)
<i>Escherichia coli</i> 803 containing pRK2013	Helper strain used for routine conjugations	Figurski and Helinski (1979)
<i>Rhizobium leguminosarum</i> J391	Streptomycin-resistant derivative of wild type strain 3841 used for expression of genes cloned in plasmid pLMB509 or pRK415	Young <i>et al.</i> (2006)
<i>Labrenzia aggregata</i> J571	<i>Labrenzia aggregata</i> LZB033 with mutation in <i>dsyB</i> gene	Curson <i>et al.</i> (2017)
<i>Labrenzia aggregata</i> J572	<i>Labrenzia aggregata</i> LZB033 with mutation in <i>dddL</i> gene	Curson <i>et al.</i> (2015)
<i>Ruegeria pomeroyi</i> DSS-3	<i>Ruegeria pomeroyi</i> DSS-3 strain used for positive control in DMSP catabolism	Todd <i>et al.</i> (2012)
pLMB509	Plasmid vector for taurine-inducible expression of cloned genes in <i>Rhizobium</i>	Tett <i>et al.</i> (2012)
pRK415	Wide host-range plasmid vector with IPTG-inducible <i>lac</i> promoter	Keen <i>et al.</i> (1988)
pRK2013	Helper plasmid used in triparental matings	Figurski and Helinski (1979)
pEX-K4	Plasmid vector containing synthesized genes	Eurofins Genomics
pBIO2275	<i>Prymnesium parvum</i> CCAP 946/6 <i>DSYB</i> cloned in pRK415	Curson <i>et al.</i> (2018)
pBIO2358	<i>Prymnesium parvum</i> HIK PR1A <i>DSYB</i> , amplified from cDNA, cloned in pRK415	This Study
pBIO2359	<i>Prymnesium parvum</i> HIK PR1A <i>DSYB</i> , codon-optimised, synthesised and cloned in pLMB509	This Study
pBIO2360	<i>Prymnesium parvum</i> HIK PR1A <i>Alma</i> -like gene, codon-optimised, synthesised and cloned in pLMB509	This Study

2.2.2 *Prymnesium* non-standard growth conditions

Standard algal growth conditions were set at temperature of 22 °C, light intensity of 120 $\mu\text{E m}^{-2} \text{s}^{-1}$, salinity of 35 practical salinity units (PSU), nitrogen concentration of 882 μM and phosphorus concentration of 36.2 μM . For increased and decreased salinity, the amount of salts added to the artificial seawater were adjusted to give a salinity of 5, 10, 35, and 50 PSU. For increased (High N or HN) or decreased (Low N or LN) nitrogen cultures, the f/2 medium was adjusted to contain 8820 μM (1000% of standard f/2) or 44.1 μM (5% of standard f/2), respectively. For H_2O_2 experiments, 0.25 mM, 0.75 mM or 2 mM of H_2O_2 were added to the cultures and samples were taken immediately before the addition of H_2O_2 , after 0.5-hour, 1 hour, and after 3 hours of treatment.

2.2.3 Sample preparation from cultures

For *Prymnesium* cultures: Sample for RNA/DNA extraction was obtained by filtering 50-100 ml of *Prymnesium* culture onto 47 mm 1.2 μm RTTP polycarbonate filters (Fisher Scientific, UK), and filters were stored in 2 mL centrifuge tubes, flash-frozen with liquid nitrogen, and stored at -80 °C in 2 ml centrifuge tubes until further processing.

For bacterial cultures: Sample for RNA/DNA extraction was obtained by centrifuging 1-2 mL overnight grown culture onto a microcentrifuge tube at maximum speed for 2 minutes. The supernatant was discarded and bacterial pellet was either processed immediately for nucleic acid extraction or flash frozen with liquid nitrogen and at -80 °C in 2 ml centrifuge tubes until further processing.

To obtain samples for DMSP measurement in *Prymnesium* by Gas Chromatography (GC), 30-50 ml of culture was filtered onto 47 mm GF/F glass microfiber filters (Fisher Scientific, UK) using a Welch WOB-L 2534 vacuum pump, and filters were then blotted on paper towel to remove excess liquid and stored at -20 °C in 2 ml centrifuge tubes for particulate DMSP measurement. All processes were done in triplicates.

To obtain samples for Prymnesin detection and characterisation in *Prymnesium* by Liquid Chromatography Mass Spectrometry (LC-MS), biomass from 150 ml algal culture was harvested by centrifugation (4000 \times g for 5 minutes) and the supernatant was discarded. The cells were

suspended in cold acetone (2 mL, -20 °C) and subjected to vortex mixing for two minutes. The resulting suspensions were then centrifuged at 30,000 × g for 5 minutes. The supernatant was discarded, and the pellets were subjected to two more cycles of the same acetone wash procedure. The cell pellets were then resuspended in methanol (MeOH, 2 mL) and vortex mixed for two minutes, after which time the cell debris was pelleted by centrifugation (30,000 × g for 5 minutes) and the supernatant was collected. This methanol extraction was repeated two more times, followed by three rounds of analogous extraction using n-propanol (n-PrOH). The MeOH and n-PrOH extracts were combined, dried in vacuo (Speed VAC, Vacuum Centrifuge Concentrator) and stored at -20 °C until further use.

2.2.4 Algal cell counting and PAM fluorometry

To monitor and quantify the growth of algal cultures, samples were removed and diluted (dependent on the level of growth) in artificial seawater (ESAW), and cell counting was done using a CASY model TT cell counter (Sedna Scientific). The effect of stress on potential maximum quantum yield of photosystem II was monitored by measuring Fv/Fm values (Butler, 1978) using a Pulse-Amplitude Modulation (PAM) fluorometer (WATER-PAM, Heinz Walz, Germany) (Schreiber et al., 1986; Bramucci et al., 2015). All PAM measurements were done at the same time when samples were taken for cell counting and measured as much as possible at the beginning of the light cycle. Samples were diluted in sterile ESAW medium and adjusted within the detection range of the PAM fluorometer. Samples were maintained at 21°C or ambient temperature throughout handling. A dark adaption period of 5 min was used before a saturating pulse was applied. The fluorescence readings were taken in triplicate at intervals of 1 min 30 s to calculate the minimal dark fluorescence (F0), the maximum dark fluorescence (Fm), and the photosystem II (PSII) maximum efficiency (Fv/Fm), $Fv/Fm = (Fm - F0)/Fm$ (Schreiber et al., 1986; Baker, 2008). Triplicate readings of each sample were averaged to determine the maximum quantum efficiency.

2.3 Nucleic acid extraction

2.3.1 Environmental DNA and RNA extraction and purification

Environmental DNA samples were extracted using a modified sodium dodecyl sulfate (SDS)-based protocol (Burgmann et al., 2003). The pelleted biomass was added to a 2.0 ml screw-cap

tube of Lysing matrix E beads (MP Biomedicals UK) and mixed with 60 μl of 10% (w/v) SDS extraction buffer. Cells were lysed in a FastPrep instrument (MP Biomedicals UK) for 2 x 30s at 6.0 ms^{-1} and supernatants were extracted twice using phenol:chloroform:isoamyl alcohol (25:24:1) and chloroform:isoamyl alcohol (24:1). Nucleic acids were precipitated with either ice-cold isopropanol or polyethylene glycol (PEG) 6000 solution (20%) and dissolved in 100 μl of nuclease-free water (Ambion, Thermo Fisher Scientific).

Total environmental RNA extraction was performed on frozen pelleted samples by directly adding 1 mL of prewarmed (65°C) TriReagent (Life Technologies) or Trizol Reagent (Sigma-Aldrich), followed by Lysing matrix E beads (MP Biomedicals UK). Cells were disrupted using an MP FastPrep instrument set at maximum speed for $3 \times 30 \text{ s}$. Following a 5 min recovery time at room temp, samples were centrifuged at $13,000 \text{ g}$, 4°C , for 2 min. The supernatant was transferred to a 2 ml screwcap tube containing 1 ml 95% ethanol and RNA was extracted using a Direct-zol RNA MiniPrep kit (Zymo Research, R2050), according to the manufacturer's specifications. Extracted RNA was DNase treated with TURBO DNA-free DNase (Ambion, Thermo Fisher, UK) according to the manufacturer's protocol. The absence of DNA in RNA samples was confirmed by PCR using 16S primers 27F and 1492R (Lane et al., 1985, Table 2.3).

All environmental DNA and RNA samples were quantified using a NanoDrop 2000 UV-Vis Spectrophotometer (Thermo Scientific) or a Qubit RNA/DNA HS assay kit (Thermo Fisher Scientific). RNA integrity is further assessed using an automated electrophoresis system, Experion™ (Bio-Rad Laboratories). RNA extracts from environmental samples were further reverse transcribed with random hexamer primers (Invitrogen) and M-MLV reverse transcriptase (Promega) for 16S rRNA amplicon sequencing, qPCR and RT-qPCR.

2.3.2 Bacterial DNA extraction and purification

DNA was extracted from bacterial cultures by either using a modified SDS-based protocol detailed in the previous section (Section 2.3.1) or by using a modified phenol-chloroform method. For modified phenol-chloroform protocol: the bacterial pellets were resuspended in 250 μl Buffer P1, mixed by inversion with 250 μl Lysis Buffer P2, and 350 μl Neutralization Buffer P3 (Qiagen Buffers, Qiagen) immediately after. Samples were left on ice for up to 5 minutes, and then centrifuged for 10 minutes at maximum speed. The supernatant was removed to a clean microcentrifuge tube, mixed with 400 μl Phenol:Chloroform:Isoamyl Alcohol 25:24:1 (v/v) and

vortexed for 5 – 10 seconds until the mixture was homogenised. Samples were centrifuged for 2 minutes at maximum speed, and the top aqueous layer was removed to a new microcentrifuge tube, to which 800 µl of 100% ice-cold ethanol was also added. Tubes were mixed by inversion and spun for 10 minutes at maximum speed. The supernatant was discarded, and 500 µl of 70% ethanol was added over the pellet. Samples were once again spun for 2 minutes at maximum speed, and the ethanol removed. The pellet was air-dried for 20-30 mins before being resuspended in 50-100 µl nuclease-free water (Ambion, Thermo Fisher Scientific). DNA was quantified with a Nanodrop spectrophotometer (Thermo Scientific) and stored at -20 °C until further analysis.

2.3.3 *Prymnesium* RNA extraction and purification

RNA extraction from *Prymnesium* culture samples was performed on frozen pelleted or filtered samples by directly adding 1 mL of prewarmed (65°C) TriReagent (Life Technologies) or Trizol reagent (Sigma-Aldrich), followed by Lysing matrix E beads (MP Biomedicals UK). *Prymnesium* cells were disrupted using an MP FastPrep-24 instrument set at maximum speed for 3 cycles of 30 s. Following a 5 min recovery time at room temp, samples were centrifuged at 13,000 g, 4 °C, for 2 min. The supernatant was transferred to a 2 ml screwcap tube containing 1 ml 95% ethanol and RNA was extracted using a Direct-zol RNA MiniPrep kit (Zymo Research, R2050), according to the manufacturer's specifications. Genomic DNA was removed by treating samples with TURBO DNA-free DNase (Ambion) according to the manufacturer's protocol. The absence of DNA in RNA samples was confirmed by PCR using 16S rDNA primers. RNA was quantified with a Nanodrop spectrophotometer or a Qubit RNA HS assay kit (Thermo Fisher Scientific).

2.4 *Prymnesium* whole transcriptome sequencing

Cultures of newly isolated *P. parvum* HIK PR1A grown on high salinity (to induce DMSP synthesis genes) were harvested at mid-exponential phase by centrifugation at 6,000 rpm. Total RNA extraction was performed using the method detailed above (Section 2.3.3). RNA was quantified using a Qubit 3.0 Fluorometer, following the protocol of the Qubit Broad Range RNA Assay Kit (Thermo Fisher Scientific), and was stored at -80 °C until needed. Total RNA integrity and cRNA target size distribution were assessed using the Experion™ Automated Electrophoresis System (Bio-Rad Laboratories, UK). Purified high quality RNA samples were then sent to Luxembourg Center for Systems Biomedicine (LCSB) Sequencing Platform, University of Luxembourg for

library construction and RNA sequencing. The final library was subsequently loaded to a 500-cycle MiSeq reagent cartridge for sequencing by using MiSeq (Illumina) platform having sequenced runs of 2 × 150 paired-end reads.

2.5 16S rRNA gene amplicon sequencing (environmental samples)

Pooled biological replicates of DNA and cDNA samples from bloom (April 2015) and non-bloom (September 2016) samples, were selected for 16S rRNA/rDNA amplicon sequencing. The primer set 515F/806R of the V4 hypervariable region of the 16S rRNA gene (Caporaso et al., 2012) was used for amplification. These primers provide sufficient resolution for the taxonomic classification of microbial sequences. Amplification and amplicon sequencing were performed by MR DNA (Shallowater, TX, USA). Sequencing was performed on a MiSeq system (300bp paired-end) according to manufacturer instructions, obtaining between 106k-257k reads per sample with an average length of 300 bp. The resulting datasets were analysed by sequence analysis and phylogenetic classification using QIIME 1 (Caporaso et al., 2010). 16S Amplicon Sequencing data was provided by Dr. Jennifer Pratscher.

2.6 *In silico* sequence analysis

2.6.1 Identification of *DSYB* and *Alma*-like genes in *P. parvum*

De novo reconstruction of transcriptome from RNA-seq data was performed using Trinity platform (Haas et al., 2013) and fasta file database was created by Dr. Simon Moxon. To search for *DSYB* and *Alma*-like gene sequences in the HIK PR1A transcriptome assembly, local BlastP searches was done on fasta file database and probed using a curated *DSYB* protein sequence from *P. parvum* as published in Curson et al. (2018) and ALMA family protein sequences in *E. huxleyi* as reported in Alcorombi et al. (2015).

2.6.2 Sequence optimization and gene synthesis

Identified *DSYB* and *Alma*-like genes selected to be synthesised were codon-optimised for expression in *E. coli* and modified to avoid the presence of XbaI, NdeI and EcoRI within their

sequences using Invitrogen GeneArt®. Genes were synthesised either using the facilities provided by the John Innes Centre (JIC) or through Eurofins Genomic Services.

2.6.3 Primer design for PCR, qPCR and RT-PCR

Primers for qPCR and RT-qPCR (Table 2.3) were designed, using Primer3Plus (Untergasser et al., 2012) to amplify a 100-150 bp region, with an optimum melting temperature of 60° C. Melting temperature difference between primers in a pair was 2° C and GC content was kept between 40% and 60%. The primer pairs were checked to avoid stable homo- and heterodimers as well as hairpin structures using the IDT (Integrated DNA Technologies) Oligoanalyzer 3.1 tool (<https://www.idtdna.com/calc/analyzer>). Primer efficiencies were all 90–110% and within recommended limits.

Primers for PCR amplification of full-length *DSYB* from *P. parvum* cDNA were designed and codon optimised to be expressed in *E. coli* using the same process as above but with the insertion of restriction sites, Ribosomal Binding Site (RBS) sequence and Pribnow box upstream of the start codon. All oligonucleotide primers were synthesized by Eurofins Genomics.

Table 2.3. List of oligonucleotide primers used in this study.

Primer Name	Sequence (5' to 3')	Use
PpDSYBp1	AAGGGATCCGAAAGGAGATATAATGCTGCG CCTCGCCCCTCG	Cloning of <i>P. parvum</i> HIK PR1A <i>DSYB</i> into pRK415 for pBIO2358
PpDSYBp2	ATATAGGTACCTTATGGTTTGAAGCGACG ATGA	Cloning of <i>P. parvum</i> HIK PR1A <i>DSYB</i> into pRK415 for pBIO2358
qParv_1_F	CTCAACATCGACGAGCTCAA	qPCR and RT-qPCR amplification of <i>P. parvum</i> HIK PR1A <i>DSYB</i>
qParv_1_R	GTTGGGCGAGAGAGTGTACC	qPCR and RT-qPCR amplification of <i>P. parvum</i> HIK PR1A <i>DSYB</i>
PrymF	TGTCTGCCGTGGACTTAGTGCT	qPCR amplification of <i>P. parvum</i> ITS2 region from Zamor et al. (2012)
PrymR-3	ATGGCACAACGACTTGGT	qPCR amplification of <i>P. parvum</i> ITS2 region from Zamor et al. (2012)
dmdAUF160	GTICARITITGGGAYGT	qPCR amplification of bacterial <i>dmdA</i> gene in environmental samples from Varaljay et al. (2010)

dmdAUR697	TCIATICKITCIATIAIRTTDGG	qPCR amplification of bacterial <i>dmdA</i> gene in environmental samples from Varaljay et al. (2010)
DddPUf	ATGTTCCGACCCGATGAACathmgntaygc	qPCR amplification of bacterial <i>dddP</i> gene in environmental samples from Liu et al. (2018)
DddPUr	CCGCACTCCTGGAACcanggrtngt	qPCR amplification of bacterial <i>dddP</i> gene in environmental samples from Liu et al. (2018)
27F	AGAGTTTGATCCTGGCTCAG	Forward primer used to amplify the 16S rRNA gene
1492R	GGTACCTTGTACGACTT	Reverse primer used to amplify the 16S rRNA gene
Euk_A	AACCTGGTTGATCCTGCCAGT	Forward primer used to amplify the 18S rRNA gene for identification from <i>P. parvum</i>
Euk_B	TGATCCTTCTGCAGGTTACCTAC	Forward primer used to amplify the 18S rRNA gene for identification from <i>P. parvum</i>

* Restriction sites included in primers for cloning are underlined

2.7 Quantitative polymerase chain reaction (qPCR)

2.7.1 *Prymnesium* ITS2 copy numbers in field samples

To study the abundance of *P. parvum* internal transcribed spacer (ITS2) copies in broad waters, real-time qPCR method previously described by Galluzzi et al. (2008) and qPCR primers PrymF and PrymR-3 (Table 2.3) used by Zamor et al. (2012) were optimised and utilised.

2.7.2 Reverse transcription reaction

Complementary DNA or cDNA was synthesised from RNA samples by reverse transcription of 1 µg DNA-free RNA using the QuantiTect Reverse Transcription Kit (QIAGEN) following manufacturers protocol. No reverse transcriptase and no template controls were performed to confirm that samples were DNA-free and that the reactions were free of contaminants.

2.7.3 *DSYB* abundance (qPCR) and transcription (RT-qPCR)

To study *P. parvum DSYB* abundance and transcription in laboratory and broad-water samples, qPCR Primers were designed as discussed in detail in section 2.6.3 and listed Table 2.3.

2.7.4 qPCR and RT-qPCR analyses

Quantitative PCR was performed with a StepOnePlus instrument (Applied Biosystems) equipped with a CFX96 Real-time PCR detection system (BioRad), using a standard SensiFAST SYBR Hi-ROX Kit (Bioline) as per the manufacturer's instructions for a three-step cycling program. The 25 μL reaction mixture contained 12.5 μL of SYBR[®] Green JumpStart™ Taq ReadyMix™ (Merck), 0.15 μM of each primer, 200 ng BSA ml^{-1} , 3.0 mM MgCl_2 , and 2.0 μL template DNA and cDNA. Gene abundance/expression measurement for each sample was performed using three biological replicates, each with three technical replicates. Control DNA consisted of pGEMT-Easy (Promega) containing the fragment created by the RT-qPCR primer pair for each gene tested (made through PCR on synthesized cDNA, cloning in *E. coli* 803 and purifying using a Miniprep Kit (Qiagen)). For each gene, the cycle threshold (C_T) values of the technical and biological replicates were averaged and manually detected outliers were excluded from further analysis. Standard curves of control DNA were calculated from five points of 1:10 serial dilutions. The efficiency for qPCR and RT-qPCR assay was 98%.

2.7.5 Post-run analysis

Analysis of the melting temperatures were performed. For each condition and gene, the cycle threshold (C_t) values of the technical and biological replicates were averaged. Analysis of the post-run melting curve was also performed. Manually detected outliers were excluded from further analysis.

2.8 Genetic manipulations

2.8.1 *In vitro* genetic manipulation

2.8.1.1 Polymerase chain reaction (PCR)

Genes were amplified using polymerase chain reaction (PCR) in a Thermal Cycler using either standard 25 µl or 50 µl PCR mixes. Standard 25 µl PCR mixes contained 12.5 µl MyFi™ DNA Polymerase (enzyme/buffer/dNTPs/DMSO), 0.5 µl template (50–100 ng), 0.5 µl of 20 pmol of F and R primers and 11 µl nuclease-free H₂O. For larger reaction volumes, the components were adjusted proportionally. Oligonucleotide primers used in this study were synthesised by Eurofins Genomics (Table 2.3). To amplify genes from *Prymnesium*, complementary DNA (cDNA) was used as template. DNA was also amplified from bacterial colonies were also amplified. For colony PCR, a sterile toothpick was used to gently touch a colony, the toothpick was introduced into PCR tube containing 20 µl sterile water. The tube was microwaved for 10 seconds, and 1 µl aliquot of the lysed mixture was diluted in 10 µl sterile water and used in PCR mixture/reaction.

2.8.1.2 Agarose gel electrophoresis

Products from PCR amplifications were visualised using gel electrophoresis. Gels were made to 1 – 1.5% (w/v) agarose using 1 x TAE Buffer (Tris-Acetate-EDTA 50 x stock: 242 g Tris base, 57.1 ml glacial acetic acid, 100 ml 500 mM EDTA (pH 8.0), water to 1 liter. A 1 x solution contains 40mM Tris, 20 mM acetic acid, and 1 mM EDTA), melted/dissolved and cooled to 50°C before adding 3-5 µl Ethidium Bromide (EtBr, 10 mg/ml) and pouring into gel trays to solidify. Samples were loaded into wells alongside a 1 KB Plus DNA ladder (Invitrogen) for size reference. Gels were typically run at 80 V for 60-90 minutes, and the separation of DNA fragments was visualised using a UV gel imaging Doc System (BioRad).

2.8.1.3 PCR purification protocol

PCR products were recovered and purified using the Roche High Pure PCR Product Purification Kit following manufacturer's instructions or user manual. The purified PCR product was eluted from the column using 50 µl sterile water, collected in a 1.5 ml microcentrifuge tube.

2.8.1.4 Gel extraction protocol

DNA fragment/band was excised from the agarose gel using sterile razor blade under UV illuminator. The sliced gel fragment was placed in a labeled microfuge tube. Subsequent, DNA extraction was carried out using the QIAquick Gel Extraction (QIAGEN) kit following the manufacturer's instructions. Dissolved gel samples are precipitated with an equal volume of isopropanol and 10 µl of 3 M Sodium acetate. DNA was eluted using 30 – 50 µl of sterile nuclease-free water collected in a 1.5 ml microcentrifuge tube. DNA sample was stored at -20 °C until further processing.

2.8.1.5 Cloning into pRK415 and pLMB509

PCR amplified gene from cDNA and synthesised genes in plasmids were cloned or subcloned into pRK415 and pLMB509, respectively. Oligonucleotide primers used for molecular cloning were synthesized by Eurofins Genomics (Table 2.3). Routine restriction digestions and ligations for cloning were performed as described in Downie et al. (1983). Sequencing of plasmids and PCR products was performed by Eurofins Genomics.

The PCR amplified *DSYB* gene from *P. parvum* HIK PR1A complementary DNA was cloned into the isopropylthiogalactoside (IPTG)-inducible wide host range expression plasmid pRK415 (Keen et al., 1988). Synthesised *DSYB* and *Alma*-like genes from *P. parvum* HIK PR1A were subcloned into pLMB509 (Tett et al., 2012), a taurine-inducible plasmid. All cloned genes were expressed in *Rhizobium leguminosarum* and *Labrenzia aggregata*. Restriction enzymes used were NdeI, Acc651 or EcoRI. All plasmid clones are described in Table 2.2.

2.8.1.6 pGEM-T Easy cloning

The pGEM-T Easy Vector System (Promega) was utilised for creating clone libraries and standards for qPCR. Fragments to be cloned were amplified using PCR and then purified by either PCR purification kit or gel extraction. Ligations were set up after calculating the appropriate volumes of PCR products using the insert:vector molar ratio 1:3. The equation below was used to calculate the volumes:

$$\frac{\text{ng of vector (50 ng)} \times \text{kb size of insert}}{\text{kb size of vector (3 kb)}} \times 3 = \text{ng insert}$$

A standard ligation mix consisted of 5 μ l 2X Rapid Ligation Buffer, 1 μ l pGEM-T Easy Vector (50 ng), X μ l PCR product, 1 μ l T4 DNA ligase (3 Weiss units/ μ l) and nuclease - free water to reach a final volume of 10 μ l. Positive controls were also set up with 2 μ l control insert DNA (provided in the kit) in the place of the PCR product. Reactions were mixed well and incubated overnight at 4 °C. Ligations were transformed by heat shock into *E. coli* JM101 competent cells as described below, with 5 μ l ligation added to 100 μ l competent cells, alongside controls. Transformed cells were plated on LB/ampicillin/IPTG/X-Gal agar plates, with 100 μ l of the ligation on one plate, and the rest on the other plates including the positive control and negative control cells. Plates were incubated overnight at 37 °C and then checked for successful cloning using a blue-white screening, where white colonies have the *lacZ* gene successfully disrupted. These are picked and checked using restriction digests or PCR.

2.8.2 *In vivo* genetic manipulation

2.8.2.1 Competent cells preparation

A small volume (5 ml LB) starter culture was prepared by inoculating with *E. coli* (803/JM101) and incubated overnight at 37 °C. This was then inoculated in a 1:100 dilution to 100 ml LB and incubated at 37 °C, 200 rpm for 2 – 3 h (until it reached OD₆₀₀ 0.2 – 0.4). The culture was transferred into 2 x 50 ml sterile falcon tubes, and cells were retrieved using a pre-cooled centrifuge at 4 °C, spinning at 4000 rpm for 10 minutes. Falcon tubes containing pellets were carefully transferred and kept on ice and the supernatant was decanted or removed. Both pellets were carefully mixed with 10 ml ice cold 0.1M CaCl₂ and left on ice for 1 hour. The mix was again centrifuged as before, and the supernatant removed. The pellets were resuspended in 2 ml of ice cold 0.1M CaCl₂. Cells were left on ice for at least 3 h prior to cell transformations or stored overnight in the fridge.

2.8.2.2 Heat shock transformations

50 to 100 ng of recombinant plasmid DNA was added to 100 μ l competent *E. coli* cells and incubated on ice 1 h. A tube containing cells with no DNA added was used as negative control. Samples were heat shocked at 42 °C for 3 minutes and transferred to ice for 5 minutes. 500 μ l LB was added to the cells and incubated at 37 °C for 60 – 90 minutes. Cells were plated on LB agar

containing ampicillin ($100 \mu\text{g ml}^{-1}$). For molecular cloning IPTG and X-gal was also added to the medium and white/blue screening was performed.

2.8.2.3 Conjugation by triparental mating

Tri-parental mating was utilised to transfer plasmids from transformed *E. coli* to *Rhizobium leguminosarum* or *Labrenzia aggregata* by conjugation. The donor strain of *E. coli* that contains the plasmid conjugate into the Host strain, through the kanamycin-resistant *E. coli* strain 803 (pRK2013) helper strain (Figurski & Helinski, 1979). To do this, recombinant plasmid containing *E. coli*, helper plasmid pRK2013 containing *E. coli* and the heterologous host *R. leguminosarum* or *L. aggregata* were mixed in rich TY (*R. leguminosarum*) or YTSS (*L. aggregata*) media plates. Control crosses were also set up with just the helper and host, and just the donor and helper. Plates were incubated overnight at 28 °C. The bacteria mix was then plated on fresh TY or YTSS media plates containing selective antibiotics and incubated at 28 °C for 2-3 days. Successful crosses were checked and confirmed using colony PCR.

2.8.2.4 Plasmid extractions from Minipreps/Midipreps

For Minipreps: Plasmid DNA was extracted from overnight 2-3 mL cultures at 28 – 37°C (depending on bacterial cells), using the QIAprep Spin Miniprep Kit (QIAGEN) following manufacturer's instructions. Around 30 - 50 μl nuclease-free water was added to the spin column to elute the purified plasmid DNA. Concentration was quantified by nanodrop and plasmid was stored at - 20°C. Plasmids used in this study are listed in Table 2.2.

For Midipreps: High concentration plasmid DNA was extracted from 100 ml culture using the Plasmid Midiprep kit (QIAGEN), with the QIAGEN-tip 100 column following user's instructions. In brief, DNA was eluted from the column using 5 ml Buffer QF. To precipitate DNA 3.5 ml of room-temperature isopropanol was added to the eluted DNA and mixed. The mixture was separated into 1.5 microcentrifuge tubes and centrifuged immediately at maximum speed for 30 minutes. The supernatant was discarded and the DNA pellets washed with 500 μl 70% ethanol, centrifuging at maximum speed for 10 minutes. The ethanol was removed, and the DNA pellet left to 'air-dry' for 5 - 10 minutes, then re-dissolved in 100 - 150 μl of nuclease-free water. Concentration was quantified by nanodrop, and plasmid was stored at – 20 °C.

2.8.2.5 Restriction digests (FastDigest enzymes)

Digestions of DNA were carried out using Thermo Scientific FastDigest restriction enzymes. Up to 16 μl of DNA (depending on concentration), 1 μl Enzyme 1, 1 μl Enzyme 2, 2 μl FastDigest Buffer and distilled water were mixed in a microcentrifuge tube to a total mix volume of 20 μl . The mixture was incubated at 37 °C for up to 30 minutes, and then inactivated by incubation at either 65 °C or 80 °C for 5 or 20 minutes. If necessary, the DNA digest was dephosphorylated by adding 1 μl alkaline phosphatase, 2.5 μl of buffer and 1.5 μl nuclease-free water and incubated for up to 60 minutes. Digested DNA was then visualised on a 1% agarose gel, and the correct sized fragment was extracted.

2.9 Metabolite analysis

2.9.1 Quantification of DMSP

To measure DMSP by gas chromatography (GC) assays, headspace DMS produced either directly by the sample or by the alkaline lysis of DMSP was measured. All DMSP measurements were performed using a gas chromatograph equipped with flame photometric detector - GC-FPD (Agilent 7890A GC fitted with a 7693 autosampler) fitted with an HP-INNOWax 30 m x 0.320 mm capillary column (Agilent Technologies J & W Scientific) containing Poropack-Q and using nitrogen as the carrier gas (flow rate, 30 ml/min) at 200°C. All measurements on the GC were performed using 2 ml glass serum vials containing 300 μl liquid samples and sealed with PTFE/rubber crimp caps. For the measurement of DMSP in culture, 200 μl culture was added into a 2 ml glass vial and DMSP was alkaline lysed to DMS with the addition of 100 μl of 10 M NaOH and immediately crimp-sealed. For the measurement of DMSP in methanolic extracts, an aliquot of 200 μl of the extract was added into a 2 ml glass vial and 100 μl of 10 M NaOH was added and serum vial was immediately crimped. All crimp-sealed serum vials were incubated at 22°C overnight in the dark before subjecting to GC assays to ensure complete alkaline lysis of DMSP. An 8-point calibration curve was produced by alkaline lysis of DMSP standards in 100% methanol to check the consistency and accuracy of the assay (Fig. 2.4). The detection limit for headspace DMS was 0.15 nmol in MeOH. DMSP used as standard was synthesized from DMS (Sigma-Aldrich) as described in (Todd et al., 2010).

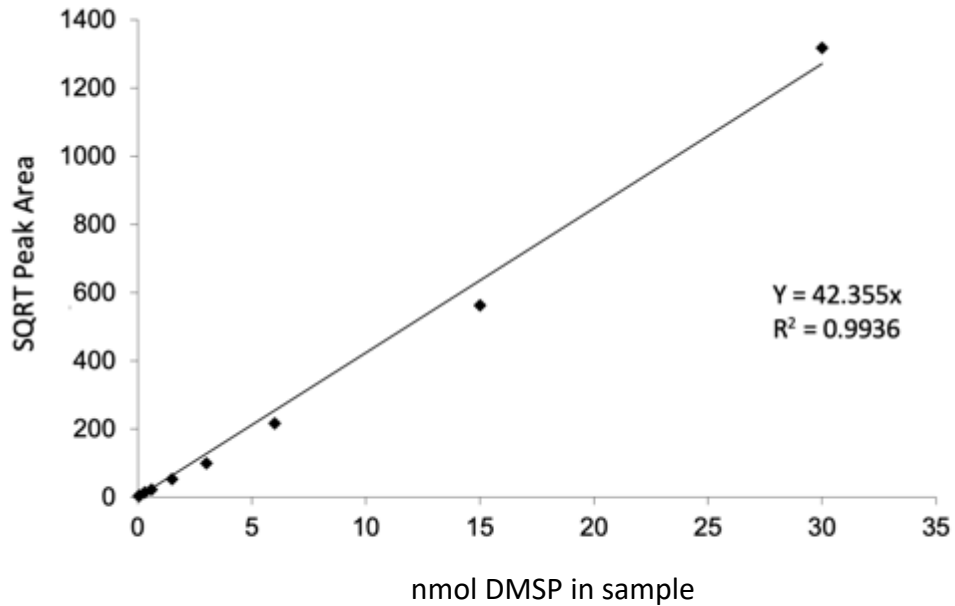


Figure 2.4. Calibration curve used to calculate DMSP concentrations in samples from DMS released via alkaline lysis. The curve was produced using known concentrations of DMSP ranging from 0.15 nmol to 30 nmol in 200 μ l MeOH added with 100 μ l 10M NaOH then incubated overnight in the dark.

2.9.2 LC-MS detection of toxins

Analysis of the *Prymnesium* Toxins was performed using an LC-MS on a Synapt G2-Si mass spectrometer coupled to an Acquity UPLC system (Waters, Manchester, UK) at the John Innes Center (JIC) with the help of Dr. Gerhard Saalbach and Dr. Carlo de Oliveira-Martins. The extracts were first dissolved into 1000 μ l of 50% EtOH. 7 μ l aliquots of samples were injected onto an Acquity UPLC® BEH C18 column, 1.7 μ m, 1 x 100 mm (Waters) and eluted with a gradient of 1-60% acetonitrile in 0.1% formic acid in 6 min at a flow rate of 0.08 ml min⁻¹ with a column temperature of 45°C. The mass spectrometer was controlled using Masslynx 4.1 software (Waters) and operated in positive MS-ToF and resolution mode with a capillary voltage of 3 kV and a cone voltage of 40 V in the m/z range of 100-2000. Leu-enkephalin peptide (0.25 μ M, Waters) was infused at 10 μ l min⁻¹ as a lock mass and measured every 30 s.

2.10 Protein quantification

Quantification of protein concentration by Bradford assay

In order for DMS/DMSP concentrations to be quantified by cell growth, the protein in culture was measured. This was achieved by recovering cells from 1 ml culture through centrifugation for 1 minute at maximum speed, and resuspending in 500 μ l Tris-HCl buffer (50mM, pH 7.5). Following this resuspension, the cells are lysed using sonication, for three repeats of 10 seconds, being kept on ice in between. Following sonication, samples were centrifuged at max speed for 10 minutes, and 20 μ l of the supernatant was mixed with 980 μ l Bradford Reagent. This was added to a cuvette and the absorption measured using a spectrometer set to OD595. A 4-point protein standard graph was produced (Fig. 2.5), using known concentrations of BSA. Standards include dH₂O alone, and concentrations of 100, 200, and 400 μ g/ml. This enables the calculation of the μ g protein in each culture.

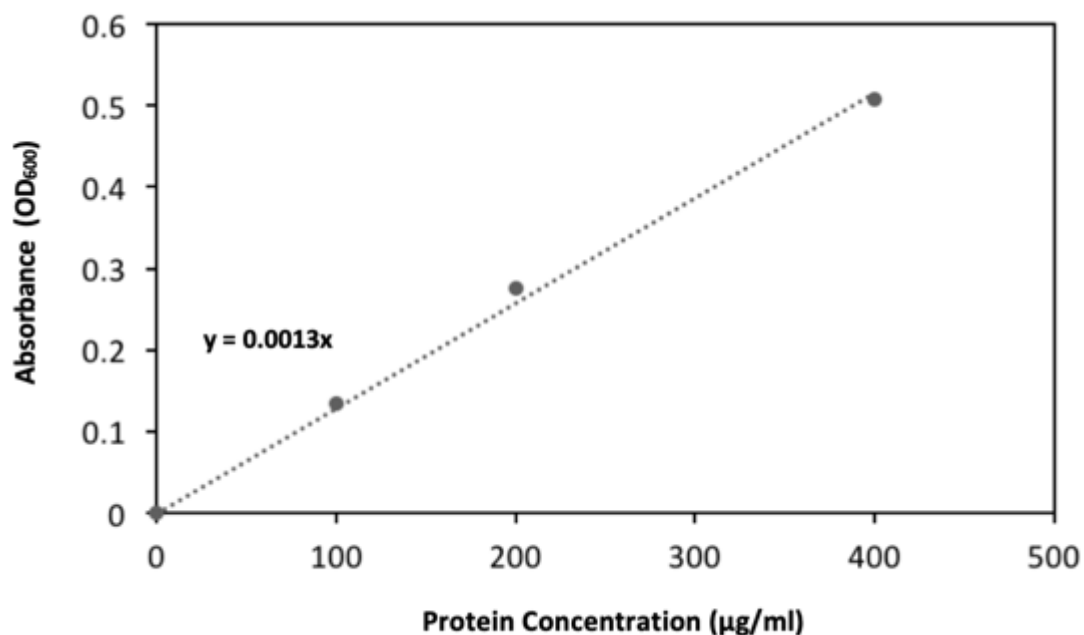


Figure 2.5. Calibration curve used to calculate protein concentration in in Bradford Reagent. The absorbance measured in OD600 of four BSA standards of known concentration, plotted with line of best fit to calculate protein concentrations of unknown samples.

2.11 Catalysed reporter deposition - fluorescence *in situ* hybridization (CARD-FISH)

To elucidate the microbial community associated with *Prymnesium parvum* cells, CARD-FISH technique was utilised. Cy3 labelled group-specific probes (Thermo Fisher): EUB338 i-iii targeting most bacteria, ALF968 targeting most *Alphaproteobacteria*, HGC69a targeting *Actinobacteria*, GAM42a targeting many members of the *Gammaproteobacteria*, BET42a targeting the *Betaproteobacteria*, and NON EUB as a control probe, were used to characterize bacterial groups. Briefly, a non-axenic *P. parvum* cells at exponential phase was collected, filtered and 3X washed with sterile 5 PSU Enriched Seawater, Artificial Seawater (ESAW) medium to remove algal detached bacterial cells in medium then gently centrifuged (700 rpm) for 10 minutes. The algal pellet was then resuspended in ESAW and an aliquot of 1 mL was fixed with 4% formaldehyde-phosphate buffered saline (PBS) overnight in the dark at room temperature. Volumes of 100 μ L fixed cells were then filtered onto 47 mm 3.0- μ m track-etched isopore membrane filters and washed with 10 mL of 0.2 μ m filtered deionised water. Filters were air-dried, dehydrated in ethanol series (50, 80, 96% and a final step of 70 % at -20 °C for 12 h to reduce chlorophyll autofluorescence) and air dried and stored at -20 °C.

Hybridization and washing proceeded as described in Amann et al. (1990) and Daims et al. (1999). Hybridized filters were mounted on a glass slide that contains the DNA stain DAPI and antifade agent (CitiFluor) and viewed using a Zeiss LSM 510 Meta confocal laser scanning microscope (LSM 510 Meta, Zeiss, Oberkochen, Germany). Stacked optical sections (z-stacks) of probe-labeled bacteria images were captured using AxioCam HRc and post-processed using Leica Application Suite X (LAS X) software program.

2.12 Statistical significance and standard deviation

Statistical methods for RT-qPCR are described in the relevant section above. All measurements for DMSP, Toxin production, or *DSYB* enzyme activity (in cell lysate experiments or enzyme assays) are based on the mean of three biological replicates per condition tested. Additionally, figures contain error bars, which represent the standard deviation between biological replicates. All experiments were performed at least twice unless otherwise stated. To identify statistically significant differences between standard and experimental conditions, a two-tailed paired

Student's t-test ($P < 0.05$) was applied to the data, using Microsoft Excel. Pearson product moment correlation coefficient was used ($p < 0.05$, $p < 0.01$, $p < 0.001$) to measure correlation between environmental parameters, cell counts, DMSP measurements. Analysis of variance (ANOVA) was used to analyze the difference between varying conditions and DMSP production.

Chapter 3

***Prymnesium parvum* associated microbiomes: their potential role in harmful algal bloom (HAB) formation and biogenic sulfur cycling**

A part of this chapter is published online as:

Wagstaff B.A., Pratscher J., Rivera P.P.L., Hems E.S., Brooks E., Rejzek M., Todd J.D., Murrell J.C., and Field R.A. (2020). Dissecting the toxicity and mitigating the impact of harmful *Prymnesium* blooms in the UK waters of the Norfolk Broads. bioRxiv 2020.03.26.010066

3.1 Introduction

The ichthyotoxic haptophyte, *Prymnesium parvum*, has gained its notoriety to invade a range of aquatic environments at high densities and elicit devastating ecosystem and economic effects. The development of *P. parvum* blooms is believed to be due to a combination of several environmental and biological factors such as eutrophication, increasing temperature, light change, ecosystem disturbance (mainly due to human activities), hydrology (current and river flow), water chemistry (pH, conductivity, salinity, carbon availability, etc.), and organism's ecological strategies. However, the main combination of these factors that drives the formation and maintenance of these blooms is still poorly understood.

Some life strategies of *P. parvum* allows it to proliferate and outcompete other native phytoplankton in the environment. These include diverse nutrient acquisition (Beszteri et al., 2012; Liu et al., 2015), mixotrophy (Carvalho & Graneli, 2010; Brutemark & Graneli, 2011), encystment or excystment (Green et al., 1982; Wang & Wang 1992), and production of a broad range of natural products including allelochemicals (toxins) (Kozakai et al., 1982; Igarashi et al., 1999; Manning & La Claire, 2010; Bertin et al., 2012) that kill or inhibit the growth of other phytoplankton groups (Graneli & Hansen, 2006). Furthermore, algal-bacterial associations can also influence its persistence and expansion.

The microenvironment of each HAB species is different from each other. Therefore, bacterial communities associated with HAB forming organism have been found to have specific order and structure rather than randomly assigned communities (Imai et al., 1995; Fukami et al., 1992). For example, in haptophytes (i.e., coccolithophores), a recent study has found that they harbour richer bacterial communities compared to dinoflagellates and diatoms, suggesting that they possess a greater range of available niches, as well as novel niches (Green et al., 2015). It is widely known that these algal-bacterial interactions or associations can be antagonistic or parasitic, symbiotic or mutualistic (Amin et al., 2015), commensalistic (Carillo et al, 2006), or just pure competition (Grossart, 1999) and these biotic interactions are crucial in the aquatic/marine environment as they control nutrient cycles and biomass production in the trophic web (Seymour et al., 2017). In a mutualistic relationship, heterotrophic bacteria can feed on the dissolved organic material (DOM) released by the algal cells (Riquelme et al., 1988) and in exchange they promote algal growth through certain complex communication mechanisms and production of inorganic nutrients (Ramanan et al., 2016).

P. parvum and other haptophytes are known to be prodigious producers of the sulfur metabolite DMSP in the marine and aquatic systems (Keller et al., 1989, Caruana & Malin, 2014). DMSP is an ecologically important metabolite and the precursor compound of dimethyl sulfide (DMS), a climate-active gas that induces atmospheric cloud formation and may affect Earth's Climate. This increased amount of DMSP in water during *P. parvum* bloom events are likely to attract and sustain bacterial species capable of catabolizing this compound. Hence, we investigated the *P. parvum* (bloom) associated microbial communities and their role in HAB formation and DMSP/DMS cycling. We assessed the bacteria and phytoplankton community diversity change *In Situ* during *P. parvum* bloom and non-bloom scenario through 16S rRNA gene amplicon sequencing and optical microscopy. Culture dependent methods were employed to identify bacterial groups associated with *P. parvum* blooms and bacteria capable of degrading DMSP produced by the haptophyte. Also, through the use of catalyzed reporter deposition - fluorescence *in situ* hybridization (CARD-FISH), I detected the microbial groups associated with *P. parvum* cells that may aid in understanding the relationship between the host algae and its associated microbiome. Finally, we investigated the abundance of genes involved in DMSP degradation and evaluate their potential relevance in sulfur cycling in the Hickling Broad.

3.2 Methods

3.2.1 Hickling Broad sampling

In Spring 2015, an outbreak of toxic *Prymnesium* bloom led to a major fish-killing event on Hickling Broad and surrounding areas. An estimate of 15,000+ fish were killed during this single event and prompted an immediate rescue of almost three-quarters of a million fish from Hickling and Somerton Broad to safer waters by the Environmental Agency (EA, 2015). A team of scientists and experts from the John Innes Center (JIC) and University of East Anglia (UEA) of the Norwich Research Park were invited to sample the area to study the microbial community and toxicity in the waters of Hickling broad. Water and biological samples were taken from Hickling Broad during the *P. parvum* bloom in April 2015 and another sampling was done in a non-bloom condition in September 2016. This is to compare the changes in microbial community in the water column using 16S rRNA gene amplicon sequencing.

In 2017, when I started my study on *Prymnesium* and sulfur cycling on the broads, I joined the regular sampling schedule set by the Broads Authority (BA). Regular water sampling was done

every two weeks from April 2017 until March 2018. A set of 4 x 50 ml and 1 x 250 ml water samples were taken from each of the 5 sampling points (See Fig. 2.2) following a transect across Hickling Broad and in concordant with the 12 regular sampling sites set up by the Broads Authority. Additional 2L Nunc bottles filled with Broad water were taken for phytoplankton identification and community monitoring, and these were immediately fixed onboard with Lugol's iodine solution. All samples were collected at approximately 20 cm depth, making sure to exclude the surface layer. Samples were returned immediately (within 3h of sampling) to the Department of Biological Sciences, UEA for microscopy, genomic, and metabolite processing.

3.2.2 Phytoplankton community analysis by microscopy

Lugol's fixed water samples were allowed to settle following an improvised Utermöhl technique (Utermöhl, 1958). Between 50 and 100 mL of the sample were dispensed into settling chambers and cells were allowed to settle for at least 15 and up to 30 h. The overlying water was removed carefully by decanting and pipetting and kept in 20 ml vials. Microalgal community cell counts were measured by adding 1 ml of fixed sample into Sedgewick rafter chamber and counting the number of algal cells using bright field microscopy (Serfling, 1949). Cells were counted with $\times 100$, $\times 200$ and $\times 400$ magnifications using a Carl Zeiss inverted microscope. Phytoplankton were identified to the lowest possible taxonomic level using appropriate literature (CEN, 2004) and keys for marine and freshwater environments (Tomas, 1997; Cox, 1996; Botes, 2003; Huynh & Serediak, 2006; John et al., 2003; Karlson et al., 2010). A minimum of 500 individual units were counted, leading to a counting error not exceeding 10% (Lund, 1958). Identification was limited to 14 dominant genera in >100 samples analysed.

3.2.3 Nucleotide extraction and purification

For environmental DNA and RNA extraction, the same procedures highlighted in sections 2.3.2 and 2.3.3 were followed. All environmental nucleotide (DNA and RNA) samples were quantified using a NanoDrop 2000 UV-Vis Spectro-photometer (Thermo Scientific) or a Qubit RNA/DNA HS assay kit (Thermo Fisher Scientific). RNA integrity is further assessed using an automated electrophoresis system, Experion™ (Bio-Rad Laboratories).

3.2.4 16S rRNA gene amplicon sequencing

16S rRNA gene amplicon sequencing was done on samples taken of the first two sampling occasions in April 2015 and September 2016. In brief, pooled biological replicates of DNA and cDNA samples from bloom (April 2015) and non-bloom (September 2016) samples, were selected for 16S rRNA/rDNA amplicon sequencing. This was again repeated for samples taken from bloom (June 2017) and non-bloom (November 2017). The primer set 515F/806R of the V4 hypervariable region of the 16S rRNA gene (Caporaso et al., 2012) was used for amplification. These primers provide sufficient resolution for the taxonomic classification of microbial sequences. Amplification and amplicon sequencing were performed by MR DNA (Shallowater, TX, USA). Sequencing was performed on a MiSeq system according to manufacturer instructions, obtaining between 106k-257k reads per sample with an average length of 300 bp. The resulting datasets were analysed by sequence analysis and phylogenetic classification using QIIME 1 (Caporaso et al., 2010). 16s Amplicon sequencing data was provided by Dr. Jennifer Pratscher.

3.2.5 Isolation of bacterial strains

At the height of a more recent bloom of *P. parvum* in June 2017, sampling for bacterial isolation was done to look at *P. parvum* bloom associated bacterial community and screen whether there are other potential players in DMSP/DMS production in Hickling Broads. Water samples were collected into 250 ml wide mouth sterile reagent bottles taken from station 6 (high *P. parvum* cell counts) and brought back to the laboratory for processing. 4 x 50 mL aliquots of the sample were spun down to 1 mL concentrate and a serial dilution was performed to a dilution factor of 10^{-5} , then 100 μ l of serially diluted samples were added to previously prepared agar plates. Four types of growing medium were used - LB, MB, YTSS and R2A containing mixed carbon sources, with no selective pressure other than selection for heterotrophic bacteria. Spread plates were incubated at a lower temperature of 20°C to approximate that of the waters sampled and colonies of different morphologies were purified to single colonies. Figure 3.1 shows sample of different bacterial isolates grown in YTSS media.

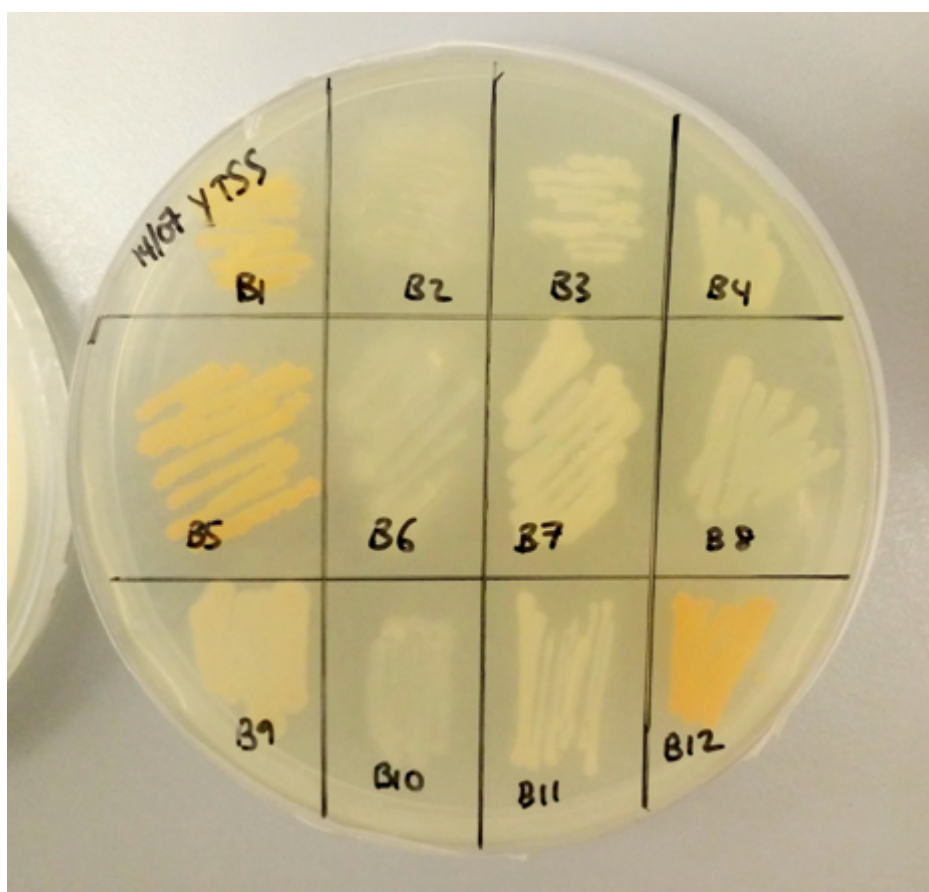


Figure 3.1. Example of purified bacterial isolates from Hickling Broad grown in YTSS agar plate displaying morphological variations.

3.2.6 Screening for DMSP-producing and -catabolizing bacteria

Purified bacterial isolates were picked and inoculated into a 5 mL liquid medium (depending on which solid media it was grown) and incubated overnight at 28 °C. Then 1 mL aliquots of liquid cultures were spun down and pelleted. The bacterial pellets were then resuspended in 200 µl modified Basal Media (MBM) minimal media (no carbon source) and transferred into 2 mL crimp-topped vials. Each vial was then added with 100 µl 10 M NaOH and sealed with sterile Teflon coated butyl rubber septa and incubated for 24 hrs in the dark at room temperature. This is to alkaline hydrolyse any endogenous DMSP produced by bacteria. DMSP/DMS measurement was done using gas chromatography (GC).

The bacterial isolates were also screened for their ability to generate DMS and/or methanethiol (MeSH) when incubated with DMSP. This was done by pelleting 1 mL of each bacterial culture and washing the pellet by resuspending the pellet in 1 mL MBM minimal media. This was

repeated for three times before finally resuspending the bacterial pellet in 300 μ L MBM minimal media enriched with 0.5 mM DMSP using sterile 2 mL crimp-topped vials. The vials were sealed using sterile Teflon coated butyl rubber septa and incubated in the dark for 48-72 hrs at room temperature. Bacteria capable of producing DMS and Mesh was then determined through DMS and Mesh measurement using GC. Vials containing a known DMSP degrading bacteria, *Ruegera pomeroyi* DSS-3, was used as positive control and vials containing only minimal media with DMSP were used as negative control and treated the same way as the bacterial isolate samples. All samples were done in triplicates.

3.2.7 Gas chromatography (GC) analysis

Determination of DMS/P in sample vials was performed by gas chromatography (GC) assays as detailed previously in Chapter 2, Section 2.9.1. In brief, this involved the measurement of headspace DMS, either directly produced by the sample, bacterial cleavage of DMSP, or via alkaline lysis of DMSP by injecting 100 μ l of headspace gas into a gas chromatograph equipped with flame photometric detector - GC-FPD. All measurements on the GC were performed using 2 ml glass vials containing 300 μ l liquid samples and sealed with PTFE/rubber crimp caps. Endogenous DMSP in samples was measured as DMS following alkaline hydrolysis through the addition of 100 μ l 10 M NaOH to 200 μ l culture. Vials were crimp sealed immediately, incubated at 22°C for 24 h in the dark, and then run in the GC. An eight-point calibration curve was performed regularly to check the consistency and accuracy of the assay.

3.2.8 Bacterial DNA extraction and purification

Bacterial isolates with DMSP-dependent DMS and/or methanethiol production phenotypes were inoculated into a fresh liquid medium (depending on the growth media (LB, TY, YTSS, or R2A) used when they were first isolated) and grown overnight. DNA was extracted from these single strain liquid cultures using a modified sodium dodecyl sulfate (SDS)-based protocol described in Chapter 2, Section 2.3.2. All DNA was resuspended in 100 μ l of nuclease-free water (Ambion, Thermo Fisher Scientific), quantified with a Nanodrop spectrophotometer (Amersham Pharmacia Biotech, Uppsala, Sweden), and stored at -20 °C until further analysis.

3.2.9 PCR amplification of bacterial 16S rRNA genes

Primers 27F and 1492R, specifically targeting approximately 1,400-bp section of the genomic bacterial 16S rRNA gene (Lane et al., 1985), were used for PCR amplifications. The 50 µl PCR mixes include 25 µl MyFi™ DNA Polymerase, 1 µl of template DNA, 2 µl of 20 pmol of forward and reverse primers, and 22 µl of sterile H₂O. Components were adjusted accordingly for smaller PCR reactions. The reaction conditions were as follows: 95°C for 3 min; followed by 30 cycles of 95°C for 1 min, 55°C for 1 min, and 72°C for 1.5 min; and then a final extension of 72°C for 10 min. Amplified PCR products were visualized by electrophoresis on 1% agarose gel stained with ethidium bromide. Purified PCR products were then sent to Eurofins Genomics (<https://www.eurofinsgenomics.eu>, Munich, Germany) for sequencing, and the isolates were taxonomically identified using BLASTn (<https://blast.ncbi.nlm.nih.gov/Blast.cgi>).

3.2.10 Catalysed reporter deposition – fluorescence *in situ* hybridisation (CARD-FISH)

Cy3 labelled group-specific probes (Thermo Fisher): EUB338 i-iii targeting the 16S rRNA of most bacteria (Daims et al., 1999), ALF968 targeting the 16S rRNA of most *Alphaproteobacteria* (Neef A., 1997), HGC69a targeting 23S rRNA of *Actinobacteria* (Roller et al., 1994), GAM42a targeting the 23S rRNA of many members of the *Gammaproteobacteria* (Manz et al., 1992), BET42a targeting the 23S rRNA of *Betaproteobacteria* (Manz et al., 1992), and NON-EUB as a control probe (Wallner et al., 1993), were used to characterize different bacterial groups associated with *P. parvum* cells. Briefly, a non-axenic *P. parvum* strain (CCMP 946/6) from culture collection was inoculated, acclimated, and grown in filtered broad water (3 µm-pore-size filters, MF-Millipore™ Membrane Filter, Sigma Aldrich) for 7-10 days. This was done to recruit naturally occurring algal-associated bacteria from Broad water. The healthy culture at exponential phase was collected, filtered and 3X washed with sterile 5 PSU Enriched Seawater, Artificial Seawater (ESAW) medium to remove algal detached bacterial cells in medium then gently centrifuged (700 rpm) for 10 minutes. The algal pellet was then resuspended in ESAW and an aliquot of 1 mL was fixed with 4% formaldehyde-phosphate buffered saline (PBS) overnight in the dark at room temperature. Volumes of 100 µL fixed cells were then filtered onto 47 mm 3.0-µm track-etched isopore membrane filters and washed with 10 mL of 0.2 µm filtered deionised water. Filters were air dried, dehydrated in ethanol series (50, 80, 96% and a final step of 70 % at -20 °C for 12 h to reduce chlorophyll autofluorescence) and air-dried and stored at -20 °C. Hybridization and

washing proceeded as described in Amann et al. (1990) and Daims et al. (1999). Hybridized filters were mounted on a glass slide which contains the DNA stain DAPI and antifade agent (CitiFluor) and viewed using a Zeiss LSM 510 Meta confocal laser scanning microscope (LSM 510 Meta, Zeiss, Oberkochen, Germany) equipped with two HeNe lasers (543 and 633 nm, respectively) and one argon laser (458, 477, 488, and 514 nm). In order to visualize as many as possible *Prymnesium* cells within a given microscopic field, it was necessary to manually set up Z-sections for each image taken due to the uneven nature of the algal surface. Stacked optical sections (z-stacks) of probe-labeled bacteria images were captured using AxioCam HRc and post-processed using Leica Application Suite X (LAS X) software program.

3.3 Results

3.3.1 Phytoplankton community

The bi-monthly sampling on Hickling Broad from April 2017 to March 2018 has revealed that the overall phytoplankton community mainly consisted of three major phytoplankton groups – the cyanobacteria, the chlorophyta, and the diatoms. This is based on microscopic data pooled from all sampled stations at each time point. From May to October, a single haptophyte species increased its concentration with these phytoplankton groups, the Prymnesiophyte *P. parvum*. The community shifted from diatom-cyanobacteria driven community (April-May) to haptophyte-cyanobacteria dominated community (May to October) where *P. parvum* accounted for 15-20 % of the total phytoplankton community. From November onwards the community went back to being diatom-cyanobacteria dominated (Fig. 3.2). Summertime samples recorded the highest microalgal densities that could reach up to 10^7 cells L^{-1} while cell densities during spring and autumn months were found to be in the range of 10^5 - 10^6 cells L^{-1} .

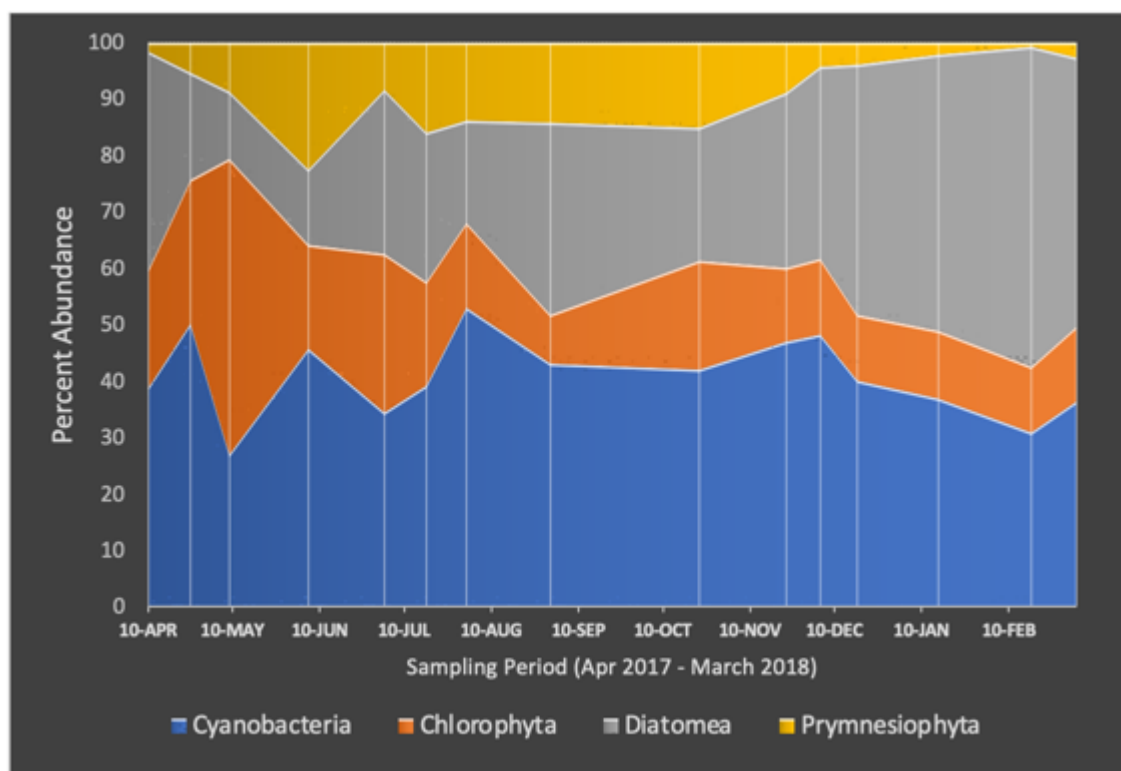


Figure 3.2. Phytoplankton community change through time on Hickling Broad as expressed in percent abundance of 4 major phytoplankton groups. Blue – Cyanobacteria, Orange – Chlorophyta, Grey – Diatomea, and Yellow – Prymnesiophyta.

Next, the phytoplankton community structure from 5 stations were compared during the height of *P. parvum* bloom (June 2017) and a non-bloom (November 2017) scenario/period (Figs. 3.3 a-d). *Cyanobacteria* was found to be consistently the major dominant phyla in both periods. But during a bloom, increased Prymnesiophyta (*P. parvum*) abundance was evident, especially at sampling station 5, where *Prymnesium* dominated consisting of almost 50% of the total phytoplankton community. On the other hand, in a non-bloom period, the three major phytoplankton groups (*Cyanobacteria*, *Chlorophyta*, and *Diatomea*) consisted of various genera almost in equal abundance (Figs. 3.3 c, d). Among the identified genera, Cyanophytes *Synechococcus* (5% in bloom vs 20% non-bloom), *Snowella* (10% bloom vs 5% non-bloom), *Agmenellum* (10% bloom vs 15-20% non-bloom), *Aphanothece* (10% bloom vs 2% non-bloom) and *Anabaena* (5-10% on both period) were found to be dominant and have shown change in abundance (Figs. 3.3 a,c). This was followed by two identified Chlorophytes *Eudorina* (25%) and *Scenedesmus* (5%) with no observable change in abundance on both sampling period. The rest of the microalgal community were composed mostly of Diatoms, identified mainly as *Melosira*,

Tabellaria, *Stephanodiscus*, *Surirella*, *Gyrosigma*, and *Nitzschia*, that all showed decrease in abundance during the bloom period (Figs. 3.3 a-d).

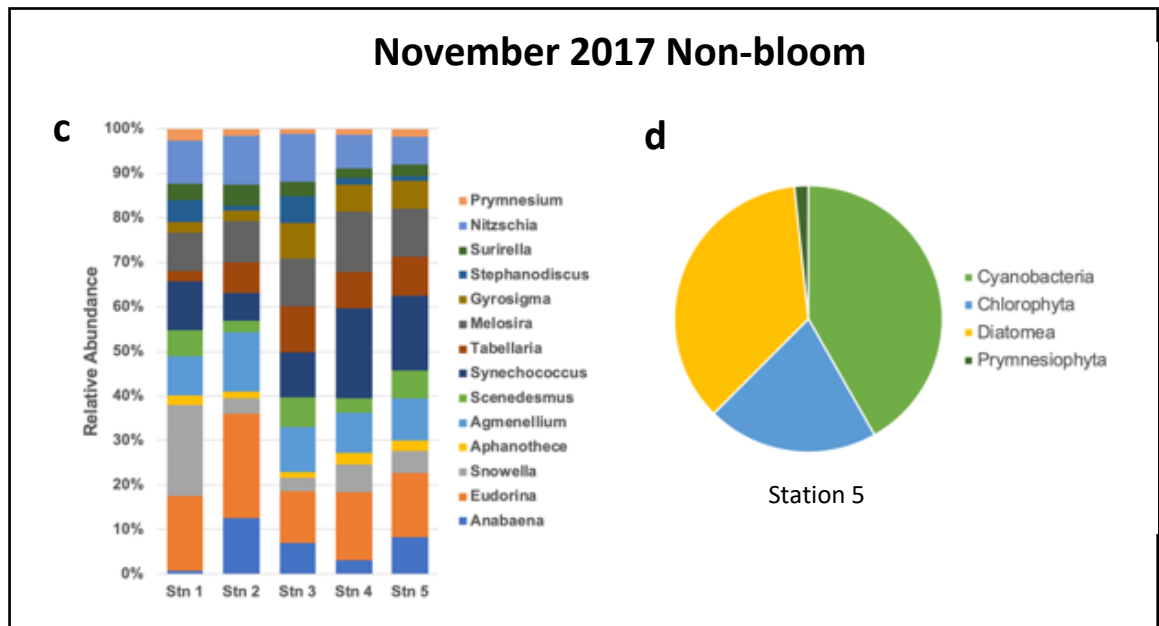
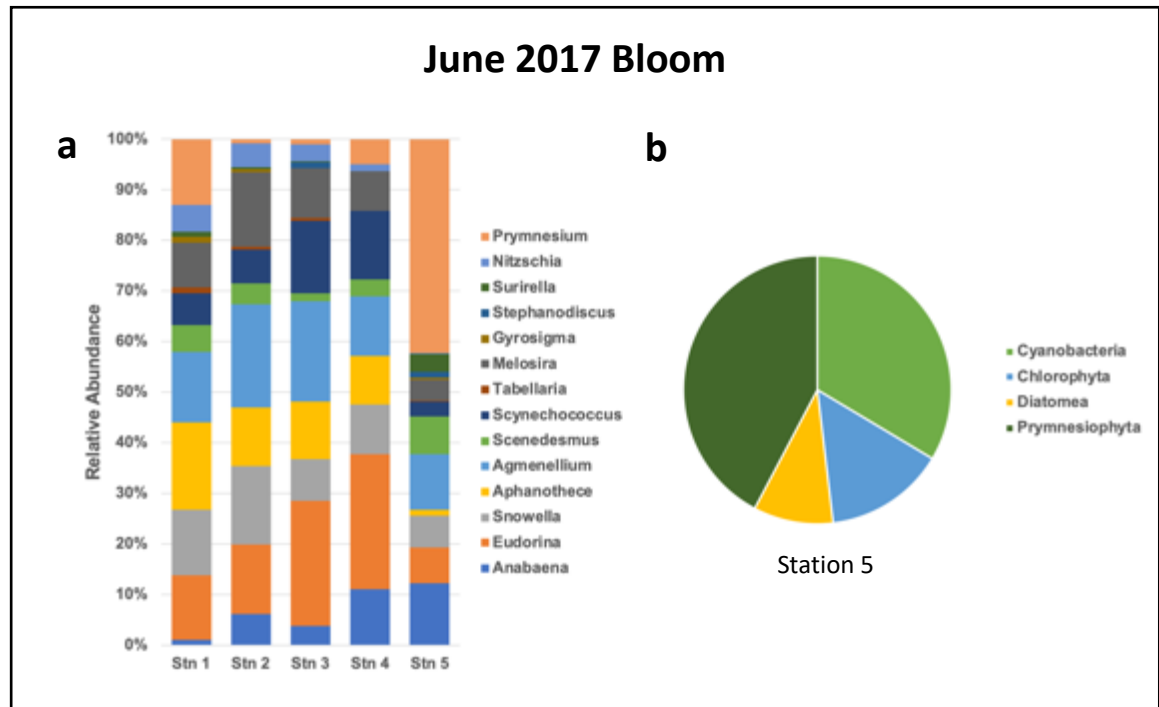


Figure 3.3. Phytoplankton community composition in bloom (Top) and non-bloom (Bottom) samples. Relative abundances of the dominant groups at the genus level (a,c). The right panel shows the composition of primary phytoplankton groups, including Cyanobacteria, Chlorophyta, Diatomea, and Prymnesiophyta at station 5 (b,d).

3.3.2 Bacterial community profiling

I compared 16S rRNA gene profiles of planktonic microbial communities in the Hickling broad to evaluate community dynamics during a massive *Prymnesium* bloom (April 2015) and non-bloom (September 2016) conditions. Community profiles of 16S rRNA genes revealed a shift in the community composition in the *Prymnesium* bloom samples compared to those dominated by different types of Cyanobacteria in non-bloom samples (Fig. 3.4 a). Prymnesiophyceae, Alphaproteobacteria, Sphingobacteriia and Betaproteobacteria were the four major dominant classes during the bloom period. During the bloom *Prymnesium* chloroplast 16S rRNA genes dominated the community in all sampling points examined, representing a mean proportion of 20-40 % of the total microbial community as compared to just 1-3% during non-bloom period. This is followed by an increase in *Alphaproteobacteria* (20-25%) higher than non-bloom condition (10-15%). *Sphingobacteria*, the majority of which were *Lewinella* (3.8%-5.6%) and *Candidatus Aquerestrus* (8.8-14%), showed increases from 0.2-0.4% and 0.1-0.6%, respectively, in the bloom versus non bloom samples. Betaproteobacteria (specifically *Methyloversatilis*, up to 5% bloom vs 0.8% non-bloom) also increased during bloom from 5-6% to about 10-15% of the community (Figs. 3.4 a, b). Cyanobacteria exhibited an inverse pattern with 28-30% dominance during non-bloom down to 2-4% during bloom period. Planctomycetia exhibited a sharp decline from 3-6% (non-bloom) to just roughly 0.5% during bloom (Figs. 3.4 a, b). The *Actinobacteria* and *Flavobacteria* groups also decreased in relative abundance during the bloom, with the maximum proportional abundance of 2.3% and 2.7% during non-bloom and 0.2% and ~1% during bloom. *Verrucomicrobiae* and *Gammaproteobacteria* showed no significant change during bloom and non-bloom maintaining the mean proportion of the community of 2-3% and 4-5%, respectively. Low proportions of *Deltaproteobacteria*, *Chlorophyceae*, *Chrysophyceae*, and *Mollicutes* occupied < 5% in both bloom and non-bloom condition (Figs. 3.4 a, b).

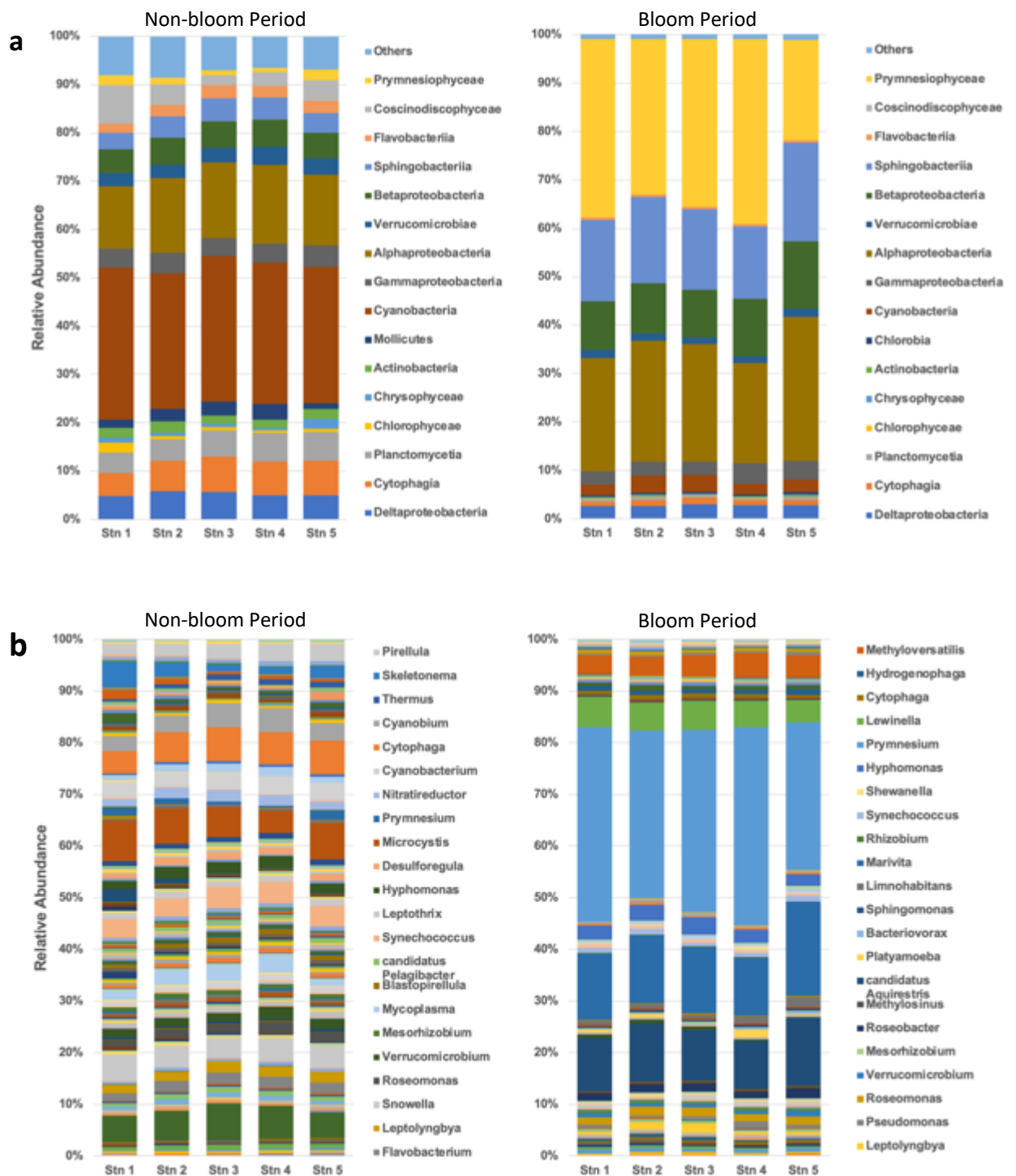


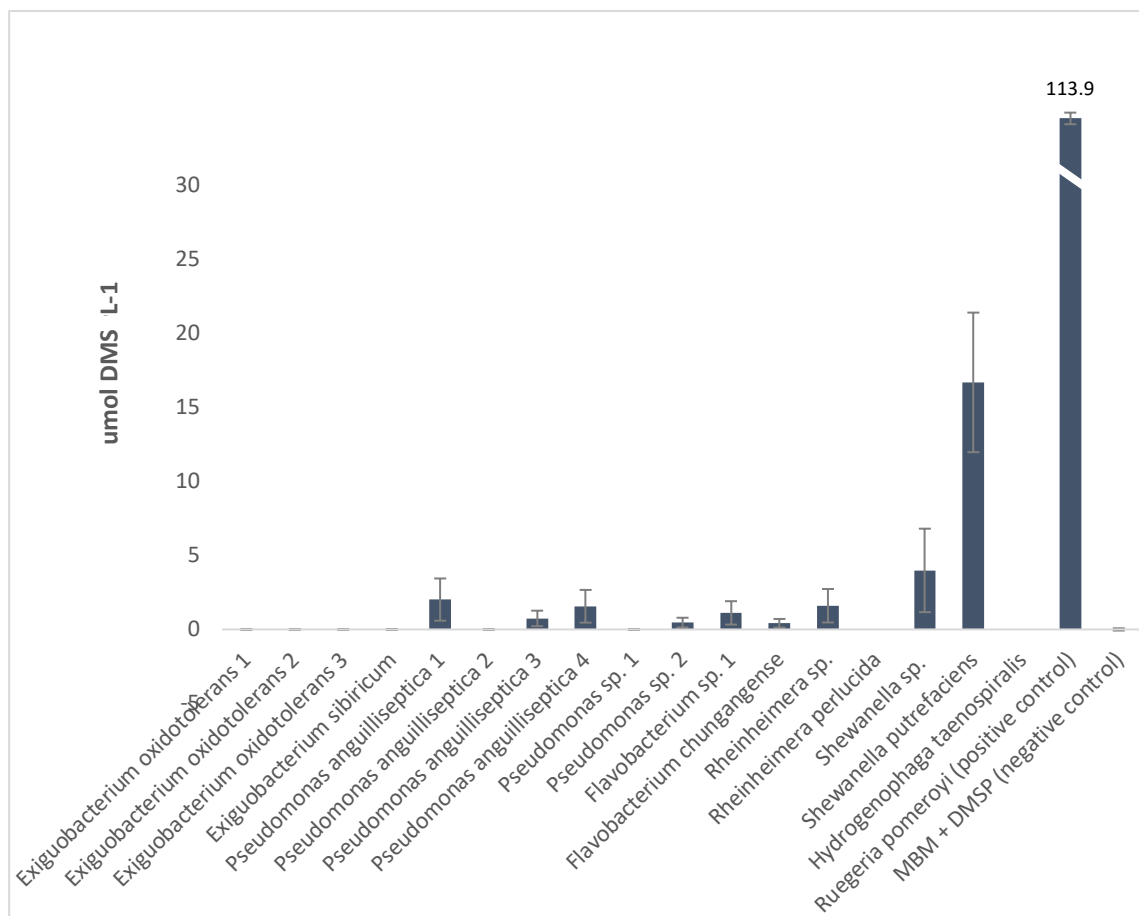
Figure 3.4. Microbial community composition in bloom and non-bloom samples. Relative abundances of the dominant groups at the class level (a) and genus level (b) obtained by 16S rRNA gene amplicon sequencing. Hickling Broad water samples collected at consistent sampling points during the harmful *P. parvum* bloom in April 2015 and during a non-bloom in September 2016. Only taxa with a combined relative abundance of $\sim 0.1\%$ are shown. Numbers refer to sampling stations on Hickling Broad.

The top 10 dominant genera in the samples during bloom (April 2015), aside from *Prymnesium*, were *Marivita*, *candidatus Aquirestris*, *Lewinella*, *Methyloversatilis*, *Hyphomonas*, *Roseomonas*, *Leptolyngbia*, *Roseobacter*, *Curvibacter*, and *Verrucomicrobium*. Other genera which showed a slight increase during bloom include: *Rhodobacter*, *Sulfuritalea*, *Labrenzia*, *Sphingomonas*, *Rhodocyclus*, *Rhodoferax*, *Desulfomonile*, and *Marinobacter* (Fig. 3.4 b). Note, that many *Roseobacter*, *Rhodobacter*, *Labrenzia* and *Marinobacter* species have previously been shown to produce and/or catabolise DMSP (Hehemann et al., 2014; Curson et al., 2008; Johnston et al., 2008; Curson et al., 2017). On the other hand, non-bloom (September 2016) community were more diverse and showed obvious overturn/change from the bloom community. The dominant genera were found to be *Microcystis*, *Plectonema*, *Cytophaga*, *Synechococcus*, *Cyanobium*, *Snowella*, *Mycoplasma*, *Cyanobacterium*, *Skeletonema*, and *Pirellula* which contributed >80% of the total quality reads. The rest of the community in small fraction include *Leptolyngbia*, *Hyphomonas*, *Nitratireductor*, *Desulfuregula*, *Verrucomicrobium*, *Flavobacterium*, *Roseomonas*, *Leptothrix*, etc. (Fig. 3.4 b). It also noteworthy at none of these genera are well known for their ability to cycle DMSP.

3.3.3 Isolation of *P. parvum* bloom-associated bacteria

The present study isolated a total of 94 pure bacterial isolates from Hickling Broad water sample taken at the height of *P. parvum* bloom in June 2017. The isolates were screened for DMSP production and none were found to produce the metabolite. However, some were shown to generate methanethiol in the absence of DMSP. This is a common trait of bacteria and is normally due to the presence of the Met- gamma lyase enzyme. Next, the isolates were also screened for their capability to generate DMS and/or MeSH when resuspended in MBM and incubated with DMSP. Seventeen suspected bacterial isolates out of 94 total isolates were chosen based on their initial GC measurements (i.e. they liberated DMS and/or MeSH) and were further investigated through DMSP incubation experiments. These bacteria were identified using 16S PCR amplification and sequencing. And among these candidate bacteria, only one was found to produce low levels of DMS when provided with DMSP, the *Shewanella putrefaciens* (Fig. 3.5). In comparison, ~6-fold higher levels of DMS were measured from *Ruegeria pomeroyi* DSS-3 as a positive control in cleaving DMSP. Unfortunately, this experiment was only preliminary and was not repeated due to the availability of *Prymnesium* bloom samples. Thus, I did not isolate bacteria with clear DMSP lyase or demethylase activity from the brackish Broads water and conclude that this is a feature of more marine systems. However, I realise that I would have had more chance

of isolating such DMSP catabolic bacteria if I had isolated the bacteria on minimal media with DMSP as the sole carbon source.

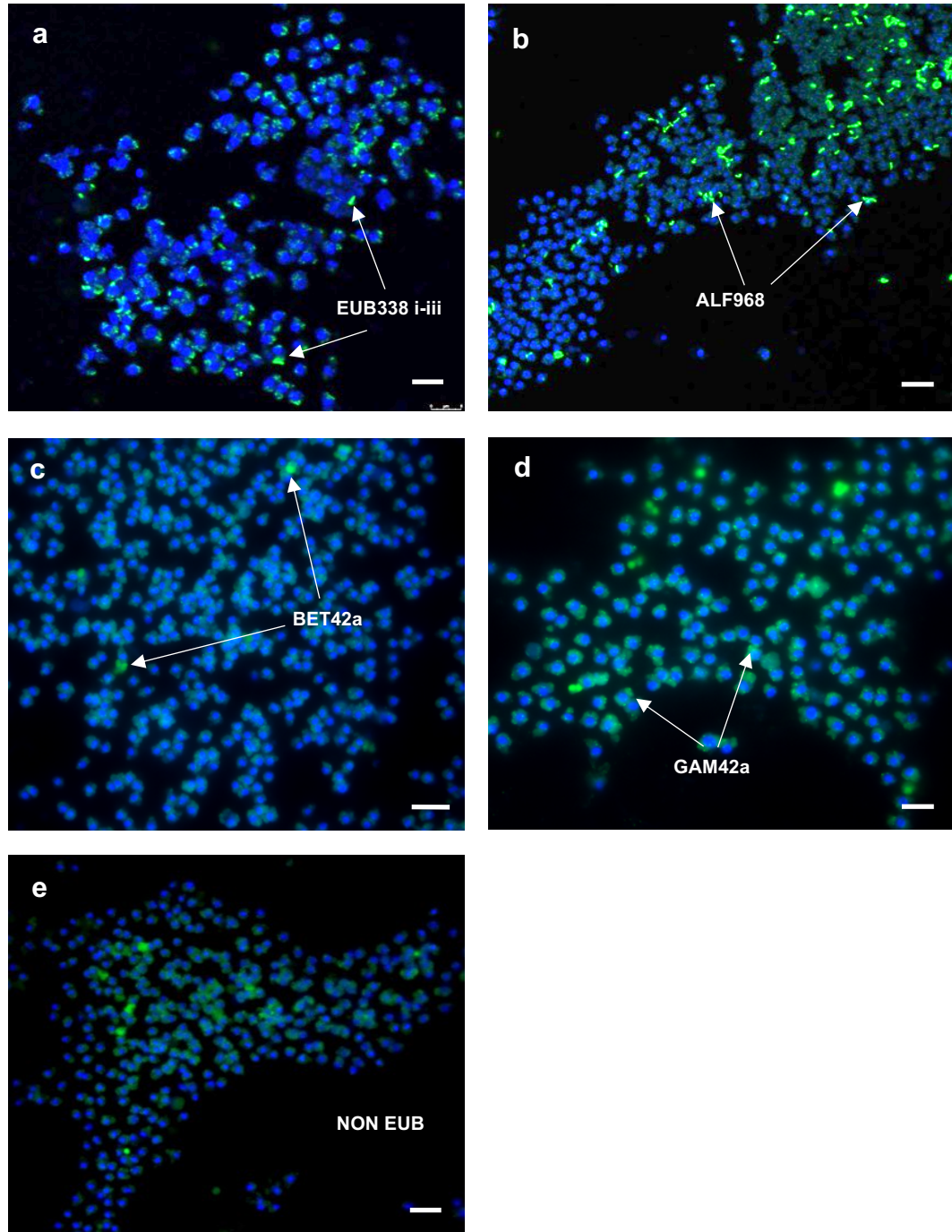


Figures 3.5. DMS production of bacterial isolates incubated in MBM media with 0.5 mM DMSP as measured by GC-FPD.

3.3.4 CARD - FISH

Fluorescence in situ hybridization (FISH) is one of the most routinely used molecular techniques in the identification and enumeration of bacteria within biological and environmental samples (Amann et al., 1990). Combining FISH with catalysed reporter deposition (CARD - FISH) has been demonstrated to substantially enhance bacterial cell detection in situ (Schonhuber et al., 1999). The use of CARD-FISH technique can detect, identify, and enumerate microorganisms without requiring culture, and therefore it has been used to help elucidate the microbial ecology of varied habitats including algal associated communities (Amann et al., 2001; Tujula et al., 2006). Here, I

used CARD-FISH technique in visualising and identifying specific bacterial populations associated with the algal cell and within the bounds of the algal phycosphere. CARD-FISH signals from bacterial cells associated with *P. parvum* cells were detected using EUB338 i-iii (targets most bacteria), ALF968 (targets most *Alphaproteobacteria*), GAM42a (targets many members of *Gammaproteobacteria*), BET42a (targets *Betaproteobacteria*) and NON-EUB (control) probes. No signals were detected using HGC69a probe (targeting *Actinobacteria*), indicating that *Actinobacteria* are less likely associated with *P. parvum*. In addition, images of DAPI-stained *P. parvum* cells were also made possible to visualize the entire microbial community. Images of the bacterial community associated with *P. parvum* cell is demonstrated in Fig. 3.6 a-e.



Figures 3.6. Confocal laser scanning micrographs of bacterial cells attached to *P. parvum* cells visualized by CARD-FISH using Cy3-labelled probes. Colored green is the probe-conferred signal and blue is the DAPI stain. Bacteria detected with EUB338 i–iii probes (a); *Alphaproteobacteria* were detected using ALF968 probe (b); *Betaproteobacteria* were detected using BET42a (c); *Gammaproteobacteria* were detected using GAM42a (d); and a NON EUB probe as a control for non-specific binding of EUB 338 on *P. Parvum* cells (e). The scale bar in all panels is 8 μm .

3.4 Discussion

There have been a limited number of studies assessing the effect of *P. parvum* blooms on the eukaryotic and prokaryotic community in aquatic systems. Even less so on *P. parvum*'s associated microbiomes (both endophytic and epiphytic) and the biotic interactions between them. Here, I showed the shift of phytoplankton community structure in response to *Prymnesium* bloom formation through time and how the bloom influenced the heterotrophic bacterial taxa in inland lake systems, e.g. Hickling Broad. The isolation, characterization and visualisation of *P. parvum*-associated bacteria further illuminate the importance of these biotic interactions and their potential active role in the biogeochemical cycling in this type of aquatic system.

3.4.1 Phytoplankton community change

In the late 60's, a series of changes happened to the ecosystem of Hickling Broad. These include: enhanced eutrophication due to agricultural runoff, fish stock loss due to fish-killing harmful algal blooms, increased water turbidity which led to the decline of aquatic plants, increased saline intrusion, etc. These changes have triggered a switch mechanism in the conversion of a submerged plant-dominated to phytoplankton-dominated ecosystem. Initially, anthropogenic eutrophication and guantrophication by black-headed gulls (*Larus ridibundus*) which roosted on the broads, were thought to be the major contributors to this ecosystem change (Moss & Leah, 1982). But later on, studies have revealed that the increased salinity in the area was the main culprit for this ecosystem switch (Moss et al., 1991; Bales et al., 1993; Irvine et al., 1993).

Previous surveys on Hickling broad found that the phytoplankton community is mainly governed by two phases, a diatom-dominated phase during winter to spring and a cyanobacterial phase during summer to early winter (Leah et al., 1978; Bales et al., 1993). The seasonal diatom (with chlorophyte) spring bloom is fueled by winter build-up of silicate and nitrogen due to tidal flushing of nutrient-rich waters from the Heigham Sound (Agricultural runoff). But in summer where riverine inflow is low, nutrients become deficient leading to opportunistic N-fixing cyanobacteria to dominate (Moss & Bales, 1989). This trend has largely been maintained since the 80's unless interrupted by sporadic *P. parvum* blooms.

My data showed that in June 2017, *P. parvum* cells were very abundant compared to diatoms and cyanobacteria especially in station 5 (where previous records of fish kills were observed).

This seemed to be rather unusual given that the N-fixing cyanobacteria and other cyanophytes should succeed the diminishing diatom spring bloom. Typically, filamentous and N-fixing cyanobacteria dominate when dissolved nutrient pools are depleted in late spring to early summer (Bales et al., 1993). Many cyanobacteria species have a lower optimum N : P ratio for growth than other eukaryotic phytoplankton and are thus generally favored during periods of N depletion (Dokulil & Teubner, 2000). But based on archival records, *P. parvum* blooms in the past tend to occur between April to September on the broads when conditions are favorable (Bales et al., 1993). This trend mirrored the pattern observed in Scandinavian lake waters, where opportunistic *P. parvum* blooms occur after the diatom spring bloom and just before the filamentous and N-fixing cyanobacteria come to dominate (Edler, 1979; Johnsen et al., 1997; Fistarol et al., 2003). In the non-bloom period (November 2017), the phytoplankton biomass consisted mostly of cyanobacteria and diatoms, followed by chlorophytes. Cyanobacteria are known to be fast-growing nutrient opportunists and can compete with other slow-growing nutrient specialists via exploitative resource competition (Vallina et al., 2014). They are considered nuisance organisms, as some species can form large floating mats and may release toxins into lake waters (Huisman et al., 2005). So far, there has been no report of cyanobacterial toxicity on Hickling broads but the presence of potentially toxic species was documented within neighboring broads and connecting rivers (Phillips et al., 2005; Hunter et al., 2008). Diatoms (*Melosira*, *Surirella*, *Stephanodiscus*, *Nitzschia*, and *Tabellaria*) were abundant in the community during winter-spring but declined in summer when nutrients ran out (Bales et al., 1993).

P. parvum's success in dominating over other phytoplankton groups is believed to be due to the release of allelopathic substances (allelopathy). Allelopathic effects of *P. parvum* exudates (e.g. Pymnesin toxins) have been demonstrated to affect cyanobacteria, cryptophytes, diatoms and dinoflagellates (Fistarol et al., 2003; Barreiro et al., 2005). These allelopathic substances inhibit other phytoplankton cells competing for light and nutrients (Fistarol et al., 2003; Uronen et al., 2005; Graneli & Johansson, 2003; Graneli et al., 2008). For *P. parvum*, these allelochemicals could be the same toxins that wreak havoc and thus work not only as defense, but also, by killing competitors, thus improving algal survival and competitiveness under extreme low nutrient conditions (Graneli et al., 2008). Apart from this, *P. parvum* can rely on mixotrophy to access resources it needs to maintain its population throughout seasons and for surviving population to seed the next opportunistic bloom event.

3.4.2 *P. parvum* bloom-associated microbial communities

The interactions between phytoplankton and bacteria are an important aspect of the microbial loop in aquatic/marine biogeochemical cycling (Ramanan et al., 2016; Mayali, 2018). Phytoplankton serve as the primary source of organic nutrients for heterotrophic microbes and the abundance of the bacteria has been shown to have a positive correlation with algal concentrations (Kjelleberg et al., 1993). Their physical relationship, which may be mutually beneficial and extend from intracellular to extracellular interactions. By providing a habitat to the intracellular bacteria, the algae benefit from the nutrients synthesized by these endophytes (Seibold et al., 2001). Bacteria colonizing the surface give them access to nutrients, protection against toxins, and protection against predators (Dang & Lovell, 2000). Bacteria adhering to algal cells are potentially important players in the dynamics of HABs and this action may be either direct or indirect.

Community profiles of microbial 16S rRNA genes revealed shifts in the community structure as driven by *P. parvum* blooms. *Alphaproteobacteria*, *Sphingobacteriia* (Bacteroidetes), and *Betaproteobacteria* were the primary bacterial groups found to be enhanced during the bloom period. This is in concordance with previous studies that showed *Alphaproteobacteria* and *Sphingobacteriia* (Bacteroidetes) as the typical communities associated with harmful algal blooms or HABs (DeLong et al., 1993; Fandino et al., 2006; Hatton et al., 2012) and found to be the predominant bacterial communities attached to algal cell surfaces (Kodama et al., 2006). *Betaproteobacteria* on the other hand, are found to be numerically abundant and common inhabitants of freshwater environments (Glöckner et al., 2000). They are opportunistic, rapidly respond to nutrient pulses/shifts (like for example the broadland system) and are likely to be associated with phytoplankton bloom exudates (Šimek et al., 2008).

For bacteria linked to DMSP/DMS cycling, *Marivita* and *Roseobacter* were the two dominant Alphaproteobacteria found in our *Prymnesium* bloom samples. They are members of the Roseobacter clade, a group characterized as ecological generalists and known to mediate key biogeochemical processes such as biogenic sulfur cycling (DMSP/DMS) in marine environments (Brinkhoff et al., 2008; Buchan et al., 2005; Curson et al., 2011) and some members can also be found in lake environments (Budinoff et al., 2011). *Marivita* display diverse metabolic capacities in acquiring nutrients and energy sources. They have been found to catabolise DMSP to form methanethiol (via demethylation) or DMS (via cleavage) (Moran et al., 2012). Recently, Zheng et

al. (2019) reported *Marivita* sp. Associated with *Synechococcus* (Cyanobacteria), possessed both the demethylation pathway (*dmdABCD*) and the cleavage pathway (*dddD* and *dddL*) for DMSP metabolism, suggesting that this bacterium may benefit from its association with DMSP-producing cyanobacteria. Furthermore, dimethyl sulfoxide (DMSO) reductases (*dmsABC*) that catalyze the reduction of DMSO to dimethyl sulfide (DMS) and complete gene cluster conferring the capacity to oxidize inorganic sulfur to sulfate (*soxRSVWXYZABCDF*) were also found in its genome (Zheng et al. 2019).

The genus *Roseobacter* has been widely reported to degrade a variety of dissolved low-molecular-weight organics (e.g., DMSP) during phytoplankton blooms (Green et al., 2004; Jasti et al., 2005; Wagner-Dobler & Biebl, 2006). Their ability to degrade DMSP has been extensively studied (Ledyard et al., 1993; Gonzalez & Moran 1997; Wagner-Dobler & Biebl, 2006) and some *Roseobacter* species were found to catabolize DMSP through the various DMSP lyase genes, in particular *dddP* (Todd et al., 2009; Curson et al., 2011; Hehemann et al., 2014). They are known to dominate the bacterioplankton communities in environments with high DMSP concentrations, such as phytoplankton blooms (González et al., 2000, Riemann et al., 2000) or polar waters (Wagner-Dobler & Biebl, 2006). *Hyphomonas* sp. isolated from saltmarsh sediments have been found to produce DMS from Methanethiol (MeSH) (Carrion et al., 2019). *Roseomonas* have been detected in various habitats like drinking water (Gallego et al., 2006), lake-bottom sediments (Jiang et al., 2006), and in lake water communities associated with cyanobacterial blooms (Eiler & Bertilsson, 2004).

Other bacterial groups that were found to dominate in our *Prymnesium* bloom samples were members of *Sphingobacteriia* (Bacteroidetes), specifically *Lewinella* and *Candidatus aquirestris*. Most *Lewinella* species have the hydrolyzing ability which indicates their ability to utilize complex carbon sources such as starch, chitin, casein, and cellulose (Holt, 1989; Khan et al., 2007). *Sphingobacteriia* species appear to have a strong dependency on nutrient load or phytoplankton blooms in freshwater lake systems (Newton et al., 2011). *Candidatus aquirestris* on the other hand, is a cosmopolitan inhabitant of hard-water lakes (Hahn & Schauer, 2007). Betaproteobacterial *Methyloversatilis* are known to utilize methanol, methylated amines, formaldehyde, methanethiol and formate, as well as a variety of multi-carbon compounds. They harbor methanethiol oxidase (MTO) - encoding genes giving them the ability to degrade methanethiol (MT) through MT oxidase (MTO) enzymes (Eyice et al., 2018). MT oxidation is a significant step in the sulfur cycle for MT is an intermediate during DMSP degradation via

demethylation pathway and an intermediate of dimethylsulfide (DMS) degradation (Lomans et al., 1999, 2002; Bentley & Chasteen, 2004; Schäfer et al., 2010; Eyice et al., 2018).

In non-bloom period, bacterial community structure in the broads was more diverse (α diversity) and complex. *Cyanobacteria*, *Alphaproteobacteria*, *Cytophagia*, *Planctomycetia*, *Betaproteobacteria*, *Gammaproteobacteria*, *Sphingobacteriia*, *Diatomea*, *Delta-proteobacteria*, and *Verrucomicrobiae* were the classes found to be relatively high in abundance. This community structure represents typical aquatic bacterial populations of freshwater lake and riverine systems (Glöckner et al., 2000; Zwart et al., 2002; Eiler & Bertilsson, 2004). Most of these bacterioplankton groups are associated with cyanobacterial species where they can prey on or thrive on organic substrates/nutrients they produce (van Hannen et al., 1999; Rashidan & Bird, 2001).

3.4.3 Bacterial isolation and screening for DMSP/DMS production

The occurrence of HABs such as *P. parvum* blooms releases large amount of secondary metabolites like methyl-sulfur compounds (DMSP and DMS) into the surrounding waters. This in turn this likely influenced the microbial community and enhanced recruitment/growth of bacterial species capable of metabolizing these compounds. In this study, I screened for culturable bacteria from *Prymnesium* bloom samples to find out whether there are DMSP producing bacteria associated with *P. parvum*. Among the 94 isolates, no isolate was found to produce DMSP but some were found to produce methanethiol (Mesh), suggesting that *P. parvum* might be the only source of DMSP in the Broads. I then investigated the production of DMS and Mesh on these suspected isolates when DMSP was added to the cultures suspended in minimal media. Based on my preliminary data, only one suspected isolate bacterium showed low DMSP lyase activity – the *Shewanella putrefaciens* isolate. This bacterium is commonly found in water-related environments such as marine, rivers, lakes, sewage, and hypoxic/anoxic sediments (Bulut et al., 2004; Basir et al., 2012). Curson et al. (2011) examined the Ddd⁺ phenotype of *S. putrefaciens* CN-32 strain and showed that it is capable of breaking down DMSP to produce DMS. Unfortunately, no further investigation was done on *Shewanella* and the experiment was not repeated due to lack of *Prymnesium* bloom samples. A more robust experimental design is warranted to further elucidate the relationship between bloom-associated bacteria and bloom forming *Prymnesium*, especially in terms of DMSP/DMS cycling.

3.4.4 CARD-FISH on *P. parvum*

The algal phycosphere is a mutually beneficial region around the algal cell (Bell & Mitchell, 1972) where growth-promoting nutrients are exchanged between phytoplankton and bacteria, the latter are especially found to feed on dissolved organic material (DOM) released by the algal cells (Riquelme et al., 1988). In order to visualise/detect microbial community present in the *P. parvum* phycosphere, I used the CARD–FISH technique. This technique has been demonstrated previously to substantially enhance microbial detection *in situ* (Schonhuber et al., 1999) and has been used for the identification of pelagic marine Bacteria (Pernthaler et al., 2002), *Cyanobacteria* (Schonhuber et al., 1999), and sedimentary marine Archaea and Bacteria (Ishii et al., 2004). My CARD-FISH results revealed that there are a plethora of bacteria living around or on the haptophyte and mainly confined to three major bacterial taxa – the *Alpha-*, *Beta-* and *Gammaproteobacteria*. Actinobacteria on the other hand, were not detected around or attached to *Prymnesium* cells, despite being a ubiquitous and dominant component of freshwater or lake bacterial communities. Previous field and microcosms studies have found a decrease in this group of bacteria during *P. parvum* blooms (Jones, 2012; Acosta et al., 2015). Overall, my CARD-FISH results reflected the results we have found earlier on the microbial community change as affected by *P. parvum* blooms using 16S rRNA gene probing.

3.5 Conclusion

The present study revealed the profound effect of the occurrence of *P. parvum* blooms on the diversity and composition of freshwater/brackish water microbial communities. Most of these changes include: an abrupt change in phytoplankton composition, decrease in diversity, and decline in relative abundances of certain phytoplankton groups such as diatoms, cyanobacteria, and chlorophytes. *P. parvum* blooms, on the other hand, enhanced the growth of HAB-related bacterial species such as the members of specific heterotrophic bacterial groups including Alphaproteobacteria, Gammaproteobacteria, and Bacteroidetes which possibly depended on phytoplankton-derived high molecular and low molecular organic compounds. The change in microbial and algal community structure during *P. parvum* bloom and non-bloom period provided insights onto algal-microbial interactions based on their co-occurrence, which has the potential to influence biogeochemical cycling and shaping future microbial/planktonic communities. Furthermore, 16S rRNA gene probing and fluorescence *in situ* hybridisation (FISH) allowed us to identify and enumerate the bacterial communities associated with *P. parvum*. And

these communities, alongside their interaction with *P. parvum*, are likely to have a multitude of direct and indirect effects on the algal bloom success.

Chapter 4

Investigating the ecological role of DMSP on the expansion and success of destructive harmful algal blooms (HABs) in the Norfolk Broads

This chapter is being prepared for publication:

Rivera, P.P.L., Zhou, S., Curson, A.J., Pratscher J., Brooks E., Field R.A., Murrell, J.C., and J.D. Todd (2020). Understanding the ecological role DMSP on the expansion and success of ecosystem destructive harmful algal blooms (HABs) in shallow wetland/lake systems

4.1 Introduction

Harmful algal blooms (HABs) occur when there's a sudden or explosive growth of toxin-producing algae that can cause harm to animals, humans, and affect local ecology (Anderson, 1989). HABs are a major issue in marine, brackish, and freshwater systems worldwide (Watson et al., 2015). They are known to cause disruptions in microbial ecosystems that result in ecological imbalance, contamination, or collapse of aquatic food webs (Buskey et al., 2001; Gobler et al., 2005). There are several factors that may influence the formation and prevalence of HABs. These include increased nutrient loading (eutrophication), changes in water temperature, availability of light, pH, and water movement (Anderson, 2014).

Prymnesium parvum is a haptophyte alga known to form harmful algal blooms leading to devastating fish kills in brackish water and inland lakes systems worldwide including the Norfolk Broads, UK. (Holdway et al., 1978; Edvardsen and Paasche, 1998; Seger et al., 2015). *Prymnesium* HABs are characterized by their seasonal recurrence, rapid proliferation, wide salinity and temperature tolerance, as well as the production of highly potent ichthyotoxins, known as prymnesins, that are fatal to all gill-breathing organisms (Shilo, 1967; Meldahl et al., 1995; Manning & La Claire). Since its first confirmed occurrence on the Norfolk Broads in the late 60's, blooms of *P. parvum* have been investigated due to increasing frequency and severity (Davies, 1977), often resulting in thousands of fish mortalities and affecting the local economy (Wagstaff et al., 2017).

The factors contributing to the formation, maintenance, and control of *P. parvum* blooms are not well known, but the alga has been known to possess several physiological characteristics that allow it to proliferate in a variety of habitats. It has a wide salinity tolerance (euryhaline) allowing it to establish in brackish to saline lake waters. *P. parvum* is also known to survive in a broad range of temperatures (eurythermal) where blooms appear not to follow fixed seasonality depending on the area or environments they tend to bloom. *P. parvum* also produces a myriad of toxins that negatively affect gill breathing animals and can lead to massive fish kills in the bloom-affected area. In the laboratory, these toxins have been shown to affect zooplankton grazers, and other members of the plankton (Edvardsen & Imai, 2006; Fistarol et al., 2003; Skovgaard & Hansen, 2003; Manning & La Claire, 2010). *P. parvum* is also a mixotrophic organism, combining phototrophy with a well-developed ability to capture, subdue and ingest (phagotrophy) a wide variety of microbial species including its predator. This physiological duality

presumably provides a huge ecological advantage relative to other algae and heterotrophic protists especially when conditions are limiting, and thus may play a role in bloom formation and maintenance (Tillmann, 1998; Tillmann, 2003).

Haptophytes are generally known to produce high intracellular levels (up to 300 mM) of the sulfur metabolite dimethylsulfoniopropionate (DMSP) and, through the action of DMSP lyase enzyme/s, the gas dimethylsulfide (DMS) (Keller et al., 1989; Sievert et al., 2007, Seymour, 2014). DMSP is one of Earth's most abundant organosulfur compounds, with eight billion tons produced in its surface waters annually by many phytoplankton, some plants, corals and bacteria (Gali et al., 2015; Zhang et al., 2019). Once released into the aquatic environment, DMSP is an important nutrient for marine microorganisms providing carbon, sulfur and/or energy demands (Zubkov et al., 2001; Curson et al., 2011; Zhang et al., 2019). Many marine microorganisms import and use DMSP for its anti-stress properties or catabolise it via two enzymatic pathways: demethylation and cleavage (Villa-Costa et al., 2006; Curson et al., 2011; Moran et al., 2012).

DMSP demethylation via the bacterial DMSP demethylase (DmdA), prominent in alphaproteobacterial SAR11 and *Roseobacter* bacteria, is believed to be the major pathway accounting ~75% of DMSP catabolism (Kiene & Linn, 2000; Howard et al., 2006; Howard et al., 2008; Zhang et al., 2019). In contrast, seven different DMSP lyases (DddD, DddL, DddP, DddQ, DddW, DddY, DddK) exist in diverse bacteria and some ascomycete fungi, and one eukaryotic DMSP lyase (Alma1) (Curson et al., 2011; Alcolombri et al., 2015; Johnston et al., 2016). DddP is the most environmentally abundant DMSP lyase and thus it is often used to assay for the presence DMSP producing organisms in marine samples (e.g., Williams et al., 2019; Sun et al., 2020).

To date most microalgal DMSP/DMS research has focused on spatial and temporal distributions in marine environments (Kiene & Linn, 2000; Jiao et al., 2003; Kumar et al., 2009) with less emphasis devoted to the mechanisms of how DMSP and DMS are produced and the factors affecting production (Stefels et al., 2007). However, our recent identification of the key methylthio-hydroxybutyrate S-methyltransferase enzyme in the transamination pathway for DMSP synthesis in marine bacteria (DsyB), and its eukaryotic counterpart (DSYB) in most haptophytes and dinoflagellates and many other phytoplankton, allows DMSP production in the environment to be monitored at the genetic level (Curson et al., 2017, Curson et al., 2018). In the lab, *P. parvum* CCAP946/6 was shown to enhance DMSP synthesis under raised salinity, and

DMSP and DSYB were localised to the chloroplasts and mitochondria in this marine strain, consistent with DMSP having a role as an organelle-specific osmolyte or in oxidative stress protection (Curson et al., 2018).

There have been no studies examining DMSP production and its catabolism by HAB algae, like *P. parvum*, and associated bacteria in a brackish water environment. Given the low salinity (3-5 PSU) of the Broads and that *P. parvum* DMSP synthesis is down-regulated by low salinity, the prediction would be that DMSP production and cycling is of low significance in such environmental settings. This study shows something quite different. Here, we collected, characterized the physicochemical properties and studied the abundance and active transcription of *P. parvum* cells in Broads water samples over a season in 2017. The standing stock DMSP concentration and the abundance and transcription of key DMSP synthesis and catabolic genes were also monitored to determine the importance of *P. parvum* and bacteria in DMSP cycling in the Broads waters. The ability of these Broads strains to produce and degrade DMSP was compared to those of marine origin from culture collections. Thus, this study provided novel insights into the functional/ecological role of DMSP in natural *P. parvum* blooms and the associated microbial community in brackish waters and if these environments are potentially important sources of DMS.

4.2 Methods

4.2.1 Sampling site, sample collection and processing

Field sampling was done on Hickling Broad (52°44'N, 1°34'E) where *Prymnesium* blooms occur almost annually (See Chapter 2, Fig. 2.1) from April 2017 to March 2018. Broad- water samples were taken fortnightly from each of the 5 sampling stations/sites following a transect across the whole broad (See Chapter 2, Fig. 2.2). Additional 2L sampling bottles were filled with water collected for phytoplankton identification and enumeration, and immediately fixed onboard with Lugol's iodine solution. All samples were collected at ~20 cm depth. During each sampling event, water physicochemical parameters were recorded. *In situ* measurements of salinity (conductance) pH, DO, and temperature were collected using YSI Professional Pro Meter (YSI Instruments, United States). Another set of samples were collected by the Broads Authority (BA) for Chl-a, Ammonium (NH₄⁺), nitrate (NO₃⁻), and phosphate (PO₄³⁻) measurements. These were sent out to the Environmental Agency (EA) for further processing. The rest of the samples were returned immediately (within 3h of sampling) to the Department of Biological Sciences, UEA for genomic and metabolite preparations. See Chapter 2 for complete details of field sampling.

Samples were immediately processed in the laboratory on the same day they were taken from the Hickling Broads. In preparing samples for DNA isolation, two 50mL plastic tubes containing algal biomass were immediately pelleted by centrifugation (6000 rpm, 4°C) for 10 min. Pellets were resuspended in 1 ml nuclease-free water (Ambion, Thermo Fisher Scientific). Suspensions from the same sampling point were pooled yielding pooled tubes of spun-down 100 ml broad-water. Cell suspensions were subsequently pelleted (10,000 rpm, 4°C) in 2 mL centrifuge tubes for 1 min, the supernatant was discarded, and cell pellets were flash frozen with liquid nitrogen, and stored at -80 °C until further processing. To process water samples for RNA isolation, 50 ml of algal biomass was filtered onto 47 mm 1.2 µm RPT polycarbonate filters (Fisher Scientific, UK) and filters were stored in 2 mL centrifuge tubes, flash-frozen with liquid nitrogen, and stored at -80 °C until further use. Broad water samples for DMSP quantification by Gas Chromatography (GC), were prepared by filtering 50-100 ml of broad water samples from each site onto 47 mm GF/F glass microfiber filters (Fisher Scientific, UK) using a Welch WOB-L 2534 vacuum pump, and filters were then blotted on paper towel to remove excess liquid and stored individually in 2 ml centrifuge tubes, flash frozen and stored at -80 °C. All processes were done in triplicates.

For algal identification and counting via microscopy, water samples taken from the Broads were fixed using Lugol's reagent and were allowed to settle following an improvised Utermöhl technique (Utermöhl, 1958). Between 50 and 100 mL of the sample were dispensed into settling chambers and cells were allowed to settle for at least 15 and up to 30 h. The overlying water was removed using pipetting, and then stored in 20 ml vials in the dark until further analysis using direct microscopic technique.

4.2.2 Isolation of *Prymnesium* strains

P. parvum strains HIK PR1A, HIK PR6H, and HIK PR12D were isolated from the Hickling Broad during a mild *P. parvum* bloom in June 2017 and *P. parvum* strains WBF PRC1 and WBF PRD2 were isolated from the Woodbridge Fen Fisheries, Suffolk Broads during a mixed *P. parvum* and cyanophyte bloom in February 2018. To do this, broad water samples (50 ml) from Hickling broad and Woodbridge Fen Fisheries were inoculated into f/2 medium-Si (100 ml, 5 PSU). Several *P. parvum* strains were picked and made monoclonal by micropipetting single cells through several rinses of sterile medium (Andersen & Kawachi, 2005) and transferred into 96 -well plates. Isolates were then allowed to grow for 2-3 weeks with the same growth conditions for the algal cultures mentioned above. Isolates from enriched cultures were further made free from other contaminating picoplankton by serial dilution. Semi-axenic strains were transferred to 42-well plates and allowed to grow for approximately 2-3 weeks. Cultures were then made axenic by treatment with multiple rounds of antibiotics (see 'Algal Growth Media' in the next section). The absence of any contaminating bacteria was confirmed by epifluorescence microscopy of culture samples stained with DAPI (Porter & Feig, 1980). Clonal cultures were then carefully transferred and up-scaled to 75 cm³ cell culture flasks (Nunc™ EasyFLASK with Filter Caps, ThermoFisher Scientific) containing 20-40 ml modified F/2 medium-Si. New *P. parvum* strains used in this study are listed in Chapter 2, Table 2.2.

4.2.3 Algal and bacterial growth media

All Algal cultures were grown in f/2 medium (Guillard, 1975) made with enriched seawater artificial water (ESAW) (Berges et al., 2001) or sterilised/autoclaved broad-water without adding Na₂SiO₃ at 22°C with a light intensity of 120 μEm⁻² s⁻¹ and a light/dark cycle of 16h light/8h dark. Algal growth media were modified according to the requirements of the experimental conditions being tested. For non-axenic *Prymnesium* strains, cultures were treated with multiple rounds of

antibiotic treatment (streptomycin (400 μgml^{-1}), chloramphenicol (50 μgml^{-1}), gentamicin (20 μgml^{-1}) and ampicillin (100 μgml^{-1}) were added) prior to experiments. Test cultures with and without antibiotic treatments showed no significant difference in total DMSP in samples.

Escherichia coli was grown in Luria-Bertani (LB) (Sambrook et al., 1989) complete medium at 37 °C. *Rhizobium leguminosarum* J391 was grown in tryptone yeast (TY) (Beringer, 1974) complete medium or RM minimal medium (with 10mM succinate as carbon source and 10mM NH_4Cl as nitrogen source) at 28 °C. *Labrenzia aggregata* J571 (Curson et al., 2017) was grown in YTSS (Gonzalez et al., 1996) complete medium or MBM (Baumann & Baumann, 1981) minimal medium (with 10mM succinate as carbon source and 10mM NH_4Cl as nitrogen source) at 30 °C. Where necessary, antibiotics were added to bacterial cultures at the following concentration: streptomycin (400 $\mu\text{g ml}^{-1}$), kanamycin (20 $\mu\text{g ml}^{-1}$), spectinomycin (200 $\mu\text{g ml}^{-1}$), gentamicin (20 $\mu\text{g ml}^{-1}$), ampicillin (100 $\mu\text{g ml}^{-1}$). Strains used in this study are listed in Chapter 2, Table 2.2.

4.2.4 Algal cell counting and PAM fluorometry

To monitor and quantify the growth of algal cultures, samples were removed and diluted (dependent on the level of growth) in artificial seawater (ESAW), and cell counting was done using a CASY model TT cell counter (Sedna Scientific). The effect of stress on the potential maximum quantum yield of photosystem II was monitored by measuring F_v/F_m values (Butler, 1978) using a PAM fluorometer (WATER-PAM, Heinz Walz, Germany) (Schreiber et al., 1986; Bramucci et al., 2015). All PAM measurements were done at the same time when samples were taken for cell counting and measured as much as possible at the beginning of the light cycle. Samples were diluted in a sterile ESAW medium and adjusted within the detection range of the PAM fluorometer. Samples were maintained at 21°C or ambient temperature throughout handling. Triplicate readings of each sample were averaged to determine the maximum quantum efficiency.

4.2.5 Nucleic acid extraction

For extracting DNA from post-Field processed samples, a modified sodium dodecyl sulfate (SDS)-based protocol was used. In brief, the previously prepared biomass pellet was added to a 2.0 ml screw-cap tube of Lysing matrix E beads (MP Biomedicals UK) and mixed with 60 μl of 10% (w/v) SDS extraction buffer. Cells were lysed in a FastPrep instrument (MP Biomedicals UK) for 2 x 30s

at 6.0 ms^{-1} and supernatants were extracted twice using phenol:chloroform:isoamyl alcohol (25:24:1) and chloroform:isoamyl alcohol (24:1). Nucleic acids were precipitated with either ice cold isopropanol or polyethylene glycol (PEG) 6000 solution (20%) and dissolved in 100 μl of nuclease free water (Ambion, Thermo Fisher Scientific).

The total RNA extraction from environmental samples was performed on frozen pelleted or filtered samples (see 'Sample Processing') by directly adding 1 mL of prewarmed (65°C) Trizol reagent (Sigma-Aldrich), followed by Lysing matrix E beads (MP Biomedicals UK). Cells were disrupted using an MP FastPrep instrument set at maximum speed for $3 \times 30 \text{ s}$. Following a 5 min recovery time at room temp, samples were centrifuged at 13,000 g, 4°C , for 2 min. The supernatant was transferred to a 2 ml screwcap tube containing 1 ml 95% ethanol and RNA was extracted using a Direct-zol RNA MiniPrep kit (Zymo Research, R2050), according to the manufacturer's specifications. Genomic DNA was removed by treating samples with TURBO DNA-free DNase (Ambion) according to the manufacturer's protocol. The absence of DNA in RNA samples was confirmed by PCR using primers 27F and 1492R (Lane et al., 1985, Table 2.3).

All DNA and RNA samples were quantified using a NanoDrop 2000 UV-Vis Spectro-photometer (Thermo Scientific) or a Qubit RNA/DNA HS assay kit (Thermo Fisher Scientific). RNA integrity is further assessed using an automated electrophoresis system, Experion™ (Bio-Rad Laboratories). Complementary DNA from RNA samples was produced by reverse transcription of 1 μg DNA-free RNA using the QuantiTect Reverse Transcription Kit (Qiagen) following manufacturer's protocol. No reverse transcriptase and no template controls were performed to confirm that samples were DNA-free and that the reactions were free of contaminants. All nucleic acid samples were stored at -80°C until further processing.

4.2.6 Whole transcriptome sequencing

Cultures at the late exponential growth stage of newly isolated *P. parvum* HIK PR1A grown on high salinity (50 PSU, to induce DMSP synthesis genes) were harvested by centrifugation at 6,000 rpm. Total RNA extraction was performed using the method detailed in the previous section. RNA was quantified using a Qubit 3.0 Fluorometer, following the protocol of the Qubit Broad Range RNA Assay Kit (Thermo Fisher Scientific). RNA integrity was assessed using the Experion™ Automated Electrophoresis System (Bio-Rad Laboratories, UK) in combination with Experion™ RNA StdSens Analysis Kit and Chips (Fig. 4.1).

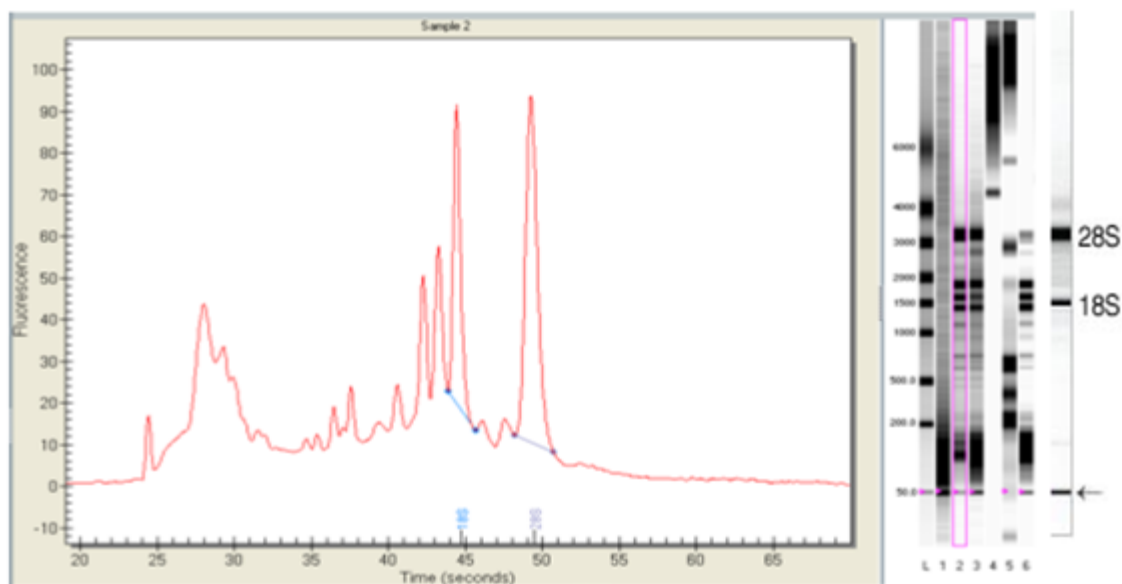


Figure 4.1. High-quality algal RNA on well number 2 from 6 RNA isolations made from *P. parvum* cells HIK PR1A. Approximately 200 ng total RNA were analysed on an Experion™ RNA StdSens Chip, using the eukaryotic total RNA software. The electropherogram feature well-defined peaks for 18S and 28S rRNAs, with a ratio of > 2.

The purified high quality RNA samples were then sent to Luxembourg Center for Systems Biomedicine (LCSB) Sequencing Platform, University of Luxembourg for library construction and RNA sequencing. The final library was subsequently loaded to a 500-cycle MiSeq reagent cartridge for sequencing by using MiSeq (Illumina) platform having sequenced runs of 2×150 paired-end reads.

4.2.7 *DSYB* and *Alma*-like in *P. parvum*

De novo reconstruction of the *P. parvum* transcriptome from RNA-seq data was performed using Trinity platform (Haas et al., 2013) and a local fasta file database of the transcriptome was created by Dr. Simon Moxon. To search for *DSYB* and *Alma*-like gene sequences in the HIK PR1A transcriptome assembly, a local blastp of fasta file database was probed using a curated *DSYB* protein sequence from *P. parvum* as published in Curson et al. (2018) and *Alma* family protein sequences in *E. huxleyi*, as reported in Alcorombi et al. (2015). Identified *DSYB* and *Alma*-like sequences obtained were codon-optimized and synthesized for expression in *E. coli*. More details can be found in ‘Genetic manipulations’ section of Chapter 2.

4.2.8 Primer design, real-time qPCR, and RT-qPCR

To study the abundance and transcription of *P. parvum* DSYB in laboratory and broad-water samples, qPCR Primers (Chapter 2, Table 2.3) were designed, using Primer3Plus (Untergasser et al., 2012), to amplify a 100-150 bp region, with an optimum melting temperature of 60° C. Melting temperature difference between primers in a pair was 2° C and GC content was kept between 40% and 60%. The primer pairs were checked to avoid stable homo- and heterodimers as well as hairpin structures using the IDT (Integrated DNA Technologies) Oligoanalyzer 3.1 tool (<https://www.idtdna.com/calc/analyzer>). Primer efficiencies were all 90–110% and within recommended limits. To study the abundance of *P. parvum* internal transcribed spacer (ITS2) copies in broad waters, real-time qPCR method previously described by Galluzzi et al. (2008) and qPCR primers PrymF and PrymR-3 (Table 2.3) used by Zamor et al. (2012) were optimised and utilised.

Quantitative PCR was performed with a C1000 Thermal cycler equipped with a CFX96 Real-time PCR detection system (BioRad), using a SensiFAST SYBR Hi-ROX Kit (Bioline) as per the manufacturer's instructions for a three-step cycling program. The 25 µL reaction mixture contained 12.5 µL of SYBR® Green JumpStart™ Taq ReadyMix™ (Merck), 0.15 µM of each primer, 200 ng BSA ml⁻¹, 3.0 mM MgCl₂, and 2.0 µL template DNA and cDNA. Gene abundance/expression measurement for each sample was performed using three biological replicates, each with three technical replicates. The pGEMT-Easy (Promega) plasmid containing the gene fragment created by the RT-qPCR primer pair for each gene tested (made through PCR on synthesized cDNA, cloning in *E. coli* 803 and purifying using a Miniprep Kit (Qiagen) was used as control DNA. For each gene, the cycle threshold (C_T) values of the technical and biological replicates were averaged and manually detected outliers were excluded from further analysis. Standard curves of control DNA were calculated from five points of 1:10 serial dilutions. The efficiency for qPCR and RT-qPCR assay was 98%. See Chapter 2 for more details.

4.2.9 Genetic manipulations

Amplification of the full-length *DSYB* gene from *P. parvum* HIK PR1A was attempted using PCR on complementary DNA (cDNA) from *P. parvum* HIK PR1A and *DSYB* primers (PpDSYB) described in Curson et al. (2018) designed to the sequenced *P. parvum* strain. Several attempts were made with varying PCR conditions, but these were not successful. Instead, new *P. parvum* *DSYB* (whole gene) primers were designed, based on the RNA-seq data, specifically to amplify *P. parvum* HIK PR1A *DSYB* (Chapter 2, Table 2.3). In designing the primers for full-length *P. parvum* *DSYB*, as detailed in Chapter 2, a ribosomal binding site and pribnow box upstream of the start codon was incorporated into the 5' primer to allow gene expression in heterologous host bacteria. The successfully amplified *P. parvum* *DSYB* gene was then cloned into the isopropylthiogalactoside (IPTG)-inducible wide host range expression plasmid pRK415 (Keen et al., 1988) using *Eco*R1 and *Acc*65I restriction enzymes for the expression in *Rhizobium* and *Labrenzia*.

The *DSYB* and *Alma*-like genes identified from *P. parvum* HIK PR1A transcriptome were also codon-optimized using Invitrogen GeneArt for expression in *E. coli*/*Rhizobium* and sent to Eurofins Genomics for gene synthesis. The synthesized *DSYB* gene or *Alma*-like gene in the vector pEX-K4 (Eurofins Genomics) was then subcloned into pLMB509 (Tett et al., 2012), a taurine inducible plasmid for the expression of genes in *Rhizobium* and *Labrenzia*, using *Nde*I and *Eco*R1 restriction enzymes.

pLMB509 or pRK415 clones containing *DSYB* or *Alma*-like gene was transferred to *E. coli* by transformation, and *Rhizobium leguminosarum* J391 or *Labrenzia aggregata* *dsyB*⁻ J571 or *Labrenzia aggregata* *dddL*⁻ J572 by conjugation, in a triparental mating using the helper plasmid pRK2013 (Figurski & Helinski, 1979). Routine restriction digestions and ligations for cloning were performed essentially as in Downie et al. (1983). Sequencing of plasmids and PCR products was performed by Eurofins Genomics. All plasmid clones are described in Table 2.2. The oligonucleotide primers used for molecular cloning were synthesized by Eurofins Genomics and are detailed in Chapter 2, Table 2.3.

4.2.10 MTHB S-methyltransferase assays

MTHB S-methyltransferase activities of pLMB509 and pRK415 clones containing the *DSYB* gene in *R. leguminosarum* J391 and *L. aggregata* J571 *dsyB*⁻ were monitored following the method described in Curson et al. (2018). In brief, cultures were grown (in triplicate) overnight growth

medium (TY for *Rhizobium* and YTSS for *Labrenzia*); 1 ml of cultures were centrifuged at 12,000 rpm for 2 min, resuspended in the same volume of minimal media (RM for *Rhizobium* and MBM for *Labrenzia*) and then diluted 1:50 into 5 ml minimal media with 10 mM taurine/IPTG (to induce expression, Sigma-Aldrich, T0625), 0.5 mM DL-MTHB (Sigma-Aldrich, 55875), 0.1 mM L-methionine and gentamicin, and incubated at 28-30 °C for 24 h before sampling for gas chromatography (GC) analysis (see 'Quantification of DMSP by GC') to determine the amount of DMSP product.

Protein concentrations were determined using the Bradford method (BioRad). This was achieved by recovering cells from 1 ml culture through centrifugation for 1 minute at maximum speed and resuspending in 500 µl Tris-HCl buffer (50mM, pH 7.5). After resuspension, the cells were lysed using sonication, for three repeats of 10 seconds and kept on the ice in between. Following sonication, samples were centrifuged at max speed for 10 minutes, and 20 µl of the supernatant was mixed with 980 µl Bradford Reagent. This was added to a cuvette and the absorption measured using a spectrometer set to OD₅₉₅. A four-point protein standard graph was produced, using known concentrations of BSA. Standards include distilled H₂O alone, and concentrations of 100, 200, and 400 µg/ml. This enables the calculation of the of µg protein in each culture. Control assays of *Rhizobium* or *Labrenzia* containing pLMB509 or pRK415 were carried out, as above, and gave no detectable DSYB activity. MTHB S-methyltransferase activities were expressed as pmol DMSP (µg protein)⁻¹, assuming that all the DMSP is derived from DMSHB through DMSHB decarboxylase activity.

4.2.11 *Alma* DMSP *in vitro* and *in vivo* cleavage assays

DMSP lyase activities of pLMB509 clones containing the *Alma*-like gene in *E. coli* 803 and *L. aggregate* J572 *dddL* were tested through *in vitro* and *in vivo* assays. For the *in vitro* assay, cultures were grown overnight in growth medium (LB for *E. coli* and YTSS for *Labrenzia*). Following overnight incubation, 50 µL of cultures were inoculated or subcultured into 300 µL of minimal medium (M9 for *E. coli* and MBM for *Labrenzia*) in 2 ml glass vials with 10 mM Succinate, 10 mM NH₄⁺, 10 mM Taurine (to induce gene expression) and 5 mM DMSP, vials were crimp sealed and left to grow for 24-48 h at 28 °C before assaying by GC.

For *In vivo* assay, culture cells were pelleted at 10,000 rpm, resuspended in 1 ml of 50 mM Tris-HCl buffer (pH 7), 4°C, then lysed by sonication (3 × 10 s) with a Markson GE50 Ultrasonic

Processor. Samples were spun for 5 min at 12,000 rpm to remove cell debris, then a sample of the cell-free extract (300 µl) was added to vials with 5 mM DMSP, crimped and incubated for an appropriate time (30 min to 6h) before assaying by GC (see 'Quantification of DMSP by GC' in Chapter 2, Section 2.9.1).

4.2.12 *Prymnesium* DMSP lyase activity

Prymnesium whole cells and cell lysate DMSP lyase activities were tested through *in vivo* and *in vitro* assays. For whole cell cultures, *Prymnesium* cells were concentrated by centrifuging 50 mL of culture at late exponential phase for 5 min at 6,000 rpm. After centrifugation, *Prymnesium* cells were resuspended and washed in its native media and this process was repeated twice. An aliquot of 300 µL of the resuspended sample was transferred to GC vial and added with 5 mM DMSP. Vials were immediately sealed and incubated at 22°C for 30 mins to 3 hours prior to GC analysis. To test for *P. parvum in vitro* DMSP lyase activity, *P. parvum* cell lysate was prepared by centrifuging 100 ml of culture at late exponential phase for 10 min at 6,000 rpm. The pellet was washed with 20 mM HEPES, 150 mM NaCl, pH 7.5 and resuspended in 2 ml buffer supplemented with EDTA-free protease inhibitor (Roche complete Tablets, Mini EDTA-free, EASYpack). Cells were sonicated 3 × 20 s to lyse, with 50 s recovery time at 4 °C. The resulting lysate was dialysed at 4 °C overnight against 20 mM HEPES, 150 mM NaCl, pH 7.5 to remove native DMSHB/DMSP. Lyase activity was monitored by performing *in vitro* enzyme assays in GC vials containing 300 µl lysate reactions added with 1 mM DMSP. GC reaction vials were immediately sealed/crimped and incubated at 22 °C for 24 h in the dark before GC analysis.

4.2.13 Quantification of DMSP and DMS by GC

Gas Chromatography (GC) assays involved measurement of headspace DMS, either directly produced or via alkaline lysis of DMSP, using a flame photometric detector (Agilent 7890 A GC fitted with a 7693 autosampler) and an HP-INNOWax 30 m × 0.320 mm capillary column (Agilent Technologies J&W Scientific). All headspace GC measurements were performed using 2 ml glass serum vials containing 0.3 ml liquid samples and sealed with PTFE/rubber crimp caps.

Quantification of DMSP from algal samples filtered on GF/F glass microfiber filters (see 'Sampling methods') was performed following methanol extraction. Filters were folded, placed in a 2 ml centrifuge tube and 1 ml 100% methanol was added. Samples were stored for 24 h at -20 °C to allow the extraction of cellular metabolites, then 200 µl of the methanol extract was added to a

2ml vial, 100 µl 10M NaOH was added and vials were crimp sealed immediately, incubated at 22°C for 24h in the dark and monitored by GC. Control samples in which DMSP standards were added to algal sample filters prior to methanol extraction showed that all standards were recovered following the extraction and measurement procedure. Calibration curves were produced by alkaline lysis of DMSP standards in water (for *Rhizobium* or *Labrenzia* MTHB *S*-methyltransferase assays) or 100% methanol (for algal methanol extracts). The detection limit for headspace DMS from DMSP was 0.015 nmol in water and 0.15 nmol in methanol.

For DMSP measurements of *L. aggregata* and *R. leguminosarum* cultures expressing *DSYB*, 200 µl of each culture (from MTHB *S*-methyltransferase assays) was added to a vial then 100 µl of 10 M NaOH was added to lyse the DMSP, and vials were immediately sealed and incubated at 30°C for 6-12 h (to allow the release of DMS into the headspace) before assaying by GC. For DMSP lyase due to cloned *Alma*-like gene expressed in *E. coli* and *L. aggregata*, vials containing cell-free extracts incubated with DMSP (300 µl) were run through the GC using the headspace method mentioned above. All experiments described here used three biological replicates. Estimated intracellular concentrations of DMSP (expressed in mM) are based on estimates of protein content per cell (Simon & Azam, 1989) and reported cell volumes

4.3 Results

4.3.1 Seasonal abundance of *Prymnesium*

Hickling Broad waters were sampled fortnightly at five stations (Fig. 4.2) from April 2017 to February 2018 and the numbers of *P. parvum* cells in the samples were counted by microscopy and recorded with the physicochemical properties of the water (Fig. 4.2, Table 4.1).

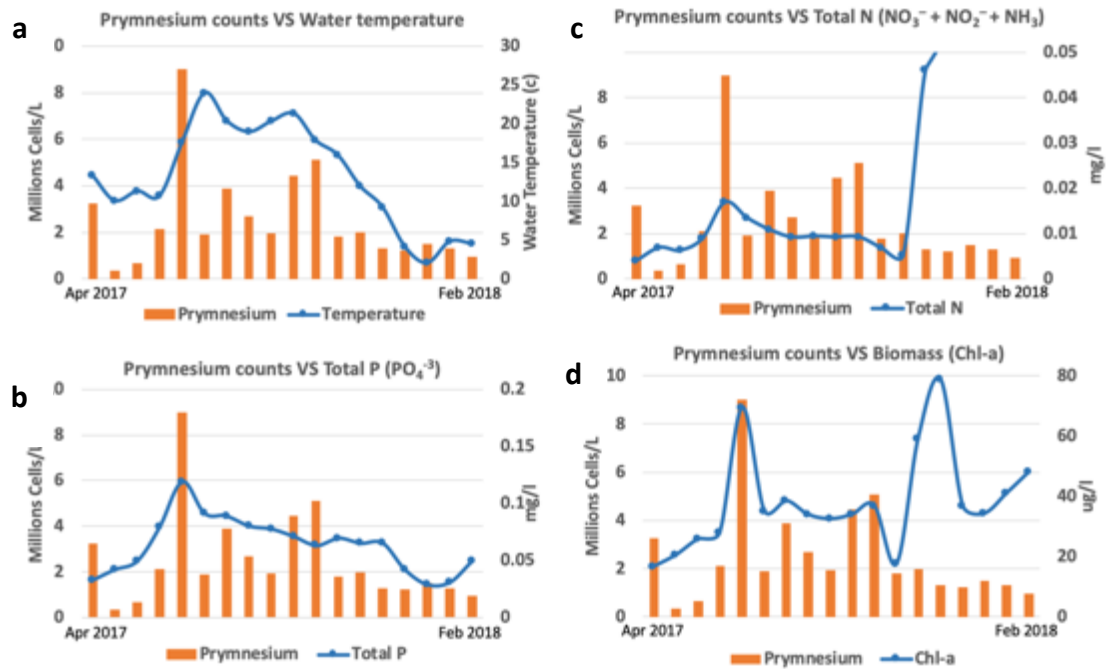


Figure 4.2. Hickling broad water biogeochemical properties and algal biomass. Time series for April 2017 (left) and February 2018 (right) of a, b: Water temperature and total P (PO_4^{3-}) concentration; c, d: Total inorganic N concentration ($\text{NO}_3^- + \text{NO}_2^- + \text{NH}_3$) and Biomass (Chl-a) the water column. Bars chronologically represent *P. parvum* counts (millions).

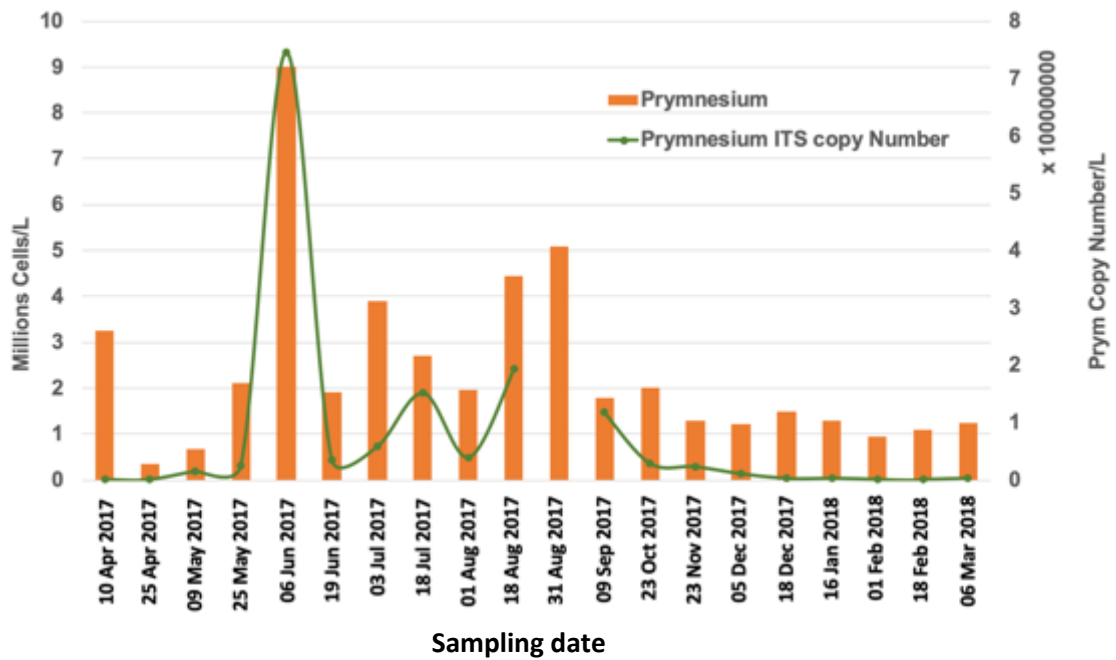
The trend in physico-chemical characteristics of Hickling broads reflected the seasonality with a single mild disturbance event of *P. parvum* bloom in June. Surface broad water temperature in spring was found to be around 4 °C followed by progressive warming in summer with a range from 16 to 24 °C (Fig. 4.2 a) reaching a maxima in June that coincided with a high abundance of *P. parvum* cells in the water column (~ 9 million cells L^{-1}). A subsequent cooling was observed through fall and winter with winter minima of approximately 2 °C. Total phosphate concentrations were mostly constant and remain relatively high throughout the sampling period with concentrations ranging between 50-125 μgL^{-1} (Fig. 4.2 b) and a peak observed in summer to early autumn, which coincided with increased abundance of *P. parvum* cells (Figs. 4.2 a and 4.2 b). A slight decrease in dissolved oxygen levels (DO) was also observed during the main *P. parvum* bloom peak in June and total suspended solid levels (TSS) were highest in these samples (Table 4.1). A Pearson correlation coefficient was conducted to examine the relationships between *Prymnesium* cell counts and Broad water physicochemical properties. *Prymnesium* counts and total phosphate was more strongly correlated, $r(18) = 0.66$, $p < .01$, than water temperature $r(18) = 0.58$, $p < .01$, and salinity $r(18) = 0.46$, $p < .05$. DO is negatively correlated, $r(18) = -0.54$, $p < .05$.

There was no obvious correlation on other measured water parameters and *P. parvum* abundance including, total nitrogen (TN comprising $\text{NH}_4^{2+} + \text{NO}_3^- + \text{NO}_2^-$), which have been previously proposed to stimulate *P. parvum* bloom onset (Lindholm et al., 1999; Litchman, 2010; Roelke et al., 2012; Patiño et al., 2014). In fact, the highest recorded *P. parvum* numbers were seen when the water inorganic nitrogen (IN)/inorganic phosphorous (IP) ratios, based on TN and TP, were relatively low at 0.32 (Table 4.1). Hickling broad has very low levels of TN ranging from ~ 5 to $>50 \text{ ugL}^{-1}$ (Fig. 4.2 C) with a winter mean concentration up to $\sim 50 \text{ ugL}^{-1}$. Low TN was observed from April to October and abruptly increased in December through March due to increased rainfall and tidal flushing of nutrient-rich waters from the Heigham Sound (Agricultural runoff) (Moss & Bales, 1989; Bennion, 2001; Hickling Broad Dossier, 2016). A large *Chl-a* spike ($69.6 \text{ }\mu\text{gL}^{-1}$) was observed during the June *P. parvum* bloom and another spike was observed in October and remained relatively high through winter months, which is apportioned to cyanobacteria and diatoms (Phillips et al., 2005) due to increased total nitrogen in the water column. Conversely, pH and salinity slightly decreased during the winter months (Table 4.1).

Table 4.1. Physical and chemical parameters in water samples from Hickling broad (station 5) during the course of the study period

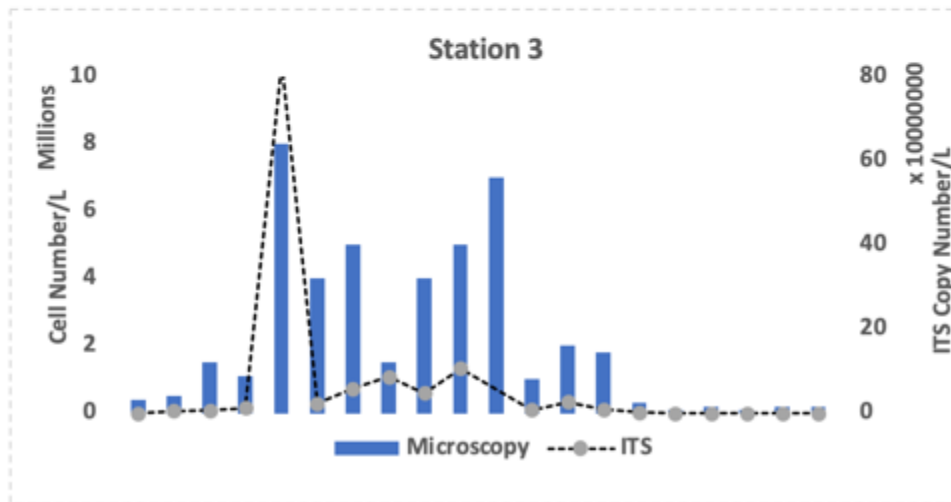
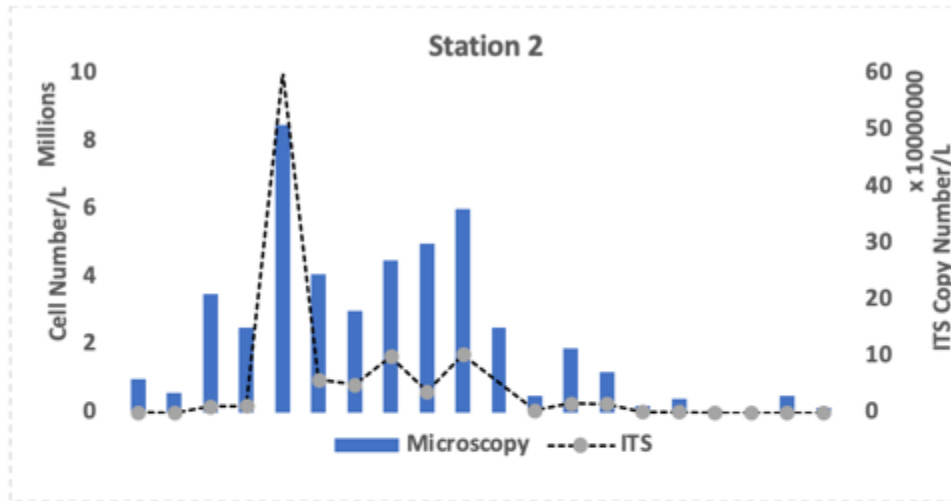
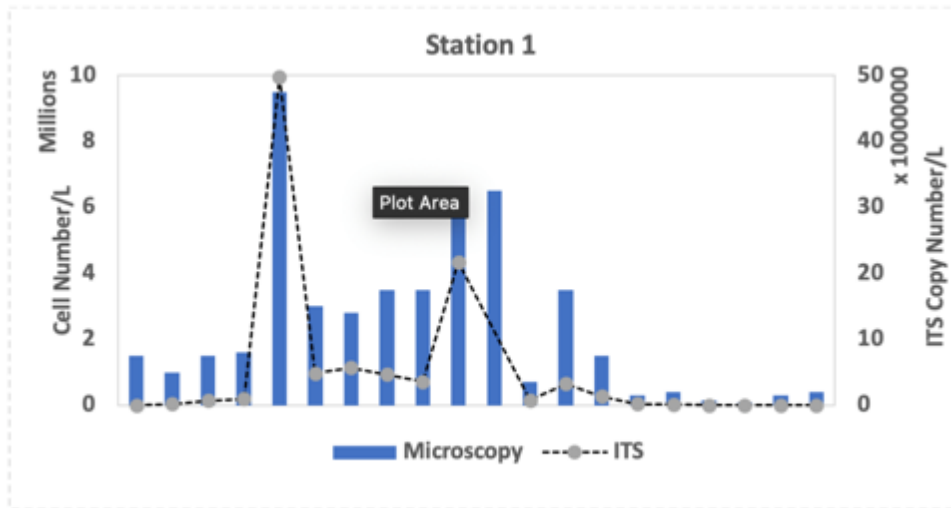
Date	Temp. (°C)	Diss. O ₂ (mg L ⁻¹)	pH	Salinity (‰)	SRP (µM)	NO ₂ ⁻ (µM)	NO ₃ ⁻ (µM)	NH ₄ ⁺ (µM)	DIN (µM)	N:P ratio	Chl-a (ugL ⁻¹)	TSS (mg/l)
10/04/2017	13.4	13.59	8.15	5.7	1.07	0.07	0.36	0.14	0.57	0.54	16.9	7.4
25/04/2017	10.1	13.5	8.17	5.9	1.36	0.07	0.36	0.14	0.57	0.42	20.8	5.2
09/05/2017	11.3	13.5	8.31	6.04	1.60	0.07	0.36	0.24	0.67	0.42	25.9	9.1
25/05/2017	10.7	11.02	8.79	5.76	2.55	0.07	0.36	0.37	0.80	0.31	28.1	n.m.
06/06/2017	17.6	9.35	8.62	5.91	3.84	0.07	0.39	0.78	1.24	0.32	69.6	29.8
19/06/2017	24	10	8.61	6.25	2.94	0.07	0.39	0.68	1.14	0.39	35.3	n.m.
03/07/2017	20.4	11	9.04	6.04	2.87	0.07	0.37	0.38	0.82	0.29	38.6	25.5
18/07/2017	19	10.94	8.97	5.96	2.58	0.07	0.36	0.36	0.79	0.30	34	n.m.
01/08/2017	20.4	10.94	8.6	6.06	2.50	0.07	0.36	0.24	0.66	0.27	32.7	25.4
18/08/2017	21.3	n.m.	8.74	5.9	2.29	0.07	0.36	0.36	0.79	0.34	34	n.m.
31/08/2017	17.9	11.36	8.37	6.08	2.03	0.07	0.36	0.27	0.70	0.34	37	15.9
15/09/2017	16	12.06	8.1	6.2	2.24	0.07	0.36	0.16	0.59	0.26	17.8	20.1
23/10/2017	12	n.m.	7.99	5.99	2.11	0.07	0.36	0.14	0.57	0.27	59.4	10.6
23/11/2017	9.3	11.3	7.93	5.4	2.11	0.22	3.05	0.14	3.41	1.61	79	15.9
05/12/2017	4.1	13.27	n.m.	6.5	1.35	0.22	3.31	0.19	3.72	2.75	37.1	7.5
18/12/2017	2.1	n.m.	n.m.	n.m.	0.94	0.41	19.56	6.18	26.15	27.93	34.4	5.9
16/01/2018	4.9	10.38	7.52	4.7	1.94	1.07	53.97	13.85	68.89	35.56	41	10.1
01/02/2018	4.6	16.4	7.63	5.3	1.60	1.09	54.83	10.35	66.27	41.30	48.4	12.7
18/02/2018	2.8	17.92	7.86	5.3	1.55	0.75	62.75	0.66	64.17	41.40	48.8	13.7
06/03/2018	2.6	16.3	7.76	5.1	1.79	0.44	53.83	0.85	55.12	30.76	35.8	15.7

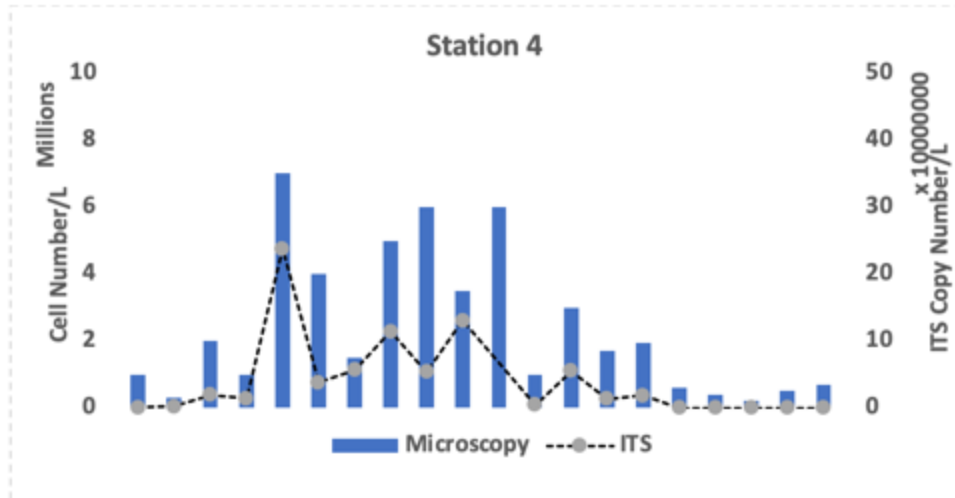
Concomitantly, sensitive qPCR methods were also employed to monitor the abundance of the *P. parvum* internal transcribed spacer (ITS) region within environmental DNA samples (Fig. 4.3).



Figures 4.3. Monitoring of *P. parvum* cells by basic microscopy (bar) and *P. parvum* ITS copies through qPCR (line) in the broad water samples from Hickling Broad at station 5. Showing trend of *P. parvum* population dynamics from April 2017 to March 2018. Values represent the average of three replicates with their respective standard deviations.

For this, total DNA was extracted from all Hickling water samples from stations 1- 5, and qPCR was done. *P. parvum* abundance estimates by both qPCR (line) and microscopy (bar) were very similar and highly correlated, $r(18) = 0.895$, $p < .001$, to each other over time in station 5 and rest of other sampling stations (Station 1: $r(18) = 0.917$, $p < .001$, Station 2: $r(18) = 0.769$, $p < .001$, Station 3: $r(18) = 0.748$, $p < .001$, and Station 4: $r(18) = 0.832$, $p < .001$) (Fig. 4.3 and Fig. 4.4). Station 5, previously found to be the site of the most devastating fish kills in a *P. parvum* bloom event of 2015 (Wagstaff et al., 2018), had the highest *P. parvum* values via both methods. The highest *P. parvum* abundance by either method was recorded during the onset of summer months and lasted until early autumn reaching to a maximum of 9 million cells L^{-1} (8.3×10^8 copies L^{-1}) in June 2017. These levels are just below the arbitrary bloom threshold number of about 10 million cells L^{-1} and *P. parvum* counts for the rest of the year remained at lower levels below 2 million cells L^{-1} ($<1 \times 10^6$ copies L^{-1}).

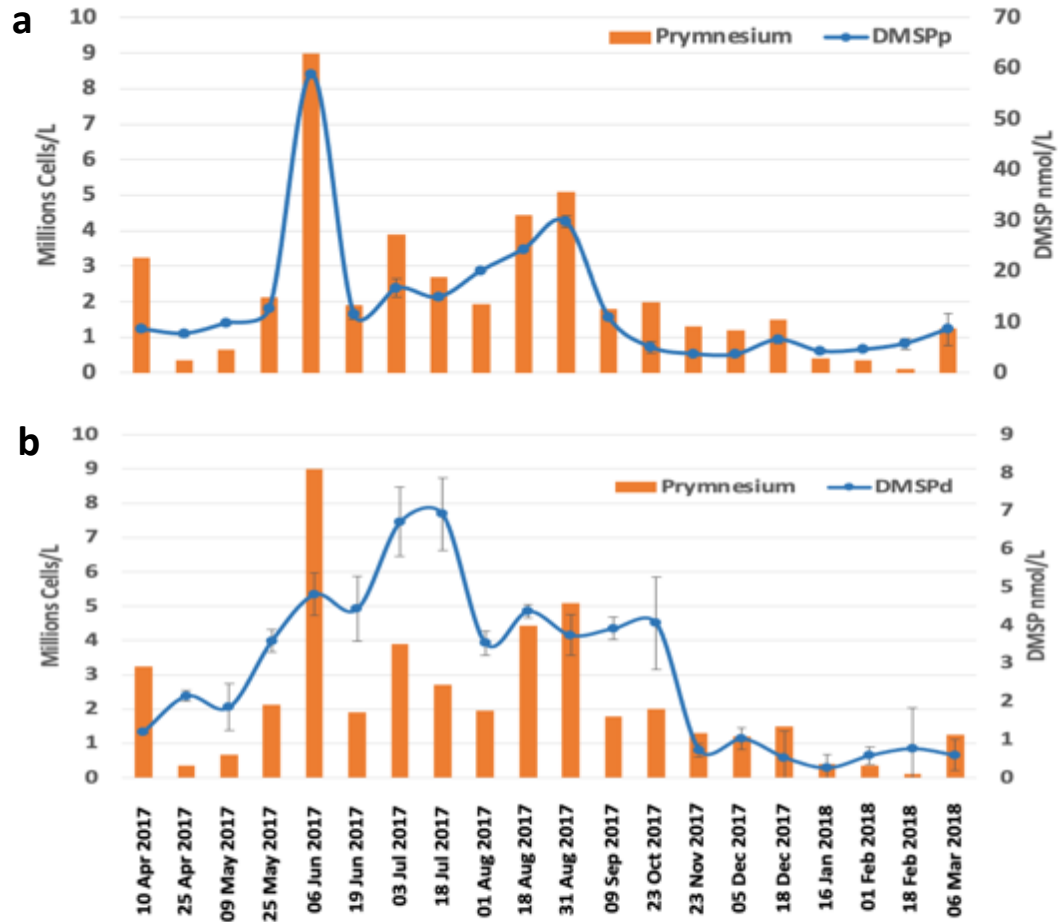




Figures 4.4. *P. parvum* cell counts by optical microscopy (bar) and *P. parvum* ITS copies through qPCR (line) in the broad water samples from Hickling Broad at four sampling stations. Showing trend of *P. parvum* population dynamics from April 2017 to March 2018.

4.3.2 Is *Prymnesium* a significant source of DMSP in the Broads

Having studied the dynamics of *P. parvum* abundance in Broad water samples, these same samples were examined for their DMSP levels within the algae (DMSP particulate, with a size > 0.4 μm) and in bacteria and water (DMSP dissolved, size < 0.4 μm). Interestingly, significant levels of $\sim 4\text{--}60 \text{ nmol L}^{-1}$ particulate DMSP_p were detected within Broads samples despite their brackish nature, which were comparable to those found in marine surface waters (Gali, 2015). Furthermore, the seasonal pattern of *Prymnesium* cell numbers (Fig. 4.5, bar) correlated (DMSP_p: $r(18) = 0.95$, $p < .001$ and DMSP_d: $r(18) = 0.64$, $p < .01$) with the average DMSP concentrations (Fig 4.5, line) in the water column and was characterized by a steep peak with concentration up to 58.8 nmol L^{-1} in June 2017 during the height of *P. parvum* bloom (Fig. 4.5)



Figures 4.5. Comparison of *P. parvum* abundance estimates obtained via microscope (bar) and DMSP concentrations (blue line) at station 5 from April 2017 to March 2018 in Hickling Broad. (a) Particulate DMSP (DMSP_p) vs *P. parvum* counts and (b) dissolved DMSP (DMSP_d) vs *P. parvum* counts. Values represent the average of three replicates with their respective standard deviations.

Relatively lower DMSP_p concentrations (less than 10 nmol L⁻¹) were measured before and after the blooming period (Fig. 4.5). Throughout the season, but most prominently in the *P. parvum* bloom event, DMSP was also detected in the dissolved fraction and thus could be a nutrient for microbial communities. Alternatively, it is possible that smaller microorganisms, e.g., bacteria, in these samples also produce DMSP (Curson et al., 2017; Williams et al., 2018), but based on my initial screening on culturable bacteria in Chapter 3, I haven't found any.

4.3.3 *P. parvum* DMSP production in the Broads

To provide further insight into *P. parvum* DMSP production in the Broads, we set out to measure the abundance and transcription of the *P. parvum* DMSP synthesis gene (*DSYB*) in the water samples. For this, we needed to isolate natural Broads *P. parvum* strains to enable identification of their specific *DSYB* gene/s and to design specific primers targeting them. Water samples were taken from the Broads during the minor *P. parvum* bloom of June 2017 (Fig. 4.3) and through a combination of single-cell micropipetting and antibiotic treatments, we isolated and made axenic cultures of Hickling *P. parvum* strains HIK PR1A, HIK PR6H, and HIK PR12D (Fig. 4.6).

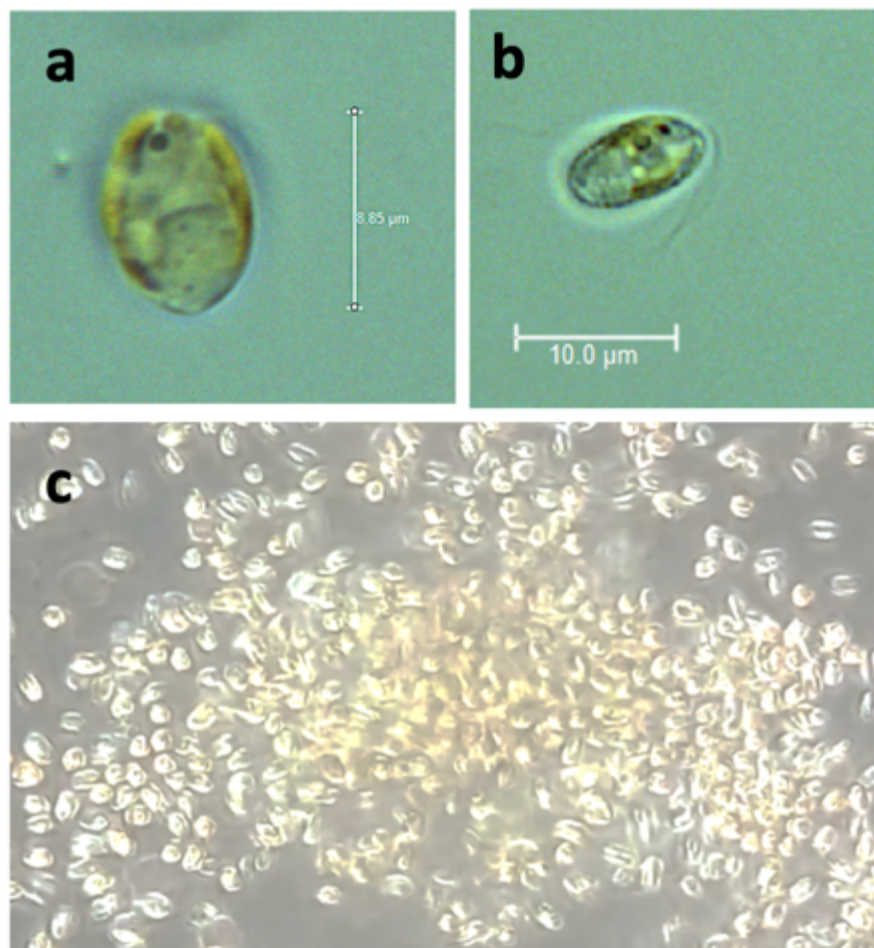
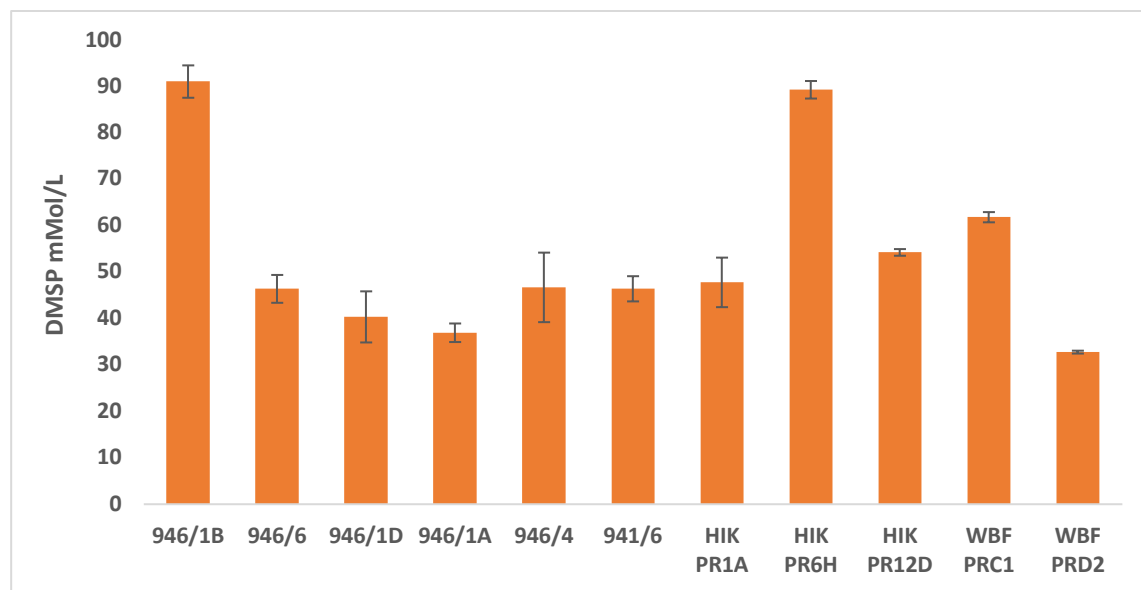


Figure 4.6. Light microscopy images of *P. parvum* HIK PR1A (a), HIK PR6H (b) and axenic culture of HIK PR1A at exponential phase (c).

These axenic strains were first shown to synthesise DMSP, see below, (Fig. 4.7). Then, from one of these strains *P. parvum* HIK PR1A, high-quality total RNA was extracted and sent out to Luxembourg Centre for Systems Biomedicine (LCSB) for RNA sequencing. A *DSYB* gene homolog and 99% identical to functional *P. parvum* *DSYB* from CCAP946/6 (Curson et al., 2018) at the nucleotide and protein level, respectively, was identified in *P. parvum* HIK PR1A.



Figures 4.7. Comparison of DMSP produced (DMSP per cell volume) by different strains of *P. parvum* from culture collections as well as the newly isolated strains from Hickling Broad, Norfolk and Woodbridge Fen Fisheries, Suffolk. All cultures were grown at 35 PSU salinity and DMSP was measured at the late exponential phase (22 days).

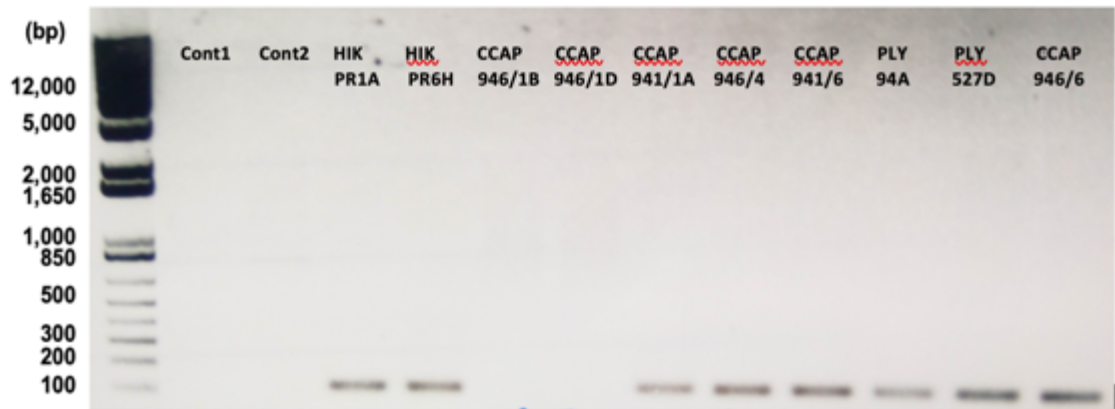
To determine if this candidate *DSYB* gene in HIK PR1A was functional, it was cloned into expression vectors and assayed in *R. leguminosarum* J391 and an *L. aggregata dsyB⁻* mutant J571 for methylthiohydroxybutyrate S-methyltransferase activity (Table 4.2). The cloned HIK PR1A *DSYB* conferred this activity to *R. leguminosarum* J391 and fully complemented the bacterial *dsyB⁻* mutant for its DMSP production (Table 4.2). Thus, *DSYB* gene from *P. parvum* HIK PR1A is functional.

Table 4.2. DMSP production by *Rhizobium leguminosarum* and *Labrenzia aggregata* expressing cloned *P. parvum* *DSYB* gene and DMS production of *Escherichia coli* and *Labrenzia aggregata* mutant with cloned *Alma* gene

Strains	Growth Medium	DMS/DMSP production (pmol µg protein ⁻¹)
<i>Labrenzia aggregata</i> LZB033	MBM (minimal)	8.4 ± 2.2
<i>Rhizobium leguminosarum</i> J391 (Control)	RM (minimal) + 0.5 mM Met + 0.5 mM MTHB	ND
<i>Labrenzia aggregata</i> J571 (LZB033 <i>dsyB</i> -) (Control)	MBM (minimal) + 0.5 mM Met + 0.5 mM MTHB	ND
<i>Rhizobium leguminosarum</i> J391:PBIO2359 (cloned <i>P. parvum</i> HIK PR1A synthesized <i>DSYB</i>)	RM (minimal) + 0.5 mM Met + 0.5 mM MTHB	26.54 ± 2.7
<i>Labrenzia aggregata</i> J571:PBIO2359 (cloned <i>P. parvum</i> HIK PR1A synthesized <i>DSYB</i>)	MBM (minimal) + 0.5 mM Met + 0.5 mM MTHB	12.19 ± 0.6
<i>Labrenzia aggregata</i> J571:PBIO2358 (cloned <i>P. parvum</i> HIK PR1A <i>DSYB</i> from cDNA)	MBM (minimal) + 1 mM Met + 0.5 mM MTHB	12.33 ± 0.1
<i>Escherichia coli</i> 803:PBIO2360 (cloned <i>P. parvum</i> HIK PR1A synthesized <i>Alma</i> -like gene)	MBM (minimal) + 10 mM Succinate + 5 mM DMSP	ND
<i>Labrenzia aggregata</i> J572 <i>dddL</i> ⁻ :PBIO2360 (cloned <i>P. parvum</i> HIK PR1A synthesized <i>Alma</i> -like gene)	MBM (minimal) + 10 mM Succinate + 5 mM DMSP	ND

*ND, not detected.

I designed and optimized specific qPCR primers (Chapter 2, Table 2.3) to the HIK PR1A *DSYB*, which amplify a 130 bp *DSYB* fragment from DNA and cDNA from *P. parvum* cultures and environmental samples (Fig. 4.8). Note these primers amplify a specific *DSYB* fragment from both Broads isolates, HIK PR1A and HIK PR6H and most of *P. parvum* strains from culture collections (Fig. 4.8).



Figures 4.8. Gel electrophoresis image showing the optimised PCR amplification of *DSYB* using qPCR primers on 10 different *P. parvum* strains from culture collections as well as the 2 newly isolated strains for Hickling Broad and water control (Cont1/2). This amplification was carried out using the primer set qParv_1_F and qParv_1_R, amplifying a 130bp fragment. Run against a 1Kb Plus ladder.

These *DSYB* primers were used in qPCR and RT-qPCR on community DNA and cDNA extracted from the Broads samples to measure the abundance and transcription of *P. parvum DSYB* allowing for comparison to the temporal pattern of DMSP levels in the water column. *P. parvum DSYB* copy ($r(18) = 0.807$, $p < .001$) and transcript numbers ($r(18) = 0.736$, $p < .01$) clearly followed the general same trend as for DMSP concentration and *Prymnesium* cells in the water samples (Fig. 4.9 a). *P. parvum DSYB* copy numbers and transcripts were highest in samples corresponding to the two most significant peaks of *P. parvum* cell numbers and DMSP content, the largest being in June (20.9×10^6 copies L^{-1} and 9.1×10^6 copies L^{-1}) with $58.8 \text{ nmol } L^{-1}$ DMSP, and then a peak of $29.7 \text{ nmol } L^{-1}$ DMSP in August 2017 (18.6×10^6 copies L^{-1} and 11×10^6 copies L^{-1}). This data is consistent with *P. parvum* being responsible for much of the DMSP in the environmental samples and is the first time *DSYB* has been targeted and linked to DMSP production in any aquatic sample.

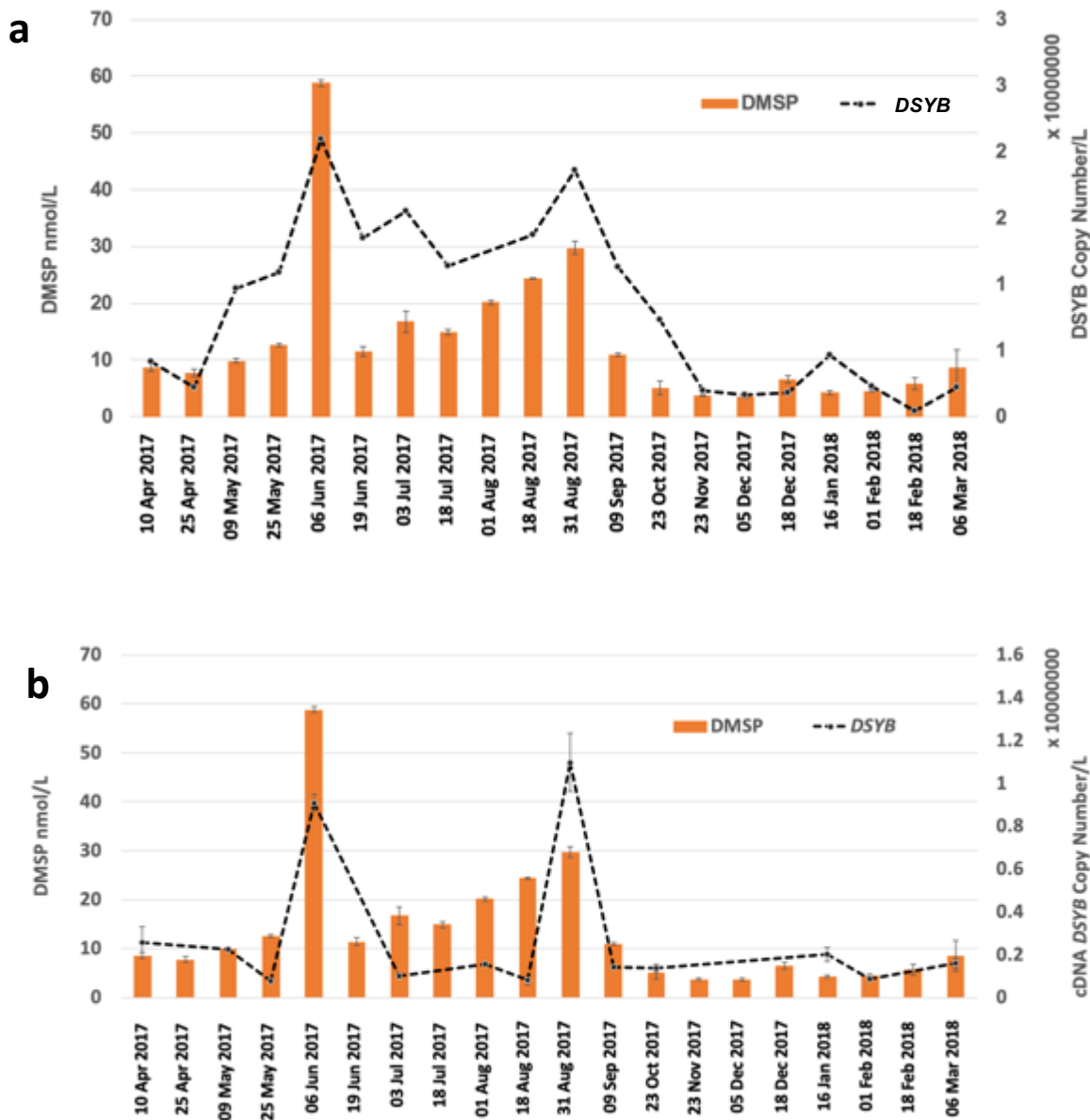


Figure 4.9. Comparison of DMSP concentrations (bar) as measured by GC and *DSYB* abundance via qPCR (dash line) (a) and *DSYB* transcript copies via RT-qPCR (b) at station 5 from April 2017 to March 2018 in Hickling broad.

4.3.4 Does *P. parvum* cleave DMSP?

Although many algae, including *P. parvum*, contain candidate Alma DMSP lyase enzymes, it is difficult to predict functional Alma enzyme unless they have very high similarity to *Emiliania huxleyi*, *Isochrysis galbana*, and *Symbiodinium sp.* Alma (Alcolombri et al., 2015). The assembled *P. parvum* HIK PR1A transcriptome was shown to contain a candidate Alma DMSP lyase, 99 % identical to those in other marine *P. parvum* strains, but only ~ 28.35 % identical to the functional *E. huxleyi* Alma1. The HIK PR1A candidate Alma was cloned and assayed for DMSP lyase activity in *E. coli* and a *Labrenzia aggregata dddL⁻* mutant (J572). In both these heterologous hosts, the candidate Alma enzyme was shown to have no significant DMSP lyase activity compared to control experiments (Table 4.2). Furthermore, the Broads *P. parvum* strains and those of marine origin from culture collections (e.g. CCMP 946/6) were incubated in the presence of 5 mM DMSP, but no DMSP lyase activity was detected. It is possible that the extracellular DMSP is not imported or able to interact with intact *P. parvum* DMSP lyases, thus, *P. parvum* cell-free extracts were also incubated with 1 mM DMSP, and again no significant DMSP lyase activity was observed. These data are consistent with the *P. parvum* Alma-like proteins not being functional DMSP lyases and these important HAB algae not having DMSP lyase activity. More relevantly to *P. parvum*, the data suggest that DMSP may be an important molecule that the algae does not want to degrade. Further work is required to establish what defines a functional Alma family DMSP lyase and to establish the source DMSP in the dissolved fraction.

4.3.5 Broads Bacterial DMSP Catabolism (Temporal Change)

Having established that similar amounts of DMSP exist in the brackish Broads water as in many surface seawater samples and that some bacteria associated to *P. parvum* blooms are known for their ability to catabolise DMSP, e.g., *Roseobacter*, and that I isolated a *Shewanella* strain capable of cleaving DMSP from Broads water, we investigated the potential for bacterial catabolism in these samples. To do this, RT-qPCR was done on environmental RNA from the Broads samples to target transcription of the DMSP demethylase gene *dmdA* (Varaljay et al., 2010; Levine et al., 2012) and the most abundant DMSP lyase gene *dddP* (Todd et al., 2009; Liu et al., 2019). Despite the presence of some Roseobacters, many of which are known to contain *dmdA* and *dddP*, in water samples with high *P. parvum* counts, *dmdA* (degenerate primer pair) was not successfully amplified from any sample. This is entirely consistent with DMSP demethylation and *dmdA* being characteristic of marine environments. In contrast, *dddP* was amplified but only at very low levels

between 1.1×10^3 to 9.1×10^4 transcripts L^{-1} (1.29×10^4 transcripts L^{-1} average). The *dddP* transcript levels did not correlate with DMSP levels nor the abundance of *P. parvum* or its demise (Fig. 4.10). However, it should be noted that only standing stock DMSP concentrations were measured and DMSP turnover and DMS production rates, not considered here, are required for a better indication of whether DMSP catabolism is an important process in these waters. Also, *dddP* is only one of seven known bacterial DMSP lyase genes (Sun et al., 2016; Johnston et al., 2016), and the others were not investigated here. Nevertheless, given *dddP* transcripts were detected, this likely indicate that these brackish waters are potential sources of DMS, fed by algal derived DMSP.

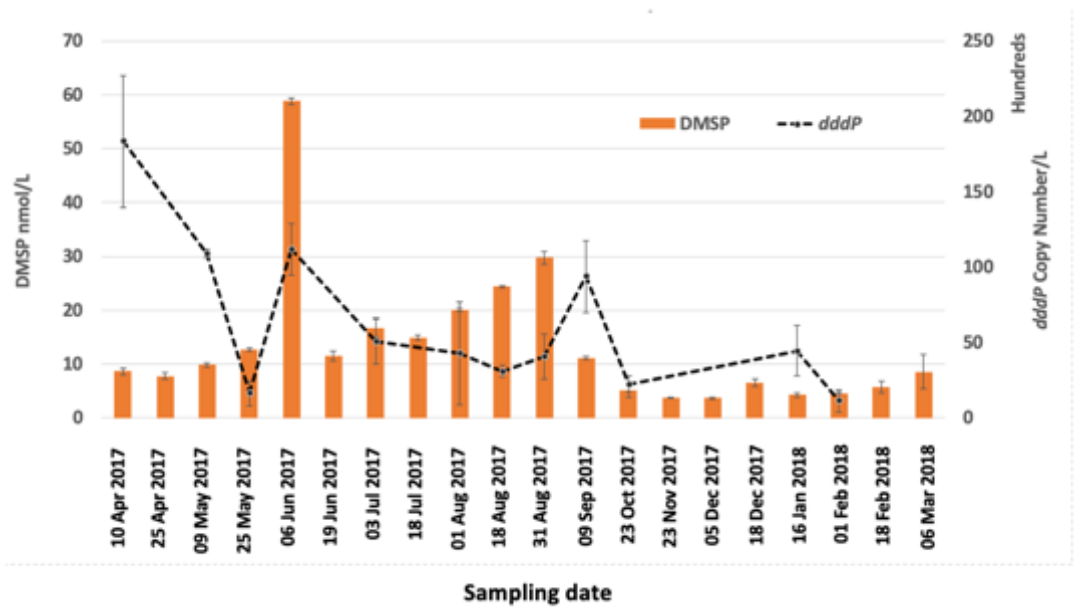


Figure 4.10. Comparison of DMSP concentrations (bar) as measured by GC and bacterial *dddP* transcription copies through RT-qPCR at station 5 from April 2017 to March 2018 in Hickling broad.

4.4 Discussion

The observations presented in this study provide new insights into the ecological role/s of DMSP on the survival and expansion of *P. parvum* blooms in shallow lake systems. It increased our understanding of DMSP production and biogenic sulfur cycling for these systems as influenced by recurring HAB events. To our knowledge, this is the first study that investigated the abundance and transcription of key eukaryotic DMSP synthesis gene (*DSYB*) in relation to DMSP concentrations and algal populations in the field.

4.4.1 *P. parvum* and DMSP

One ecological strategy that favour *P. parvum* expansion and establishment success is the ability to synthesize and utilize DMSP and DMS. Haptophytes (like *P. parvum*), dinoflagellates and chrysophytes are prolific producers of DMSP (Keller et al., 2012). About 90% of the reduced sulfur found in algae is in the form of DMSP, but much about the regulation of its biosynthesis and uptake is still not fully understood (Gage et al., 1997). Nevertheless, many of the proposed roles for these compounds would be beneficial to phytoplankton trying to survive in an ever-changing environment. Several proposed physiological functions include roles as an osmolyte (compatible solute), antioxidant, predator deterrent, photosynthetic overflow mechanism, a signalling molecule, antimicrobial/antiviral, cryoprotectant, as a means of balancing excess cellular energy. (Kirst et al., 1990; Karsten et al., 1996; Wolfe & Steinke, 1997; Stefels & van Leeuwe, 1998; Stefels, 2000; Sunda et al., 2002; Raina et al., 2013). Only few studies focus on DMSP/DMS cycling in freshwater systems (Ginzburg et al., 1998; Sela-Adler et al., 2015; Brailsford et al., 2020), as DMSP/DMS production is thought to be prevalent only in marine and estuarine environments.

In studying an inland brackish/freshwater inland lake, the Hickling broad, we found that DMSP production showed positive correlation ($r = 0.95$, $p < 0.001$) with the abundance of *P. parvum* cells based on microscopic data and molecular probing (qPCR, *P. parvum* ITS2), suggesting that *P. parvum* cells were most likely to be the main drivers of DMSP production in this inland lake system.

4.4.2 *P. parvum* DMSP synthesis and breakdown

We isolated strains of *P. parvum* specific to Hickling broad, sequenced/characterized their DMSP synthesis gene (*DSYB*), proved that it is functional and that *DSYB* abundance and expression in the environment correlates with the particulate DMSP concentration in the water column. We tested a candidate Alma DMSP lyase from Broads *P. parvum* isolates and found it was not functional and that the isolates themselves lacked DMSP lyase activity, indicating an important role for DMSP for this haptophyte.

Only a few species of freshwater phytoplankton are known to produce DMSP/DMS (Ginzburg et al., 1998; Steinke et al., 2018), and their cellular production were small compared to organisms originating from the marine environment, e.g., *P. parvum*. Our broad's *P. parvum* strains produce DMSP up to $\sim 90 \text{ mmol L}^{-1}$ cell volume, similar to what has been reported in the past (Keller, 1989; Hatton et al., 2007) and in other *P. parvum* strains isolated from various marine and aquatic habitats (this study). Furthermore, we investigated the possible presence of bacterial DMSP catabolic (*dddP* and *dmdA*) genes, which are known to be active during DMSP release from phytoplankton during cell death (autolysis) or grazing in marine field samples. We found no detectable DMSP demethylation genes in the broads samples and only very low *dddP* levels, suggesting that either DMSP breakdown in freshwater/brackish water systems might be governed by other DMSP lyase/degrading genes yet to be identified or that these processes are no relevant in these ecosystems. It is noteworthy that we did not examine the abundance of *dddY* which is known to exist in some *Shewanella* spp. like those I isolated in the previous chapter.

4.5 Conclusion

This study provides new insights into the functional/ecological role of DMSP on the survival and expansion of invasive HAB-forming organisms such as *P. parvum*. Significant correlations between *P. parvum* population, DMSP concentrations, and *DSYB* gene abundance/transcription were found, implying that DMSP production on the broads was mainly due to the presence of *P. parvum* cells. Furthermore, it demonstrates the importance of algal-derived DMSP and the potential for its breakdown in lake systems. The significance of these processes to global biogeochemical cycling and if they are a significant source of climate active gases requires further investigation.

Chapter 5

Effects of growth phases, salinity, nutrients, and oxidative stress on DMSP production of the haptophyte algae *Prymnesium parvum*

This chapter is being prepared for publication:

Rivera, P.P.L., Zhou, S., Curson, A.J., Pratscher J., Brooks E., Field R.A., Murrell, J.C., and J.D. Todd. Understanding the ecological role DMSP on the expansion and success of ecosystem destructive harmful algal blooms (HABs) in shallow wetland/lake systems.

5.1 Introduction

Dimethylsulfoniopropionate (DMSP) is a ubiquitous sulfur metabolite compound found throughout the marine and other aquatic environments because it constitutes a major intracellular solute of most dinoflagellates, haptophytes, diatoms, other phytoplankton, macroalgae, and corals (Kettles et al., 2014; Gage et al., 1997; Raina et al., 2013). There are several known physiological functions for DMSP in micro- and macroalgae. In marine microalgae, it is one of the major compatible solutes that stabilises enzymatic processes and regulates osmotic pressure. It serves as a methyl donor in cell metabolism (Kirst, 1996, Randal et al., 1996, Stefels, 2000) and potentially serves as a ballast mechanism in an aflagellate phytoplankton (Lavoie et al., 2016). It was also found to have a grazing repellent function (Wolfe & Steinke., 1997; Strom et al., 2003) and potentially have an ecological side effect as an info-chemical (Steinke et al., 2002). As a signaling molecule, DMSP production and breakdown has been reported to be involved in antiviral defense mechanisms and sulfide detoxification (Havill et al., 1985; Evans et al., 2006; Seymour et al., 2010). DMSP was also found to have a cryoprotective function in polar macroalgae (Karsten et al., 1996) for they have higher intracellular DMSP content compared to their tropical and sub-tropical counterpart. In some organisms, DMSP and its downstream products may function as antioxidants that can scavenge toxic intracellular hydroxyl and reactive oxygen radicals (Sunda et al., 2002).

However, despite these numerous developments in understanding the physiological significance or role of DMSP in these organisms, there are still many uncertainties in predicting the role of this molecule in organisms, the variability of its production and the subsequent release of DMS into the atmosphere (Kettle et al., 1999). This is partly due to the fact that there is no direct link between DMS emission and primary production (Leck et al., 1990), chlorophyll or any taxon-specific marker pigment concentration (Andreae 1990; Kiene et al., 2000; Dacey et al., 1998) but the main reason behind this is that there are great uncertainties surrounding DMSP production at different physiological states of the studied organisms and their response to changing environmental conditions.

DMSP production is known to be affected by many biotic and abiotic factors such as, growth phase, salinity, light, temperature, nutrients, and oxidative stress (van Rijssel & Gieskes 2002; Sunda et al., 2002; Spielmeyer & Pohnert, 2012; Arnold et al., 2013). Some studies have reported a decrease in the intracellular DMSP content of the dinoflagellate *A. carterae* during the growth

from the log phase to stationary phase (Simó et al., 1998; Hatton & Wilson, 2007). On the other hand, other studies observed an increase in DMSP and DMS production until late stationary to senescent stages of growth in different taxa (dinoflagellates, prasinophytes, coccolithophores, and diatoms) with a positive correlation with cell density (Zhuang et al., 2011; Liu et al., 2014). Therefore, DMSP production varies between taxa and dependent on the algal growth stage or phase.

Among abiotic factors, salinity in particular, has been extensively shown to regulate DMSP production and accumulation in algae and higher plants (Stefels, 2000). An increase of DMSP production and accumulation with salinity has been observed for different microalgal species such as diatoms (i.e. *Skeletonema costatum*), prymnesiophytes (i.e. *Phaeocystis spp.*) and some dinoflagellates (Vairavamurthy et al., 1985; Dickson & Kirst, 1986; Karsten et al., 1992; Stefels, 2000; Zhuang et al., 2011; Kettles et al., 2014). This is also supported by studies done in the field, where they found positive correlations between DMSP and salinity from the estuarine to the coastal and shelf environments (Iverson et al., 1989; Sciare et al., 2002). The accumulation or release of DMSP in response to the extreme environmental salinity gradients encountered by sea-ice diatoms is well documented (Lyon et al., 2016). They can accumulate DMSP in higher concentrations than their low DMSP producer counterparts (Keller et al., 1989). Thus, indicates the importance of DMSP as an osmoregulatory compound especially in halotolerant species of microalgae.

DMSP production was also previously assumed to be influenced by nitrogen concentration because high DMS concentrations were found mostly in the oligotrophic environment. It was proposed that under low nitrogen conditions, high sulfate environments, such as in seawater, DMSP might substitute its nitrogenous organic analog glycine betaine (GBT) (Andreae, 1986; Thierstein & Young, 2004). However, there is no clear evidence of the reciprocity between the intracellular content of DMSP and GBT due to the dominance of DMSP in most algal species investigated (Keller *et al.*, 1999). Nonetheless, DMSP synthesis is related to the cellular nitrogen metabolism, since the deamination of its amino acid precursor methionine releases reduced nitrogen for other cellular function (Greene, 1962; Gage et al., 1997, Stefels, 2000). Thus, nitrogen availability affects key metabolic pathways involved in the growth and overall survival of phytoplankton. N-limitation causes a reduction in the accumulation of free nitrates, amino acids and proteins. Furthermore, N-limitation affects algal photosynthesis inducing oxidative stress by causing excessive accumulation of carbon components and reduction in electron

transfer (Hockin et al., 2012). Increased intracellular DMSP production was reported in phytoplankton cultures grown under low nitrogen growth conditions (Turner et al., 1988; Gröne & Kirst, 1992; Matrai & Keller, 1994; Stefels & van Boekel, 1993; Sunda, 2007). For the diatom *Thalassiosira pseudonana*, the synthesis of DMSP is upregulated when cells reach the N-limited conditions (Hockin et al., 2012; Bromke et al., 2013; Kettles et al., 2014). The same was observed in chain-forming coastal diatom *Skeletonema costatum* (Sunda et al., 2007). DMSP is likely to have a role in alleviating the oxidative stress produced by N limitation (Sunda et al., 2002; Hockin et al., 2012). For haptophytes, such as *E. huxleyi*, cultures grown in no nitrate supplemented media showed higher intracellular DMSP concentration as compared to cultures grown in media with nitrate supplement (Green & Leadbeater, 1994). In contrast, Sunda et al. (2007) reported that under nitrogen-limited conditions, *E. huxleyi* (CCMP 374) showed no significant increase in DMSP production. Therefore, increased DMSP production due to N availability might not be true for all DMSP-producing phytoplankton or even between strains of the same species.

Nutrient limitation can cause metabolic imbalances that can disrupt the photosynthetic mechanism of phytoplankton. This can lead to an increase in the production of short-lived reactive oxygen species (ROS) and increase oxidative stress (Sunda et al., 2002) for ROS such as hydrogen peroxide and hydroxyl radicals are by-products of photosynthesis (Niogi, 1999). ROS can be neutralized or sequestered by DMSP through oxidation to form DMSO (Kinsey et al., 2016). Therefore, the generation of ROS under oxidative stress condition promotes DMSO production (Sunda et al., 2002; Kinsey et al., 2016) and the intracellular DMSP/DMSO ratio serves as an indicator of oxidative stress (Hatton & Wilson, 2007). This suggests DMSP's role as an antioxidant compound with overlapping functions in redox control.

In this chapter, I examined the effect of biotic factors such as different growth phases/stages and the presence of viral-like particles (VLPs) on growth response and intracellular DMSP production in *P. parvum*. In addition, the effect abiotic variables such as growth-limiting nutrients (i.e. nitrogen, N), presence of ROS (hydrogen peroxide, H₂O₂) to induce oxidative stress, and varying salinity was also investigated. Results generated from these investigations will provide a better understanding of the effect of these biotic and abiotic variables on DMSP production and regulation of an invasive bloom-forming haptophyte *P. parvum* and how these variables could impact the biogeochemical sulfur cycling in areas where they tend to bloom.

5.2 Methods

5.2.1 Strains of *Prymnesium* tested

Xenic and axenic cultures of *P. parvum* CCAP946/1B, *P. parvum* CCAP946/6, *P. parvum* CCAP946/1D, *P. parvum* CCAP941/1A, *P. parvum* f. *patelliferum* CCAP946/4, and *P. parvum* CCAP941/6 from culture collections and newly isolated strains, *P. parvum* HIK PR1A, *P. parvum* HIK PR6H, *P. parvum* HIK PR12D, *P. parvum* WBF PRC1 and *P. parvum* WBF PRD2, were used in this the study. Full details of all the strains origin, growth maintenance, and isolation process are previously discussed in Chapter 2.

At the start of each experiment, experimental flasks were inoculated with a *P. parvum* stock culture in the late exponential growth phase to obtain an initial cell density of 10^4 cells ml^{-1} . The inoculation marked the starting time of the experiments. Sampling was done in the middle of the photoperiod over the course of each experiment to avoid the possibility of any existing diurnal rhythm in the algal cell division.

5.2.2 Biomass sampling and preparation

The sampling for DMSP detection and measurement by GC was carried out by either vacuum filtration or centrifugation as described in Chapter 2. In brief, when using the filtration method, *P. parvum* cultures were filtered onto 47 mm GF/F glass microfiber filters (0.7 mm particle retention rate) using a vacuum pump at the lowest possible pressure to avoid algal cell breakage. Filters were fitted into 2 ml screw-capped tubes and added with 1 mL of Methanol (MeOH) to extract the algal metabolite then stored overnight at 4°C in the dark before DMSP measurement by Gas Chromatography (GC), otherwise stored -80 °C for future measurements. For centrifugation, *P. parvum* cultures were centrifuged and pelleted. The pellets were transferred to a 2 ml screw-capped tube and 1 mL of MeOH was added to extract the algal metabolites. The mixtures were stored overnight at 4 °C before DMSP measurement using the GC or stored at -80 °C for future measurements. Methanolic metabolite extraction was used for all *Prymnesium* samples throughout the entire study.

5.2.3 Growth measurements

To monitor and measure the number of *P. parvum* cells in the cultures, aliquot samples at certain time points was taken and cell counting was done using a CASY TT cell counter. Temporal variations in the potential maximum quantum yield of photosystem II was monitored by measuring Fv/Fm ratio using a PAM fluorometer (WATER-PAM, Heinz Walz, Germany). All PAM measurements were done at the same time when samples were taken for cell counting. Full details of cell count measurement and PAM fluorometry were described in Chapter 2.

5.2.4 Intracellular DMSP Measurements

To detect and measure DMSP by gas chromatography (GC) assays, headspace DMS produced from the alkaline lysis of DMSP was measured. All DMSP measurements were performed using a gas chromatograph equipped with a flame photometric detector (GC-FPD). See Chapter 2, Section for more details on DMSP measurement via headspace method.

5.2.5 *P. parvum* growth phases

Since stock cultures of *P. parvum* strains were maintained at different salinity, growth curves were first determined at this condition (Supplementary Fig. 5.1). Then, batch cultures of newly isolated *P. parvum* strains were gradually acclimated with increasing salinity until they reached 35 PSU. This was done by multiple rounds of subculturing until new generations of *P. parvum* strains (new strains) stabilised at this salinity. New growth curves were generated, and algal growth phases/stages were identified for biomass sampling for DMSP measurements. Five sampling time points were used based on these curves: day 16 for mid-exponential phase, day 22 for early stationary phase, day 28 for stationary phase, and days 36, 46 as senescent phases (Fig. 5.1, red arrows). Five strains of *P. parvum* from culture collections and two newly isolated strains were used for this growth phase-influenced DMSP production experiment.

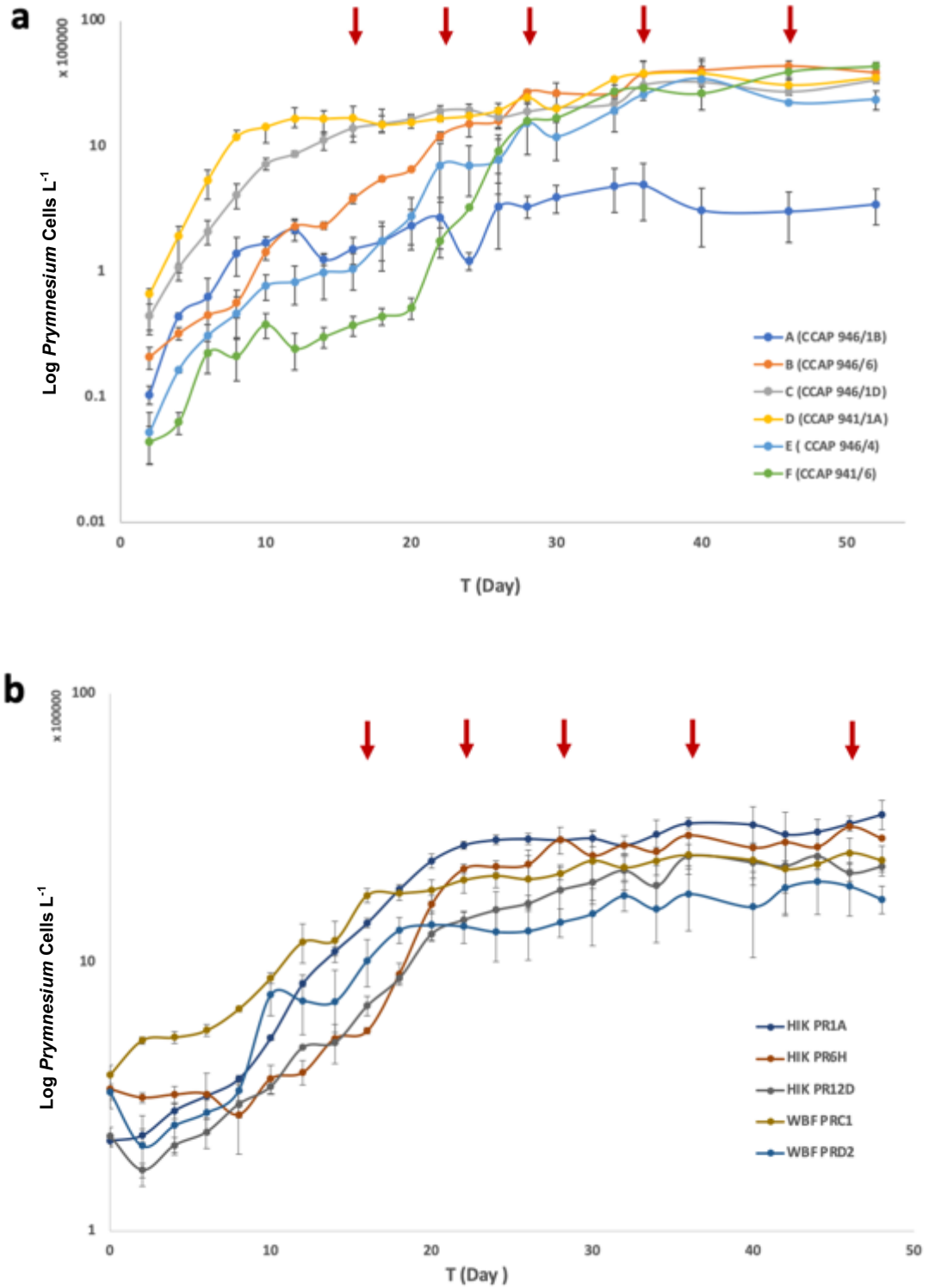


Figure 5.1. Growth curves of different *P. parvum* strains obtained from culture collections (a) and newly isolated *P. parvum* strains from Hickling Broad and Woodbridge Fen Fisheries (b). Red arrows indicate the sampling time points.

An accidental generation of non-motile state of *P. parvum* cells known as 'cysts' (Fig. 5.2, see figure below) was discovered for *P. parvum* CCAP 946/6 strain cultures in F/2 agar plates that was previously prepared for immunogold labelling and left in the plant growth room for 3 years without any intervention.



Figure 5.2. Light micrograph of intact resting 'cysts' of *Prymnesium parvum* CCAP 946/6 formed on the surface of solid f/2 agar plate stored for 3 years. Scale bar = 10 μm .

The viability of these cysts cells was tested and confirmed by inoculating the non-motile cells into fresh liquid growth medium and allowing them to grow. After a few days, germination occurred, and several vegetative cells were found in the liquid culture confirming the viability of the resting cells to germinate. Resting stages of *P. parvum* are rarely reported and no *Prymnesium* cysts have been found in the field or *in situ*. Only a few studies have reported their occurrence either from cultured strains or by microscopical observation of cyst formation (Pienaar, 1980; Wang & Wang, 1992; Beltrami et al., 2007), and they are difficult to generate in laboratory condition. The role of the resting cyst in the life cycle/history and survival of *Prymnesium* is still ambiguous.

DMSP from these non-motile cells was also measured to elucidate the intracellular DMSP values in *P. parvum* at its cyst or resting stage form. This was done by gently scraping off the algal colonies at the surface of the agar plates and resuspending cells in ESAW media. Once suspended, the colonies were gently agitated by vortexing to separate the aggregated cells. Then, the same sample preparation procedure for cell counting and metabolite extraction were done as detailed in Chapter 2.

5.2.6 Different salinity treatments

Before starting the actual salinity treatments, stock cultures of *P. parvum* strains (CCAP946/1B, CCAP946/6, CCAP946/1D, CCAP941/1A, CCAP946/4, CCAP941/6 and HIK PR1A) were inoculated into low (10 PSU), standard normal (35 PSU) and high salinity (50 PSU) media allowing the cells to acclimate in different salinity regimes. The third generation of these cultures was used as the starting stocks for salinity treatments. Three salinity treatments were tested (5, 10, and 50 PSU) and compared with a control of normal standard salinity (35 PSU). Each of the 3 conditions including control was performed in 3 replicate flasks. To obtain the salinities described above, the amount of salts added to the artificial seawater ESAW medium (described in Chapter 2) were adjusted. Erlenmeyer flasks (250 ml volume) containing f/2 enriched ESAW medium at varying salinities were then inoculated with pre-acclimated stock culture to obtain 200 ml of starting batch cultures at approximately 10^4 cells ml⁻¹. Algal cell counts were monitored at regular intervals where the inoculation marked as the starting time of the experiment (Day 0 or T = 0). The cultures were monitored until they reached the late stationary or senescent phase, but my DMSP investigations focused on the period of late exponential growth or early stationary (Day 22) where it was found to be the peak of DMSP production for *P. parvum* based on DMSP measurement at different growth phases.

5.2.7 Varying nitrogen conditions

The effect of varying nutrients (Nitrogen, N) on the growth and DMSP production of *P. parvum* was investigated. For increased (High N or HN) or decreased (Low N or LN) nitrogen, the f/2 medium was adjusted to contain 8820 μ M (1000% of standard f/2) or 44.1 μ M (5% of standard f/2), respectively. Standard f/2 media was used as normal control (NN or NP). For varying nitrogen treatments, *P. parvum* strains CCAP 946/1B, CCAP 946/6, CCAP 946/1D, PLY 595, PLY 94A, and HIK PR1A were used. Erlenmeyer flasks (250 ml volume) containing the modified f/2 enriched ESAW medium were inoculated with a stock culture to obtain 200 ml of starting batch cultures with cultures containing approximately 10^4 cells ml⁻¹. Each of these conditions was performed in 3 culture replicates. Algal cell counts were monitored at regular intervals where the inoculation marked as the starting time of the experiment (Day 0 or T = 0). The cultures were monitored until they reached the late stationary or senescent phase, biomass sampling was taken at early stationary phase (Day 22) where it was found to be the peak of DMSP production for *P. parvum* based on the initial DMSP measurement at different growth phases.

5.2.8 Oxidative stress (H₂O₂) treatments

To investigate the effect of oxidative stress on DMSP production of *P. parvum*, a short-term ROS exposure experiment through the addition of hydrogen peroxide (H₂O₂) was done. Naturally, H₂O₂ (10-100 nM) is one of the short-lived ROS by-products of phytoplankton during oxidative metabolic processes. Its overproduction, however, can lead to oxidative stress (Sunda et al., 2002). For this experiment, cultures of *P. parvum* CCAP 946/6 were treated with different H₂O₂ concentrations. 0.25 mM, 0.75 mM or 2 mM of H₂O₂ was added to the culture and biomass sample was taken immediately after the addition of H₂O₂ (0 h), after 0.5 h, 1 h and 3 h for cell counting and DMSP measurement. A non-H₂O₂ treated culture was maintained as control. Each of these conditions was performed in 3 replicate cultures. Concentration of H₂O₂, was visually checked (Fig. 5.3) and monitored using Quantofix® semi-quantitative test strips (Peroxide 100, Sigma Aldrich, UK, 1-100 mg/L sensitivity).

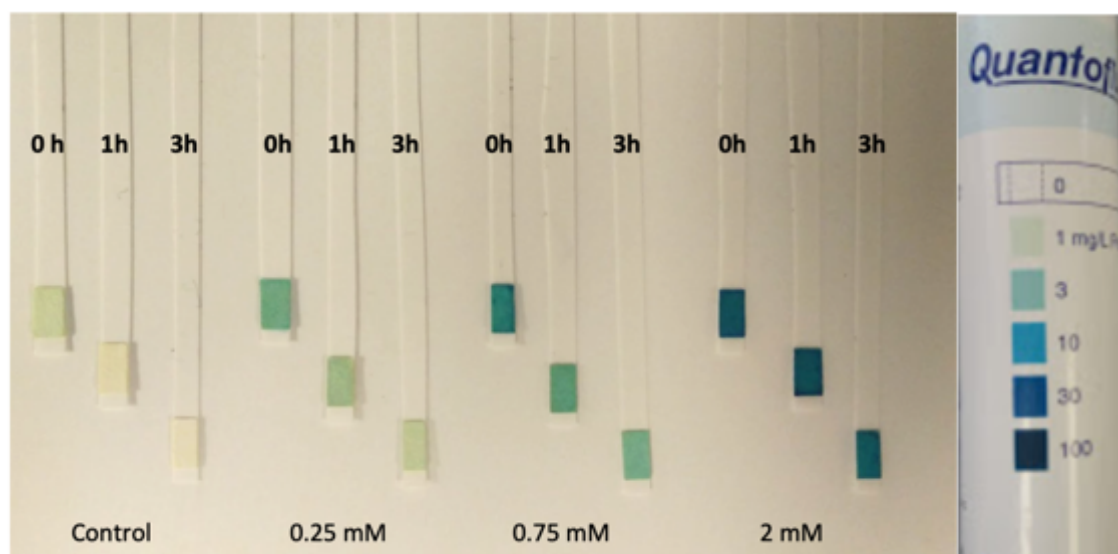


Figure 5.3. Concentrations of H₂O₂ in the culture replicates were monitored at the start and at the end of the exposure experiment using Quantofix® test strips. Left shows the indicator levels of the peroxide.

5.2.9 Viral-like particles (VLP) exposure experiment

Viral infection has been shown to cause substantial production and release of DMSP and DMS in haptophytes (Malin et al., 1998; Evans et al., 2006) and this is believed to have a significant contribution to the global sulfur cycle. The recent isolation of *Prymnesium parvum* virus

(PpDNAV) from Hickling broad has been shown to have algicidal activity on 33% of *Prymnesium* strains tested and was found to have high specificity on *P. parvum* CCAP 946/6 strain (Wagstaff et al., 2017). This gave me an opportunity to test the effects of this *Prymnesium*-specific virus on DMSP production in *P. parvum*.

Unfortunately, the cryopreserved viral particles were not viable when tried to be revived and no copies were deposited into culture collections (Wagstaff, pers. comm.). This brought me back to Hickling broad to isolate these viral-like particles (VLPs). In brief, water samples taken from Hickling broad were centrifuged at 3000 g to separate the heavy suspended fraction from the light fraction. The supernatants were pooled together and subsequently filtered three times through 0.22 µm pore-size filters (Sartorius AG, Goettingen, Germany). The resulting filtrate was then concentrated using 100 kDa MW cut-off spin filters (Amicon Ultra 15, Merck Millipore, Watford, UK) to give 1 mL of viral-like particles concentrate and stored at -20°C until needed.

The algicidal activity of the VLP concentrate was first tested on small-scale cultures of *P. parvum* CCAP 946/6 and Hickling broad's *P. parvum* HIK PR6H. Since the virus has been proven to infect CCAP 946/6 effectively (Wagstaff et al., 2017), and HIK PR6H strain as native strain where the VLPs were isolated. A small volume (20 µl) of VLP concentrate was added to each of exponentially growing cultures of both strains in 25 Nunc cell culture flasks containing 20 ml culture. No-VLP added culture was used as a control. Cultures were visually inspected for signs of cell lysis every day for 2-3 days. For CCAP 946/6 strain, control culture showed continued growth whereas the VLP treated cultures showed signs of cell lysis or culture clearance (Fig. 5.4). As for HIK PR6H strain, all cultures continued to grow healthily, and no culture clearance was observed. (Supplementary Fig. 5.2). Therefore, the algalytic activity is only effective to CCAP 946/6 strain. This was repeated at least three times to confirm the host specificity. New populations of infectious agents/VLPs were obtained by taking the supernatant of a lysed CCAP 946/6 culture and the same procedure was employed in preparation for the next batch of VLP concentrate for larger batch cultures.

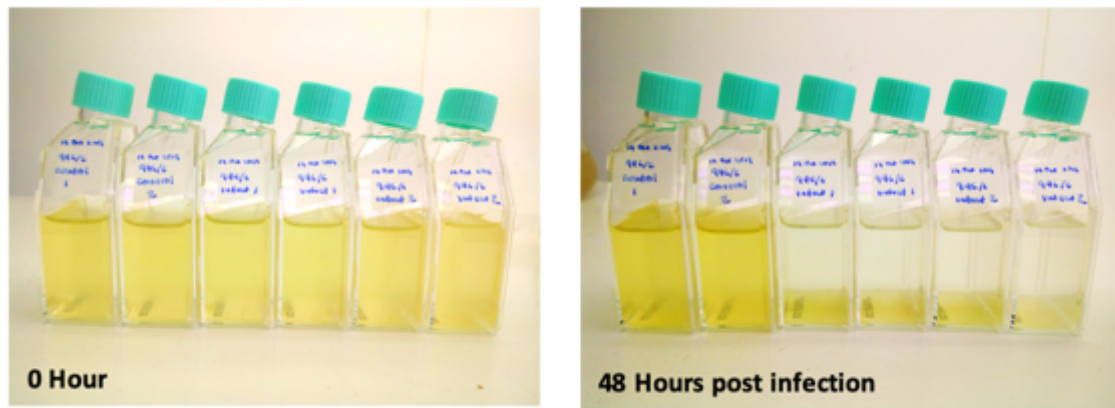


Figure 5.4. Initial VLP treatments on *P. parvum* CCAP 946/6 cultures. (Left) is the set of cultures at the start of infection; (Right) is the set of cultures at 48-h post-infection. Culture ‘clearance’ or collapse is observed on treated replicates as compared to the control cultures.

The previously prepared VLP concentrate was then used for a larger set-up using Erlenmeyer flasks containing 100 mL of *P. parvum* CCAP 946/6 cultures. Once the cultures reached the late exponential stage, an aliquot of 100 μ L of VLP concentrate was added to each of the three replicate cultures, this marked as the starting time of the experiment (T = 0 h). A set of triplicate culture was kept as non-treated control. Intracellular DMSP was monitored for 24 hours at five time points (0h, 3h, 6h, 9h and 24h). After this, a separate experiment was done, and the period of observation and sampling was extended up to 14 days. Intracellular DMSP was monitored at day 0, 3, 7 and 14 post-infection. Due to time constraints and limited materials at hand, the identity of these VLP was not determined, hence, I just used the term viral-like particles (VLPs).

5.2.10 *DSYB* transcription at varying salinity and nitrogen conditions

P. parvum *DSYB* transcription in varying salinity and nutrient conditions were also investigated following the methods described in Chapter 2. Briefly, algal biomass for RT-qPCR was harvested at the same time (late exponential stage) with the algal biomass for DMSP measurements. These were then pelleted immediately and subjected to RNA isolation and reversed transcribed to make complimentary DNA. *DSYB* transcription was measured using the previously designed qPCR Primers (Chapter 2, Table 2). Quantitative PCR was performed with a C1000 Thermal cycler equipped with a CFX96 Real-time PCR detection system (BioRad). Gene abundance/expression measurement for each sample was performed using three biological replicates, each with three

technical replicates. The efficiency for qPCR and RT-qPCR assay was 98%. See Chapter 2 for a more detailed procedure.

5.3 Results

5.3.1 *Prymnesium* DMSP in various studies

During this study, intracellular DMSP detected in all tested *P. parvum* strains ranged between 8 to 270 mmolL⁻¹ cell volume. I compared these results to previously published culture experiments involving various *P. parvum* strains and their intracellular DMSP concentrations (Table 5.1).

Table 5.1. Intracellular concentration of DMSP in different cultures of *Prymnesium* from various studies

Strain	DMSP Concentration per L Cell Volume	References
<i>Prymnesium parvum</i>	112 mMol	Keller, 1989
<i>Prymnesium parvum</i> CCAP 946/1D	25.21 mMol	Hatton & Wilson, 2007
<i>Prymnesium parvum</i> B127.9 (Gottingen, FRG)	125 mMol	Dickson & Kirst, 1987
<i>Prymnesium parvum</i> CCAP 946/6	54.3 ± 5.97 mMol	Curson et al., 2018
	46.4 ± 3.00 mMol	This Study
<i>Prymnesium parvum</i> CCAP 941/6	20.6 ± 3.05 mMol	Curson et al., 2018
	46.4 ± 3.05 mMol	This Study
<i>Prymnesium parvum</i> CCAP 946/1A	53.8 ± 4.58 mMol	Curson et al., 2018
	36.9 ± 1.99 mMol	This Study
<i>Prymnesium parvum</i> CCAP 941/1D	35.5 ± 1.50 mMol	Curson et al., 2018
	40.4 ± 5.51 mMol	This Study
<i>Prymnesium parvum</i> CCAP 946/1B	48.4 ± 6.29 mMol	Curson et al., 2018
	91.1 ± 3.49 mMol	This Study

<i>Prymnesium parvum</i> CCAP 946/4	25.3 ± 2.39 mMol	Curson et al., 2018
	46.7 ± 7.49 mMol	This Study
<i>Prymnesium parvum</i> CCAP 946/6	16.2 ± 4.4 fmol*	Thume et al., 2018
<i>Prymnesium parvum</i> (Axenic) CCAP 946/6	17.4 ± 2.6 fmol*	Thume et al., 2018
<i>Prymnesium parvum</i> HIK PR1A	47.8 ± 5.34 mMol	This Study
<i>Prymnesium parvum</i> HIK PR6H	89.3 ± 1.89 mMol	This Study
<i>Prymnesium parvum</i> HIK RR12D	54.3 ± 0.72 mMol	This Study
<i>Prymnesium parvum</i> WBF C1	61.9 ± 1.09 mMol	This Study
<i>Prymnesium parvum</i> WBF D2	32.8 ± 0.31 mMol	This Study
<i>Prymnesium</i> sp. PLY 595	61.8 ± 1.47 mMol	This Study
<i>Prymnesium parvum</i> PLY 94A	45.7 ± 5.86 mMol	This Study

* Concentration per cell

The collated results have shown that intracellular DMSP contents of *P. parvum* tested from different culture experiments are within range but not similar to each other. This suggests that DMSP concentration is strain-specific and potentially dependent on the growth phase/stage when sampling. This variation in DMSP concentrations within the same species proved that DMSP production is different between type strains and can be influenced by its genetic make-up, environmental conditions, or affected by their combination. In the following sections, I investigated these variables that are likely to influence *P. parvum* DMSP production.

5.3.2 DMSP production at different growth stages

DMSP production in axenic cultures of my *P. parvum* isolates from the Broads at different growth stages were analysed and compared to those from strains available in culture collections. The growth curves of these strains are shown in Fig. 5.1. The growth patterns observed during the 52-day monitoring period were consistent with those of algal blooms in the natural environment. Algal growth stages start with small growth lag phase, followed by a quick exponential growth phase, then a prolonged stationary growth phase, and finally senescent/death phase. For all *P. parvum* strains observed, the first few days of slow growth was followed by the fast-developing phase between day 10-24 and reached their maximum abundance on day 26, remaining at that level thereafter. I did not observe any senescent phase throughout the experiment due to time limitations. *P. parvum* growth cycle could last beyond 52-day period especially in laboratory-controlled conditions.

The Fv/Fm ratio, which indicates the condition of the photosystem during the experiment, varied from 0.48 to 0.67 during the exponential phase, varied from 0.44 to 0.67 during the early stationary phase, slowly decreased (from 0.59 to 0.39) during the stationary to late stationary phase (Fig. 5.5).

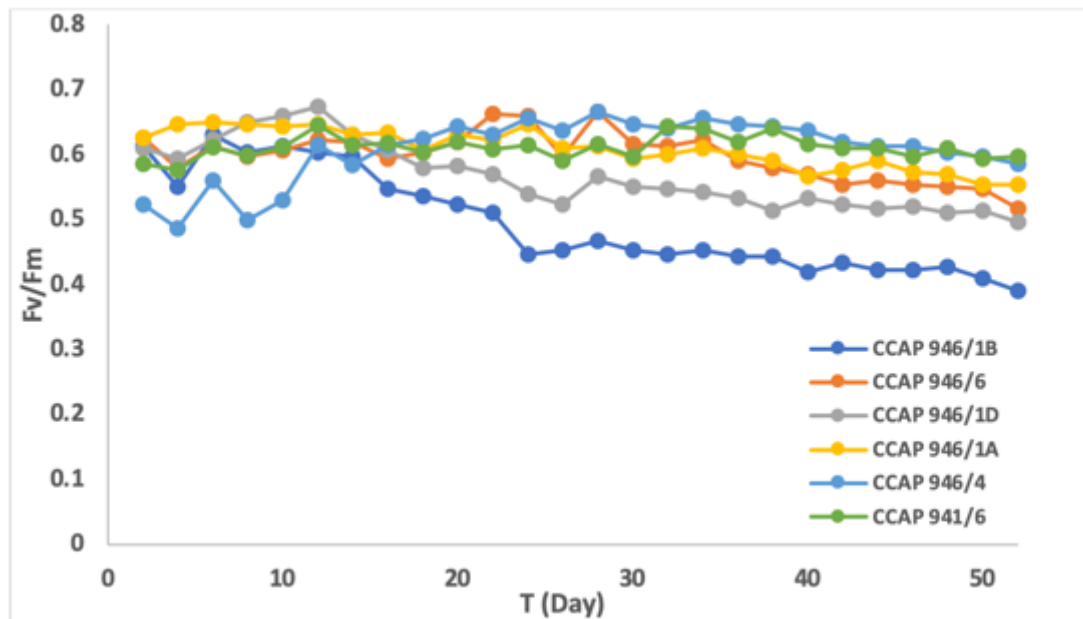


Figure 5.5. Variation in Fv/Fm ratio *P. parvum* strains grown under controlled culture conditions during the 52-day monitoring.

Next, I determined the DMSP levels within the different strains at different growth phases (Fig. 5.6). Samples taken at day 16 represented mid exponential phase, day 22 for late exponential phase, then day 28 for stationary phase, and both day 36 and 46 for late stationary phase. Results showed that all strains except of strain CCAP 946/1B, produce very similar the amounts of DMSP that ranged between 9 to 51 mmol L⁻¹ cell volume (Fig. 5.6)

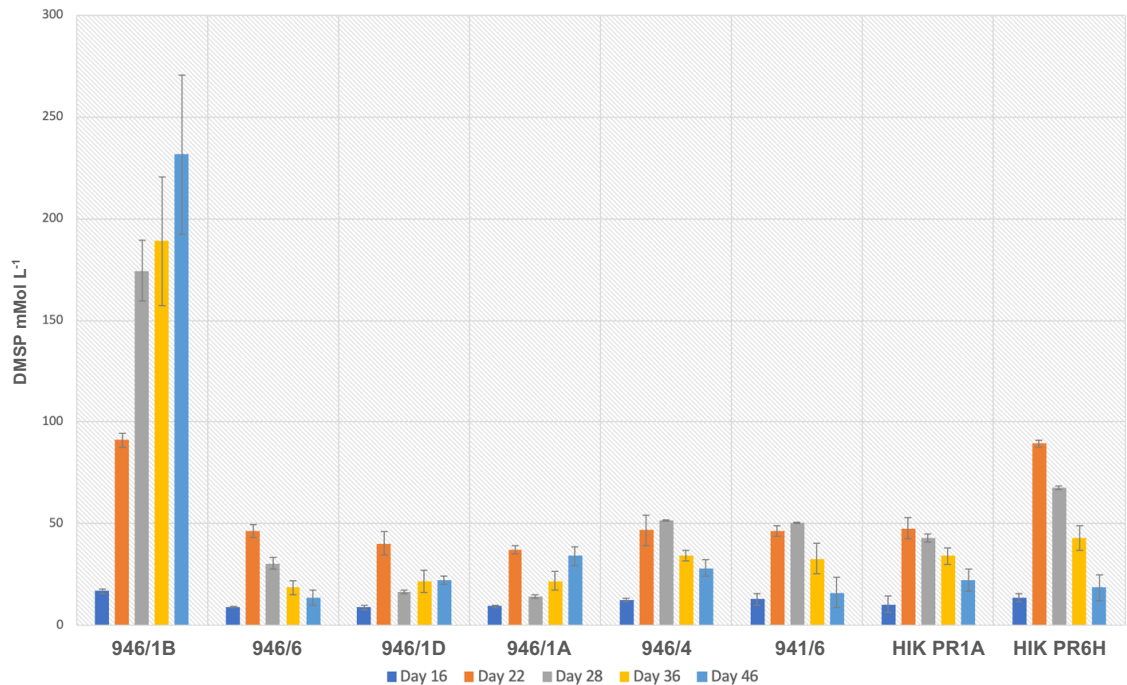


Figure 5.6. DMSP concentrations of different *P. parvum* strains, including two of the newly isolated strains, at different growth phases. Day 16 - mid exponential phase, day 22 – early stationary phase, day 28 – stationary phase, and days 36, 46 as late stationary to senescent phases.

DMSP production, apart from with CCAP 946/1B, increased rapidly during the exponential phase and reached its maximum on day 22-24 (late exponential phase), and started to decrease production on stationary phase until late stationary to senescent phases. The decrease in DMSP production at stationary phase and thereafter is associated with physiological stress conditions (e.g nutrient limitation) that led to growth limitation. For CCAP 946/1B, DMSP production continued to increase even until the late stationary phase to senescent phases. This possibly due to continued cell replication/division in replacement to cell autolysis thereby maintaining DMSP base quota and the carry-over of inactive cells (no growth) from late exponential phase (Laroche et al., 1999).

The discovery of non-motile cells or 'cysts' of *P. parvum* CCAP 946/6 in F/2 agar plates that was stored and left in the plant growth room for 3 years without any intervention gave me an opportunity to determine the intracellular levels of DMSP at its resting state. I measured the intracellular DMSP content of these cyst cells and compared it to the intracellular DMSP at its vegetative growth phases (Fig. 5.7).

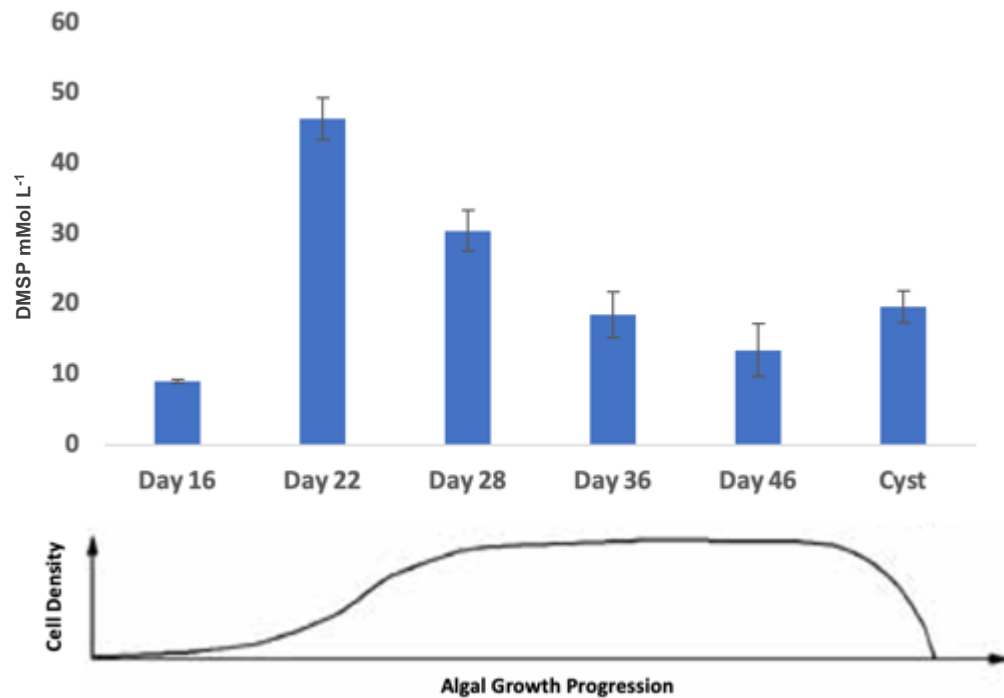


Figure 5.7. DMSP concentration of *P. parvum* CCAP 946/6 strain at different growth phases including dormant cyst phase. Day 16 - exponential phase, day 22 -early stationary phase, day 28 - stationary phase, days 36, 46 as late stationary to senescent phases, and non-motile 'cysts' as resting phase/stage in f/2 solid agar plates.

I found that that even at resting phase/stage *P. parvum* CCAP 946/6 contained approximately 20 mmolL⁻¹ of DMSP, which is double the amount of DMSP (~ 10 mmolL⁻¹) produced at early exponential phase (Day 16) (Fig. 5.7), suggesting that DMSP is an important molecule for this haptophyte even at dormant or 'seed' state.

5.3.3 Effect of varying salinity

The effect of varying salinity on DMSP production of different *P. parvum* strains was investigated (Fig. 5.8 a, b). All *P. parvum* cultures (including a newly isolated strain HIK PR1A) grown in salinities 5, 10, 35, and 50 followed similar pattern and had similar intracellular DMSP concentrations (Fig. 5.8 a). There was significant effect of the strain ($F = 13.74$, $p < .001$), salinity ($F = 159.79$, $p < .001$), and both combined ($F = 3.82$, $p < .001$) on the DMSP values.

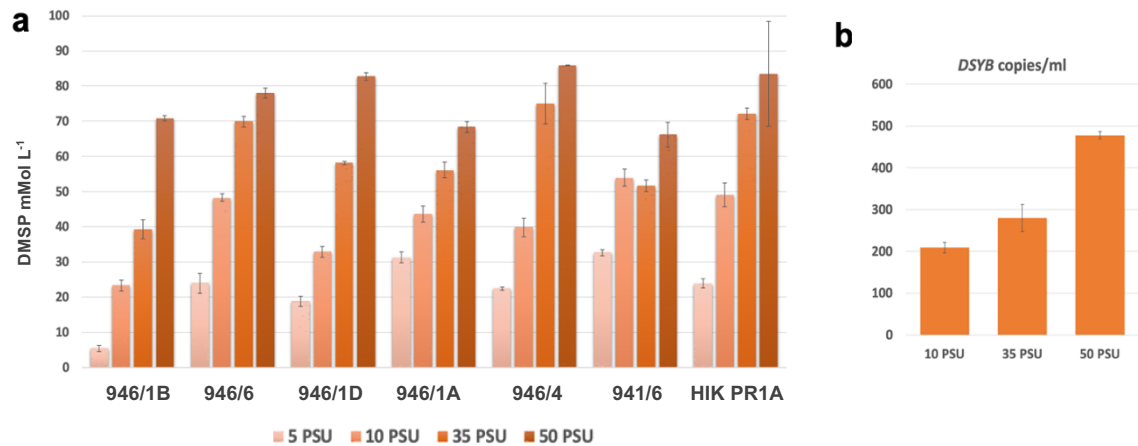


Figure 5.8. DMSP concentrations of different *P. parvum* strains at different salinity regimes (5, 10, 35, and 50 PSU) (a) and *P. parvum* HIK PR1A *DSYB* transcription at three salinity conditions (b).

DMSP was progressively accumulated at higher levels in *P. parvum* in response to increased salinity (between 10-90%). This supports previous published results that showed increased salinity enhances DMSP production in many marine phytoplankton (Zhuang *et al.*, 2011; Kettles *et al.*, 2014) and supports a role for DMSP as a significant osmolyte for coping with salinity stress in *P. parvum* (Dickson & Kirst, 1987). The transcription of *DSYB*, the key gene encoding the *S*-methyltransferase gene of the transamination DMSP synthesis pathway, in my Hickling *P. parvum* strain was also enhanced (25-56%) by increasing salinity (Fig. 5.8 b), consistent with work published in Curson *et al.* (2018) where DMSP production in six *Prymnesium* strains was investigated by me. My results, together with previous studies, support DMSP playing an osmoregulatory role in *P. parvum*. This osmotic regulation (through production of DMSP) is particularly crucial in the long-term survival of *Prymnesium* especially in brackish shallow lakes (3-5 PSU), like the Hickling broad, where frequent sea flooding and increased anthropogenic catchment modifications (Roberts *et al.*, 2019) have caused large seasonal fluctuations in salinity.

Furthermore, the increasing salination of Hickling broad over time due to these factors may have given a competitive advantage to *P. parvum* allowing it to grow and proliferate over less saline tolerant freshwater phytoplankton species.

5.3.4 Effect of varying nitrogen

Next, I examined the effect of nutrient imbalance (nitrogen, N) on DMSP production by *P. parvum* (Fig. 5.9 a, b). Limitation by nutrients leads to metabolic imbalances that can further lead to increased oxidative stress in organisms. It has been proposed that DMSP could act as antioxidative stress protectant together with its cleavage products that scavenge reactive oxygen species (Sunda et al., 2007). Thus, I subjected several *P. parvum* strains to low and high nitrogen conditions to see the effects on DMSP production. For nitrogen depleted (LN) and repleted (HN) *P. parvum* cultures, results showed no significant change in intracellular DMSP concentrations between strains ($F = 1.36$, $p = 0.261$), varying N ($F = 1.25$, $p = 0.298$) and both combined ($F = 0.97$, $p = 0.484$) (Fig. 5.9 a) and they were all comparable to values observed in normal conditions (NN), suggesting that nitrogen does not affect DMSP production in *P. parvum*. This is consistent with my findings in the field samples (Chapter 4) and the findings of Curson et al. (2018). Interestingly, this is not what happens in bacteria that make DMSP or diatoms, both of which have been shown to upregulate DMSP production by low N/N limitation. Note there is a low observed DMSP concentration in 595 and HIK PR1A strains under the low nitrogen (LN) conditions and this is likely due to cultures reaching stationary phase faster than N -replete cultures (NN & HN). Thus, my sampling during the late stationary phase rather than the early stationary phase may be the explanation. *DSYB* Transcription levels of in these samples show no clear differences between the treatments which is consistent with the DMSP measurements (Fig. 5.9 b).

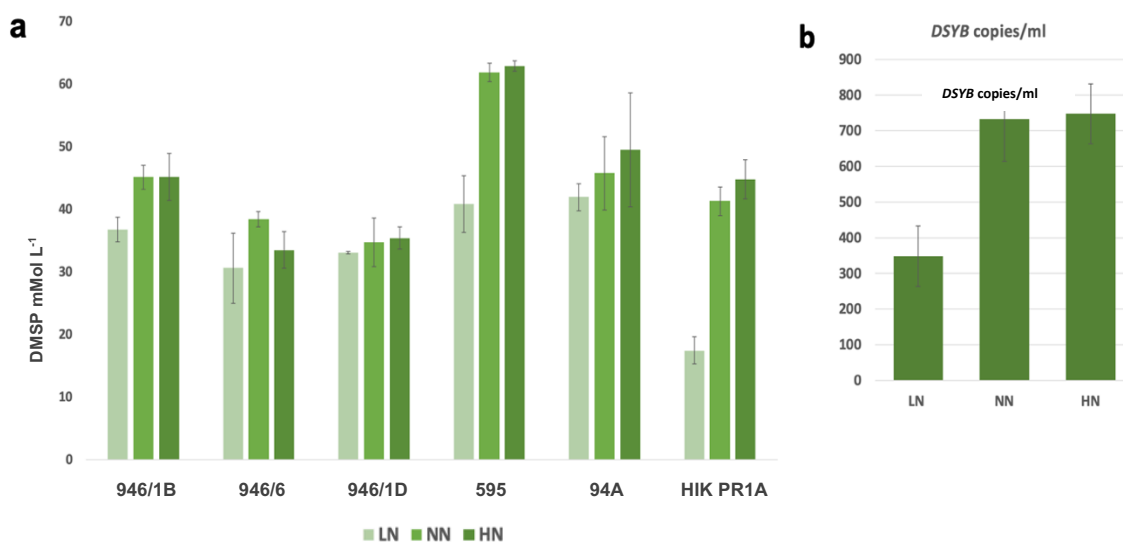


Figure 5.9. DMSP concentrations of different *P. parvum* strains grown at different nitrogen concentrations (LN - Low N or N - deplete, NN - Normal N, and HN - High N or N - replete) (a) and *P. parvum* HIK PR1A *DSYB* transcription at these conditions (b).

5.3.5 Effect of oxidative stress

To evaluate the effect of oxidative stress on *P. parvum*'s DMSP production, cultures of CCAP 946/6 strain were exposed to different H₂O₂ (ROS) concentrations (0.25 mM, 0.75 mM and 2 mM). The intracellular DMSP concentrations of H₂O₂ treated cultures plus non-treated control were measured at the beginning (0 h), after 0.5 h, 1 h, and 3 h of exposure. Results indicated that there were no apparent increase in DMSP concentration of the treated culture but, instead, a sudden decrease in particulate DMSP in all H₂O₂-treated cultures especially at 1 hour post-treatment (Fig. 5.10). It is possible that this results from a biological use of DMSP to sequester free radicals. Perhaps, DMSP is oxidized to DMSOP under these conditions to help protect against oxidative stress (Thume et al, 2018). To be able to answer these questions I would have needed to monitor DMSP production and turnover rates, which was not done here.

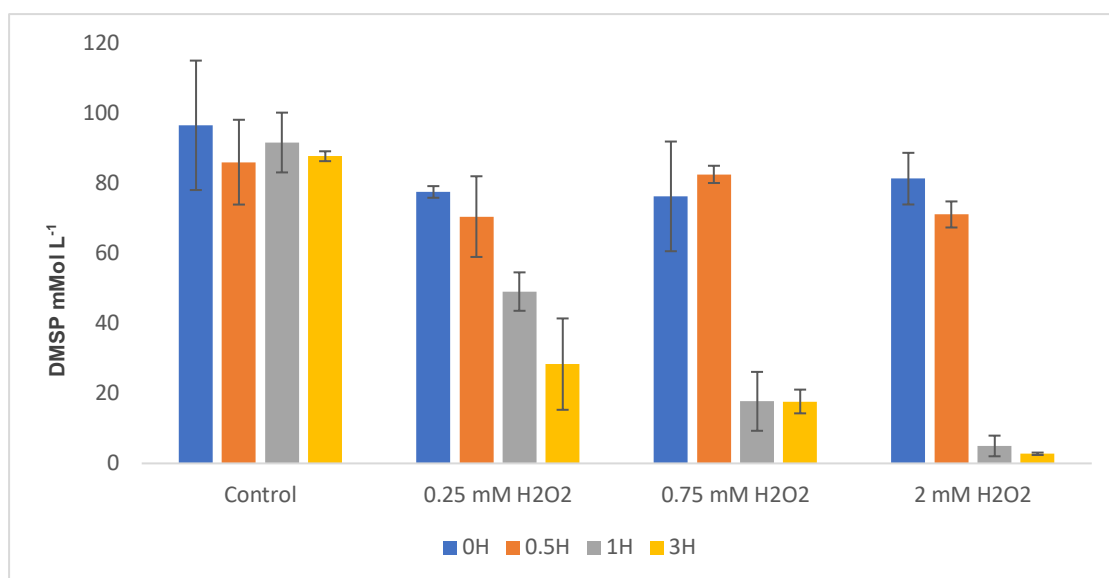


Figure 5.10. Intracellular DMSP concentration (mMol L^{-1}) of *P. parvum* CCAP 946/6 treated with H_2O_2 (ROS). Cultures grown in F/2 medium mixed in artificial seawater in standard conditions, were treated with 0.25 mM, 0.75 mM, and 2 mM of H_2O_2 . No H_2O_2 – treated cultures were maintained as control. Samples were taken immediately after the addition of H_2O_2 (0 h), after 0.5 h, after 1 h, and after 3 h. Results are shown as means \pm standard deviation of 3 independent cultures.

The decrease in DMSP were more pronounced on cultures treated with higher H_2O_2 concentration (0.75 mM or 2 mM). Decrease in DMSP values were attributed to induction of cell lysis/death and culture collapse by the strong oxidant or from the turnover of DMSP that was not monitored. In contrast, when I used the same method on two model diatoms, *Thalassiosira pseudonana* CCMP 1335 and *Phaeodactylum tricornutum* CCAP 1055/1, I found that they could tolerate these concentrations of H_2O_2 and a small increase in their intracellular DMSP were observed (See Supplementary Fig. 5.3). So, it seems that *P. parvum* cells have higher sensitivity to these levels of H_2O_2 which potentially could be very useful in terms of algal bloom control or mitigation measure and management. Previous studies have used H_2O_2 treatments as a fast, effective management measure to combat harmful algal blooms (HABs) such as toxic cyanobacteria and dinoflagellates (Drabkova et al., 2007; Matthijs et al., 2012; Burson et al., 2014).

5.3.6 Effect of viral-like particles (VLPs)

The effect of VLPs on *P. parvum* CCAP 946/6 cells was explored to determine the lytic cycle and to determine whether it will induce DMSP production in the algae. At 24 h post-infection, the *P.*

parvum cells exhibited signs of distress, slowed mobility, and started to lyse as visually confirmed under the microscope (not shown). Some cells formed aggregates and sedimented at the bottom of the culture flask. Cells were re-suspended by gentle shaking and sampled to determine the number of remaining viable cells using Casy Counter. The time before symptoms of infection or the incubation period was therefore presumed to be within 24 h and intracellular DMSP concentrations were first measured within this time frame (Fig. 5.11 a).

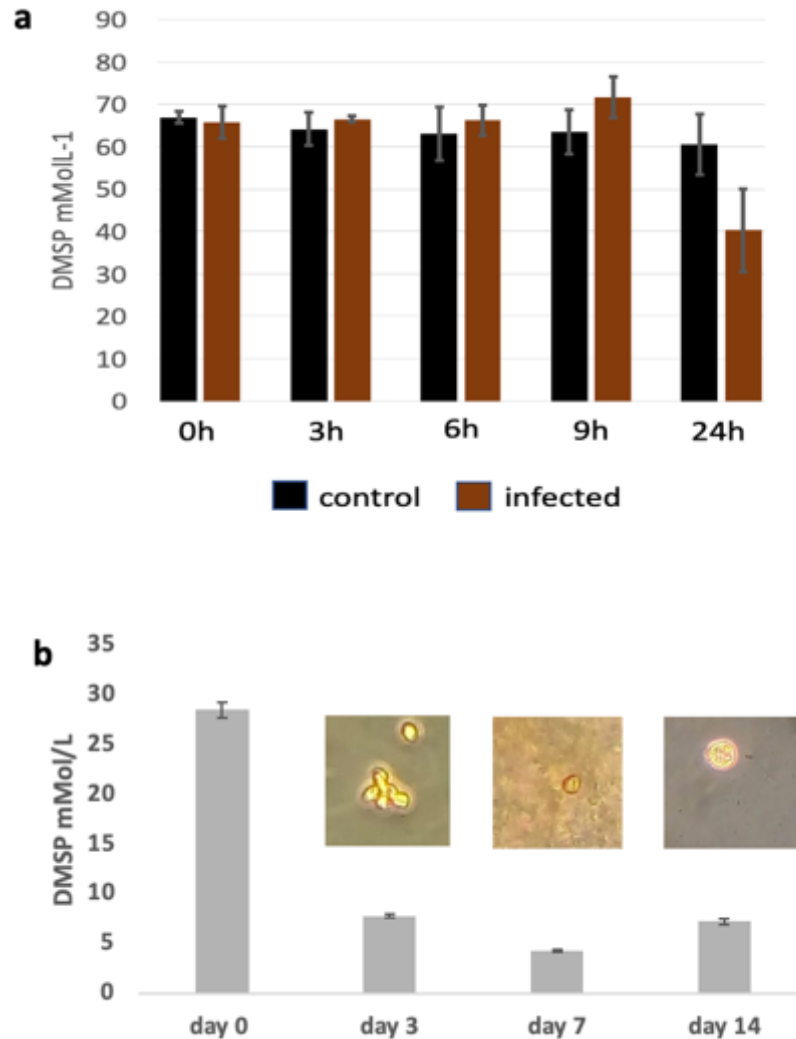


Figure 5.11. Intracellular DMSP concentration (mMol L^{-1}) of *P. parvum* CCAP 946/6 infected with VLP. Cultures grown in standard F/2 medium mixed in artificial seawater under conditions were treated with 0.1 % v/v of VLP concentrate. Non-infected cultures were maintained as control. Samples were taken immediately after the addition of VLP (0h, 3h, 6h, 9h, and 24h) (a). Same experiment was repeated and extended to 14-day period. Cell morphological changes were also observed through microscopy (b). Results are shown as means \pm standard deviation of 3 independent cultures.

When *P. parvum* cells were exposed to VLPs, there was no apparent increase in DMSP production on the first few hours, but a sharp decrease at 24-hour post infection was observed, which marked the start of the 'eclipse' period. This period reflects the time between infection and algal cell death (cell lysis) and based on cell count data (Supplementary Figure 5.4), the eclipse period was roughly judged to be 24–48 h post-infection. Most of the cells were non-viable (observed cell bursting/lysis through microscopy) after this period indicating detrimental effects of the VLPs on most of *P. parvum* CCAP 946/6 cells. The non-VLP treated control cultures continued to grow over the 24-h duration of the experiment.

Another experiment was done with extended period of incubation up to 14 days (Fig. 5.11 b). Since not all cells lysed during the viral treatment, it is interesting to determine what might be some form of mechanism that these cells employed to become resistant to viral attacks. DMSP was monitored and a decreasing trend of DMSP was observed from 0 - 7 days of VLP infection. Surprisingly, significant amount of particulate DMSP was still present even after 14 days of infection which might indicate the presence non-infected cells. When observed under the microscope the cells seemed to produce temporary or pellicle cysts which can potentially serve as propagules (seed) for the next batch of algal cells once the virus disappears. Therefore, this might be a form of escape/defense mechanism for *P. parvum* for VLP attacks.

5.4 Discussion

Intracellular DMSP production and regulation of *P. parvum* in batch cultures at different growth phases and under different salinity, varying nutrient (N), exposure to reactive oxygen species and viral-like particles were investigated in order to identify or elucidate the possible physiological roles of DMSP in this invasive haptophyte.

5.4.1 Production at different growth phases

DMSP production of different *P. parvum* strains tested at different growth stages follows the same trend with the exception of one strain, *P. parvum* CCAP 946/1B. The average DMSP concentrations range from ~ 10 to 50 mMol L^{-1} . The observed DMSP production was low during mid-exponential phase and reached its maximum at day 22 (late exponential phase) and then gradually decreased during stationary to late stationary phases. The increase in DMSP production during exponential growth and subsequent gradual decline can be explained by the fact that at

the beginning of the cell growth the nutrients were adequate, and conditions became limiting when cells reached maximum growth when nutrient supply was diminished. In addition, cell growth starts to decline during stationary phase and the eventual apoptosis and cell autolysis releases the intracellular DMSP to the culture medium. This is in concordance with previous reports on DMSP production at different physiological stages of marine phytoplankton (Matrai & Keller, 1994; Keller, 1999; Zhuang et al., 2011) where they found decrease in particulate DMSP during the late stationary to senescent phases of the algal culture.

On the other hand, the observed increase in DMSP production of *P. parvum* CCAP 946/1B throughout physiological stages until late stationary phase, suggests that the algae maintained its base DMSP quota through active replication and carryover of non-active intact algal cells where DMSP remained largely intracellular (Laroche et al., 1999). I didn't observe any obvious senescent phase in all cultures tested. *P. parvum* growth cycle or any phytoplankton could last beyond 40-day period especially in laboratory-controlled conditions. Therefore, no data related to DMSP production during senescent phase of *Prymnesium* cultures was presented.

The trend observed between cell counts/abundance and DMSP concentration implied direct relationship between intracellular DMSP and the algal biomass. Furthermore, the circumstantial generation of *P. parvum* cyst cells of strain CCAP 946/6 gave me a chance to determine the intracellular DMSP concentration at its non-motile or dormant state. I found that the intracellular DMSP of cyst cells were of considerable amount suggesting that DMSP is an important molecule for these dormant cells and may potentially play a role in algal cyst germination or "reseeding". Further investigation is warranted to study the importance of DMSP on microalgal cysts.

5.4.2 Effect of varying salinity and nitrogen

DMSP is produced and accumulated as a compatible solute in some haptophytes (Vairavamurthy et al., 1985; Stefels, 2000; Blunden et al., 1992; Stefels et al., 2007), prasinophytes (Dickson & Kirst, 1986) and green macroalgae (Dickson et al., 1980; Karsten et al., 1991). But some macroalgal species, do not respond to salinity change by producing more DMSP like for example in epiphytic tropical dinoflagellate *Gambierdiscus belizeanus* (Edwards et al., 1987; Van Alstyne et al., 2003; Gwinn et al., 2019). Some low DMSP producers like dinoflagellates *Pfiesteria piscicida*, *Ceratium longipes*, and *Gambierdiscus toxicus* produce DMSP in very small amounts that it is unlikely to act as an osmolyte (Caruana & Malin, 2013). Additionally, DMSP

concentration remains stable under salinity changes in some other organisms such as the terrestrial plant *Spartina anglica* (van Diggelen et al., 1986).

In this study, I found that DMSP production was significantly affected by salinity change in *P. parvum* (Fig. 5.8 a). All *P. parvum* cultures (including a newly isolated strain) grown in varying salinities (5, 10, 35, and 50 PSU) followed the same pattern and had similar intracellular DMSP concentrations. DMSP concentration in *P. parvum* was universally enhanced and progressively accumulated as I increased the salinity regime (between 10-90%) and the osmolyte action may therefore be linked to their use for coping with salinity stress. *DSYB* transcription was also enhanced by increasing salinity and similar to Curson et al. (2018). In short, DMSP per cell volume decreased with low salinities and increased with high salinities. This allows *P. parvum* to easily adapt to rapid change in salinity, especially in saline-influenced lake systems, like the Hickling broad, where they can easily invade, establish and develop toxic algal blooms. Thus, this haptophyte species is not affected by a drastic variation in salinity caused by tidal exposure, evaporation, desiccation, precipitation and many other contributing processes taking place in this type of aquatic environment. My results, together with previous studies, support that DMSP does play an osmoregulatory role in some organisms, like *P. parvum*, especially when they are exposed to high magnitude of salinity shifts and increased salinification. Moreover, with the increasing tidal incursions in freshwater habitats around the world due to climate change and sea level rise, *P. parvum* invasion and bloom formation are likely to increase and become more frequent in the future.

There is some evidence suggesting that varying nutrient levels can modulate the intracellular concentrations of DMSP (Turner et al., 1988; Keller et al., 1999; Stefels, 2000; Sunda et al., 2002). For example, *Prymnesium's* close relative *E. huxleyi* has been found to produce more DMSP when grown under N-limited conditions and this was thought to be due to the cells having the ability to switch between production of DMSP and its functional nitrogen analog, glycine betaine (GBT) and other N-containing compatible solutes (Green & Leadbeater, 1994). But in contrary, Sunda et al. (2007) reported that *E. huxleyi* grown in limited N showed no significant increase in DMSP production. Nitrogen limitation causes a reduction in the accumulation of free nitrates, amino acids and proteins (Bucciarelli & Sunda, 2003). Furthermore, N limitation leads to metabolic imbalances that can disrupt the photosynthetic mechanism of the algae leading to oxidative stress.

Here, in this study, I investigated the the effect of varying nitrogen conditions (low - LN, normal - NN, high nitrogen - HN) on DMSP production of *P. parvum* (Fig. 5.9). For nitrogen depleted (LN) and repleted (HN) *P. parvum* cultures, results have shown no significant increase in intracellular DMSP concentrations (Fig. 5.9 a) and they were all comparable to values observed in normal conditions (NN), suggesting that nitrogen levels do not significantly impact DMSP production in *P. parvum*. The observed low DMSP concentration in HIK 1A strain during the low nitrogen conditions was likely due to growth decline because I took samples too late during the late stationary phase rather than the start of stationary phase. *P. parvum* *DSYB* transcription for this strain (Fig. 5.9 b) also reflects DMSP concentrations. These results are consistent with the findings of Curson et al. (2018) where nitrogen limitation didn't affect DMSP production in six *P. parvum* strains. Interestingly, this is in contrast to what was observed in bacteria or diatoms that make DMSP, both of which have been shown to upregulate DMSP production by low N or N limitation (Bucciareli & Sunda, 2003; Curson et al., 2017).

One reason that might explain why DMSP was not enhanced during N limitation in *P. parvum* is that the organism is capable of both photoautotrophy (photosynthesis) and heterotrophy (mainly phagotrophy) to supplement its nutritional needs (Carvalho and Granéli, 2010; Granéli et al., 2012; Liu et al., 2016). As a mixotrophic (photoautotrophy + heterotrophy) organism, it is capable of utilizing both inorganic, dissolved organic or particulate nutrients, therefore inorganic N limitation may not particularly affect the algal nutritional balance. The uptake of organic nutrients can be used to compensate for low inorganic nutrient concentrations (Granéli & Carlsson, 1998; Legrand et al., 2001; Lindehoff et al., 2011). Furthermore, single cell stable isotope probing and NanoSIMS imaging analysis provided evidence that *P. parvum* relies heavily on heterotrophy as a supplemental source of nitrogen (Carpenter et al., 2018). The study also showed that *P. parvum* displayed no preference for uptake of the nitrogen from prey or inorganic nutrients (nitrate) when both sources are available.

5.4.3 Other tested variables: ROS and VLPs

Sunda et al. (2002) proposed that DMSP and its related breakdown products constitute an antioxidant system in marine microalgae when cells undergo oxidative stress due to the overproduction of reactive oxygen species (ROS). ROS is normally produced in algae and acts as a secondary messenger in numerous metabolic processes. Under abiotic induced stresses, the balance between production and suppression of ROS disappears and causes build-up of ROS

(Rezayian et al., 2019). ROS is very harmful when produced at high concentrations and can lead to oxidative stress leading to cellular damage. All algae have mechanisms to cope with an overabundance of ROS like superoxide O_2^- , H_2O_2 , and OH radical and maintain them under oxidative stress. They produce multiple enzymes (e.g. superoxide dismutases, catalases, glutathione reductase, etc.) and compounds to deal with ROS before they can damage the cell components. Abiotic factors such as osmotic stress, high or low temperature, nutrient limitation, high light, and chemical toxicity can increase ROS production levels. In support to DMSP's role as an antioxidant, Sunda et al. (2002) demonstrated that in both *Thalassiosira pseudonana* (low DMSP producer) and *Emiliana huxleyi* (high DMSP producer) induced increase in intracellular DMSP levels when subjected to increased UV radiation, increased Cu^{2+} , low CO_2 and low iron (Fe).

Following this proposed function, I tried to replicate this oxidative stress study by examining the effect of exogenous H_2O_2 on DMSP production of *P. parvum*. There was no obvious increase in intracellular DMSP concentration found but, instead, a sudden decrease in particulate DMSP in all H_2O_2 -treated cultures especially at 1 hour post-treatment. There is a possibility that the observed decrease in intracellular DMSP results from a biological use of DMSP to sequester free radicals. Perhaps, DMSP is oxidized to DMSOP under these conditions to help protect against oxidative stress (Thume et al., 2018). To prove this, however, is to measure DMSP and its turnover rates which was not done in this study. My results are not comparable to what was found by Sunda et al. (2002) for they use different methods in their study, but it suggests that *P. parvum* acute exposure to ROS doesn't lead to an increase in DMSP production.

DMSP and its downstream products have been implicated in cellular defence against grazing (Wolfe et al., 1997) and viral infection (Evans et al., 2006; Evans et al., 2007). Viruses are pervasive components of the aquatic environment (Jacquet *et al.*, 2010). They play a key role in regulating both prokaryotic and eukaryotic (algal) bloom dynamics (Furhman, 1999) and are therefore considered to influence major biogeochemical cycles (Suttle, 2005). But algal bloom collapse due to viral attack may not annihilate all cells, some cells may remain uninfected (Jacquet et al., 2002) and some even continued to coexist with their viral pathogen (Thyrhaug et al., 2003). This suggests that some algae may have innate defence mechanisms to combat viral infection through the production of certain compounds. Studies have reported that increased DMSP lyase (DLA) activity in some high DMSP-producing haptophytes, such as *E. huxleyi*, has potent antiviral effects due to the release DMSP cleavage products (DMS and Acrylic Acid) that may serve as an algal chemical defence mechanism against viruses (Malin et al., 1998; Evans et

al., 2005; Evans et al., 2006). However, the mechanism of how these algae utilise such secondary metabolic products as a form of chemical defence against viruses is not fully elucidated.

The novel *Prymnesium parvum* virus (PpDNAV) have been demonstrated to infect and lyse 5 out of 15 tested *P. parvum* strains (Wagstaff et al., 2017). The cryopreserved virions were not viable anymore when 'attempted to revive'. So, instead I isolated the Virus-like particles (VLPs) from the waters taken from Hickling broad. I used these VLPs against *P. parvum* strain CCAP 946/6 (the same strain lysed by pPDNAV) and it conferred effective algalytic activity. Several cycles of infections and generations of virions were made in order to confirm the algalytic activity. The lytic cycle was determined based on the period of incubation, eclipse, and appearance of lysed cells found in all replicated infection cycles. The incubation period was found to be within 24 hours, the eclipse is within 48-72 hours, and rapid cell lysis occurred after 72 hours of infection. I monitored the DMSP content of the cells during the incubation period (24 h) and found no change but DMSP values decreased after this period which indicated the decline in cell health and biomass for most of the cells started to lyse. A similar trend was found in *E. huxleyi* CCMP 1516 when subjected to viral infection (Evans et al., 2007), with intracellular DMSP declining in parallel with cell density. Unfortunately, neither dissolved DMSOP, DMSP, nor DMSP cleavage products (DMS and Acrylic Acid) were measured throughout my investigation and given that an in vitro assay was used, I can only speculate that DMSP is released into the media upon cellular breakdown and no DMSP cleavage happened since *P. parvum*'s DMSP lyase 'Alma' is non-functional as I have found in Chapter 4.

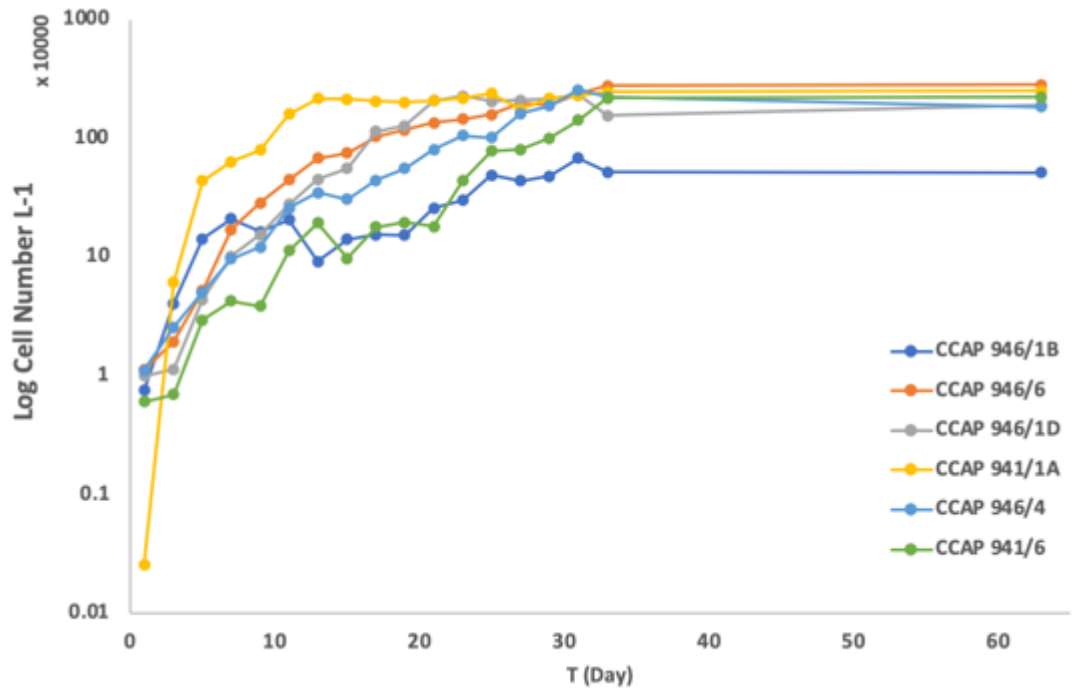
In a separate experiment, I found that not all cells were susceptible to VLP infection, and the formation of temporary cysts was observed. And this was supported by the significant amount of particulate DMSP still present in the samples. As far as I know, there were no reports of induced cyst formation as a form of temporary escape strategy for *P. parvum* against its viral pathogen. On the other hand, Frada et al. (2008) have found that there is a clear difference in viral susceptibility between life cycle stages with different ploidy levels of coccolithophore *Emiliania huxleyi* to *E. huxleyi* viruses (EhVs). They found that the haploid cells of *E. huxleyi* is unrecognizable and therefore resistant to EhVs that kill the diploid cells. Since *P. parvum* was proposed to have haplodiplontic life cycle, this strategy might be as well utilised during the algal-viral interaction.

It is important to note that these experiments are preliminary and additional work is needed to examine what actually happens *in vivo* during viral infection, especially on the expression of DMSP synthesis gene *DSYB* and algal DMSP lyase gene '*ALMA*'. DMSP cleavage products DMS, Acrylate and DMSO should be also monitored to gain more insights.

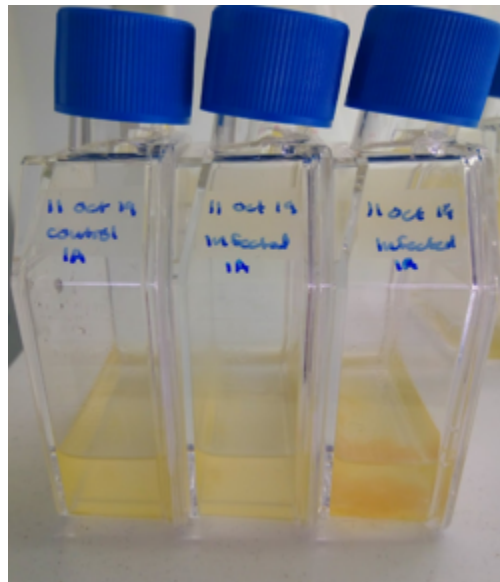
5.5 Conclusion

In this chapter, I found growth related variations in DMSP production and first to report the intracellular DMSP content of *P. parvum* at its resting state or cysts. This suggests DMSP's potential role in cyst maintenance, excystment, and bloom reseeding. Moreover, my results showed that *P. parvum* DMSP production is mainly influenced by salinity among the abiotic variables tested and DMSP act as an important osmolyte compound especially at higher salinity conditions. Osmotic regulation for turgor pressure is a fundamental process for most aquatic/marine algal species. Invasive organisms like *P. parvum* that are adapted to their brackish or salinized habitat have developed or maintained strategies such as DMSP synthesis to survive huge salinity shifts, outcompeting other native freshwater or brackish water algal species. This in turn brought to light the significance of haptophyte blooms in this type of ecosystem as a potential source of DMSP and DMS and a potential contributor to the local sulfur cycle. Nutrient limitations or overabundance did not affect DMSP production in *P. parvum* and this was reflected in the transcription of DMSP synthesis gene, *DSYB* for *P. parvum*, which as a mixotrophic organism, has several nutritional strategies at its disposal. Lastly, the exposure to exogenous peroxide (induced oxidative stress) and viral-like particles (VLPs) was found to have no influence on DMSP production but found to have deleterious effects in *P. parvum* cells. These could be utilised as potential control or mitigation strategy against the toxic haptophyte blooms.

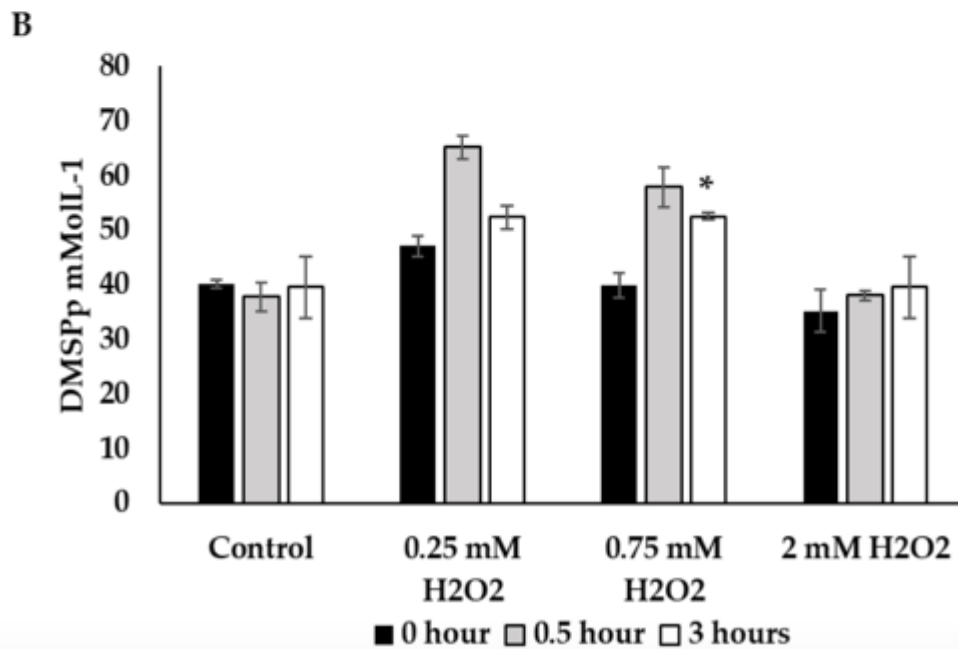
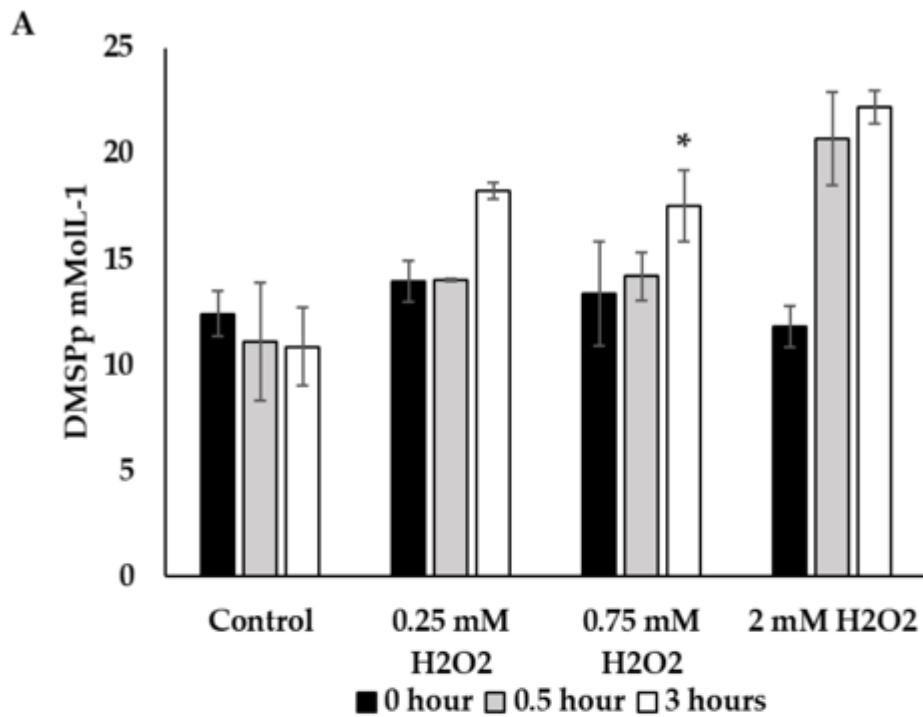
5.6 Supplementary figures



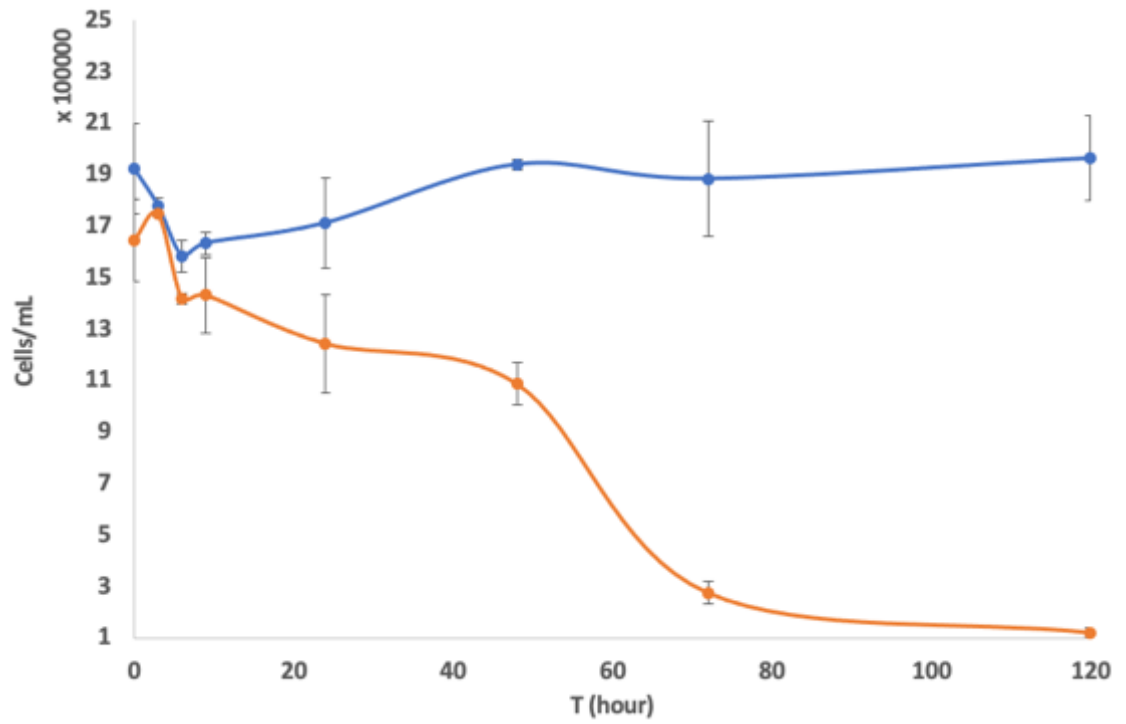
Supplementary Figure 5.1. Preliminary determination of growth curves of *P. parvum* strains obtained from culture collections.



Supplementary Figure 5.2. Initial VLP treatments on *P. parvum* HIK PR1A cultures at 72-h post-infection. VLP treatment was repeated at least 3 times to confirm resistance. No culture 'clearance' or collapse was observed on treated replicates.



Supplementary Figure 5.3. Concentration of DMSP particulate (mMolL⁻¹) on two model diatoms (A) *T. pseudonana* CCMP 1335 and (B) *P. tricornutum* CCAP 1055/1. Cultures grown in F/2 medium mixed in artificial seawater in standard conditions and no addition (control) of H₂O₂ or with addition of 0.25 mM, 0.75 mM or 2 mM of H₂O₂. Samples were taken immediately after the addition of H₂O₂ (0 h), after 0.5 h and after 3 h.



Supplementary Figure 5.4. Virus-like Particle (VLP) infection cycle propagated on *P. parvum* 946/6. The graph shows the average number of algal cells in control cultures (blue line) and VLP treated/infected cultures (orange line). Error bars represent the standard error for triplicate cultures.

Chapter 6

Detection and characterization of toxins produced by newly isolated *Prymnesium parvum* from the Broads

A part of this chapter is published as:

Wagstaff, B., Pratscher J., Rivera P.P.L., Hems E. S., Brooks E., Rejzek, M., Todd, J.D., Murrell, J.C., and Field R.A. (2021). Assessing the Toxicity and Mitigating the Impact of Harmful *Prymnesium* Blooms in Eutrophic Waters of the Norfolk Broads. *Environmental Science & Technology* 2021 55 (24), 16538-16551. DOI: 10.1021/acs.est.1c04742

6.1 Introduction

The toxic haptophyte *Prymnesium parvum* has been implicated in the production of ecosystem destructive algal blooms and devastating fish kill events worldwide every year. In the UK, recurrent *Prymnesium* blooms have been plaguing the Norfolk broads since its first reported devastating fish-killing bloom in 1969 (Holdway et al., 1978). The Norfolk broads is renowned for its unique wetland biodiversity for it is home to more than a quarter of the rarest wildlife in the UK. It also draws in tourists for high-profile angling and boating activities that generate thousands of jobs and hundreds of millions of pounds annually (Broads Authority, 2017). The persistent *Prymnesium* blooms and subsequent fish-killing events remain a serious threat to the local wildlife biodiversity, which result in a tremendous blow to the ecology as well as in the local economy.

Prymnesium parvum is known to synthesize toxigenic metabolites that have deleterious effects on gill-breathing organisms. The toxicity is attributed to, not just one single compound but, a complex mixture of toxic substances (Shilo & Sarig, 1989) which have been shown to exhibit potent cytotoxic, hemolytic, neurotoxic, and ichthyotoxic effects (Manning & La Claire, 2010). These toxins were also known to have lytic activity towards both prokaryotic and eukaryotic single-celled organisms (Yariv & Hestrin, 1961; Tillmann, 2003). The *Prymnesium* toxins include lipopolysaccharides (Paster, 1973), a galactoglycerolipid (Kozakai et al., 1982), proteolipid (Dafni et al., 1972), ladder-framed polyoxy-polyene-polyethers (Igarashi et al., 1996; Igarashi et al., 1999; Manning & La Claire, 2013; Rasmussen et al., 2016), cyclo amines (Bertin et al., 2012), reactive oxygen species (James et al., 2011; Dorantes-Aranda et al., 2015), acrylic acid from dimethylsulfoniopropionate (DMSP) breakdown (Sieburth, 1960), fatty acid amides (Bertin et al., 2012), and toxic fatty acids (Henrikson et al., 2010) with assorted fish-killing, cytotoxic, hemolytic, hepatotoxic, neurotoxic, and/or antimicrobial (allelopathic) activity (Burkholder, 2009). Only a few of these toxins have been characterized due to the complexity of separating each component and the difficulty to assess individual toxicity and there are conflicting reports of required conditions (e.g., temperature, nutrients, pH, salinity etc.) for toxin production (Maestrini & Bonin, 1981; Fistarol et al., 2003; Edvardsen & Imai, 2006).

In the mid-1990's, Igarashi and colleagues succeeded in isolating and characterizing two glycosidic hemolytic-ichthyotoxic substances, subsequently called prymnesin-1 (PRM1, C₁₀₇H₁₅₄Cl₃NO₄₄) and prymnesin-2 (PRM2, C₉₆H₁₃₆Cl₃NO₃₅) (Igarashi et al., 1996). These were the

first toxic metabolites to be chemically characterized from any isolate of *P. parvum* using modern analytical methods (Manning & La Claire, 2010). The potency of prymnesins exceeds that of the well-known toxin, saponin, and it is comparable to brevetoxin (produced by fish-killing dinoflagellate *Karenia brevis*), making prymnesins one of the highly ichthyotoxic compounds (Igarashi et al., 1999).

PRM1 and PRM2 appear to be structurally complex ladder-framed polycyclic ether compounds with remarkably distinct key features (Fig. 6.1 a) (Igarashi et al., 1996; Igarashi et al., 1999). They have double and triple carbon-carbon bonds in the unsaturated head and tail regions, an amino group, several chlorines, four 1,6-dioxadecalin units, and an assortment of sugar moieties (Fig. 6.1 a) (Igarashi et al., 1996; Igarashi et al., 1999; Manning & La Claire, 2010). Structurally, PRM1 and PRM2 are homologous compounds with a common head and backbone: they differ only in the number and in the type of sugars in the tail region, with PRM2 containing a rare L-xylose. PRM1 was shown to be slightly more polar (due to the additional sugar residues) and it elutes ahead of PRM2 in reversed-phase C-18 chromatography (Manning & La Claire, 2010) (Fig. 6.1 a).

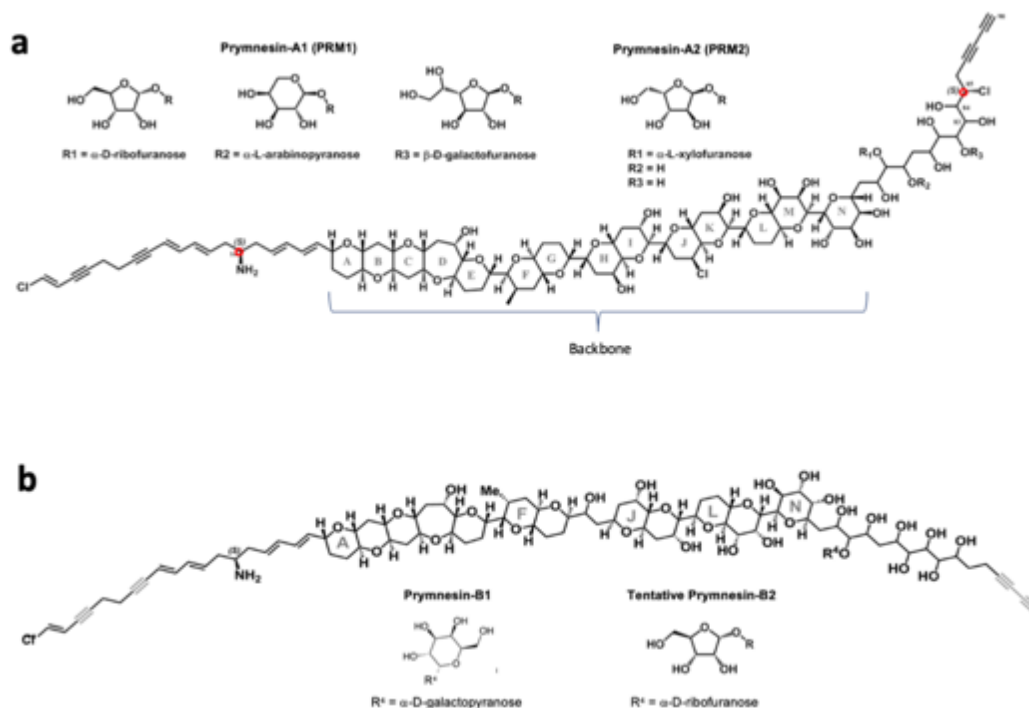


Figure 6.1. The structures of A-type and B-type prymnesins. (a) prymnesin-A1 (PRM1) and prymnesin-A2 (PRM2) toxins isolated and characterized by Igarashi et al. (1996). Synthesis studies have confirmed the absolute conformation of the ring series A-K and the sinistral (S) chiral centers at carbons C14 and

C85 highlighted in red. (b) Structure of a B-type prymnesin, notice the lack of ring-system at position H, I as it was replaced by carbon-carbon bond. prymnesin-B1 contained D-galactose and prymnesin-B2 contained D-ribose based on chiral GCMS run (Rasmussen et al., 2016).

Upon examining 10 different type strains of *P. parvum* from various places, Rasmussen et al. (2016) discovered that *P. parvum* produces not only PRM1 and PRM2 but three different types of prymnesins. They were classified/grouped as A- B- and C-type prymnesins, differentiated by the number of the core carbon atoms in the anglycone backbone of the molecule. A-type prymnesins such as PRM1 and PRM2 are the largest with 91 carbons, while the backbone of B- and C-type prymnesins contains 85 and 83 carbons, respectively (Rasmussen et al., 2016). The chemical structure for both A- and B-type prymnesins (Fig. 6.1 a,b) is well characterized whereas, the core structure of C-type prymnesins has not been elucidated (Igarashi et al., 1996; Igarashi et al., 1999; Rasmussen et al., 2016). This discovery revealed large structural diversity in the prymnesin types produced by different strains of *Prymnesium* investigated. Furthermore, each *Prymnesium parvum* strain exclusively produced only one of the three prymnesin types and never a combination (Rasmussen et al., 2016) despite producing different variants of each prymnesin type. Recently, Binzer et al., (2019) expanded this study to 26 different *P. parvum* strains and identified a total of 51 analogs of prymnesins (9 for A-type, 12 for B-type, and 30 for C-type). Differences within each prymnesin type are found in the number of chlorine (1 to 4), number of oxygen atoms, number of double bonds, and the attached sugar moieties (0 to 3) (Rasmussen et al., 2016; Hems et al., 2018; Binzer et al., 2019) (Sup. Table 6.1). They also reported that the production of A-, B- and C-type prymnesins is related to the three major clades within *P. parvum*, thus, establishing the link between chemotype and phylotype in the toxigenic haptophyte. This genotypic and phenotypic difference between strains revealed a possible existence of cryptic species within *Prymnesium parvum* and challenges its current morphological species assignment (Binzer et al., 2019).

Until now prymnesins remain difficult to quantify, despite numerous efforts and several decades of study, and the routine methodologies have not been fully established to isolate and quantify the various toxic fractions (Burkholder, 2009; La Claire et al., 2015). The use of liquid chromatography coupled with mass spectrometry (LCMS) and Nuclear Magnetic Resonance (NMR) was found to be useful and preferred analytical methods for identification and quantification of prymnesins in complex mixtures (Manning & La Claire, 2013) due to its high selectivity and sensitivity. But these procedures were very complex, expensive, and time-

consuming and quantification of toxin through MS requires purified standards which are not currently available (Manning & La Claire, 2010). To address this, a semi quantification method using a fluorometric assay, specifically a ninhydrin reaction on the conserved primary amine group of the prymnesins was developed (La Claire et al., 2015). A similar method was employed by Hems et al. (2018) where they used the conserved terminal bis-alkyne instead of the amine group for tagging the prymnesins via bioorthogonal copper-catalysed alkyne-azide cycloaddition (CuAAC) or 'click' chemistry and examined the clicked products using high performance liquid chromatography – high-resolution mass spectrometry (HPLC-HRMS). Despite these developments, the chemical isolation and quantification of individual prymnesins have proved to be tedious, and alternative assays will need to be developed for the specific *in vitro* detection of prymnesins.

P. parvum can thrive in various physical conditions, but nutrient availability has been shown to greatly influence its bloom formation and toxin production (Manning & La Claire, 2010). The effect of phosphorus is the most widely studied factor related to prymnesin toxicity. It was first demonstrated by Shilo (1969) that low phosphorus conditions resulted in increased toxicity of *P. parvum* and this trend has been confirmed in various studies (Dafni et al., 1972; Meldahl et al., 1994; Johansson & Graneli, 1999; Uronen et al., 2005; Graneli & Salomon, 2010). These lab findings were also reflected on what has been observed *in situ*, where *P. parvum* toxicity is elevated under high N:P ratios (Kartvedt et al., 1991; Lindholm et al., 1999). Overall, these observations support that toxic blooms of *P. parvum* (capable of producing massive fish kills) might occur when nutrients are sufficient and then subsequent nutrient limiting conditions could lead to an increase in cellular toxin production and the eventual release of toxins upon bloom collapse.

In this chapter, I determined the type of prymnesins produced by the newly isolated *P. parvum* strains from Hickling Broad and Woodbridge Fisheries using LC-MS. I examined the clade grouping of *P. parvum* Hickling strain using its complete ITS sequences (ITS1 & ITS2) compared to 25 other *P. parvum* strains from different culture collections and I map the type of prymnesins onto a topology tree. Lastly, preliminary results of studies on the effect of varying phosphorus conditions (Low P, Normal P, High P) and low salinity (LS) conditions on prymnesin profiles and the relative abundances of the strains were carried out and presented here.

6.2 Methods

6.2.1 Isolation of *P. parvum* broad strains

P. parvum strain HIK PR1A, HIK PR6H, and HIK PR12D were isolated from Hickling Broad, Norfolk Broads during a minor bloom of *P. parvum* in June 2017. *P. parvum* strain WBF PRC1 and WBF PRD2 were isolated from Woodbridge Fisheries, Suffolk Broads during a mixed cyanobacteria-haptophyte bloom in February 2018. Full details of the study site and the isolation process were discussed in Chapter 2.

6.2.2 Culture conditions and extraction of toxins

Prymnesin toxin extraction was performed using a modified protocol used by Manning & La Claire (2015). Batch cultures (150 mL) of *Prymnesium parvum* HIK PR1A, HIK PR6H, HIK PR12D, WBF PRC1, WBF PRD2 were grown in 5 PSU f/2 media at room temperature in a 14:10 h (light: dark) cycle as previously described in Chapter 2. After 3 weeks, when the *Prymnesium* cells reached a late exponential growth phase at cell concentrations between 5×10^5 to 2×10^6 cells mL⁻¹; cell biomass was harvested by centrifugation (4000 × g for 5 minutes) and the supernatant was discarded. The cells were suspended in cold acetone (2 mL, -20 °C) and subject to vortex mixing for two minutes. The resulting suspensions were then centrifuged at 30,000 × g for 5 minutes. The supernatant was discarded, being careful not to disturb the cell debris, and the pellets were subjected to two more cycles of the same acetone wash procedure. The acetone wash was necessary for the removal of any interfering compounds including chlorophylls and accessory pigments. The cell pellets were then resuspended in methanol (MeOH, 2 mL) and vortex mixed for two minutes, after which time the cell debris was pelleted by centrifugation (30,000 × g for 5 minutes) and the supernatant was collected. This methanol extraction was repeated two more times, followed by three rounds of analogous extraction using n-propanol (n-PrOH). The MeOH and n-PrOH extracts were combined, dried in vacuo (Speed VAC, Vacuum Centrifuge Concentrator) and stored at -20 °C until further use.

6.2.3 LC-MS detection of prymnesin toxins

Analysis of the *Prymnesium* extracts was performed using an LC-MS on a Synapt G2-Si mass spectrometer coupled to an Acquity UPLC system (Waters, Manchester, UK) at the John Innes

Center (JIC) with the help of Dr. Gerhard Saalbach and Dr. Carlo de Oliveira-Martins. The extracts were first dissolved into 1000 μL of 50% EtOH. 7 μL aliquots of samples were injected onto an Acquity UPLC[®] BEH C18 column, 1.7 μm , 1 x 100 mm (Waters) and eluted with a gradient of 1-60% acetonitrile in 0.1% formic acid in 6 min at a flow rate of 0.08 ml min⁻¹ with a column temperature of 45°C. The mass spectrometer was controlled using Masslynx 4.1 software (Waters) and operated in positive MS-Tof and resolution mode with a capillary voltage of 3 kV and a cone voltage of 40 V in the m/z range of 100-2000. Leu-enkephalin peptide (0.25 μM , Waters) was infused at 10 $\mu\text{l min}^{-1}$ as a lock mass and measured every 30 s.

6.2.4 HIK PR1A ITS sequence and phylogenetic inference

The ITS sequence (including 5.8S rDNA) of *P. parvum* HIK PR1A was determined by querying the transcriptome dataset generated previously in Chapter 4 with the available ITS gene sequences downloaded from GenBank (<https://www.ncbi.nlm.nih.gov/uea.idm.oclc.org/genbank/>) using the local Blastn. In addition, the ITS sequence of *P. parvum* UOBS-LP0109 (Texoma1) strain, isolated from Lake Texoma, Oklahoma, USA, was also queried against its publicly available transcriptome (Texoma1– Marine Microbial Eukaryote Transcriptome Sequencing Project, MMETSP) (Keeling et al., 2014) (Supp. Data). The sequences were deposited in GenBank (<https://www.ncbi.nlm.nih.gov/uea.idm.oclc.org/genbank/>) and accession numbers are provided in Supplementary Table 6.2.

The phylogeny of *P. parvum* HIK PR1A and Texoma1 strains together with other 24 different *P. parvum* strains from culture collections was inferred by analysing the 696 base-pair ITS1 and ITS2 sequences including introduced gaps. The ITS sequences of most *P. parvum* strains used in this analysis are publicly available and published in Binzer et al. (2019). Sequences were aligned using ClustalW using Mega v7 and the resulting data matrix was analysed using Bayesian approach and visualized in a maximum likelihood phylogenetic tree to observed the relatedness of the sequences. A total of 10×10^6 generations and a sampling frequency of trees for every 1000 generations was used. The robustness of the tree topology was evaluated with 1000 bootstrap replications. *Platychrysis pigra* was used as the outgroup in phylogenetic analysis.

6.2.5 Effect of varying P and low salinity on prymnesins

The effect of various phosphorous ($\text{PO}_4\text{-P}$) conditions (LP, NP, HP) and low salinity (LS) on the changes in the prymnesin profiles of *P. parvum* HIK PR1A as compared to standard conditions

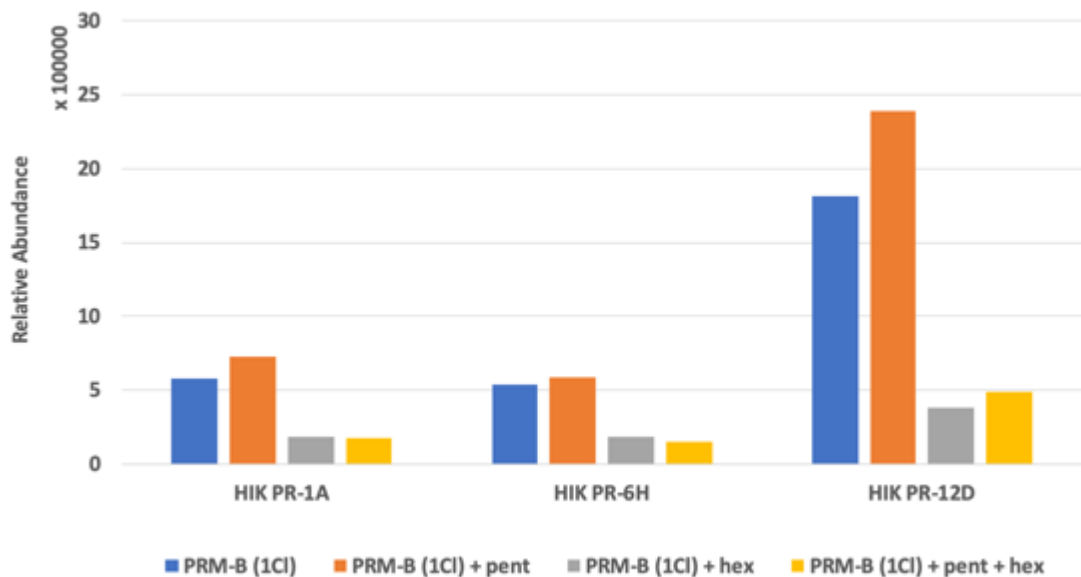
was investigated. For various P conditions and LS, batch cultures were grown following the growth in non-standard conditions described in Chapter 2. When cultures reached late exponential growth, cell biomass was harvested and pelleted by centrifugation and immediately processed for prymnesin extraction following the procedure detailed in Section 6.2.2.

Two separate experiments were done, the first was to screen for the effect of LP and LS on the prymnesin production. For the second experiment, I studied the effects of varying phosphorous availability but this time extending my conditions to not just only Low P, but also including high P conditions. Standard conditions served as control. All experiments were done in three biological replicates.

6.3 Results

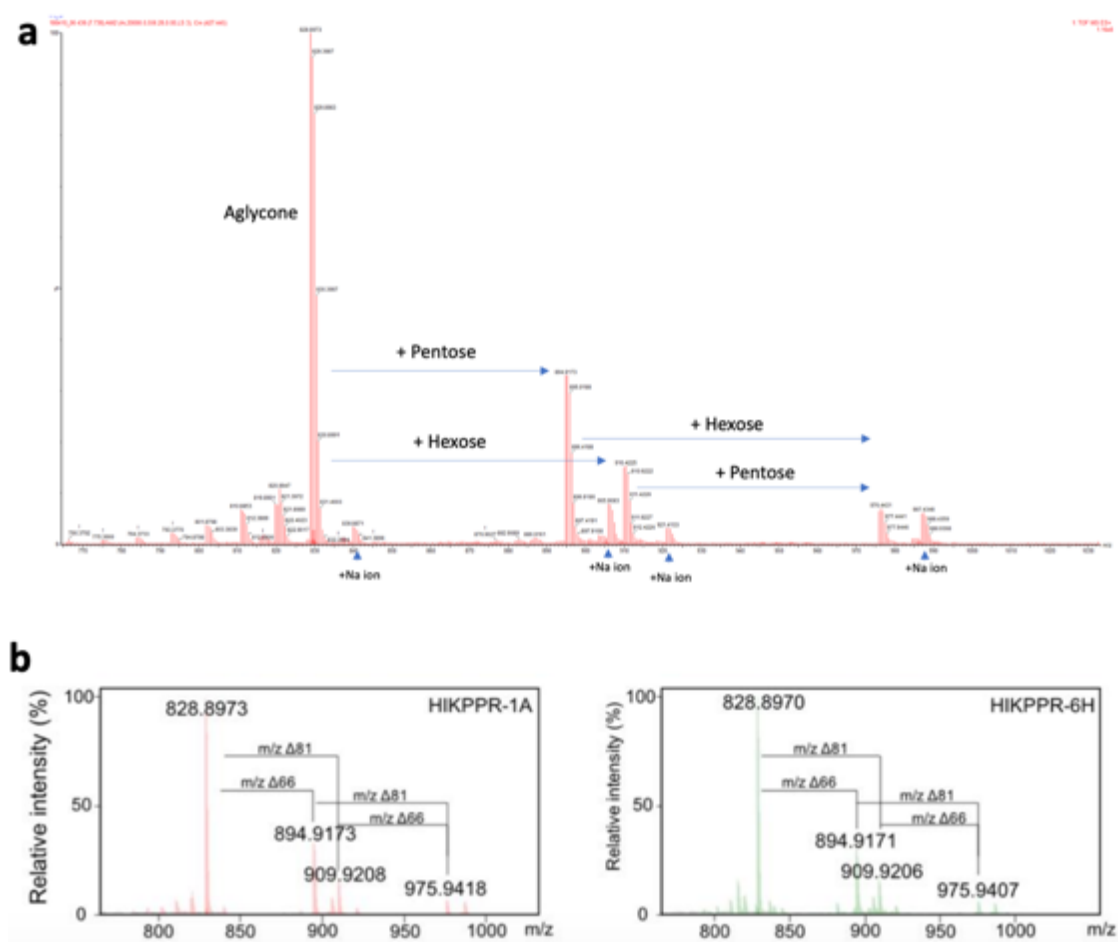
6.3.1 Prymnesin profiles of the Broads isolates

Five different strains of *P. parvum* isolated from Norfolk and Suffolk broads were grown to late exponential phase, harvested, and their prymnesins types were determined. The Hickling broad strains (HIK PR1A, HIK PR6H, and HIK PR12D) gave similar prymnesin profiles/types and were confirmed to produce the B-type prymnesins (Fig. 6.2) based on the molecular features described in Rasmussen et al. (2016). It is important to note that the results are presented as relative prymnesin abundance since there were no prymnesin reference or internal standards available.



Figures 6.2. Relative abundance of Pymnesin types found in *P. parvum* strains isolated from Hickling broad. Pymnesin-B type and sub-types were all present in the Pymnesium strains isolated from Hickling Broads. PRM-B (1Cl) - pymnesin B-type backbone with one incorporated chlorine atom; pent - pentose conjugate; hex - hexose conjugate.

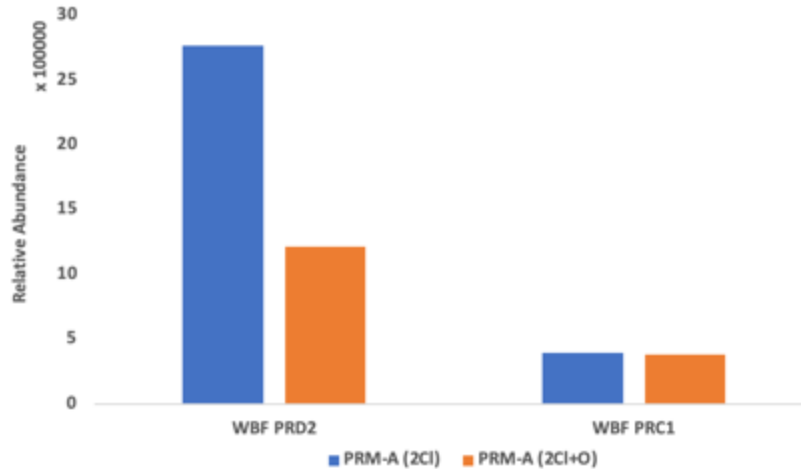
In addition to detecting signals corresponding to pymnesin-B1 type (PRM-B (1 Cl) + hexose), with 1 hexose sugar attached, we also detected m/z signals corresponding to the same toxin backbone but glycosylated with a pentose sugar (pymnesin-B2 type or PRM-B (1 Cl) + pentose), and the type toxin with both a hexose and pentose (PRM-B (1 Cl) + pentose + hexose) which Svenssen et al. (2019) detected recently in *P. parvum* strains from Denmark, Norway, and Germany. Due to poor separation of these species under our chromatography conditions, it is unclear whether the organism produces a mixture of these forms of the toxin (Fig. 6.3), or whether the loss of m/z values corresponding to these sugars is an artefact of mass spectrometry fragmentation, as is frequently the case for this class of compounds.



Figures 6.3. MS-based identification of B-type pymnesins from Hickling broad *P. parvum* isolates. (a) ESI-MS spectrum showing detection of the diagnostic signal for the aglycone backbone (m/z 828.9), mono glycosylated with a pentose (m/z 894.9), mono glycosylated with a hexose (m/z 909.9), and double glycosylated with pentose and hexose (m/z 975.9) of the B-type pymnesins from *P. parvum* HIK PR1A cell extracts. (b) Comparison of ESI-MS spectra showing detection of the diagnostic signals for B-type pymnesins of HIK PR1A (left) and HIK PR6H (right). All masses observed for the toxins have errors less than Δ 3 ppm with the exception of m/z 975.9407 of the intact double glycosylated toxin from HIK PR6H which has an error of Δ -3.8 ppm. Figure 6.3b adapted from Wagstaff et al. (2020).

Furthermore, the pymnesin profiles of two additional *P. parvum* strains isolated from Woodbridge Fen Fisheries, Suffolk during a mixed cyanobacteria- *P. parvum* bloom in January 2018 proved to be different from those isolated from Hickling. Initial toxin profiling data suggest that these two strains (WBF PRC1 and WBF PRD2), were more likely to produce A-type pymnesins (Fig. 6.4). The strains only produced two major variants of non-glycosylated A-type pymnesins (PRMA). There was a pymnesin A-type backbone with two incorporated chlorine atoms (PRM-A (2Cl)) and a pymnesin A-type backbone with two incorporated chlorine atoms

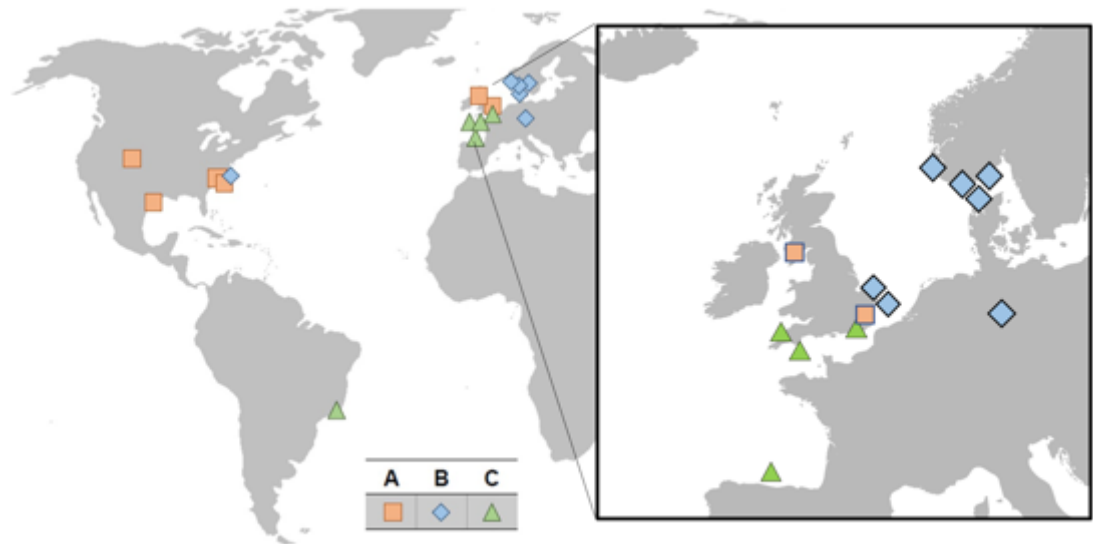
plus one oxygen atom (PRM-A (2Cl+O)). It is interesting to note that no fish kill was observed during the bloom despite its high abundance (1.8×10^5 cells mL^{-1}). Additional investigations are warranted to further study the prymnesins profiles/types from these two unique strains.



Figures 6.4. Relative abundance of Prymnesin types found in *P. parvum* strains isolated from Woodbridge Fen Fisheries. Prymnesin-A type and a sub-type were found in the strains. Apparently, only two non-glycosylated forms were found in abundance; PRM-A (2Cl) - prymnesin A-type backbone with two incorporated chlorine atoms; PRM-A (2Cl+O) - prymnesin A-type backbone with two incorporated chlorine atoms plus one oxygen atom.

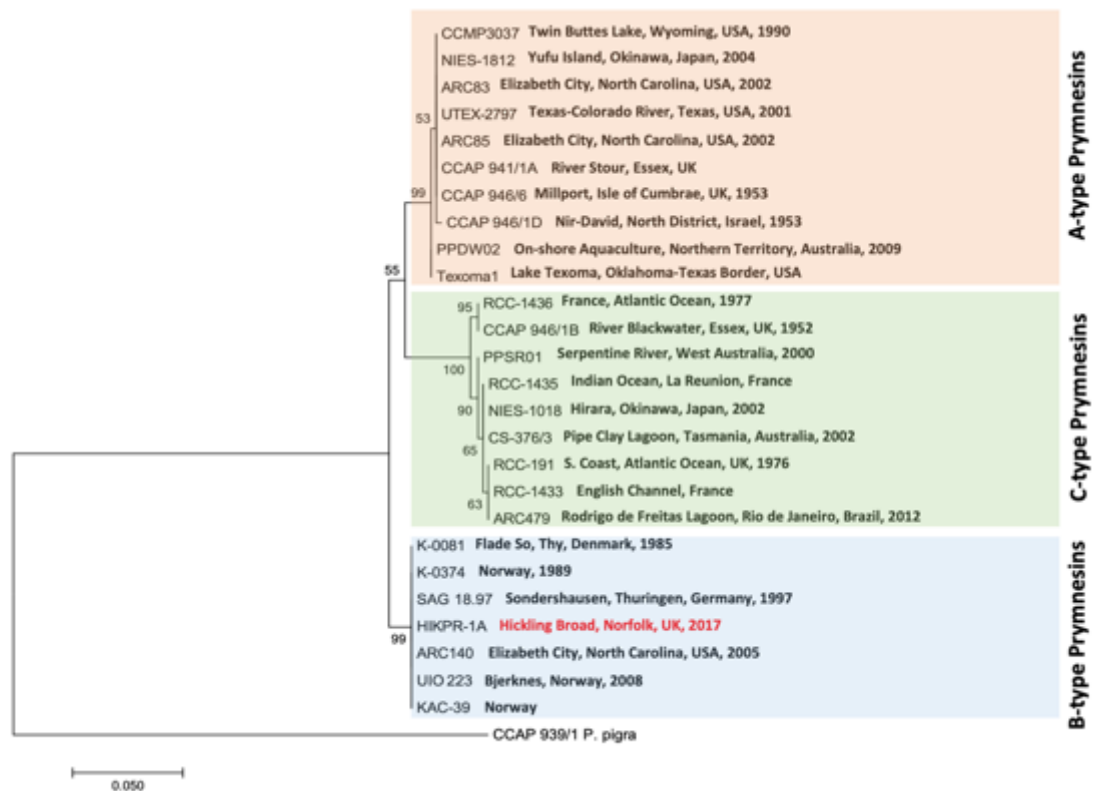
6.3.2 Distribution of *P. parvum* producing A-, B-, C-type prymnesins

Next, I looked at the global distribution pattern of *P. parvum* based on prymnesin types and mapped the Hickling *P. parvum* strain prymnesins (Fig. 6.5). The origin of all known *Prymnesium parvum* strains are illustrated on the world map and color-coded based on the type of prymnesin produced. Based on the map, I found that the Hickling broad *P. parvum* strains were the only known B-type prymnesins producing *P. parvum* in the UK. All other UK strains previously isolated and stored in culture collections were found to produce only either A-type or C-type prymnesins (Fig. 6.4). This suggests that the UK have now set a record of having *P. parvum* strains capable of producing each of the three types of prymnesins.



Figures 6.5. Geographical distribution of *Pymnesium parvum* producing A-, B-, and C-type prymnesins. Broads *P. parvum* strains were the first known strains to produce B-type prymnesins in the UK. Adapted from Binzer et al. (2019).

To build on these findings I generated a phylogenetic tree from the internal transcribed spacer regions (ITS1 and ITS2) of the nuclear ribosomal cistron using a total of 26 different *P. parvum* strains with a wide geographical distribution (including a Hickling strain (HIK PR1A) and a lake Texoma strain (Texoma1)). The tree topology using Bayesian inference is illustrated in Fig. 6.6. The Hickling *P. parvum* strain clustered with B-type prymnesins-producing strains mainly isolated from northern Europe confirming the results of toxin analysis. This signifying that Hickling *P. parvum* strains are closely related to the Scandinavian isolates. The Texoma1 strain clustered well with the ones isolated from Northern America and this might suggest that this strain is producing the A-type prymnesins.



Figures 6.6. Phylogeny of 26 widely distributed strains of *Prymnesium parvum* inferred from Bayesian analysis. Analysis was based on 696 base pairs (including introduced gaps) of internal transcribed spacers (ITS-1 and ITS-2) and the 5.8S rDNA gene. *Platychnysis pigra* was used as an outgroup. Numbers at internal nodes are posterior probabilities (≥ 0.5) from Bayesian analysis followed by bootstrap values ($\geq 50\%$) from maximum likelihood with 1,000 replications. Strain numbers and geographical origin are provided for all sequences. Branch lengths are proportional to the number of character changes.

6.3.3 Effect of varying P and low salinity on prymnesins

The effect of available nutrients (e.g. phosphorus and nitrogen) and salinity on the toxicity of *P. parvum* are well studied (Dafni et al., 1972; Baker et al., 2007; Uronen et al., 2005; Graneli & Salomon, 2010). Here, I examined the effects of these two variables on the prymnesins produced by the *P. parvum* isolated from Hickling broads. For the first experiment, *Prymnesium* cells were grown in low salt (LS) and low phosphorus (LP) conditions with cultures under normal phosphorus and salinity (NP) served as standard control. The relative ratios of individual prymnesins are shown in Fig. 6.7. Initial results suggest that the LP condition does not have any effect on the production of each prymnesin type and no significant changes were observed. The

LS condition on the other hand served to increase the ratio of non-glycosylated type and reduce those for all other glycosylated prymnesin types.

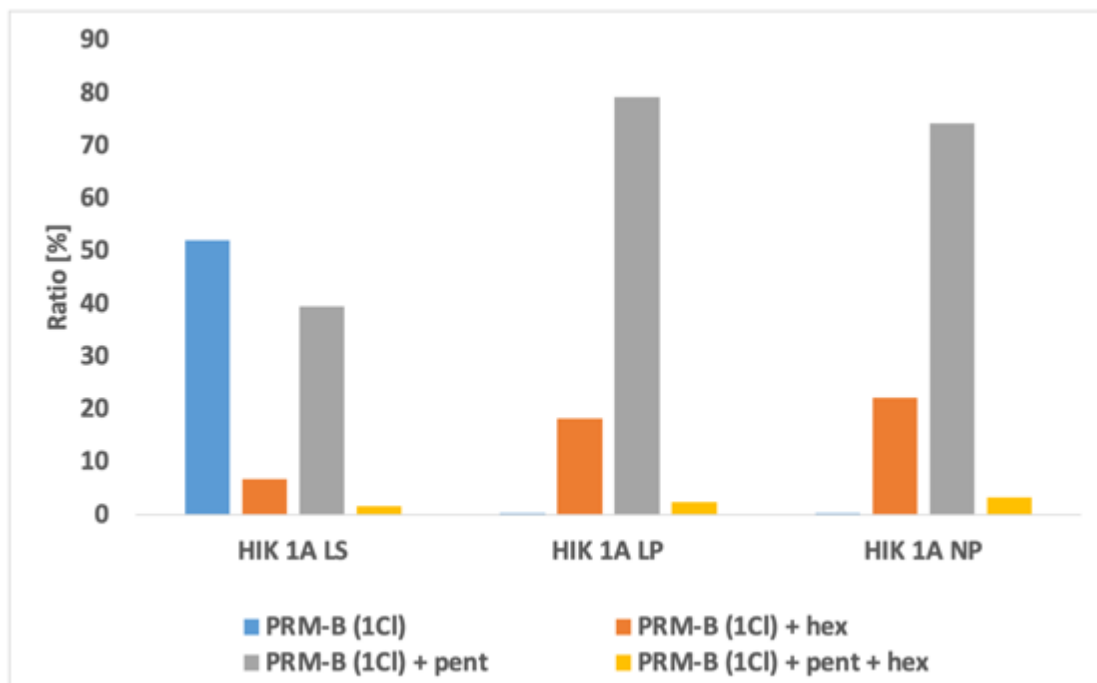
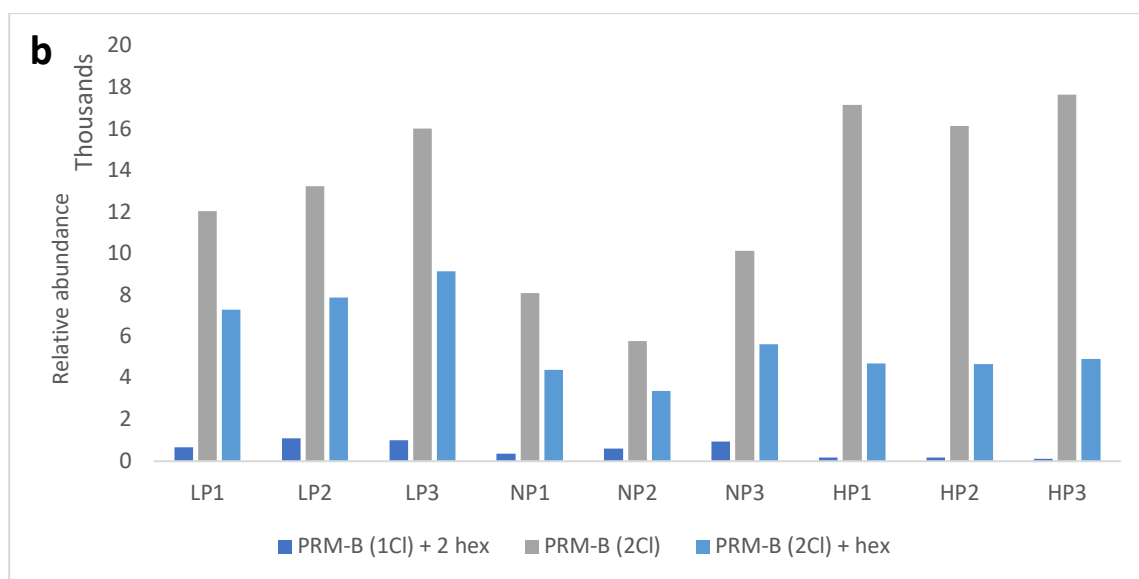
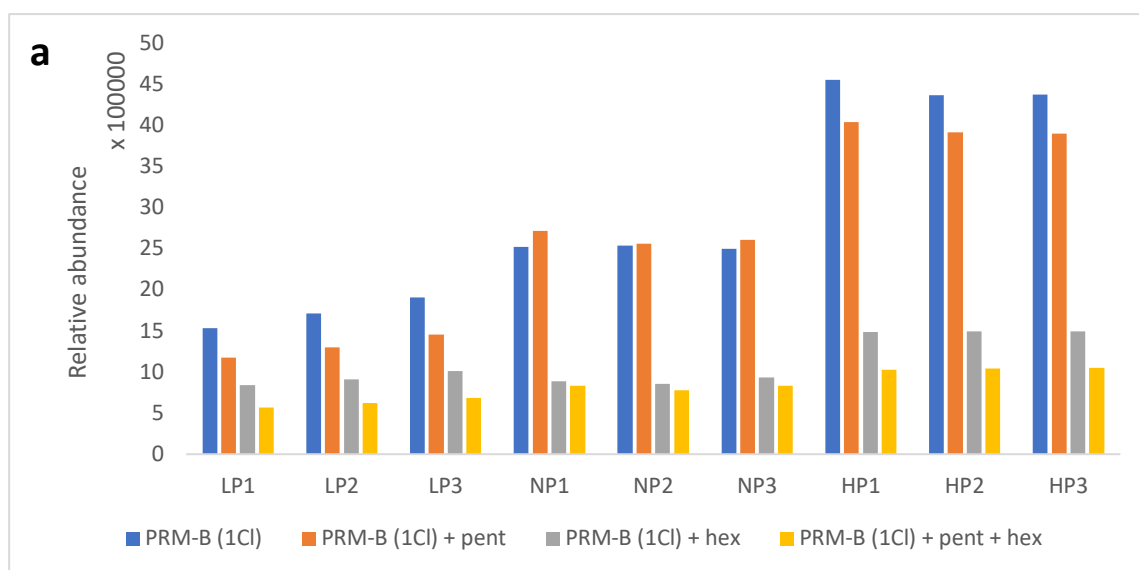


Figure 6.7. HIK PR1A manual integration: Relative ratios of the individual prymnesin peak areas as a function of the sum of all prymnesin peak areas present in the sample. Abbreviations: HIK 1A LS – low salinity culture; HIK 1A LP – low phosphate culture; HIK 1A NP – normal phosphate culture; PRM-B (1Cl) – prymnesin B-type backbone with one incorporated chlorine-atom; pent – pentose conjugate; hex – hexose conjugate.

Unconvinced with the initial results, I repeated this experiment with a wider range of phosphorus levels. This time I used low phosphorus (LP) and high phosphorus (HP) conditions with normal phosphorus (NP) as the standard control. I also searched for more prymnesin B subtype signals based on the prymnesins B-type masses reported by Rasmussen et al. (2016) (Supp. Table 6.1).

Results from the second experiment showed that the abundance of B-type prymnesin and its subtypes were enhanced when *P. parvum* is subjected to LP conditions (Fig. 6.8 a) and these were more pronounced in the relative abundance of minor prymnesins analogs/subtypes (Fig. 6.8 b). Under HP conditions, *P. parvum* prymnesin profiles were showed that non-glycosylated forms increased in abundance. These results suggest that under limiting P conditions, more glycosylated forms of prymnesin B type are produced while under replete P conditions only non-glycosylated forms were produced.



Figures 6.8. Relative abundances of the individual Prymnesin-B analogs/sub-types present in the sample grown at low, normal and high phosphate conditions. LP – low phosphate culture; NP – normal phosphate culture; HP – high phosphate culture; (a) Changes in the relative abundance of major components of B-type prymnesins; (b) Changes in the relative abundance of minor components of B-type prymnesins. PRM-B (1Cl) – prymnesin B-type backbone with one incorporated chlorine-atom; PRM-B (2Cl) – prymnesin B-type backbone with two incorporated chlorine-atoms; pent – pentose conjugate; hex – hexose conjugate. (ANOVA, Prymnesins: $F = 1620.3$, $p < .001$; Varying P: $F = 525.65$, $P < .001$; Prymnesins & Varying P: $F = 139.8$, $p < .001$).

6.4 Discussion

P. parvum blooms have been a problem on the Norfolk Broads since its first confirmed fish-killing bloom in 1969, which wiped out almost the entire fish population of the area. Since then, sporadic and recurrent *P. parvum* blooms have plagued the broads posing a serious threat to the local wildlife biodiversity, that can result in tremendous blow to its unique wetland ecosystem and local economy. In this study, I characterized the prymnesin toxins produced by broads *P. parvum* strains and compared them to other *P. parvum* strains isolated from various places. I mapped out the phylogeny of the Hickling isolate based on its full ITS sequence. Furthermore, I did some preliminary works on the effects of varying phosphorus and low salinity conditions on prymnesin production that might shed light on how these variables may influence its toxicity.

6.4.1 Hickling broad *P. parvum* produce B-type prymnesins

The three types of prymnesins (A-, B-, C-type) are differentiated by the length of the core carbon backbone of the compound (Rasmussen et al., 2016). This trait is uncommon among phycotoxins for they usually have fixed carbon backbone and changes only tend to occur on the number of side chains and functional groups attached (e.g. saxitoxins, karlotoxins, ciguatoxins, azaspiracis etc.) (Twiner et al., 2008; Cusick & Saylor, 2013; Rasmussen et al., 2016; Binzer et al., 2019).

Rasmussen et al. (2016) reported several analogs or subtypes of each type of prymnesins found in 10 different strains of *P. parvum*. These prymnesins types and subtypes vary in the number of chlorine atoms, the degree of saturation, and the number of sugar moieties attached. More of these analogs were identified recently which expanded the number to a total of 51 analogs as shown in Supp. Fig. 6.1 (Rasmussen et al., 2016; Hems et al., 2018; Binzer et al., 2019). Systematic names for these analogs were proposed based on mass spectrometric characterization (Binzer et al., 2019). The authors emphasized that these prymnesin analogs were only detected under one growth condition and some analogs that were produced at certain specific growth stages or varying culture conditions might be overlooked.

In 2015, a toxic bloom of *P. parvum* in Hickling broad caused a massive fish kill event eliminating approximately 17,000+ fish (mostly mature stocks, > 10-year-old) and evoked an immediate rescue of 750,000 fish by relocating the stressed fish stocks to non-affected waters. This event also prompted an investigation led by the team of scientists from John Innes Centre (JIC) and the

University of East Anglia (UEA) to identify the type of ichthyotoxins present in the water column. Biological samples, i.e. dead pike (*Exos lucius*), and water samples were taken and brought back to the lab for toxin extraction and analysis. Field samples were then analyzed using LC-MS using targeted approach. There were no signals corresponding to prymnesin-1 or prymnesin-2 detected from either water or fish-gill samples but masses corresponding to prymnesin-B type was detected (Supp. Fig. 6.1). Moreover, the extracted ion chromatograms suggested the B-type prymnesins were present in the dead pike samples and water samples were taken from the algal bloom-affected area. Unfortunately, isolation of the causative organism, *P. parvum*, was not successful during that time and it's difficult to prove whether the prymnesins found in the dead fish and water samples were indeed produced by the toxic haptophyte from the broads.

In June 2017, I isolated a few strains of *P. parvum* from Hickling broad and this gave us a good opportunity to study or characterize the prymnesin type they produce. Later on, additional two *P. parvum* strains were isolated from the neighboring Suffolk broads (Woodbridge Fisheries) during a suspected algal bloom in January 2018. The newly isolated strains were screened for the production of prymnesins. The Hickling broad strains were found to produce a single type of prymnesin and all were found to be B-type prymnesins while the ones isolated from Woodbridge were likely to produce A-type prymnesins. Additional confirmatory tests needed to confirm this preliminary result on Woodbridge *P. parvum* strains. Thus, the presented prymnesin results on the Hickling broad *P. parvum* strains reinforced the earlier findings on the prymnesins found in fish gills and water samples.

6.4.2 First B-type prymnesin producing *P. parvum* in the UK

I compared the prymnesin type produced by the Hickling *P. parvum* strains with other strains recently analysed and reported by Binzer *et al.* (2019) (Supp. Table 6.2) and I found that these strains were the first known B-type producing *Prymnesium* in the UK. I then looked at the biogeographical distribution pattern of prymnesins types (Fig. 6.5) hoping to uncover a trend for accounting for the observed distribution. For example, in the toxic dinoflagellate, *Alexandrium ostenfeldii*, strains from low salinity (Baltic sea) waters produce paralytic shellfish toxins only, while strains from oceanic waters (Mediterranean Sea, Northern Atlantic coast of Canada and US) produce spirolides. Strains from areas with intermediate salinity (Danish Straits) produce both types of toxins (Suikkanen *et al.*, 2013).

Surprisingly, the biogeographical distribution of the *P. parvum* strains followed no trend with A-type producing strains mostly found in North America, but also present everywhere, and B-type producing strains mainly being concentrated in Scandinavian waters, but also present in North America and now in the UK. The C-type prymnesins were present everywhere except in North America. The results presented here are in agreement with what has been observed by Rasmussen et al. (2016) and Binzer et al. (2019).

6.4.3 Phylogeny of *P. parvum*

Previous investigations suggest that *P. parvum* are divided into three major clades based on their ITS sequences (Larsen & Medlin, 1997; Lutz-Carrillo et al., 2010; Binzer et al., 2019). And recently, Binzer et al. (2019) reported that the prymnesins type distribution complemented the clade clustering suggesting links between chemotype and phylotype in *P. parvum*. This observation was also reflected in my phylogenetic results where *P. parvum* strain (HIK PR1A) clustered with B-type prymnesins producing *P. parvum* strains mostly from Northern Europe. This suggests the possibility of vector transfer between these two areas given their proximity to one another, but no current data supports this. The genetic findings of Lutz-Carrillo et al. (2010) showed that *P. parvum* strains from Scotland and the USA were remarkably similar, suggesting that *P. parvum* in the USA originated in Europe and invasion might have occurred recently. Moreover, the lake Texoma strain (Texoma1) grouped with *P. parvum* strains from North America suggesting that this strain produces A-type prymnesins.

6.4.4 Effect of Low phosphorus and low salinity on prymnesin production

Toxin production in *P. parvum*, is variable between strains (Manning & La Claire, 2010; Rasmussen et al., 2016; Svenssen et al., 2019). The total amount of toxins and composition of analogs produced can be altered by certain environmental conditions (Larsen et al, 1993; Baker et al., 2007; Freitag et al., 2011) such as salinity, growth phase, nutrients, etc. This is not uncommon for the same thing has been observed with other toxigenic bloom-forming algae-like *Karenia brevis* (Errera & Campbell, 2011), *Alexandrium spp.*, and *Karlodinium veneficum* (Place et al., 2012; Suikkanen et al., 2013).

Shilo (1969) first reported an increase in the amount of intracellular prymnesins in *P. parvum* when grown in P-limited conditions. This trend was subsequently confirmed by other studies (Dafni et al., 1972; Meldahl et al., 1994; Johansson & Graneli, 1999; Uronen et al., 2005; Graneli

& Salomon, 2010) suggesting that the toxin production of *P. parvum* is related to its growth conditions. Furthermore, studies have also directed their attention to the effects of salinity on prymnesin toxicity since *P. parvum* have a wide osmotic tolerance and earlier studies have reported higher toxicity at low salinity conditions (Parnas et al., 1963; Brand et al., 1984; Baker et al., 2007). However, Larsen and Bryant (1998) found no differences in toxicity when *P. parvum* were grown at varying salinity conditions providing conflicting results on the effects of salinity on prymnesins production.

In this study, I did some preliminary investigations on the effects of low phosphorus (LP) and low salinity (LS) conditions on the prymnesin profiles of Hickling broad *P. parvum* (HIK PR1A). My results suggest that each prymnesin analog or type/subtype changes as the algal cells undergo limiting growth due to nutrient stress and low salinity conditions. In addition, increased abundance of glycosylated analogs of prymnesin was observed which might enhanced its toxicity upon release from the algal cells through cell autolysis, breakdown due to grazing, and virulence.

6.5 Conclusion

In this chapter, I determined the prymnesin type produced by *Prymnesium parvum* strains isolated from Hickling broads and Woodbridge fisheries. The Hickling broad *P. parvum* strains produce B-type prymnesins based on LC-MS analysis. These results are in congruence with the earlier detected prymnesin-B toxin from Pike gill tissues and water samples taken during a fish-killing *Prymnesium* bloom back in 2015. This implies that the *P. parvum* prymnesins were the leading cause of fish mortalities in the area. The broads *P. parvum* were the first known B-type producing strains in the UK which might suggest that this strain was introduced more recently. Upon mapping its phylogenetic topology, the Hickling strains clustered with the B-type prymnesin producing strains from Northern Europe indicating its relatedness to this *P. parvum* group. Furthermore, initial screening results of the prymnesins isolated from Woodbridge suggest that the strains produce A-type prymnesins based on the masses of prymnesin analogs found. Further research is warranted to confirm and determine the exact characteristics of these set of prymnesins for they didn't cause any fish kills during an algal bloom event in February 2018. Finally, nutrient limiting conditions such as low phosphorus influenced the abundance of prymnesin analogs/types/subtypes and were found to enhance the abundance of glycosylated forms over non-glycosylated forms. This Indicates the significance of nutrient availability on the toxin production and toxicity of *P. parvum* cells.

6.6 Supplementary Data

Supplementary Table 6.1. All proposed systematic names of A-, B-, C-type prymnesins

	Proposed Systematic Name	Proposed Sum Formula	Exact Masses		
			[M+H] ⁺	[M+2H] ⁺²	[M+Na+H] ⁺²
A-type Prymnesins	PRM-A (2 Cl + DB)*	C ₉₁ H ₁₂₇ Cl ₂ NO ₃₁	1800.7842	900.8957	911.8867
	PRM-A (2 Cl + DB) + pentose	C ₉₆ H ₁₃₅ Cl ₂ NO ₃₅	1932.8264	966.9169	977.9078
	PRM-A (2 Cl)	C ₉₁ H ₁₂₉ Cl ₂ NO ₃₁	1802.7998	901.9036	912.8945
	PRM-A (2 Cl) + pentose	C ₉₆ H ₁₃₇ Cl ₂ NO ₃₅	1934.8421	967.9247	978.9157
	PRM-A (2 Cl) + 2 pentose + hexose	C ₁₀₇ H ₁₅₅ Cl ₂ NO ₄₄	2228.9372	1114.9722	1125.9632
	PRM-A (2 Cl + O)*	C ₉₁ H ₁₂₉ Cl ₂ NO ₃₂	1818.7948	909.9010	920.8920
	PRM-A (2 Cl + O) + pentose	C ₉₆ H ₁₃₇ Cl ₂ NO ₃₆	1950.8370	975.9221	986.9131
	PRM-A (3 Cl)	C ₉₁ H ₁₂₈ Cl ₃ NO ₃₁	1836.7609	918.8841	929.8750
	PRM-A (3 Cl) + pentose (prymnesin-2)	C ₉₆ H ₁₃₆ Cl ₃ NO ₃₅	1968.8031	984.9052	995.8962
	PRM-A (3 Cl) + pentose + hexose	C ₁₀₂ H ₁₄₆ Cl ₃ NO ₄₀	2130.8559	1065.9316	1076.9226
	PRM-A (3 Cl) + 2 pentose + hexose (prymnesin-1)	C ₁₀₇ H ₁₅₄ Cl ₃ NO ₄₄	2262.8982	1131.9527	1142.9437
B-type Prymnesins	PRM-B (1 Cl + DB)	C ₈₅ H ₁₂₀ ClNO ₂₉	1654.7707	827.8890	838.8800
	PRM-B (1 Cl + DB) + pentose	C ₉₀ H ₁₂₈ ClNO ₃₃	1786.8130	893.9101	904.9011
	PRM-B (1 Cl)	C ₈₅ H ₁₂₂ ClNO ₂₉	1656.7864	828.8968	839.8878
	PRM-B (1 Cl) + pentose (prymnesin-B2)	C ₉₀ H ₁₃₀ ClNO ₃₃	1788.8286	894.9180	905.9089
	PRM-B (1 Cl) + hexose (prymnesin-B1)	C ₉₁ H ₁₃₂ ClNO ₃₄	1818.8392	909.9232	920.9142
	PRM-B (1 Cl) + pentose + hexose	C ₉₆ H ₁₄₀ ClNO ₃₈	1950.8815	975.9444	986.9353
	PRM-B (1 Cl) + 2 hexose	C ₉₇ H ₁₄₂ ClNO ₃₉	1980.8920	990.9497	1001.9406
	PRM-B (2 Cl)	C ₈₅ H ₁₂₁ Cl ₂ NO ₂₉	1690.7474	845.8773	856.8683
	PRM-B (2 Cl) + pentose	C ₉₀ H ₁₂₉ Cl ₂ NO ₃₃	1822.7897	911.8985	922.8894
	PRM-B (2 Cl) + hexose	C ₉₁ H ₁₃₁ Cl ₂ NO ₃₄	1852.8002	926.9038	937.8947
	PRM-B (2 Cl) + pentose + hexose	C ₉₆ H ₁₃₉ Cl ₂ NO ₃₈	1984.8425	992.9249	1003.9159
	PRM-B (2 Cl) + 2 hexose	C ₉₇ H ₁₄₁ Cl ₂ NO ₃₉	2014.8531	1007.9302	1018.9211

	Proposed Systematic Name	Proposed Sum Formula	Exact Masses		
			[M+H] ⁺	[M+2H] ⁺²	[M+Na+H] ⁺²
C-type Prymnesins	PRM-C (2 Cl + 2 DB) + pentose	C ₈₈ H ₁₂₃ Cl ₂ NO ₃₅	1824.7325	912.8699	923.8609
	PRM-C (2 Cl + 2 DB) + pentose + hexose	C ₉₄ H ₁₃₃ Cl ₂ NO ₄₀	1986.7854	993.8963	1004.8873
	PRM-C (2 Cl + 2 DB) + 2 pentose + hexose	C ₉₉ H ₁₄₁ Cl ₂ NO ₄₄	2118.8276	1059.9175	1070.9084
	PRM-C (2 Cl + DB)	C ₈₃ H ₁₁₇ Cl ₂ NO ₃₁	1694.7059	847.8566	858.8476
	PRM-C (2 Cl + DB) + pentose	C ₈₈ H ₁₂₅ Cl ₂ NO ₃₅	1826.7482	913.8777	924.8687
	PRM-C (2 Cl + DB) + pentose + hexose	C ₉₄ H ₁₃₅ Cl ₂ NO ₄₀	1988.8010	994.9041	1005.8951
	PRM-C (2 Cl + DB) + 2 pentose	C ₉₃ H ₁₃₃ Cl ₂ NO ₃₉	1958.7905	979.8989	990.8898
	PRM-C (2 Cl + DB) + hexose + 2 pentose	C ₉₉ H ₁₄₃ Cl ₂ NO ₄₄	2120.8433	1060.9253	1071.9162
	PRM-C (2 Cl)*	C ₈₃ H ₁₁₉ Cl ₂ NO ₃₁	1696.7216	848.8644	859.8554
	PRM-C (2 Cl) + pentose	C ₈₈ H ₁₂₇ Cl ₂ NO ₃₅	1828.7638	914.8856	925.8765
	PRM-C (2 Cl) + 2 pentose	C ₉₃ H ₁₃₅ Cl ₂ NO ₃₉	1960.8061	980.9067	991.8977
	PRM-C (3 Cl + DB)	C ₈₃ H ₁₁₆ Cl ₃ NO ₃₁	1728.6670	864.8371	875.8281
	PRM-C (3 Cl + DB) + pentose	C ₈₈ H ₁₂₄ Cl ₃ NO ₃₅	1860.7092	930.8583	941.8492
	PRM-C (3 Cl + DB) + pentose + hexose	C ₉₄ H ₁₃₄ Cl ₃ NO ₄₀	2022.7620	1011.8847	1022.8756
	PRM-C (3 Cl + DB) + 2 pentose	C ₉₃ H ₁₃₂ Cl ₃ NO ₃₉	1992.7515	996.8794	1007.8704
	PRM-C (3 Cl + DB) + hexose + 2 pentose	C ₉₉ H ₁₄₂ Cl ₃ NO ₄₄	2154.8043	1077.9058	1088.8968
	PRM-C (3 Cl)	C ₈₃ H ₁₁₈ Cl ₃ NO ₃₁	1730.6826	865.8449	876.8359
	PRM-C (3 Cl) + pentose	C ₈₈ H ₁₂₆ Cl ₃ NO ₃₅	1862.7249	931.8661	942.8570
	PRM-C (3 Cl) + 2 pentose	C ₉₃ H ₁₃₄ Cl ₃ NO ₃₉	1994.7671	997.8872	1008.8782
	PRM-C (3 Cl) + 2 pentose + hexose	C ₉₉ H ₁₄₄ Cl ₃ NO ₄₄	2156.8200	1078.9136	1089.9046
	PRM-C (4 Cl + DB)	C ₈₃ H ₁₁₇ Cl ₄ NO ₃₁	1764.6436	882.8255	893.8164
	PRM-C (4 Cl + DB) + pentose	C ₈₈ H ₁₂₅ Cl ₄ NO ₃₅	1896.6859	948.8466	959.8376
	PRM-C (4 Cl + DB) + pentose + hexose	C ₉₄ H ₁₃₅ Cl ₄ NO ₄₀	2058.7387	1029.8730	1040.8640
	PRM-C (4 Cl + DB) + 2 pentose	C ₉₃ H ₁₃₃ Cl ₄ NO ₃₉	2028.7282	1014.8677	1025.8587
	PRM-C (4 Cl + DB) + 2 pentose + hexose	C ₉₉ H ₁₄₃ Cl ₄ NO ₄₄	2190.7810	1095.8941	1106.8851
	PRM-C (4 Cl)	C ₈₃ H ₁₁₉ Cl ₄ NO ₃₁	1766.6593	883.8333	894.8243

	PRM-C (4 Cl + 3 =O)	C ₈₃ H ₁₁₃ Cl ₄ NO ₃₄	1808.5971	904.8022	915.7932
	PRM-C (4 Cl + 3 =O) + pentose	C ₈₈ H ₁₂₁ Cl ₄ NO ₃₈	1940.6393	970.8233	981.8143
	PRM-C (4 Cl + 3 =O) + pentose + hexose	C ₉₄ H ₁₃₁ Cl ₄ NO ₄₃	2102.6922	1051.8497	1062.8407
	PRM-C (4 Cl + 3 =O + 3 O)	C ₈₃ H ₁₁₃ Cl ₄ NO ₃₇	1856.5818	928.7946	939.7855
	PRM-C (4 Cl + 3 =O + 3 O) + pentose	C ₈₈ H ₁₂₁ Cl ₄ NO ₄₁	1988.6241	994.8157	1005.8067

All proposed sum formulas are solely based on high resolution mass spectrometric characterization and the previous publications (Igarashi *et al.*, 1999; Rasmussen *et al.*, 2016; Hems *et al.*, 2018, Binzer *et al.*, 2019).

* no confirmed detection apart from in-source fragmentation

PRM-A --> A-type prymnesin with 91 carbon-atoms in the backbone

PRM-B --> B-type prymnesin with 85 carbon-atoms in the backbone

PRM-C --> C-type prymnesin with 83 carbon-atoms in the backbone

Cl --> number of chlorine-atoms in the proposed compounds

+ DB --> additional double bond

+ pentose --> pentose-conjugate attached

+ hexose --> hexose-conjugate attached

+ O --> one oxygen more, presumably in OH-group

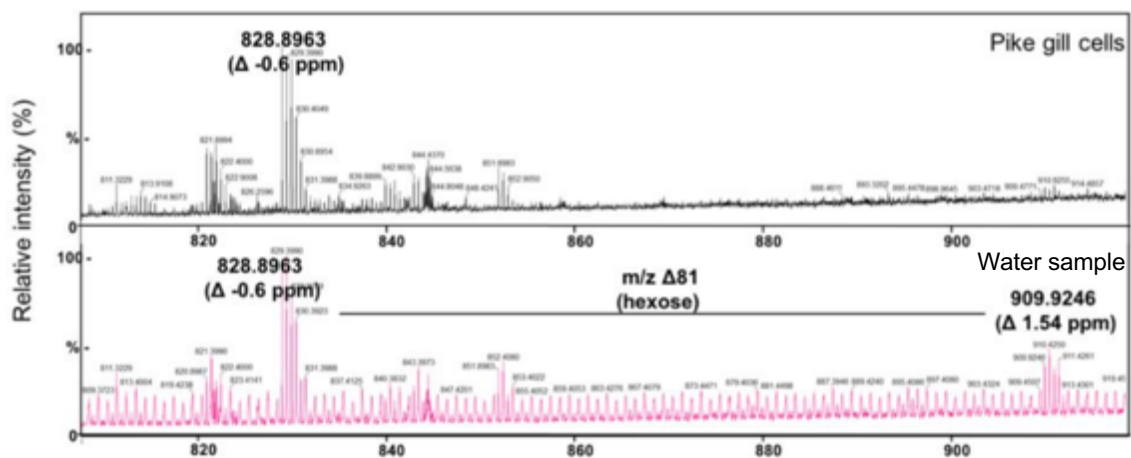
Supplementary Table 6.2. List of *Prymnesium parvum* strains, salinity and the type of prymnesin produced

Strain	Origin	Isolation year	Isolator	Source	Salinity PSU	Prymnesin Type	Accession Number
CCAP 946/1B	River Blackwater, Essex, United Kingdom	1952	Butcher	CCAP	35	C-type	MK091124
CCAP 946/6	Millport, Isle of Cumbrae, United Kingdom	1953	Droop	CCAP	35	A-type	MK091114
CCAP 946/1D	Nir-David, North District, Israel	1953	Reich	CCAP	35	A-type	MK091120
CCAP 941/1A	River Stour, Essex, United Kingdom	N/A	Butcher	CCAP	35	A-type	MK091115
CCAP 946/4 (<i>P. patelliferum</i>)	West End of Fleet, Dorset, England	1976	Hibberd	CCAP	35	A-type	
CCAP 941/6	River Stour, Essex, United Kingdom	N/A	Butcher	CCAP	35	A-type	
HIK PR1A	Hickling Broad, Norfolk, UK	2017	Rivera	This Study	35	B-type	
HIK PR6H	Hickling Broad, Norfolk, UK	2017	Rivera	This Study	35	B-type	
HIK PR12D	Hickling Broad, Norfolk, UK	2017	Rivera	This Study	10	B-type	
WBF PRC1	Woodbridge Fisheries, Suffolk, UK	2018	Rivera	This Study	10-35	A-type?	
WBF PRD2	Woodbridge Fisheries, Suffolk, UK	2018	Rivera	This Study	10	A-type?	
PLY 595 (<i>P. sp</i>)	Baltic Sea, Finland	N/A	N/A	MBACC	35	B-type	
PLY 94A	English Bay, British Columbia, Canada	N/A	N/A	MBACC	35	A-type	
PLY 527D (<i>P. patelliferum</i>)	North of Büsum, North Sea, Germany	N/A	N/A	MBACC	35	C-type	
K-0081	Flade Sø, Thy, Denmark	1985	N/A	SCCAP	30	B-type	MK091108
K-0374	Norway	1989	N/A	SCCAP	30	B-type	MK091109
SAG 18.97	Sondershausen, Thüringen, Germany	1997	Schlösser	SAG	30	B-type	MK091110
ARC140	Elizabeth City, North Carolina, USA	2005	Tomas	ARC	9	B-type	MK091111
UIO 223	Bjerknes, Norway	2008	Eikrem	NORCAA	9	B-type	MK091112
KAC-39	Norway	N/A	N/A	KAC	30	B-type	MK091113
ARC85	Elizabeth City, North Carolina, USA	2002	Tomas	ARC	9	A-type	MK091116
UTEX-2797	Texas Colorado River, Texas, USA	2001	N/A	UTEX	30	A-type	MK091117
ARC83	Elizabeth City, North Carolina, USA	2002	Tomas	ARC	9	A-type	MK091118
CCMP3037	Twin Buttes Lake, Wyoming, USA	1990	Kugrens	NCMA	30	A-type	MK091119
NIES-1812	Yufu Island, Okinawa, Japan	2004	Chikuni	NIES	30	A-type	MK091121
PPDW02	On-shore aquaculture, Northern Territory, Australia	2009	N/A	Hallegraeff G.	30	A-type	MK091122

RCC-1436	Atlantic Ocean, France	1977	N/A	RCC	30	C-type	MK091123
CS-376/3	Pipe Clay Lagoon, Tasmania, Australia	1994	LeRoi	ANACC	30	C-type	MK091125
RCC-1435	Indian Ocean, La Réunion, France	N/A	N/A	RCC	30	C-type	MK091126
NIES-1018	Hirara, Okinawa, Japan	2002	Moriya	NIES	30	C-type	MK091127
RCC-191	South Coast, Atlantic Ocean, United Kingdom	1976	N/A	RCC	30	C-type	MK091128
RCC-1433	English Channel, France	N/A	N/A	RCC	30	C-type	MK091129
ARC479	Rodrigo de Freitas Lagoon, Rio de Janeiro, Brazil	2012	Benevides	ARC	20	C-type	MK091130
PPSR01	Serpentine River, West Australia, Australia	2000	N/A	Hallegraef	30	C-type	MK091131
Texoma1	Lake Texoma, Oklahoma, USA	N/A	Hambright		30	A-type	

Collated data from this work and data provided by Binzer *et al.* (2019)

N/A - not available, ANACC - Australian National Algae Culture Collection
ARC - Algal Resources Collection, CCAP - Culture Collection of Algae and Protozoa
KAC - Kalmar Algae Collection, Linnaeus University
NIES - National Institute for Environmental Studies Collection
NCMA - National Center for Marine Algae and Microbiota (former CCMP)
NORCCA - The Norwegian Culture Collection of Algae
RCC - Roscoff Culture Collection
SCCAP – Scandinavian Culture Collection of Algae and Protozoa
SAG - Culture Collection of Algae at Göttingen University
UTEX - Culture Collection of Algae at the University of Texas at Austin



Supplementary Figure 6.1. MS-based identification of B-type prymnesins from environmental samples taken from Hickling Broad. ESI-MS spectrum showing detection of the diagnostic signal (m/z 828.8963, $\Delta -0.6$ ppm) for the backbone of the B-type prymnesins from Pike gill cells (top), and water sample (bottom) taken during the 2015 fish-killing event. ESI-MS signal corresponding to the singly glycosylated form of the toxin (m/z 909.9246, $\Delta 1.54$ ppm) could also be seen in the water sample. (Adapted from Wagstaff et al., 2020).

Supplementary Data:

696 base pairs (including introduced gaps) of internal transcribed spacers (ITS-1 and ITS-2) and the 5.8S rDNA gene of *P. parvum* strains

K-0081

ATCATTACCGGTCTTTCCACCCACACCAGTGCGTACCACTCGTCCCTTTGGGTCCGTCCGGTGCTCGCATC
GGCGGCTCATCTGTGCTCTTGCTTGAGCTGGCGCTCCGCGCGCCAGATCGGGCGGGACGCAGGCACTGTG
TCCCGGACACAGCCACATCTCCTCCTCGGCCCTCGCCGGTTCGTTGAGGATCCCCCTCGTCGTGCCCTGC
GCGTTGCGCTCTCGGGCAGCAAGAATTGTTGAAACACACAACCTCTTGTCGATGGATATCTTGCTCTCG
CAACGATGAAGAACGCAGCGAAATGCGATACGTAATGCGAATTGCAGAATTCAGTGAATCATCGAACTTT
TGAACGCAACTGGCGCTTCCAGGTTCCGCCTGGGAGCATGTTTCTTCGAGTGGCGCCTCCACCCGCTGG
GCGTGCCTCGCGCGCACATCCGATCGTGTCTGCCGTGGACTTAGTGCTGCGCCAGATCAAGGCTCGAG
CGTCGCCTGAGGGCAGCGTTGCACGGGAGGATCCTCGGATCTGACGTGTGCCGACGTGCTAGTAGGCCGC
CTACCAAGTCGTTGTGCCATCGAACGCTGCGATCTCAACCGACGCGGGGACTCGAGGACCTAGGTCGTTCG
CGTTTCCGCCCACCGGTACGCCTCGCGCGCACCATTTGGACTC

K-0374

ATCATTACCGGTCTTTCCACCCACACCAGTGCGTACCACTCGTCCCTTTGGGTCCGTCCGGTGCTCGCATC
GGCGGCTCATCTGTGCTCTTGCTTGAGCTGGCGCTCCGCGCGCCAGATCGGGCGGGACGCAGGCACTGTG
TCCCGGACACAGCCACATCTCCTCCTCGGCCCTCGCCGGTTCGTTGAGGATCCCCCTCGTCGTGCCCTGC
GCGTTGCGCTCTCGGGCAGCAAGAATTGTTGAAACACACAACCTCTTGTCGATGGATATCTTGCTCTCG
CAACGATGAAGAACGCAGCGAAATGCGATACGTAATGCGAATTGCAGAATTCAGTGAATCATCGAACTTT
TGAACGCAACTGGCGCTTCCAGGTTCCGCCTGGGAGCATGTTTCTTCGAGTGGCGCCTCCACCCGCTGG
GCGTGCCTCGCGCGCACATCCGATCGTGTCTGCCGTGGACTTAGTGCTGCGCCAGATCAAGGCTCGAG
CGTCGCCTGAGGGCAGCGTTGCACGGGAGGATCCTCGGATCTGACGTGTGCCGACGTGCTAGTAGGCCGC
CTACCAAGTCGTTGTGCCATCGAACGCTGCGATCTCAACCGACGCGGGGACTCGAGGACCTAGGTCGTTCG
CGTTTCCGCCCACCGGTACGCCTCGCGCGCACCATTTGGACTC

SAG 18.97

ATCATTACCGGTCTTTCCACCCACACCAGTGCGTACCACTCGTCCCTTTGGGTCCGTCCGGTGCTCGCATC
GGCGGCTCATCTGTGCTCTTGCTTGAGCTGGCGCTCCGCGCGCCAGATCGGGCGGGACGCAGGCACTGTG
TCCCGGACACAGCCACATCTCCTCCTCGGCCCTCGCCGGTTCGTTGAGGATCCCCCTCGTCGTGCCCTGC
GCGTTGCGCTCTCGGGCAGCAAGAATTGTTGAAACACACAACCTCTTGTCGATGGATATCTTGCTCTCG
CAACGATGAAGAACGCAGCGAAATGCGATACGTAATGCGAATTGCAGAATTCAGTGAATCATCGAACTTT
TGAACGCAACTGGCGCTTCCAGGTTCCGCCTGGGAGCATGTTTCTTCGAGTGGCGCCTCCACCCGCTGG
GCGTGCCTCGCGCGCACATCCGATCGTGTCTGCCGTGGACTTAGTGCTGCGCCAGATCAAGGCTCGAG
CGTCGCCTGAGGGCAGCGTTGCACGGGAGGATCCTCGGATCTGACGTGTGCCGACGTGCTAGTAGGCCGC
CTACCAAGTCGTTGTGCCATCGAACGCTGCGATCTCAACCGACGCGGGGACTCGAGGACCTAGGTCGTTCG
CGTTTCCGCCCACCGGTACGCCTCGCGCGCACCATTTGGACTC

HIK PR1A

ATCATTACCGGTCTTTCCACCCACACCAGTGCGTACCACTCGTCCCTTTGGGTCCGTCCGGTGCTCGCATC
GGCGGCTCATCTGTGCTCTTGCTTGAGCTGGCGCTCCGCGCGCCAGATCGGGCGGGACGCAGGCACTGTG
TCCCGGACACAGCCACATCTCCTCCTCGGCCCTCGCCGGTTCGTTGAGGATCCCCCTCGTCGTGCCCTGC
GCGTTGCGCTCTCGGGCAGCAAGAATTGTTGAAACACACAACCTCTTGTCGATGGATATCTTGCTCTCG
CAACGATGAAGAACGCAGCGAAATGCGATACGTAATGCGAATTGCAGAATTCAGTGAATCATCGAACTTT
TGAACGCAACTGGCGCTTCCAGGTTCCGCCTGGGAGCATGTTTCTTCGAGTGGCGCCTCCACCCGCTGG
GCGTGCCTCGCGCGCACATCCGATCGTGTCTGCCGTGGACTTAGTGCTGCGCCAGATCAAGGCTCGAG
CGTCGCCTGAGGGCAGCGTTGCACGGGAGGATCCTCGGATCTGACGTGTGCCGACGTGCTAGTAGGCCGC
CTACCAAGTCGTTGTGCCATCGAACGCTGCGATCTCAACCGACGCGGGGACTCGAGGACCTAGGTCGTTCG
CGTTTCCGCCCACCGGTACGCCTCGCGCGCACCATTTGGACTC

ARC140

ATCATTACCGGTCTTTCCACCCACACCAGTGCGTACCACTCGTCCCTTTGGGTCCGTTCGGTGCTCGCATC
GGCGGCTCATCTGTGCTCTTGCTTGAGCTGGCGCTCCGCGCGCCAGATCGGGCGGGACGCAGGCACTGTG
TCCCGGACACAGCCACATCTCCTCCTCGGCCCTCGCCGGTTCGTTGAGGATCCCCCTCGTCTGCCCCCTGC
GCGTTGCGCTCTCGGGCAGCAAGAATTGTTGAAACACACAACCTCTTGTCGATGGATATCTTGCTCTCG
CAACGATGAAGAACGCAGCGAAATGCGATACGTAATGCGAATTGCAGAATTCAGTGAATCATCGAACTTT
TGAACGCAACTGGCGCTTCCAGGTTCCGCCTGGGAGCATGTTTCTTCGAGTGGCGCTCCACCCGCTGG
GCGTGCCTCGCGCGCACATCCGATCGTGTCTGCCGTGGACTTAGTGCTGCGCCAGATCAAGGCTCGAG
CGTCGCTGAGGGCAGCGTTGCACGGGAGGATCCTCGGATCTGACGTGTGCCGACGTGCTAGTAGGCCGC
CTACCAAGTCGTTGTGCCATCGAACGCTGCGATCTCAACCGACGCGGGGACTCGAGGACCTAGGTCGTCG
CGTTTCCGCCACCGGTACGCCTCGCGCGCACCATTTGGACTC

UIO 223

ATCATTACCGGTCTTTCCACCCACACCAGTGCGTACCACTCGTCCCTTTGGGTCCGTTCGGTGCTCGCATC
GGCGGCTCATCTGTGCTCTTGCTTGAGCTGGCGCTCCGCGCGCCAGATCGGGCGGGACGCAGGCACTGTG
TCCCGGACACAGCCACATCTCCTCCTCGGCCCTCGCCGGTTCGTTGAGGATCCCCCTCGTCTGCCCCCTGC
GCGTTGCGCTCTCGGGCAGCAAGAATTGTTGAAACACACAACCTCTTGTCGATGGATATCTTGCTCTCG
CAACGATGAAGAACGCAGCGAAATGCGATACGTAATGCGAATTGCAGAATTCAGTGAATCATCGAACTTT
TGAACGCAACTGGCGCTTCCAGGTTCCGCCTGGGAGCATGTTTCTTCGAGTGGCGCTCCACCCGCTGG
GCGTGCCTCGCGCGCACATCCGATCGTGTCTGCCGTGGACTTAGTGCTGCGCCAGATCAAGGCTCGAG
CGTCGCTGAGGGCAGCGTTGCACGGGAGGATCCTCGGATCTGACGTGTGCCGACGTGCTAGTAGGCCGC
CTACCAAGTCGTTGTGCCATCGAACGCTGCGATCTCAACCGACGCGGGGACTCGAGGACCTAGGTCGTCG
CGTTTCCGCCACCGGTACGCCTCGCGCGCACCATTTGGACTC

KAC-39

ATCATTACCGGTCTTTCCACCCACACCAGTGCGTACCACTCGTCCCTTTGGGTCCGTTCGGTGCTCGCATC
GGCGGCTCATCTGTGCTCTTGCTTGAGCTGGCGCTCCGCGCGCCAGATCGGGCGGGACGCAGGCACTGTG
TCCCGGACACAGCCACATCTCCTCCTCGGCCCTCGCCGGTTCGTTGAGGATCCCCCTCGTCTGCCCCCTGC
GCGTTGCGCTCTCGGGCAGCAAGAATTGTTGAAACACACAACCTCTTGTCGATGGATATCTTGCTCTCG
CAACGATGAAGAACGCAGCGAAATGCGATACGTAATGCGAATTGCAGAATTCAGTGAATCATCGAACTTT
TGAACGCAACTGGCGCTTCCAGGTTCCGCCTGGGAGCATGTTTCTTCGAGTGGCGCTCCACCCGCTGG
GCGTGCCTCGCGCGCACATCCGATCGTGTCTGCCGTGGACTTAGTGCTGCGCCAGATCAAGGCTCGAG
CGTCGCTGAGGGCAGCGTTGCACGGGAGGATCCTCGGATCTGACGTGTGCCGACGTGCTAGTAGGCCGC
CTACCAAGTCGTTGTGCCATCGAACGCTGCGATCTCAACCGACGCGGGGACTCGAGGACCTAGGTCGTCG
CGTTTCCGCCACCGGTACGCCTCGCGCGCACCATTTGGACTC

CCAP 946/6

ATCATTACCGGTCTTTCCACCCACACCAGTGCGTACCACTCGTCCCTTTGGGTCCGTTCGGTGCTTCGCATC
GGCGGCTCATCTGTGCTCTAGCTCGAGCTGGCGCTCCGCGCGCCAGATCGGGTGGGACGCAGGCACTGTG
TCCTTGACACACAGCCACATCTCCTCCTCGGCCCTCGCCGGTTCGTTGAGGATCCCCCTCGTCTGCCCCCTGC
GCCTCGCGCGCTCGAGCACACAAGAATTGTTGAAACACACAACCTCTTGTCGATGGATATCTTGCTCTCG
CAACGATGAAGAACGCAGCGAAATGCGATACGTAATGCGAATTGCAGAATTCAGTGAATCATCGAACTTT
TGAACGCAACTGGCGCTTCCAGGTTCCGCCTGGGAGCATGTTTCTTCGAGTGGCGCTCCACCCGCTGG
GCGTGCCTCGCGCGCACATCCGATCGTGTCTGCCGTGGACTTAGTGCTGCGCCAGATCAAGGCTCGAG
CGTCGCTGAGGGCAGCGTTGCACGGGAGGATCCTCGGATCCTCGGTGTGCCGACGTGCTAGTAGGTTT
CCTACCAAGTCGTTGTGCCATCGAACGCTGCGATCTCAACCGACGCGGGGACGCGAGGACCTACCTAGGT
CGTCTCGACTCCGCCACCGGTACGCCTCGCGCGCACCATTTGGACTC

CCAP 941/1A

ATCATTACCGGTCTTTCCACCCACACCAGTGCGTACCACTCGTCCCTTTGGGTCCGTTCGGTGCTTCGCATC
GGCGGCTCATCTGTGCTCTAGCTCGAGCTGGCGCTCCGCGCGCCAGATCGGGTGGGACGCAGGCACTGTG
TCCTTGACACACAGCCACATCTCCTCCTCGGCCCTCGCCGGTTCGTTGAGGATCCCCCTCGTCTGCCCCCTGC
GCCTCGCGCGCTCGAGCACACAAGAATTGTTGAAACACACAACCTCTTGTCGATGGATATCTTGCTCTCG
CAACGATGAAGAACGCAGCGAAATGCGATACGTAATGCGAATTGCAGAATTCAGTGAATCATCGAACTTT

TGAACGCAACTGGCGCTTCCAGGTTCCGCCTGGGAGCATGTTTCTTCGAGTGGCGCTCCACCCGCTGG
GCGTGGCGCTCGCGCGCACATCCGATCGTGTCTGCCGCGGCCTTAGTGCTGCGCCAGATCAAGGCTCGAG
CGTCGCTGAGGGCAGCGTTGCACGGGAGGATCCTCGGATCCTCGCGTGTGCCGACGTGCTAGTAGGTTT
CCTACCAAGTCGTTGTGCCATCGAACGCTGCGATCTCAACCGACGCGGGGACGCGAGGACCTACCTAGGT
CGTCTCGACTCCGCCACCGGTACGCTCGCGCGCACCATTGGACTC

ARC85

ACCAGTGCGTACCACTCGTCCCTTTGGGTCCGTCGGTGTTCATCGGCGGCTCATCTGTGCTCTTGCTC
GCGCTGGCGCTCCGCGCGCCAGATCGGGTGGGACGCAGGCACTGTGTCCCTTGACACAGCCACATCTCCT
CCTCGGCCCTCGCGGGTCGTTGAGGATCCCTCGTGTGCTCCTGCGCCTCGCGCGCTCGAGCACACAAG
AATTGTTGAAACACACAACCTTTGTTCGATGGATATCTTGGCTCTCGCAACGATGAAGAACGCAGCGAAAT
GCGATACGTAATGCGAATTGCAGAATTGAGTGAATCATCGAACTTTTGAACGCAACTGGCGCTTCCAGGT
TCCGCTGGGAGCATGTTTCTTCGAGTGGCGCTCCACCCGCTGGGCGTGCCTCGCGCGCACATCCG
ATCGTGTCTGCCGCGCCTTCGTGCTGCGCCAGATCAAGGCTCGAGCGTCCCTGAGGGCAGCGTTGCAC
GGGAGGATCCTCGGATCCTCGCGTGTGCCGACGTGCTAGTAGGTTTCTACCAAGTCGTTGTGCCATCGA
ACGCTGCGATCTCAACCGACGCGGGGACGCGAGGACCTACCTAGGTTCGCTTCGACTCCGCCACCGGTAC
GCCTCGCGCGCACCATTGGACTC

UTEX-2797

ATCATTACCGGTCTTTCCACCCACACCAGTGCGTACCACTCGTCCCTTTGGGTCCGTCGGTGTTCATC
GGCGGCTCATCTGTGCTCTTGCTCGAGCTGGCGCTCCGCGCGCCAGATCGGGTGGGACGCAGGCACTGTG
TCCTTGACACAGCCACATCTCCTCCTCGGCCCTCGCCGGTCGTTGAGGATCCCTCGTGTGCTCCTGC
GCCTCGCGCGCTCGAGCACACAAGAATTGTTGAAACACACAACCTTTGTTCGATGGATATCTTGGCTCTCG
CAACGATGAAGAACGCAGCGAAATGCGATACGTAATGCGAATTGCAGAATTGAGTGAATCATCGAACTTT
TGAACGCAACTGGCGCTTCCAGGTTCCGCCTGGGAGCATGTTTCTTCGAGTGGCGCTCCACCCGCTGG
GCGTGCCTCGCGCGCACATCCGATCGTGTCTGCCGCGCCTTCGTGCTGCGCCAGATCAAGGCTCGAG
CGTCGCTGAGGGCAGCGTTGCACGGGAGGATCCTCGGATCCTCGCGTGTGCCGACGTGCTAGTAGGTTT
CCTACCAAGTCGTTGTGCCATCGAACGCTGCGATCTCAACCGACGCGGGGACGCGAGGACCTACCTAGGT
CGTCTCGACTCCGCCACCGGTACGCTCGCGCGCACCATTGGACTC

ARC83

ATCATTACCGGTCTTTCCACCCACACCAGTGCGTACCACTCGTCCCTTTGGGTCCGTCGGTGTTCATC
GGCGGCTCATCTGTGCTCTTGCTCGAGCTGGCGCTCCGCGCGCCAGATCGGGTGGGACGCAGGCACTGTG
TCCTTGACACAGCCACATCTCCTCCTCGGCCCTCGCCGGTCGTTGAGGATCCCTCGTGTGCTCCTGG
GCCTCGCGCGCTCGAGCACACAAGAATTGTTGAAACACACAACCTTTGTTCGATGGATATCTTGGCTCTCG
CAACGATGAAGAACGCAGCGAAATGCGATACGTAATGCGAATTGCAGAATTGAGTGAATCATCGAACTTT
TGAACGCAACTGGCGCTTCCAGGTTCCGCCTGGGAGCATGTTTCTTCGAGTGGCGCTCCACCCGCTGG
GCGTGCCTCGCGCGCACATCCGATCGTGTCTGCCGCGCCTTCGTGCTGCGCCAGATCAAGGCTCGAG
CGTCGCTGAGGGCAGCGTTGCACGGGAGGATCCTCGGATCCTCGCGTGTGCCGACGTGCTAGTAGGTTT
CCTACCAAGTCGTTGTGCCATCGAACGCTGCGATCTCAACCGACGCGGGGACGCGAGGACCTACCTAGGT
CGTCTCGACTCCGCCACCGGTACGCTCGCGCGCACCATTGGACTC

CCMP3037

ATCATTACCGGTCTTTCCACCCACACCAGTGCGTACCACTCGTCCCTTTGGGTCCGTCGCTGCTCGCATC
GGCGGCTCATCTGTGCTCTTGCTCGCGCTGGCGCTCCGCGCGCCAGATCGGGTGGGACGCAGGCACTGTG
TCCTTGACACAGCCACATCTCCTCCTCGGCCCTCGCCGGTCGTTGAGGATCCCTCGTGTGCTCCTGG
GCCTCGCGCGCTCGAGCACACAAGAATTGTTGAAACACACAACCTTTGTTCGATGGATATCTTGGCTCTCG
CAACGATGAAGAACGCAGCGAAATGCGATACGTAATGCGAATTGCAGAATTGAGTGAATCATCGAACTTT
TGAACGCAACTGGCGCTTCCAGGTTCCGCCTGGGAGCATGTTTCTTCGAGTGGCGCTCCACCCGCTGG
GCGTGCCTCGCGCGCACATCCGATCGTGTCTGCCGCGCCTTCGTGCTGCGCCAGATCAAGGCTCGAG
CGTCGCTGAGGGCAGCGTTGCACGGGAGGATCCTCGGATCCTCGCGTGTGCCGACGTGCTAGTAGGTTT
CCTACCAAGTCGTTGTGCCATCGAACGCTGCGATCTCAACCGACGCGGGGACGCGAGGACCTACCTAGGT
CGTCTCGACTCCGCCACCGGTACGCTCGCGCGCACCATTGGACTC

CCAP 946/1D

ATCATTACCGGTCTTTCCACCCACACCAGTGCGTACCACTCGTCCCTTTGGGTCCGTCCGGTGCTTGCATC
GGCGGCTCATCTGTGCTCTTGCTCGAGCTGGCGCTCCGCGCGCCAGATCGGGTGGGACGCAGGCACTGTG
TCCTTGCACACAGCCACATCTCCTCCTCGGCCCTCGCCGGTCGTTGAGGATCCCCCTCGTCGTGCTCCTGC
GCCTCGCGCGCTCGGGCACACAAGAATTGTTGAAACACACAACCTTTGTTCGATGGATATCTTGGCTCTCG
CAACGATGAAGAACGCAGCGAAATGCGATACGTAATGCGAATTGCAGAATTCAGTGAATCATCGAACTTT
TGAACGCAACTGGCGCTTCCAGGTTCCGCCTGGGAGCATGTTTCTTCGAGTGGCGCTCCACCCGCTGG
GCGTGCCTCGCGCGCACATCCGATCGTGTCTGCCGCGCCCTTAGTGTGCGCCAGATCAAGGCTCGAG
CGTCGCCTGAGGGCAGCGTTGCACGGGAGGATCCTCGGATCCTCGCGTGTGCCGACGTGCTAGTAGGTTT
CCTACCAAGTCGTTGTGCCATCGAACGCTGCGATCTCAACCGACGCGGGGACGCGAGGACCTACCTAGGT
CGTCTCGACTCCGCCACCGGTACGCCTCGCGCGCACCATTTGGACTC

NIES-1812

ATCATTACCGGTCTTTCCACCCACACCAGTGCGTACCACTCGTCCCTTTGGGTCCGTCCGGTGCTCGCATC
GGCGGCTCATCTGTGCTCTTGCCCGAGCTGGCGCTCCGCGCGCCAGATCGGGTGGGACGCAGGCACTGTG
TCCTTGCACACAGCCACATCTCCTCCTCGGCCCTCGCCGGTCGTTGAGGATCCCCCTCGTCGTGCTCCTGC
GCCTCGCGCGCTCGAGCACACAAGAATTGTTGAAACACACAACCTTTGTTCGATGGATATCTTGGCTCTCG
CAACGATGAAGAACGCAGCGAAATGCGATACGTAATGCGAATTGCAGAATTCAGTGAATCATCGAACTTT
TGAACGCAACTGGCGCTTCCAGGTTCCGCCTGGGAGCATGTTTCTTCGAGTGGCGCTCCACCCGCTGG
GCGTGCCTCGCGCGCACATCCGATCGTGTCTGCCGCGCCCTTAGTGTGCGCCAGATCAAGGCTCGAG
CGTCGCCTGAGGGCAGCGTTGCACGGGAGGATCCTCGGATCCTCGCGTGTGCCGACGTGCTAGTAGGTTT
CCTACCAAGTCGTTGTGCCATCGAACGCTGCGATCTCAACCGACGCGGGGACGCGAGGACCTACCTAGGT
CGTCTCGACTCCGCCACCGGTACGCCTCGCGCGCACCATTTGGACTC

PPDW02

ATCATTACCGGTCTTTCCACCCACACCAGTGCGTACCACTCGTCCCTTTGGGTCCGTCCGGTGCTCGCATC
GGCGGCTCATCTGTGCTCTTGCCCGAGCTGGCGCTCCGCGCGCCAGATCGGGTGGGACGCAGGCACTGTG
TCCTTGCACACAGCCACATCTCCTCCTCGGCCCTCGCCGGTCGTTGAGGATCCCCCTCGTCGTGCTCCTGC
GCCTCGCGCGCTCGAGCACACAAGAATTGTTGAAACACACAACCTTTGTTCGATGGATATCTTGGCTCTCG
CAACGATGAAGAACGCAGCGAAATGCGATACGTAATGCGAATTGCAGAATTCAGTGAATCATCGAACTTT
TGAACGCAACTGGCGCTTCCAGGTTCCGCCTGGGAGCATGTTTCTTCGAGTGGCGCTCCACCCGCTGG
GCGTGCCTCGCGCGCACATCCGATCGTGTCTGCCGCGCCCTTAGTGTGCGCCAGATCAAGGCTCGAG
CGTCGCCTGAGGGCAGCGTTGCACGGGAGGATCCTCGGATCCTCGCGTGTGCCGACGTGCTAGTAGGTTT
CCTACCAAGTCGTTGTGCCATCGAACGCTGCGATCTCAACCGACGCGGGGACGCGAGGACCTACCTAGGT
CGTCGCGACTCCGCCACCGGTACGCCTCGCGCGCACCATTTGGACTC

RCC-1436

ATCATTACCGGTCTTTCCACCCACACCAGTGCGTACCTCCCGTCCCTTTGGGTCCGTCCGGTGCTCGCGCA
TCGGCAGACCCATCTGTGCTCTTGTTCGAGCTGGCGCGCCCCGCGCGGCAGATCGGGCGGGACGCAGGCA
CTGTGTCTCGAACACAGCCACATCTCCTCATCGGCCCTCCCCGGTCGAGGAGGATCCCCCTCGACGTGCC
CATCGCGCCTCGAGCGCGGGGACGCAAGAATTGTTGAAACACACAACCTTTGTTCGATGGATATCTTGG
CTCTCGCAACGATGAAGAACGCAGCGAAATGCGATACGTAATGCGAATTGCAGAATTCAGTGAATCATCG
AACTTTTGAACGCAACTGGCGCTTCCAGGTTCCGCCTGGGAGCATGTTTCTTCGAGTGGCGCTCCACCC
GCCTGGGCGTGCCTCGCGCGCACATCCGATCGTGTCTGCCGCGCGTGTGAGCTGCGCCAGATCAAGGTT
CGAGCGTGCCTGAGGGCAGCGTTGCACGGGAGGATCCTCGGATCTGCCGCGTGTGCCGACGTGCTAGTAG
GTGCTACCAAGTCGTTGTGCCATCGAACGCTGTGATCTCAACCGACGCGGGGACGCGAGGAGATACAT
CGCGGCTCCGCCACCGGTGCGCCTCGCGCGCACCATTTGGACTC

CCAP 946/1B

ATCATTACCGGTCTTTCCACCCACACCAGTGCGTACCTCCCGTCCCTTTGGGTCCGTCCGGTGCTCGCGCA
TCGGCAGACCCATCTGTGCTCTTGTTCGAGCTGGCGCGCCCCGCGCGGCAGATCGGGCGGGACGCAGGCA
CTGTGTCTCGAACACAGCCACATCTCCTCATCGGCCCTCCCCGGTCGAGGAGGATCCCCCTCGACGTGCC
CATCGCGCCTCGAGCGCGGGGACGCAAGAATTGTTGAAACACACAACCTTTGTTCGATGGATATCTTGG
CTCTCGCAACGATGAAGAACGCAGCGAAATGCGATACGTAATGCGAATTGCAGAATTCAGTGAATCATCG

AACTTTTGAACGCAACTGGCGCTTCCAGGTTCCGCCTGGGAGCATGTTTCTTCGAGTGGCGCCTCCACCC
GCCTGGGCGTGCGCCTCGCGCGCACATCCGATCGTGTCTGCCGCGGCGTGAGCTGCGCCAGATCAAGGTT
CGAGCGTTCGCTGAGGGCAGCGTTGCACGGGAGGATCCTCGGATCTGCCCGTGTGCCGACGTGCTAGTAG
GTCGCCTACCAAGTCGTTGTGCCATCGAACGCTGTGATCTCAACCGACGCGGGGACGCGAGGAGATACAT
CGCGGCTCCGCCACCGGTGCGCCTCGCGCGCACCATTGGACTC

CS-376/3

ATCATTACCGGTCTTTCCACCCACACCAGTGCGTACCTCTCGTCCCTTTGGGTCCGTTCGGTGTCTCGCATC
GGCAGACCCATCTGTGCTCTTGTTCGAGCTGGCGCGCCCCGCGCGGCAGATCGGGCGGGACGCAGGCACT
GTGTCTCGAACACAGCCACATCTCCTCATCGGCCTCTCCCGGTTCGAGGAGGATCCCTTCGACGTGCCCA
TCGCGCCTCGAGCGCGGGGGGACGCAAGAATTGTTGAAACACACAACCTCTTGTGATGGATATCTTGGC
TCTCGCAACGATGAAGAACGCAGCGAAATGCGATACGTAATGCGAATTGCAGAATTGAGTGAATCATCGA
ACTTTTGAACGCAACTGGCGCTTCCAGGTTCCGCCTGGGAGCATGTTTCTTCGAGTGGCGCCTCCACCCG
CCTGGGCGTGCGCCTCGCGCGCACATCCGATCGTGTCTGCCGCGGCGTGAGCTGCGCCAGATCAAGGTT
GAGCGTCGCCTGAGGGCAGCGTTGCACGGGAGGATCGTCGGATCTGCCCGTGTGCCGACGTGCTAGTAGG
TCGCCTACCAAGTCGTTGTGCCATCGAACGCTGTGATCTCAACCGACGCGGGGACGCGAGGACATATATA
TCGCGGCTCCGCCACCGGTGCGCCTCGCGCGCACCATTGGACAC

RCC-1435

ATCATTACCGGTCTTTCCACCCACACCAGTGCGTACCTCTCGTCCCTTTGGGTCCGTTCGGTGTCTCGCATC
GGCAGACCCATCTGTGCTCTTGTTCGAGCTGGCGCGCCCCGCGCGGCAGATCGGGCGGGACGCAGGCACT
GTGTCTCGAACACAGCCACATCTCCTCATCGGCCTCTCCCGGTTCGAGGAGGATCCCTTCGACGTGCCCA
TCGCGCCTCGAGCGCGGGGGGAGCAGCAAGAATTGTTGAAACACACAACCTCTTGTGATGGATATCTTGG
CTCTCGCAACGATGAAGAACGCAGCGAAATGCGATACGTAATGCGAATTGCAGAATTGAGTGAATCATCG
AACTTTTGAACGCAACTGGCGCTTCCAGGTTCCGCCTGGGAGCATGTTTCTTCGAGTGGCGCCTCCACCC
GCCTGGGCGTGCGCCTCGCGCGCACATCCGATCGTGTCTGCCGCGGCGTGAGCTGCGCCAGATCAAGGTT
CGAGCGTTCGCTGAGGGCAGCGTTGCACGGGAGGATCGTCGGATCTGCCCGTGTGCCGACGTGCTAGTAG
GTCGCCTACCAAGTCGTTGTGCCATCGAACGCTGTGATCTCAACCGACGCGGGGACGCGAGGACATATATA
ATCGCGGCTCCGCCACCGGTGCGCCTCGCGCGCACCATTGGACAC

NIES-1018

ATCATTACCGGTCTTTCCACCCACACCAGTGCGTACCTCTCGTCCCTTTGGGTCCGTTCGGTGTCTCGCATC
GGCAGACCCATCTGTGCTCTTGTTCGAGCTGGCGCGCCCCGCGCGTCAGATCGGGCGGGACGCAGGCACT
GTGTCTCGAACACAGCCACATCTCCTCATCGGCCTCTCCCGGTTCGAGGAGGATCCCTTCGACGTGCTCCA
TCGCGCCTCGAGCGCGGGGGGAGCAGCAAGAATTGTTGAAACACACAACCTCTTGTGATGGATATCTTGG
CTCTCGCAACGATGAAGAACGCAGCGAAATGCGATACGTAATGCGAATTGCAGAATTGAGTGAATCATCG
AACTTTTGAACGCAACTGGCGCTTCCAGGTTCCGCCTGGGAGCATGTTTCTTCGAGTGGCGCCTCCACCC
GCCTGGGCGTGCGCCTCGCGCGCACATCCGATCGTGTCTGCCGCGGCGTGAGCTGCGCCAGATCAAGGTT
CGAGCGTTCGCTGAGGGCAGCGTTGCACGGGAGGATCGTCGGATCTGCCCGTGTGCCGACGTGCTAGTAG
GTCGCCTACCAAGTCGTTGTGCCATCGAACGCTGTGATCTCAACCGACGCGGGGACGCGAGGACATATATA
ATCGCGGCTCCGCCACCGGTGCGCCTCGCGCGCACCATTGGACAC

RCC-191

ATCATTACCGGTCTTTCCACCCACACCAGTGCGTACCTCTCGTCCCTTTGGGTCCGTTCGGTGTCTCGCATC
GGCAGACCCATCTGTGCTCTTGTTCGAGCTGGCGCGCCCCGCGCGGCAGATCGGGCGGGACGCAGGCACT
GTGTCTCGAACACAGCCACATCTCCTCATCGGCCTCTCCCGGTTCGAGGAGGATCCCTTCGACGTGCTCCA
TCGCGCCTCGAGCGCGGGGGGAGCAGCAAGAATTGTTGAAACACACAACCTCTTGTGATGGATATCTTGG
CTCTCGCAACGATGAAGAACGCAGCGAAATGCGATACGTAATGCGAATTGCAGAATTGAGTGAATCATCG
AACTTTTGAACGCAACTGGCGCTTCCAGGTTCCGCCTGGGAGCATGTTTCTTCGAGTGGCGCCTCCACCC
GCCTGGGCGTGCGCCTCGCGCGCACATCCGATCGTGTCTGCCGCGGCGTGAGCTGCGCCAGATCAAGGTT
CGAGCGTTCGCTGAGGGCAGCGTTGCACGGGAGGATCGCCGGATCTGCCCGTGTGCCGACGTGCTAGTAG
GTCGCCTACCAAGTCGTTGTGCCATCGAACGCTGTGATCTCAACCGACGCGGGGACGCGAGGACATATATA
ATCGCGGCTCCGCCACCGGTGCGCCTCGCGCGCACCATTGGACAC

RCC-1433

ATCATTACCGGTCTTTCCACCCACACCAGTGCGTACCTCTCGTCCCTTTGGGTCCGTCCGGTGCTCGCATC
GGCAGACCCATCTGTGCTCTTGTTCGAGCTGGCGCGCCCCGCGCGGCAGATCGGGCGGGACGCAGGCACT
GTGTCTCGAACACAGCCACATCTCCTCATCGGCCTCTCCCGGTTCGAGGAGGATCCCCTCGACGTGCTCCA
TCGCGCCTCGAGCGCGGGGGAGCACGCAAGAATTGTTGAAACACACAACCTCTTGTTCGATGGATATCTTGG
CTCTCGCAACGATGAAGAACGCAGCGAAATGCGATACGTAATGCGAATTGCAGAATTCAGTGAATCATCG
AACTTTTGAACGCAACTGGCGCTTCCAGGTTCCGCCTGGGAGCATGTTTCTTCGAGTGGCGCCTCCACCC
GCCTGGGCGTGCCTTCGCGCGCACATCCGATCGTGTCTGCCGCGGCGTGAGCTGCGCCAGATCAAGGTT
CGAGCGTCGCCTGAGGGCAGCGTTGCACGGGAGGATCGCCGGATCTGCCCGTGTGCCGACGTGCTAGTAG
GTGCGCTACCAAGTCGTTGTGCCATCGAACGCTGTGATCTCAACCGACGCGGGGACGCGAGGACATATAT
ATCGCGGCTCCGCCACCGGTGCGCCTCGCGCGCACCATTTGGACAC

ARC479

ATCATTACCGGTCTTTCCACCCACACCAGTGCGTACCTCTCGTCCCTTTGGGTCCGTCCGGTGCTCGCATC
GGCAGACCCATCTGTGCTCTTGTTCGAGCTGGCGCGCCCCGCGCGGCAGATCGGGCGGGACGCAGGCACT
GTGTCTCGAACACAGCCACATCTCCTCATCGGCCTCTCCCGGTTCGAGGAGGATCCCCTCGACGTGCTCCA
TCGCGCCTCGAGCGCGGGGGAGCACGCAAGAATTGTTGAAACACACAACCTCTTGTTCGATGGATATCTTGG
CTCTCGCAACGATGAAGAACGCAGCGAAATGCGATACGTAATGCGAATTGCAGAATTCAGTGAATCATCG
AACTTTTGAACGCAACTGGCGCTTCCAGGTTCCGCCTGGGAGCATGTTTCTTCGAGTGGCGCCTCCACCC
GCCTGGGCGTGCCTTCGCGCGCACATCCGATCGTGTCTGCCGCGGCGTGAGCTGCGCCAGATCAAGGTT
CGAGCGTCGCCTGAGGGCAGCGTTGCACGGGAGGATCGCCGGATCTGCCCGTGTGCCGACGTGCTAGTAG
GTGCGCTACCAAGTCGTTGTGCCATCGAACGCTGTGATCTCAACCGACGCGGGGACGCGAGGACATATAT
ATCGCGGCTCCGCCACCGGTGCGCCTCGCGCGCACCATTTGGACAC

PPSR01

CGGGGGAGCACGCAAGAATTGTTGAAACACACAACCTCTTGTTCGATGGATATCTTGGCTCTCGCAACGATG
AAGAACGCAGCGAAATGCGATACGTAATGCGAATTGCAGAATTCAGTGAATCATCGAACTTTTGAACGCA
ACTGGCGCTTCCAGGTTCCGCCTGGGAGCATGTTTCTTCGAGTGGCGCCTCCACCCGCTGGGCGTGC
CTCGCGCGCACATCCGATCGTGTCTGCCGCGGCGTGAGCTGCGCCAGATCAAGGTTTCGAGCGTCGCCTGA
GGGAGCGTTGCACGGGAGGATCGTCGGATCTGCCCGTGTGCCGACGTGCTAGTAGGTCGCCTACCAAGT
CGTTGTGCCATCGAACGCTGTGATCTCAACCGACGCGGGGACGCGAGGACATATATATCGCGGCTCCGCC
CACCGGTGCGCCTCGCGCGCACCATTTGGACTC

NIES-1017

ATCATTACCGGTCTTTCCACCCACACCAGTGCGTACCTTTTCGTCCCTCTGGGCCTGTCCGGTGCTCGCATC
GGCAGACCCATCTGTGCTCTTGTTCGAGCTGGCGCCTCCGCGCGCCAGAGCGAGCGGGACGCAGGCACTGT
GTCTCGAACACAGCCACAGCTCCTCCCGTTCGGCCTCCGGGTTCGAGGAGGATCCCCTCGACGTGCCAGC
GCGCCTCGGCGAGCGGTGGGCACGTAAGAATTGTTGAAACACACAACCTCTTGTTCGATGGATATCTTGGCT
CTCGCAACGATGAAGAACGCAGCGAAATGCGATACGTAATGCGAATTGCAGAATTCAGTGAATCATCGAA
CTTTTGAACGCAACTGGCGCTTCCAGGTTCCGCCTGGGAGCATGTTTCTTCGAGTGGCGCCTCCACCCGC
CTGGGCGTGCCTTCGCGCGCACATCCGATCGTGTCTGCCGTGGCCTTGGGCCGCGCCAGATAAAGGTTTC
GAGCGTCGCCTGAGGGCAGCGTTGCACGGGAAGATTTCGCGGATCTTGCTGTGTTGCCGACGTGCTAGTAG
GTGCGCTACCAAGTCGTTGTGCCATCGAACGCTGCGATCTCAACCGACGCGGGGCCGCGAGAAAAGTCGC
GGTCCGCCACCGGTGCGCCTCGCGCGCACCATTTGGACTC

K-0252

ATCATTACCGGTCTTTCCACCCACACCAGTGCGTACCTTTTCGTCCCTCTGGGCCTGTCCGGTGCTCGCATC
GGCAGACCCATCTGTGCTCTTGTTCGAGCTGGCGCCTCCGCGCGCCAGAGCGAGCGGGACGCAGGCACTGT
GTCTCGAACACAGCCACAGCTCCTCCCGTTCGGCCTCCGGGTTCGAGGAGGATCCCCTCGACGTGCCAGC
GCGCCTCGGCGAGCGGTGGGCACGTAAGAATTGTTGAAACACACAACCTCTTGTTCGATGGATATCTTGGCT
CTCGCAACGATGAAGAACGCAGCGAAATGCGATACGTAATGCGAATTGCAGAATTCAGTGAATCATCGAA
CTTTTGAACGCAACTGGCGCTTCCAGGTTCCGCCTGGGAGCATGTTTCTTCGAGTGGCGCCTCCACCCGC
CTGGGCGTGCCTTCGCGCGCACATCCGATCGTGTCTGCCGTGGCCTTGGGCCGCGCCAGATAAAGGTTTC
GAGCGTCGCCTGAGGGCAGCGTTGCACGGGAAGATTTCGCGGATCTTGCTGTGTTGCCGACGTGCTAGTAG

GTCGCCTACCAAGTCGTTGTGCCATCGAACGCTGCGATCTCAACCGACGCGGGGCCGCGAGAAAAAGTCGC
GGCTCCGCCACCGGTGCGCCTCGCGCGCACCATTGGACTC

Texoma1

ATCATTACCGGTCTTTCCACCCACACCAGTGCGTACCACTCGTCCCTTTGGGTCCGTCCGGTGCCTTGCATC
GGCGGCTCATCTGTGCTCTTGCTCGAGCTGGCGCTCCGCGCGCCAGATCGGGTGGGACGCAGGCACTGTGT
CCTTGACACAGCCACATCTCCTCCTCGGCCCTCGCCGGTTCGTTGAGGATCCCCCTCGTCTGCTCCTGCGC
CTCGCGCGCTCGAGCACACAAGAATTGTTGAAACACACAACCTCTTGTCGATGGATATCTTGGCTCTCGCAA
CGATGAAGAACGCAGCGAAATGCGATACGTAATGCGAATTGCGAATTCAGTGAATCATCGAACTTTTGAA
CGCAACTGGCGCTTCCAGGTTCCGCCTGGGAGCATGTTTCTTCGAGTGGCGCTCCACCCGCTGGGCGTG
CGCCTCGCGCGCACATCCGATCGTGTCTGCCGCGGCTTCGTGCTGCGCCAGATCAAGGCTCGAGCGTCGC
CTGAGGGCAGCGTTGCACGGGAGGATCCTCGGATCCTCGCGTGTGCCGACGTGCTAGTAGGTTTCTACCA
AGTCGTTGTGCCATCGAACGCTGCGATCTCAACCGACGCGGGGACGCGAGGACCTAGGTCGTCGCGACTCC
GCCACCGGTACGCTCGCGCGCACCATTGGACTC

WBF_PRC1

ATCATTACCGGTCTTTCCACCCACACCAGTGCGTACCACTCGTCCCTTTGGGTCCGTCCGGTGCCTTGCATCG
GCGGCTCATCTGTGCTCTTGCTTGAGCTGGCGCTCCGCGCGCCAGATCGGGCGGGACGCAGGCACTGTGTC
CCGGACACAGCCACATCTCCTCCTCGGCCCTCGCCGGTTCGTTGAGGATCCCCCTCGTCTGCTCCTGCGCG
TTGCGCTCTCGGGCACGCAAGAATTGTTGAAACACACAACCTCTTGTCGATGGATATCTTGGCTCTCGCAAC
GATGAAGAACGCAGCGAAATGCGATACGTAATGCGAATTGCGAATTCAGTGAATCATCGAACTTTTGAAC
GCAACTGGCGCTTCCAGGTTCCGCCTGGGAGCATGTTTCTTCGAGTGGCGCTCCACCCGCTGGGCGTGC
GCCTCGCGCGCACATCCGATCGTGTCTGCCGTGGACTTAGTGCTGCGCCAGATCAAGGCTCGAGCGTCGCC
TGAGGGCAGCGTTGCACGGGAGGATCCTCGGATCTGACGTGTGCCGACGTGCTAGTAGGCCCGCTACCAAG
TCGTTGTGCCATCGAACGCTGCGATCTCAACCGACGCGGGGACTCGAGGACCTAGGTCGTCGCGTTTTCCGC
CCACCGGTACGCTCGCGCGCACCATTGGACTC

WBF_PRD2

ATCATTACCGGTCTTTCCACCCACACCAGTGCGTACCACTCGTCCCTTTGGGTCCGTCCGGTGCCTTGCATCG
GCGGCTCATCTGTGCTCTTGCTTGAGCTGGCGCTCCGCGCGCCAGATCGGGCGGGACGCAGGCACTGTGTC
CCGGACACAGCCACATCTCCTCCTCGGCCCTCGCCGGTTCGTTGAGGATCCCCCTCGTCTGCTCCTGCGCG
TTGCGCTCTCGGGCACGCAAGAATTGTTGAAACACACAACCTCTTGTCGATGGATATCTTGGCTCTCGCAAC
GATGAAGAACGCAGCGAAATGCGATACGTAATGTGAATTCGAGAATTCAGTGAATCATCGAACTTTTGAAC
GCAACTGGCGCTTCCAGGTTCCGCCTGGGAGCATGTTTCTTCGAGTGGCGCTCCACCCGCTGGGCGTGC
GCCTCGCGTGCACATCCGATCGTGTCTGCCGTGGACTTAGTGCTGCGCCAGATCAAGGCTCGAGCGTCGCC
TGAGGGCAGCGTTGCACGGGAGGATCCTCGGATCTGACGTGTGCCGACGTGCTAGTAGGCCCGCTACCAAG
TCGTTGTGCCATCGAACGCTGCGATCTCAACCGACGCGGGGACTCGAGGACCTAGGTCGTCGCGTTTTCCGC
CCACCGGTACGCTCGCGCGCACCATTGGACTC

Partial sequence of internal transcribed spacer (ITS) gene of other *P. parvum* strains not included in the phylogenetic tree

UTEX_LB_995 (syn 946/1B)

TACCGGTCTTTCCACCCACACCAGTGCGTACCTCTCGTCCCTTTGGGTCCGTCCGGTGCCTTGCATCGGCAG
ACCCATCTGTGCTCTTGTTGAGCTGGCGCGCCCCGCGCGGCAGATCGGGCGGGACGCAGGCACTGTGTC
TCGAACACAGCCACATCTCCTCATCGGCCCTTTCGGTTCGAGGAGGATCCCCCTGACGTGCCCATCGCGC
CTCGAGCGCGGGAGCACGCAAGAATTGTTGAAACACACAACCTCTTGT

CCMP708 (syn 946/6)

TGCCGGTCTTTCCACCCACACCAGTGCGTACCAACACGTCCTTTGGGTCCGTCCGGTGCCTTGCATCGGGCGG
CTCATCTGTGCTCTAGCTCGAGCTGGCGCTCCGCGCGCCAGATCGGGTGGGACGCAGGCACTGTGTCCTT
GCACACAGCCACATCTCCTCCTCGGCCCTCGCCGGTTCGTTGAGGATCCCCCTCGTCTGCTCCTGCGCCTC
CGCGCTCGAGCACACAAGAATTGTTGAAACACACAACCTCTTGT

CCMP1296

TACCGGTCTTTCCACCCACACCAGTGCGTACCTCTCGTCCCTTTGGGTCCGTCGGTGCTCGCATCGGCAG
ACCCATCTGTGCTCTTGTTCGAGCTGGCGCGCCCCGCGGGCAGATCGGGCGGGACGCAGGCACTGTGTCT
CGAACACAGCCACATCTCCTCATCGGCCTCTTCCGGTCGAGGAGGATCCCCCTCGACGTGCCCCATCGCGC
CTCGAGCGCGGGGCACGCAAGAATTGTTGAAACACAACCTCTTGT

UWCC MI 325

TACCGGTCTTTCCACCCACACCAGTGCGTACCAATCGTCCCTTTGGGCGCGTCGGTCCTCGGATCGGCAG
TCATCTGTGCTCTTGTTCGAGCTGGCGCCTCCGGCGTCAGAGCGAGCGGGACGCAGGCACTGTGTCTCGC
ACACAGCCACACCCCTCCTCGCACGATCTCGGTGCTGTGGAGAGGATCCCCCTCGTCGTGTTACGCTGC
CCTCGGCCTGGACACACAAGAATTGTTGAAACACAACCTCTTGT

Wyoming

TACCGGTCTTTCCACCCACACCAGTGCGTACCACTCGTCCCTTTGGGTCCGTCGCTGCTCGCATCGGCGG
CTCATCTGTGCTCTTGTCTCGCGCTGGCGCTCCGCGCGCCAGATCGGGTGGGACGCAGGCACTGTGTCTT
GCACACAGCCACATCTCCTCCTCGGCCCTCGCCGGTCGTTGAGGATCCCCCTCGTCGTGCTCCTGGGCCTC
GCGCGCTCGAGCACACAAGAATTGTTGAAACACAACCTCTTGT

UTEX LB 2827

TACCGGTCTTTCCACCCACACCAGTGCGTACCACTCGTCCCTTTGGGTCCGTCGCTGCTCGCATCGGCGG
CTCATCTGTGCTCTTGTCTCGCGCTGGCTCCGCGCGCCAGATCGGGTGGGACGCAGGCACTGTGTCTTGC
ACACAGCCACATCTCCTCCTCGGCCCTCGCCGGTCGTTGAGGATCCCCCTCGTCGTGCTCCTGGGCCTCGC
GCGCTCGAGCACACAAGAATTGTTGAAACACAACCTCTTGT

LGDCBD

TACCGGTCTTTCCACCCACACCAGTGCGTACCACTCGTCCCTTTGGGTCCGTCGCTGCTCGCATCGGCGG
CTCATCTGTGCTCTTGTCTCGCGCTGGCGCTCCGCGCGCCAGATCGGGTGGGACGCAGGCACTGTGTCTT
GCACACAGCCACATCTCCTCCTCGGCCCTCGCCGGTCGTTGAGGATCCCCCTCGTCGTGCTCCTGCGCCTC
GCGCGCTCGAGCACACAAGAATTGTTGAAACACAACCTCTTGT

LGRC

TACCGGTCTTTCCACCCACACCAGTGCGTACCACTCGTCCCTTTGGGTCCGTCGCTGCTCGCATCGGCGG
CTCATCTGTGCTCTTGTCTCGCGCTGGCTCCGCGCGCCAGATCGGGTGGGACGCAGGCACTGTGTCTTGC
ACACAGCCACATCTCCTCCTCGGCCCTCGCCGGTCGTTGAGGATCCCCCTCGTCGTGCTCCTGGGCCTCGC
GCGCTCGAGCACACAAGAATTGTTGAAACACAACCTCTTGT

RB

TACCGGTCTTTCCACCCACACCAGTGCGTACCACTCGTCCCTTTGGGTCCGTCGCTGCTCGCATCGGCGG
CTCATCTGTGCTCTTGTCTCGCGCTGCGCTCCGCGCGCCAGATCGGGTGGGACGCAGGCACTGTGTCTTGC
CACACAGCCACATCTCCTCCTCGGCCCTCGCCGGTCGTTGAGGATCCCCCTCGTCGTGCTCCTGCGCCTCGC
GCGCTCGAGCACACAAGAATTGTTGAAACACAACCTCTTGT

UTEX LB 2797

TACCGGTCTTTCCACCCACACCAGTGCGTACCACTCGTCCCTTTGGGTCCGTCGCTGCTCGCATCGGCGG
CTCATCTGTGCTCTTGTCTCGCGCTGGCGCTCCGCGCGCCAGATCGGGTGGGACGCAGGCACTGTGTCTT
GCACACAGCCACATCTCCTCCTCGGCCCTCGCCGGTCGTTGAGGATCCCCCTCGTCGTGCTCCTGCGCCTC
GCGCGCTCGAGCACACAAGAATTGTTGAAACACAACCTCTTGT

Lake Diversion

TACCGGTCTTTCCACCCACACCAGTGCGTACCACTCGTCCCTTTGGGTCCGTCCGGTGCTCGCATCGGCGG
CTCATCTGTGCTCTCGCTTGAGCKGGCTCCGCGCGCCAGATCGGGCGGGACGCAGGCACTGTGTCCCGGA
CACAGCCACATCTCCTCCTCGGCCCTCGCCGGTTCGTTGAGGATCCCCCTCGTTCGTGCCCTGCCGTTGCG
CTCTCGAGCACGCAAGAATTGTTGAAACACACAACCTCTTGT

ZB1101

CCACACCAGTGCGTACCACTCGTCCCTTTGGGTCCGTCCGGTGCTCGCATCGGCGGCTCATCTGTGCTCTT
GCTCGAGCTGGCGCTCCGCGCGCCAGATCGGGTGGGACGCAGGCACTGTGTCTTGCACACAGCCACATC
TCCTCCTCGGCCCTCGCCGGTTCGTTGAGGATCCCCCTCGTTCGTGCTCCTGCGCCTCGCGCGCTCGAGCACA
CAAGAATTGTTGAAACACACAACCTCTTGTTCGATGGATATCTTGGCTCTCGCAACGATGAAGAACGCAGCG
AAATGCGATACGTAATGCGAATTGCGAATTGAGAAATTCAGTGAATCATCGAACTTTTGAACGCAACTGGCGCTTCC
AGGTTCCGCTGGGAGCATGTTTCTTCGAGTGGCGCCTCCACCCGCTGGGCGTGCGCCTCGCGCGCACA
TCCGATCGTGTCTGCCGCGGCCTTCGTGCTGCGCCAGATCAAGGCTCGAGCGTCCCTGAGGGCAGCGTT
GCACGGGAGGATCCTCGGATCCTCGCGTGTGCCGACGTGCTAGTAGGTTTCTACCAAGTCGTTGTGCCA
TCGAACGCTGCGATCTCAACCGACGCGGGGACGCGAGGACCTACCTAGGTCGTCCGACTCCGCCACCG
GTACGCCCTCGCGCGCACCATTTGGACTC

CCAP 941/6

ATCATTACCGGTCTTTCCACCCACACCAGTGCGTACCAACACGTCCCTTTGGGTCCGTCCGGTGCTTGCATCG
GCGGCTCATCTGTGCTCTAGCTCGAGCTGGCGCTCCGCGCGCCAGATCGGGTGGGACGCAGGCACTGTGTC
CTTGCACACAGCCACATCTCCTCCTCGGCCCTCGCCGGTTCGTTGAGGATCCCCCTCGTTCGTGCTCCTGCGCC
TCGCGCGCTCGAGCACACAAGAATTGTTGAAACACACAACCTCTTGTTCGATGGATATCTTGGCTCTCGCAAC
GATGAAGAACGCAGCGAAATGCGAATGCGAATTGCGAATTGAGAAATTCAGTGAATCATCGAACTTTTGAAC
GCAACTGGCGCTTCCAGGTTCCGCTGGGAGCATGTTTCTTCGAGTGGCGCCTCCACCCGCTGGGCGTGC
GCCTCGCGCGCACATCCGATCGTGTCTGCCGCGGCCTTAGTGTGCGCCAGATCAAGGCTCGAGCGTCCG
TGAGGGCAGCGTTGCACGGGAGGATCCTCGGATCCTCGCGTGTGCCGACGTGCTAGTAGGTTTCTACCAA
GTCGTTGTGCCATCGAACGCTGCGATCTCAACCGACGCGGGGACGCGAGGACCTACCTAGGTCGTCTCGAC
TCCGCCACCGGTACGCTCGCGCGCACCATTTGGACTC

12A1

GTTCCGCCAGCCGTGATGCCGCGGGAAGCTGTCCAACCTTATCATTTAGAGGAAGGAGAAGTCGTAACAAG
GTTTCCGTAGGTGAACCTGCGGAAGGATCATTACCGGTCTTTCCACCCACACCAGTGCGTACCACTCGTC
CCTTTGGGTCCGTCCGGTGCTTGCATCGGCGGCTCATCTGTGCTCTTGTCTCGAGCTGGCGCTCCGCGCGCC
AGATCGGGTGGGACGCAGGCACTGTGTCTTGCACACAGCCACATCTCCTCCTCGGCCCTCGCCGGTTCGT
TGAGGATCCCCCTCGTTCGTCTCCTGCGCCTCGCGCGCTCGAGCACA

13A5

GTTCCGCCAGCCGTGATGCCGCGGGAAGCTGTCCAACCTTATCATTTAGAGGAAGGAGAAGTCGTAACAAG
GGTTTCCGTAGGTGAACCTGCGGAAGGATCATTACCGGTCTTTCCACCCACACCAGTGCGTACCACTCGTC
CCCTTTGGGTCCGTCCGTGCTCGCATCGGCGGCTCATCTGTGCTCTTGTCTCGCGCTGGCGCTCCGCGCGC
CAGATCGGGTGGGACGCAGGCACTGTGTCTTGCACACAGCCACATCTCCTCCTCGGCCCTCGCCGGTTCG
TTGAGGATCCCCCTCGTTCGTCTCCTGGGCTCGCGCGCTCGAGCACA

CCAP 939/1 P. pigra

AGTCATATGCTTGTCTCAAAGATTAAGCCATGCATGTCTAAGTATAAGCGACTTGTACTGTGAAACTGCG
AATGGCTCATTAAATCAGTTATGGTTTATTTGATGGTACCTTACTACTTGGATAACCGTAGTAATCTAG
AGCTAATACATGCAGGAAGTCCCAGCTTTGGAAGGGATGTATTTATTAGATAAGAGACCAATCCGGCTTG
CCGGTTGCGTGCTGAGTCACAATAACTGCTCGAATCGCATGNCCTTGGCGCCGGCGATGGTTTCAATCAAAT
TTCTGCCCTATCAGCTTTTCGATGGTAGGATCGAGGCCTACCATGGCGTTAACGGGTAACGGAGAATTAGG
GTTTCGATTCCGGAGAGGGAGCCTGAGAAATGGCTACCACATCCAAGGAAGGCAGCAGGCGCGTAAATTCG
CCGAATCCTGACACAGGGAGGTAGTGACAAGAAATAACAATACAGGGCTATTTTGTCTTGTAAATTTGGAA
TGAGTACAATTTACATCTCTTACGAGGATCAATTGGAGGGCAAGTCTGGTGCCAGCAGCCGCGGTAAT
CCAGCTCCAATAGCGTATATTAAGTTGTTGAGTTAAAACGCTCGTAGTCGGATTTCCGGGCGGCTTTG

CCGGTCTGCCGCTGGGTATGCACTGGTGAGGGCGTCCCTTCCTTCCGGAGACTGGCCCTACTCTTAGCTGA
GCGGGGTCGGGAATCGGATCGTTTACTTTGAAAAAATCAGAGTGTTTCAAGCAGGCAGTTTGTCTTTGCA
TGGATTAGCATGGGATAATGAAATAGGACTTTGGTGCTATTTTGTGGTTTTCGAACACCAGAGTAATGAT
TAACAGGGACAGTCAGGGGCACTCGTATTCCGCCGAGAGAGGTGAAATTTCTCAGACCAGCGGAAGACGAA
CCACTGCGAAAGCATTGTCAGGGATGTTTTCACTGATCAAGAACGAAAGTTAGGGGATCGAAGACGATC
AGATACCGTCGTAGTCTTAACCATAAACCATGCCGACTAGGGATCGGCGGAAGTCCTCTTTTGACTCCGT
CGGCACCTTGAGGGAAACTATAGTCTTTGGGTTCCGGGGGAGTATGGTCGCAAGGCTGAAACTTAAAGG
AATTGACGGAAGGGCACCACCAGGAGTGGAGCCTGCGGCTTAATTTGACTCAACACGGGGAAACTTACCA
GGTCCAGACATTGTGAGGATTGACAGATTGAGAGCTCTTTCTTGATTTCGATGGGTGGTGGTGCATGGCCG
TTCTTAGTTGGTGGAGTGATTTGTCTGGTTAATTTCCGTTAACGAACGAGACCTTAGCCTATTAAATAGTG
ACGCGAACACTTTGTTGGCGGTTCACTTCTTAGAGGGACAACCTTGTCTTCAACAAGTGGAAAGTTTGAGGC
AATAACAGGTCTGTGATGCCCTTAGATGTTCTGGGCCGACGCGCTACACTGATGCACTCAACGAGTC
TTCGCCTTGGCCGGAAGGTCCGGGAAACCTTTTGAACCTGCATCGTGATGGGGATAGATTATTGCAACTA
TTAATCTTGAACGAGGAATTCCTAGTAAGCGCATGTCATCAGCGTGCGTTGATTACGTCCCTGCCCTTTG
TACACACCGCCCGTCGCTCCTACCGATTGAATGATCCGGTGAGGCCCCCGGACTGTGGCAACGCAGATGG
TTCGCCATCCGCGATGCCGCGGGAAGCTGTCCAAACCTTATCATTAGAGGAAGGAGAAGTCGTAACAAG
GTTTCCGTAGGTGAACCTGCGGAAGGATCATTACCGGTCTTTCCNCCCGCACTTGTGCGTACCGTTTCGG
TGGGCCTTTGCGTCCATCCGTTTCGTCTGAGGCGTGCTTTGTGGTGCCTTTTGGGACGTTTCGGGCACAGG
TTGCGTCTTGTGTTGGTGGCAGCTTGCTCGCTGTGCCGTTGTGGCATTCCCTGGAGTTTTACGGATCATA
AGCAAGACACAACCTTGTGCGATGGATATCTTGGCTCTCGCAACGATGAAGAACGCAGCGAAAATGCGATA
CGTAGTGCGAATTGCAGAATTCCGTGAATCATCGAACCTTTGAACGCAACTGGCGCTCCAGGTTCCGCC
TGGGAGCATGTCTCTTCGAGTGGCGCTCCACCCGCGTGGGCGCGCGCTGCGCGTGTCCGAACATGGCC
NCCGTTTGGGCTTTTGTGAGGCGTCGGCTAAAGGAGGGAGCGTCGTTGTGGGTCTACTGTGTCTCGCT
CCGCGGCCCGACGTGCTACAAAGGCGTTGCGTCGGAAGCGGTGGTGTGAGTCGTTTGGACTCGGCGGCGCGC
GGTGCGGCTGTTGTGTCGCGGCGCAAAGATGGAAGCGTTGGTTTGCGCCATCGAATGAGGCAAGACTACC
CGCTGAACTTAAGCATATCACTAAGCGGAGGAGAAGAACTAACCAGGATGCCCTCAGTAATGGCGAATG
AAGCGG

Chapter 7

General Discussion and Concluding Remarks

7.1 Research gaps and goals

Prymnesium parvum forms harmful algal blooms (HABs) resulting in fish kills in brackish waters across the world, including the Norfolk Broads, UK where such blooms appear to be a long-standing issue. The factors that contribute to the formation and maintenance of *P. parvum* blooms are not fully known, but this haptophyte species has been reported to have several strategies that equip it to invade and form ecosystem destructive algal blooms (EDABs) in various aquatic habitats (Gobler & Sunda, 2012; Sunda *et al.*, 2006). It is a euryhaline algae that can tolerate a wide range of salinity, allowing it to establish in brackish to freshwater inland environments, such as the broads. *P. parvum* as a mixotrophic microalga, is capable of combining photoautotrophy with heterotrophy (via phagotrophic lifestyle) in gaining its nutritional requirements. *P. parvum* also produces a suite of toxic compounds that negatively affect all gill-breathing animals that can lead to devastating fish-killing events (Evardsen & Imai, 2006; Fistarol *et al.*, 2003; Skovgaard & Hansen, 2003). Apart from toxic substances, *P. parvum* is well-known copious producer of sulfur metabolite dimethylsulfoniopropionate or DMSP.

DMSP is an environmentally important and abundant molecule in marine environments with several petagrams predicted to be produced by Earth's surface oceans (Ksionzek *et al.*, 2016). DMSP affects nutrient supply, atmospheric chemistry signalling and sulfur cycling (Kiene *et al.*, 2000). Most marine phytoplankton, including *P. parvum*, synthesise DMSP via the transamination pathway (Gage *et al.*, 1997). Our recent identification of the key methylthiohydroxybutyrate *S*-methyltransferase enzyme in the transamination pathway for DMSP synthesis in marine bacteria (DsyB), and its eukaryotic counterpart (DSYB) in most phytoplankton, allows DMSP production in the environment to be monitored at the genetic level (Curson *et al.*, 2017, Curson *et al.*, 2018). There have been no studies examining DMSP production and its catabolism by HAB algae, like *P. parvum*, and associated bacteria in a brackish water environment. Given the brackish nature (3-5 PSU) of the Broads and that *P. parvum* DMSP synthesis is down-regulated by low salinity, the prediction would be that DMSP production and cycling is of low significance in such environmental settings.

The goal of this study was to obtain a more developed understanding of the cellular processes involved in the production of DMSP and its by-product DMS, the factors affecting it, and their roles in the toxic bloom-forming haptophyte *Prymnesium parvum*, using combined quantitative chromatography and functional genomic approaches. This phytoplankton has been implicated in

the recurring fish kills which have proven to be a real problem on the Norfolk Broads over the years. Examining DMSP/DMS importance to the algae will shed light on understanding its invasiveness and persistence.

Therefore, to tackle some fundamental gaps in knowledge surrounding the role of DMSP in toxic haptophyte *P. parvum* and its contribution to sulfur cycling, I divided this study into four core sections addressing the following specific goals:

- 1. Determine the effects of *P. parvum* blooms on the Hickling Broad phytoplankton and bacterial community structure and identify the bacterial groups associated with *P. parvum* cells.**
- 2. Determine the temporal change in DMSP production and *DSYB* abundance in Hickling Broad and investigate the potential biological roles of DMSP and DMS in *P. parvum* bloom initiation and maintenance.**
- 3. Determine physiological and environmental variables that drive *P. parvum* DMSP production on the broads.**
- 4. Characterize the toxins produced by novel strains of *P. parvum* isolated from Hickling Broad which will be essential in future HAB control and mitigation.**

Most microalgal DMSP and DMS research focuses on the spatio-temporal distributions and factors controlling DMSP/DMS cycling in the marine environment. By contrast, minimal attention has been given to brackish water and/or freshwater systems. Research presented in this thesis significantly improves the current understanding of sulfur cycling in brackish water ecosystems, in particular by determining the functional/ecological role of DMSP in *P. parvum* blooms and the associated microbial community. In this chapter, I summarise results presented in this study and develop a wider view on DMSP/DMS cycling in brackish waters. I conclude by identifying future research directions that would improve our understanding of sulfur cycling in brackish and freshwater systems as influenced by HAB events and further emphasize the importance of algal-microbial interactions in modulating such biogeochemical process.

7.2 Key findings described in this thesis

7.2.1 *Prymnesium parvum* blooms affect Hickling Broads prokaryotic and eukaryotic communities

The effect of *P. parvum* bloom on the eukaryotic (phytoplankton) and bacterial community structure was examined in samples collected in Hickling Broad (**Chapter 3**). For phytoplankton community, the general cyclical pattern observed is mainly influenced by seasonal change. Bi-monthly sampling also revealed that the overall phytoplankton community on Hickling broad consisted of three major phytoplankton groups; *cyanobacteria*, *chlorophyta*, and diatoms based on 17 taxa of phytoplankton identified via microscopy. The episodic disturbance due to *P. parvum* bloom in the summer months resulted in major shift in the phytoplankton community when elevated numbers of haptophyte *Prymnesium* overshadowed and dominated the community. *Prymnesium parvum* alone was accounted for 15-20 % of the total community during such a bloom. Despite this major shift in the community during summer, in autumn through spring, the plankton community composition recovered and went back to a cyclical seasonal pattern with a mixed diatom-cyanobacteria dominated community.

The effect of the *P. parvum* bloom on bacterial community structure was investigated through 16S rRNA gene amplicon sequencing analysis during the bloom and non-bloom conditions. This revealed a drastic shift in the bacterial community composition. *P. parvum* chloroplast 16S rRNA genes dominated the community in all sampling locations examined, representing between 20% and 41% of the total microbial community in bloom samples compared to those dominated by different types of Cyanobacteria in non-bloom samples. In the non-bloom period, levels of *P. parvum* were as low as only 1-3% of the total population, and a much more diverse microbial community was seen. *Prymnesiophyceae*, *Alphaproteobacteria*, *Sphingobacteriia* (*Bacteroidetes*) and *Betaproteobacteria* were the four major dominant classes found to be enhanced during the *P. parvum* bloom period. Cyanobacteria on the other hand, exhibited an inverse pattern with 28-30% dominance during non-bloom down to 2-4% during bloom period. *Planctomycetia*, *Actinobacteria*, and *Flavobacteria* also exhibited decline in abundance during the bloom period.

The changes observed in this study are in agreement with what was previously observed in *P. parvum* bloom colonised communities such as the increased abundance in *Alphaproteobacteria* and *Bacteroidetes*. These two groups are dominant in bacterial communities attached to algal

cell surfaces during HAB events (Kodama *et al.*, 2006; Acosta *et al.*, 2015). The decline in abundance of ubiquitous limnetic bacteria, *Actinobacteria* (Newton *et al.*, 2011), was also observed during *P. parvum* blooms in lake Texoma, US (Jones, 2012). The author speculated that conspicuous absence may indicate a negative effect from the exposure of algal excreted toxins, or ecological vulnerability as a preferential prey source. Furthermore, when probed using catalysed reporter deposition with *in situ* hybridisation (CARD-FISH), no Actinobacterial groups were found attached/associated with *P. parvum* cells which supported our results and previous results. The detection of CARD-FISH signals for *Alphaproteobacteria*, *Betaproteobacteria* and *Gammaproteobacteria* surrounding or attached to *Prymnesium* cells highlighted the fact that these bacterial groups were favoured during *P. parvum* bloom events and such microbial interactions might have a role in *P. parvum* bloom establishment and control.

P. parvum blooms release a variety of metabolite compounds, such as DMSP, into the surrounding waters. This in turn influences the bacterial community and enhances the recruitment or growth of bacterial species capable of assimilating and/or metabolizing these compounds (Howard *et al.*, 2008). Exogenous labile DMSP can be assimilated by opportunistic bacterioplankton as a compatible solute or osmoprotectant especially during the unfavorable osmotic condition (Mason & Blunden, 1989, Wolfe, 1996, Cosquer *et al.*, 1999; Malmstom *et al.*, 2004). Also, in marine surface water, DMSP supports 1–13% of the bacterial carbon demand (Kiene & Linn, 2000) and it is essentially important as a reduced organic sulfur source, like for example the dominant heterotrophic bacteria SAR11 and *Roseobacter* group, which require exogenous sources of reduced sulfur for growth (Tripp *et al.*, 2008). A wide variety of marine microorganism import (Vila *et al.*, 2004; Howard *et al.*, 2008) and catabolize DMSP (Curson *et al.*, 2011; Moran *et al.*, 2012), but less is known for brackish water bacterioplankton.

In this study, I found an increased abundance of bacterial groups linked to DMSP/DMS cycling such as members of the *Roseobacter/Rhodobacter* clade, *Marivita* and *Roseobacter*. These groups are known to dominate the bacterioplankton communities in aquatic/marine environments with high DMSP concentrations, such as phytoplankton blooms, and mediate biogenic sulfur cycling. (Brinkhoff *et al.*, 2008; Buchan *et al.*, 2005; Budinoff *et al.*, 2011; Curson *et al.*, 2011). However, upon investigating there were no detectable DMSP demethylation genes (*dmdA*) suggesting that this process is not important in these brackish systems (**Chapter 4**). However, The DMSP lyase gene *dddP* and its transcripts were detected, albeit at low levels, suggesting that DMSP lysis is at least occurring in these brackish waters. There was no correlation

between *dddP* abundance and *P. parvum* though. It would be interesting in the future to analyse the abundance of the other known DMSP lyase genes, particularly *dddY* that is known to function in *Shewanella* spp. (Curson et al., 2011), Ddd+ strains of which were isolated from the bloom samples.

The effect of *P. parvum* on microbial communities perhaps derives from the direct effects of a variety of metabolite compounds produced by this species on a wide range of organisms (Skovgaard & Hansen, 2003). For example, the variety of toxic substances (**Chapter 6**) produced by *P. parvum* have been shown to affect phototrophic and heterotrophic species of the microbial plankton, and its phagotrophic capabilities allow the ingestion of taxa ranging in size from bacteria to zooplankton that can be significantly larger than the alga (Tillmann, 2003; Acosta et al., 2015). Furthermore, the release of DMSP by *P. parvum* during bloom events attract and encourage the growth of microbial groups that are capable of assimilating and metabolising DMSP. The observed shift in both microbial and algal community structure during *P. parvum* bloom and non-bloom provided insights onto algal-microbial interactions based on their co-occurrence, which has the potential to influence biogeochemical processes and shaping future microbial/planktonic communities.

7.2.2 Seasonal dynamics of *Prymnesium parvum* in Hickling Broad

In studying the *P. parvum* bloom dynamics, combined microscopy and sensitive qPCR methods were employed to enumerate and monitor the seasonal populations of the *P. parvum* on Hickling Broad. *P. parvum* cell counts (through microscopy) and ITS abundance (through qPCR) were measured and correlated with Broad water physico-chemical parameters (**Chapter 4**). My results showed that the seasonal change in Broad water temperature positively correlated with cell counts and ITS abundance of *P. parvum*. The temperature has been previously reported to influence *Prymnesium* bloom initiation and success (Larsen et al., 1998; Baker et al., 2007). Furthermore, previous results (2015-2016) on *P. parvum* ITS abundance showed that blooms of *P. parvum* strongly correlated with an increase in Broad water temperature (Wagstaff et al., 2020), where high ITS copies of *P. parvum* were recorded in August 2016 when the temperature was elevated (21 °C). Subsequently, the abundance of *P. parvum* decreased throughout the later summer leading into autumn months (August to October) with *P. parvum* ITS copies remained low consistently throughout winter and spring (November to May) where minimum temperatures were recorded.

Total phosphate (TP) concentrations were mostly constant and remain relatively high throughout the sampling period with concentrations ranging between 50-125 $\mu\text{g L}^{-1}$. TP levels were slightly elevated during the summer months which coincided with increased abundance of *P. parvum* cells, but no obvious correlation was established. A decrease in dissolved oxygen (DO) levels was also observed during the main *P. parvum* bloom peak in June and total suspended solid levels (TSS) were highest in these samples owing to the increased plankton and microbial biomass due to seasonal forcing. There was no obvious correlation observed between any other of the measured water parameters and *P. parvum* abundance including, total nitrogen (TN, comprising $\text{NH}_4^{2+} + \text{NO}_3^- + \text{NO}_2^-$) and salinity, which have been previously proposed to stimulate *P. parvum* bloom onset (Lindholm et al., 1999; Litchman, 2010; Roelke et al., 2012; Patiño et al., 2014). In fact, the highest recorded *P. parvum* numbers were seen when the water N:P ratio was low. A large *Chl-a* spike was observed during the June *P. parvum* bloom and another spike was observed in October and remained relatively high through winter months, which is apportioned to cyanobacteria and diatoms (Phillips et al., 2005). Likely due to increased total nitrogen loading in the water column because of increased rainfall and tidal flushing of nutrient-rich waters from the Heigham Sound (Agricultural runoff) (Moss & Bales, 1989; Philipps, 1977; Bennion, 2001; Hickling Broad Dossier, 2017).

7.2.3 *Prymnesium parvum* as a major source of DMSP in the Broads

DMSP levels in Hickling Broad water samples were measured from April 2017 to March 2018. Interestingly, significant levels of ~ 4 to 60 nmol L^{-1} particulate DMSP_p (Fig. 4.5) were detected within Broads samples despite their brackish nature, which was comparable to those found in marine surface waters (Gali, 2015). Furthermore, the seasonal pattern of *Prymnesium* cell numbers and abundance strongly correlated with the average DMSP concentrations in the water column and was characterized by a steep peak with concentration up to 58.8 nmol L^{-1} in June 2017 during the height of *P. parvum* bloom. Lower DMSP concentrations were measured before and after the bloom period indicating that *P. parvum* is the main source of DMSP in the Broad water. Throughout the season, but most prominently in the *P. parvum* bloom event, DMSP was also detected in the dissolved fraction and thus could be a nutrient for microbial communities. Alternatively, it is possible that smaller microorganisms, e.g., bacteria, in these samples also produce DMSP (Curson et al., 2017; Williams et al., 2018), but based on my initial screening on culturable bacteria (**Chapter 3**), I only found one.

7.2.4 Hickling *P. parvum* *DSYB* abundance and transcription

Further insight into *P. parvum* DMSP production in the Broads was made by measuring the abundance and transcription of the *P. parvum* DMSP synthesis gene (*DSYB*) in the Broad water samples. I isolated natural Broads *P. parvum* strains to identify their specific *DSYB* gene/s and to design specific qPCR primers targeting them (**Chapter 4**). High quality total RNA was extracted from one of the Hickling broad isolates, *P. parvum* HIK PR1A, and sent out to Luxembourg Centre for Systems Biomedicine (LCSB) for RNA sequencing. *DSYB* and catabolising gene *Alma*-like gene sequences in the HIK PR1A transcriptome assembly created by Dr. Simon Moxon, was queried using local BLAST searches and probed using a curated *DSYB* protein sequence from *P. parvum* as published in Curson et al. (2018) and *Alma* family protein sequences in *E. huxleyi* as reported in Alcorombi et al. (2015).

DSYB primers were designed and used in qPCR and RT-qPCR on community DNA extracted from the Broads samples to measure the abundance and transcription of *P. parvum* *DSYB* allowing for understanding temporal patterns of DMSP levels in the water column. *P. parvum* *DSYB* copy and transcript numbers clearly followed a similar trend to DMSP concentration and *Prymnesium* cells in the water samples (Fig. 4.9). *P. parvum* *DSYB* copy number and transcripts were highest in samples corresponding to the two most significant peaks of *P. parvum* cell numbers and DMSP content, the largest being in June (20.9×10^6 copies L⁻¹ and 9.1×10^6 copies L⁻¹) with 58.8 nmolL⁻¹ DMSP, and then a peak of 29.7 nmol L⁻¹ DMSP in August 2017 (18.6×10^6 copies L⁻¹ and 11×10^6 copies L⁻¹). This data is consistent with *P. parvum* being responsible for much of the DMSP in the environmental samples and is the first time *DSYB* has been targeted and linked to DMSP production in any aquatic sample.

7.2.5 Does *P. parvum* cleave DMSP? and who cleaves DMSP on the Broads?

Although many algae, including *P. parvum*, contain candidate *Alma* DMSP lyase enzymes, it is difficult to predict functional *Alma* enzyme unless they have very high identity to *Emiliana huxleyi*, *Isochrysis galbana*, and *Symbiodinium* sp. *Alma*1 (Alcolombri et al., 2015). The assembled *P. parvum* HIK PR1A transcriptome was shown to contain a candidate *Alma* DMSP lyase gene, 99 % identical to those in other marine *P. parvum* strains, but only ~ 28.35 % identical to the functional *E. huxleyi* *Alma*1 (**Chapter 4**). The HIK PR1A candidate *Alma* was cloned and assayed for DMSP lyase activity in *E. coli* and a *Labrenzia aggregata* *dddL*⁻ mutant (J572). In both these

heterologous hosts, the candidate Alma enzyme was shown to have no significant DMSP lyase activity compared to control experiments (Table 4.2). Furthermore, the Broads *P. parvum* strains and those of marine origin from culture collections (e.g., CCMP 946/6) were incubated in the presence of DMSP, but no DMSP lyase activity was detected. It is possible that the extracellular DMSP is not imported or able to interact with intact *P. parvum* DMSP lyases, thus, *P. parvum* cell-free extracts were also incubated with DMSP, and again no significant DMSP lyase activity was observed. These data are consistent with the *P. parvum* Alma-like proteins not being functional DMSP lyases and these important HAB algae not having DMSP lyase activity. More relevantly to *P. parvum*, the data suggest that DMSP may be an important molecule that the algae do not want to degrade. Further work is required to establish what defines a functional Alma family DMSP lyase and to establish the source DMSP in the dissolved fraction.

Having established that similar amounts of DMSP exist in the brackish Broad waters as in many surface seawater samples and that some bacteria associated with *P. parvum* blooms are known for their ability to catabolise DMSP, e.g., *Roseobacter* (**Chapter 3**), we investigated the potential for bacterial catabolism in these samples. RT-qPCR was done on environmental RNA from the Broads samples to target transcription of the DMSP demethylase gene *dmdA* (Varaljay et al. (2010) and Levine et al. (2012) and the most abundant DMSP lyase gene *dddP* (Todd et al., 2009; Liu et al., 2019). Despite the presence of some Roseobacters, many of which are known to contain *dmdA* and *dddP*, in samples with high *P. parvum* counts, *dmdA* was not successfully amplified from any sample. This is entirely consistent with DMSP demethylation and *dmdA* being characteristic of marine environments (Howard et al., 2006; Bullock et al., 2017). In contrast, *dddP* was amplified but only at very low levels between 1.1×10^3 to 9.1×10^4 transcripts L^{-1} (1.29×10^4 transcripts L^{-1} average) (**Chapter 4**). The *dddP* transcript levels did not correlate with DMSP levels nor the abundance of *P. parvum* or its demise (Fig. 4.10). However, it should be noted that only standing stock DMSP concentrations were measured and DMSP turnover rates, was not done here, which are required for a better indication of activity. Also, *dddP* is only one of seven known bacterial DMSP lyase genes (Sun et al., 2016; Johnston et al., 2016), and the others were not investigated including *dddY* that is known to function in *Shewanella* spp. (Curson et al., 2011). Nevertheless, given *dddP* transcripts likely indicate that these brackish waters are potential sources of DMS, fed by algal derived DMSP.

7.2.6 Factors affecting *P. parvum* DMSP production

Intracellular DMSP production and regulation of *P. parvum* in batch cultures at different growth phases and under different salinity, varying nutrient (N), exposure to reactive oxygen species and viral-like particles were investigated (**Chapter 5**) to identify or elucidate the possible physiological roles of DMSP in this invasive bloom-forming haptophyte, with relevance to the Broads conditions.

DMSP production is dependent on the physiological phase/stage of the algae. The average DMSP concentrations range from ~ 10 to 50 mMol L^{-1} . The observed DMSP production trend started with low production during the mid-exponential phase and reached its maximum at day 22 (late exponential phase) and then gradually decreased during stationary to late stationary phases. This is in concordant with previous reports on DMSP production at different physiological stages of other DMSP-producing marine phytoplankton (Matrai & Keller, 1994; Keller, 1999; Zhuang et al., 2011) where they found a decrease in particulate DMSP during the late stationary to senescent phases of the algal culture. I didn't observe any obvious senescent phase in all cultures tested, for *parvum* growth cycle or any phytoplankton could last beyond study period especially in laboratory-controlled conditions. On the other hand, DMSP of *P. parvum* dormant non-motile cells or 'cysts' were found to be of considerable amount suggesting that DMSP is an important molecule for these cyst cells and may play an important role during algal cyst germination and reseedling. Further studies are needed to elucidate the importance of DMSP on microalgal cysts.

Among the abiotic variables tested, I found that DMSP production was significantly affected by salinity change in *P. parvum* (Fig. 5.8). DMSP concentration in *P. parvum* were all enhanced and progressively accumulated as I increased the salinity regime (between 10-90%) and the osmolyte action may therefore be linked to their use for coping with salinity stress. *DSYB* transcription was also enhanced by increasing salinity and this reflected what was observed in Curson et al. (2018). In short, DMSP per cell volume decreased with lower salinities and increased with raising salinities. This allows *P. parvum* to easily adapt to rapid change in salinity, especially in saline-influenced lake systems (e.g. the Broads), where they can easily invade, establish and develop toxic algal blooms. Thus, this haptophyte species can cope with variation in salinity caused by tidal exposure, evaporation, desiccation, precipitation, and many other contributing processes taking place in this type of aquatic environment. My results, together with previous studies (Vairavamurthy et al., 1985; Blunden et al., 1992; Stefels et al., 2007), support that DMSP does

play an osmoregulatory role in some organisms, like *P. parvum*, especially when they are exposed to the high magnitude of salinity shifts and increased salinification.

There is some evidence suggesting that varying nutrient levels can modulate the intracellular concentrations of DMSP (Turner et al., 1988; Keller et al., 1999; Stefels, 2000; Sunda et al., 2002). In this study, I found no significant increase in intracellular DMSP and *DSYB* transcriptions of *P. parvum* when subjected to low or high nitrogen (LN, HN) conditions. These results are consistent with the findings of Curson et al. (2018) where nitrogen limitation didn't affect DMSP production in six *P. parvum* strains. Furthermore, similar results were found by Sunda et al. (2007) on *E. huxleyi* grown in limited N that showed no significant increase in DMSP production. Interestingly, this is in contrast to what was observed in bacteria and diatoms that make DMSP, both of which have been shown to upregulate DMSP production by low N or N limitation (Bucciareli & Sunda, 2003; Curson et al., 2017).

DMSP and its related breakdown products constitute an antioxidant system in marine microalgae when cells undergo oxidative stress due to overproduction of reactive oxygen species (ROS) (Sunda et al., 2002). I tried to replicate this oxidative stress experiment in the present study by examining the effect of exogenous H₂O₂ on DMSP production of *P. parvum*. There was no obvious increase in intracellular DMSP concentration found but, instead, a sudden decrease in particulate DMSP in all H₂O₂-treated cultures was observed. There is a possibility that observed decrease in intracellular DMSP results from a biological use of DMSP to sequester free radicals. Perhaps, DMSP is oxidized to DMSOP under these conditions to help protect against oxidative stress (Thume et al., 2018). To prove this, however, is to measure DMSP and its turnover rates which was not done in this study.

The effect of virus-like particles (VLPs) isolated from Hickling broad waters on DMSP production by *P. parvum* DMSP was tested since DMSP and its catabolites have been implicated in cellular defence against viral infection (Evans et al., 2006; Evans et al., 2007). I found no change in intracellular DMSP concentrations in response to viral infection but did see a sudden decrease in DMSP after the incubation period which may indicate the decline in cell health and biomass as most of the cells had likely started to lyse. There is again the possibility that the observed decline in intracellular DMSP results from a biological use of DMSP to fight viral titers. DMS and acrylic acid, both cleavage products of DMSP breakdown, have been shown to inhibit *E. huxleyi* virus (Evans et al., 2007). Unfortunately, neither dissolved DMSP nor cleavage products (DMS and

acrylic acid) were measured throughout the period of my investigation and given that an in vitro assay was used, I can only speculate that DMSP is released into the media upon cellular breakdown and no DMSP cleavage happened since *P. parvum*'s DMSP lyase 'ALMA' is non-functional as I have found in **Chapter 4**.

7.2.7 Ichthyotoxins produced by Broads *P. parvum*

Biological and water samples taken from *P. parvum* bloom event in 2015 have been found to be contaminated with B-type prymnesins based on LC-MS data (Wagstaff, 2018). But it was not confirmed whether prymnesins found in the dead fish and water samples were indeed produced by the toxic haptophyte from the broads. In the present study, I managed to isolate a few strains of *P. parvum* from Hickling broad and characterized the prymnesin type they produce (**Chapter 6**). The Hickling broad *P. parvum* strains produce B-type prymnesins based on LC-MS analysis. These results are in congruence with the earlier detected prymnesin-B toxin from Pike gill tissues and water samples taken during a fish-killing *Prymnesium* bloom back in 2015. This proved that the *P. parvum* prymnesins were likely the leading cause of fish mortalities in the area. Furthermore, I found that the broads *P. parvum* were the first known B-type producing strains in the UK, which might suggest that this strain was introduced more recently. Upon mapping its phylogenetic topology, the Hickling strains clustered with the B-type prymnesin producing strains from Northern Europe indicating its relatedness to this *P. parvum* group. Examining further the biogeographical distribution of the *P. parvum* strains, no trend was observed. This agrees with what has been previously observed by Rasmussen et al. (2016) and Binzer et al. (2019).

Previous investigations suggest that *P. parvum* are divided into three major clades based on their ITS sequences (Larsen & Medlin, 1997; Lutz-Carrillo et al., 2010; Binzer et al., 2019). And recently, Binzer et al. (2019) reported that the prymnesins type distribution complemented the clade clustering suggesting links between chemotype and phylotype in *P. parvum*. This observation was also reflected in my phylogenetic results where *P. parvum* strain HIK PR1A clustered with B-type prymnesins producing *P. parvum* strains mostly from Northern Europe. This suggests the possibility of vector transfer between these two areas given their proximity to one another, but no current data supports this.

Toxin production in *P. parvum*, is variable between strains (Manning & La Claire, 2010; Rasmussen et al., 2016; Svenssen et al., 2019). The total amount of toxins and composition of

analogs produced can be altered by certain environmental conditions (Larsen et al, 1993; Baker et al., 2007; Freitag et al., 2011) such as salinity, growth phase, nutrients, etc. In this thesis, I did some preliminary investigations on the effects of low phosphorus (LP) and low salinity (LS) conditions on the pycnospirins profiles of Hickling broad *P. parvum* HIK PR1A. These two factors have been widely reported to affect toxin production (Larsen et al, 1993; Baker et al., 2007). Since there is no standard available for pycnospirins, exact quantification remains a problem. LC-MS data can only provide the relative abundance of each pycnospirin analog/type. Based on my results, I can only infer that each pycnospirin analog changes as the algal cells undergo limiting growth due to nutrient stress. In addition, an increased abundance of glycosylated analogs of pycnospirin were observed which might enhance its toxicity upon release from the algal cells through cell autolysis, breakdown due to grazing, and virulence. This indicated the significance of nutrient availability on the toxin production and toxicity of *P. parvum* cells. Furthermore, the Broads is a eutrophied system with high seasonal fluctuations in nutrients (Phillips & Jackson, 1990; Irvine et al., 1993; Lau & Lane, 2002; Phillips et al., 2005), this potentially explains the frequent occurrence of fish kills due to *P. parvum* in such shallow lake environment.

7.3 Limitations of the Study

7.3.1 *P. parvum* effects on eukaryotic and prokaryotic communities

The phytoplankton community data presented in this study only covered a single seasonal cycle in 2017 which captured a small episodic disturbance in summer months due to *P. parvum* bloom. The observed 2017 *P. parvum* bloom, however, was not as massive as the 2015 bloom that led to a fish kill event, therefore, changes in the phytoplankton community structure may be different between these two bloom events. Furthermore, phytoplankton organisms were visualized and enumerated using the traditional microscopical technique which on its own have certain limitations or disadvantages despite being the benchmark methodology. Some phytoplankton species are too small to be identified by light microscopy, therefore, underestimating the total diversity of phytoplankton present in the sample. The change in microbial community abundance through 16S rRNA gene amplicon sequencing was done only during the height of *P. parvum* bloom in 2015 and compared to a non-bloom period in 2016 and the changes in the bacterioplankton communities as influenced by seasonal variations was not presented. More and longer data sets are needed to establish the effects of *P. parvum* blooms on the phytoplankton and microbial communities.

7.3.2 DMSP turnover

The turnover of DMSP in Hickling broad was not investigated in the present study. Only particulate and some dissolved fraction were measured in the field samples as described in Chapter 4. It is highly recommended to study the biological turnover of DMSP and its breakdown product DMS to further give insight on how fast DMSP and DMS are consumed in this type of system. In addition, DMSP turnover could have possibly explained the observed decrease in intracellular DMSP in *P. parvum* cells when exposed to reactive oxygen species (ROS) and viral-like particles (VLPs).

7.3.3 Quantitation of prymnesins in the broads

Ideally MS-based techniques of quantitating prymnesins require purified standards of prymnesins analog as a bare minimum. This means that a pure standard is required for each one of representative analog for each prymnesin type and subtypes. Unfortunately, prymnesins are difficult to isolate and purify due to the complexity of their nature. There are no currently available commercial standards for Prymnesins. In Chapter 6, I can only detect and identify the type of toxin produced by the Hickling or Woodbridge *P. parvum* strain based on the MS signals and infer the relative abundance of these different prymnesin types/analogs. A new approach should be designed and utilised to, at least indirectly, measure Prymnesin in the samples.

7.4 Recommendations for Future Research

This research has increased our understanding of DMSP production in brackish shallow lakes as mediated by harmful algal blooms of *Prymnesium parvum*, filling the gap of DMSP/DMS cycle in this type of environment that is often overlooked, but more questions arise from this study that need to be dealt with and which will open more opportunities to do more study.

7.4.1 Further work on broad/lake systems DMSP/DMS production

The present study showed *P. parvum* as the major source of DMSP on the Broads, but not all broads/lakes have been colonised by *P. parvum*. Other brackish water systems could have been invaded by different DMSP-producing phytoplankton or bacterioplankton which have yet to be

identified. More work is needed to establish the overall effect of these organisms on the biogeochemical processes, such as sulfur cycling, in this type of aquatic environment.

Moreover, this thesis only covered the levels of DMSP found in the Broad's water column and didn't include DMS and sedimentary DMSP pool (base hydrolysable DMS, Kiene et al., 1988; DMSP_{bound}, Sela-Adler et al., 2015) concentrations. It would be interesting to look at the levels of DMSP in the sediment and compare them to the water column fraction. The sediment-associated pool of DMSP is likely due to sinking detritus, benthic epipelagic microorganisms, algal cysts, and particle adsorbed DMSP.

7.4.2 Fate of algal-derived DMSP on the Broads

More studies should be done to determine the fate of DMSP once released into the surrounding water during algal autolysis and bloom collapse. In this research, we detected DMSP lyase gene in Broad water samples which suggest the presence of bacterial groups capable of catabolising DMSP to form DMS. Future investigations should be directed to determine the spatial and temporal distribution of key bacterial and algal DMSP-degrading genes to better understand the biological turnover of DMSP on the Broads and the functional roles of DMSP-degrading bacteria in this type of aquatic system. Culture-dependent methods should also be done to complement the data derived from these investigations. Samples should have been plated on basal media with DMSP as the sole carbon source and bacteria capable of growing on this condition should have been isolated and purified.

7.4.3 *Prymnesium*-bacterial interactions

An important area for further research would be to investigate *Prymnesium*-bacterial interactions happening within the algal phycosphere. This microscale environment is the planktonic version of the rhizosphere in higher plants. The CARD-FISH results presented in this study found numerous groups of bacteria attached to the *Prymnesium* cells indicating potential interactions between the host algae and the bacterial communities. Such interactions can be symbiotic, parasitic, commensalistic, antagonistic, or just direct competition. The exchange in metabolites, allelochemicals, infochemicals, vitamins etc. (e.g. DMSP and prymnesins) within this interface could exert influence on the ecosystem-scale biogeochemical processes, like sulfur cycling.

7.4.4 Field measurements of prymnesins

The identification of prymnesins types produced by Hickling *P. parvum* strains in the present study set a precedent to develop and/or design methods for directly or indirectly measuring prymnesins in the Broad water. Such toxin quantitation methods will help managers and stakeholders in predicting and controlling the negative impacts of *P. parvum* HABs in affected areas.

7.5 Concluding Remarks

DMSP is an important osmolyte produced in large quantities by phytoplankton, and an important component of the global geochemical sulfur cycle. Previous investigations on DMSP production and regulation have been limited to estuarine and marine environments and production of DMSP in brackish water or freshwater environments were thought to be of low significance.

In this thesis, I investigated the natural cycling of DMSP by harmful algal bloom (HAB)-forming and fish-killing haptophyte *Prymnesium parvum* on shallow brackish water lakes – the Broads through chromatographic and molecular techniques. I found significant levels of DMSP on the broads over a season. *P. parvum* counts/abundance, its DMSP synthesis gene (*DSYB*) transcripts and DMSP are strongly correlated, indicating that this HAB alga as the main producer of DMSP on the Broads. *P. parvum* strains did not produce DMS themselves, and despite significant DMSP levels in Broads water, bacteria with the potential to catabolise DMSP through the DddP DMSP lyase or DmdA DMSP demethylase were rare or undetected in Broads water, respectively. This is consistent with DMSP having an important role in these organisms and these catabolic systems being marine. *P. parvum* DMSP production was upregulated during the late exponential to early stationary phase and by raised salinity, consistent with stress response and osmoregulatory functions.

Knowledge derived from this PhD study provides novel insights into the role of brackish water HAB in DMSP dynamics of lake systems, their role in local biogenic sulfur cycling, and the prymnesin toxins they produce.

8 REFERENCES

- Alcolombri, U., Ben-Dor, S., Feldmesser, E., Levin, Y., Tawfik, D. S. and Vardi, A. 2015. Identification of the algal dimethyl sulfide–releasing enzyme: A missing link in the marine sulfur cycle. 348 (6242), pp. 1466–1469.
- Amann, R.I., Krumholz L., and Stahl, D.A. 1990. Fluorescent oligonucleotide probing of whole cells for determinative, phylogenetic, and environmental studies in microbiology. *J. of Bac.*, vol. 172:2, pp. 762–770.
- Amin, S.A. et al. 2015. Interaction and signalling between a cosmopolitan phytoplankton and associated bacteria. *Nature* 522, pp. 98–101.
- Andersen, R.A. and Kawachi, M. 2005. in *Algal Culturing Techniques* (ed. Anderson, R. A.) Elsevier Acad. Press. pp. 83–101.
- Anderson, D.M. 1989. Toxic algal blooms and red tides: A global perspective, p. 11–16. *In* T. Okaichi, D. M. Anderson, and T. Nemoto (eds.), *Red Tides: Biology, Environmental Science and Toxicology*. Elsevier, New York.
- Anderson D.M. 2014. HABs in a changing world: a perspective on harmful algal blooms, their impacts, and research and management in a dynamic era of climactic and environmental change. *Harmful Algae 2012: Proceedings of the 15th International Conference on Harmful Algae : October 29 - November 2, 2012, CECO, Changwon, Gyeongnam, Korea. International Conference on Harmful Algae (15th : 2012 : Changwon, Gyeongnam, Kore..., 2012, pp. 3–17.*
- Andreae, M.O., 1990. Ocean-atmosphere interactions in the global biogeochemical sulfur cycle. *Marine Chemistry*, 30, pp.1–29.
- Andreae, M.O. and Crutzen, P.J. 1997. Atmospheric aerosols: biogeochemical sources and role in atmospheric chemistry. *Science*. 276, pp. 1052-1058.
- Archer, S. D., Ragni, M., Webster, R., Airs, R. L. and Geider, R.J. 2010. Dimethyl sulfoniopropionate and dimethyl sulfide production in response to photoinhibition in *Emiliana huxleyi* . *Limnol. Oceanogr.* 55, pp. 1579– 89.
- Arnold, H., Kerrison, H., and Steinke, M. 2013. Interacting effects of ocean acidification and warming on growth and DMS-production in the haptophyte coccolithophore *Emiliana huxleyi*. *Glob. Chang. Biol.* 19, pp. 1007–1016.
- Ayers, G.P. and Gras, J.L. 1991. Seasonal relationship between cloud condensation nuclei and aerosol methanesulphonate in marine air. *Nature*. 353, pp. 834 – 835.

- Baker, J.W., Grover, J.P., Brooks, B.W., Ureña-Boeck, F., Roelke, D.L., Errera, R. et al. 2007. Growth and toxicity of *Prymnesium parvum* (Haptophyta) as a function of salinity, light, and temperature. *J Phycol.* 43 (2), pp. 219–227
- Bales, M., Moss, B., Phillips, G., Irvine, K., and Stansfield, J. 1993. The changing ecosystem of a shallow, brackish lake, Hickling Broad, Norfolk, U.K. II. Long-term trends in water chemistry and ecology and their implications for restoration of the lake. *Freshwat. Biol.* 29, (1), pp. 141-165.
- Balls, H., Moss, B., and Irvine, K. 1989. The loss of submerged plants with eutrophication I. Experimental-design, water chemistry, aquatic plant and phytoplankton biomass in experiments carried out in ponds in the Norfolk Broadland *Freshw. Biol.*, 22 (1989), pp. 71-87.
- Barber, M.A. 1914. The pipette method in the isolation of single micro-organisms and in the inoculation of substances into living cells: With a technique for dissection, staining, and other processes carried out under the higher powers of the microscope. *Philippine J. Sci. B.* 9, pp. 307–360.
- Barak-Gavish, N., Frada, M.J., Ku, C., Lee, P.A., DiTullio, G.R., Malitsky, S., Aharoni, A., Green, S.J., Rotkopf, R., Kartvelishvily, E., Sheyn, U., Schatz, D. and Vardi A. 2018. Bacterial virulence against an oceanic bloom-forming phytoplankter is mediated by algal DMSP. *Sci Adv* 4, 5716.
- Basir, N., Yong, A.M.L. and Chong, V.H. 2012. *Shewanella putrefaciens*, a rare cause of splenic abscess. *Journal of Microbiology, Immunology and Infection.* 45(2), pp. 151–53.
- Baumann, P. and Baumann, L. 1981. *The Prokaryotes*. Springer-Verlag.
- Berdalet, E., Fleming, L.E., Gowen, R., Davidson, K., Hess, P., Backer, L.C., Moore, S.K., Hoagland P. and Enevoldsen, H. 2015. Marine harmful algal blooms, human health and wellbeing: challenges and opportunities in the 21st century. *J. Mar. Biol. Assoc., U K.*
- Berges, J.A., Franklin D.J. and Harrison, P.J. 2001. Evolution of an artificial seawater medium: Improvements in enriched seawater, artificial water over the last two decades. *Journal of Phycology*, 37(6), pp. 1138–1145.
- Beringer, J.E. 1974. R factor transfer in *Rhizobium leguminosarum*. *J. Gen. Microbiol.* 84, pp. 188–198.
- Bertin, M.J., Zimba, P.V., Beauchesne, K.R., Huncik, K.M. and Moeller, P.D.R. 2012. Identification of toxic fatty acid amides isolated from the harmful alga *Prymnesium parvum* Carter. *Harmful Algae.* 20, pp. 111-116.

- Beszteri, S., Yang, I., Jaeckisch, N., Tillman, U., Frickenhaus, S., Glöckner, G., et al. 2012. Transcriptomic response of the toxic prymnesiophyte *Prymnesium parvum* (N. Carter) to phosphorus and nitrogen starvation. *Harmful Algae* 18, pp. 1–15.
- Binzer, S.B., Svenssen, D.K., Daugbjerg, N., Alvez-de-Souza, C., Pinto, E., Hansen, P.J., Varga, E. 2019. A-, B- and C-type prymnesins are clade specific compounds and chemotaxonomic markers in *Prymnesium parvum*. *Harmful Algae*, 81, pp. 10-17.
- Bold, H.D. And Wynne, M.J. 1983. Introduction to the algae, 2nd Ed. Prentice-Hall, Inc. Englewood Cliffs, NJ. pp. 417-428.
- Boyle, J.F., Sayer, C.D., Hoare, D., Bennion, H., Heppel, K., Lambert, S.J., Appleby, P.G., Rose, N.L., and Davy, A.J. 2016. Toxic metal enrichment and boating intensity: sediment records of antifoulant copper in shallow lakes of eastern England. *J. Paleolimnol.* 55, pp. 195–208.
- Brailsford, F.L., Glanville, H.C., Wang, D., Golyshin, P.N., Johnes, P.J., Yates, C.A., Jones, D.L. 2020. Rapid depletion of dissolved organic sulphur (DOS) in freshwaters. *Biogeochemistry* 149 (1), pp. 105-113.
- Bratbak, G., 1996. Viral activity in relation to *Emiliania huxleyi* blooms: a mechanism of DMSP release?. *Oceanographic Literature Review*, 7(43), p. 691.
- Broads Authority. 2015. Broads Authority, Norwich, UK.
<http://www.broads-authority.gov.uk/education/about-the-broads.html>
- Broads Authority. 2017. Broads Plan 2017: Partnership strategy for the Norfolk and Suffolk Broads. Norwich, UK: Broads Authority.
http://www.broads-authority.gov.uk/data/assets/pdf_file/0012/976728/Broads-Plan-2017.pdf
- Broads Authority. 2019. Broads Authority, Norwich, UK.
<https://www.visitthebroads.co.uk/discover-the-broads/wildlife-in-the-broads>
- Bromke, M. A., Giavalisco, P., Willmitzer, L. and Hesse, H. 2013. Metabolic analysis of adaptation to short-term changes in culture conditions of the marine diatom *Thalassiosira pseudonana*. *PLoS One* 8, pp. 1–11.
- Brummett, A.E., Schnicker, N.J., Crider, A., Todd, J.D. and Dey, M. 2015. Biochemical, kinetic, and spectroscopic characterization of *Ruegeria pomeroyi* DddW — a mononuclear iron-dependent DMSP lyase. *PLOS ONE*, 10.
- Brutemark, A. and Granéli, E. 2011. Role of mixotrophy and light for growth and survival of the toxic haptophyte *Prymnesium parvum*. *Harmful Algae* 10, pp. 388–394.

- Bucciarelli, E., and Sunda, W. G. 2003. Influence of CO₂, nitrate, phosphate, and silicate limitation on intracellular dimethylsulfoniopropionate in batch cultures of the coastal diatom *Thalassiosira pseudonana*. *Limnol. Oceanogr.* 48: 2256–2265.
- Bulut, C., Ertem, G., Gokcek, C., Tulek, N., Bayar, M.A. and Karakoc, E. 2004. A rare cause of wound infection: *Shewanella putrefaciens*. *Scand J Infect Dis.* 36, pp. 692-694.
- Bürgmann, H., Widmer, F., Sigler, W.V. and Zeyer J. 2003. mRNA extraction and reverse transcription-PCR protocol for detection of nifH gene expression by *Azotobacter vinelandii* in soil. *Appl Environ Microbiol.* 69, pp. 1928-1935.
- Burson, A., Matthijs, H.C., de Bruijne, W., Talens, R., Hoogenboom, R., Gerssen, A., Visser, P.M., Stomp, M., Steur, K., van Scheppingen, Y. and Huisman, J. 2014. Termination of a toxic *Alexandrium* bloom with hydrogen peroxide. *Harmful Algae.* 31, pp. 125-135.
- Butler, W.L. 1978. Energy distribution in the photochemical apparatus of photosynthesis. *Annual Review of Plant Physiology* 29, pp. 345– 378.
- Caporaso, J.G., Kuczynski, J., Stombaugh, J., Bittinger, K., Bushman, F.D., Costello, E.K., et al. 2010. QIIME allows analysis of high-throughput community sequencing data. *Nat Methods.* 7, p. 335.
- Caporaso, J.G., Lauber, C.L., Walters, W.A., Berg-Lyons, D., Huntley, J., Fierer, N. et al. 2012. Ultrahigh-throughput microbial community analysis on the Illumina HiSeq and MiSeq platforms. *The ISME journal.* 6, pp. 1621.
- Caron, D.A., Alexander, H., Allen, A.E., Archibald, J.M., Armbrust, E.V. et al. 2017. Probing the evolution, ecology and physiology of marine protists using transcriptomics. *Nat. Rev. Micro.* 15, (1), pp. 6-20.
- Carpenter, K.J., Bose, M., Polerecky, L., Lie Alle, A.Y., Heidelberg K.B. and Caron D.A. 2018. Single-Cell View of Carbon and Nitrogen Acquisition in the Mixotrophic Alga *Prymnesium parvum* (Haptophyta) Inferred From Stable Isotope Tracers and NanoSIMS. *Frontiers in Marine Science.* Vol. 5: p. 157.
- Carrión, O., Pratscher, J., Richa, K., Rostant, W.G., Farhan Ul Haque, M., Murrell, J.C. and Todd, J.D. 2019. Methanethiol and Dimethylsulfide Cycling in Stiffkey Saltmarsh. *Front. Microbiol.* 10, p. 1040.
- Carrillo, P., Medina-Sánchez, J.M., Villar-Argaiz, M., Delgado-Molina, J.A. and Ballejos, F.J. 2006. Complex interactions in microbial food webs: Stoichiometric and functional approaches. *Limnetica.* 25, pp. 189–204.
- Carter, N. 1937. New or interesting algae from brackish water. *Archiv für Protistenkunde* 90: 1-68.

- Carvalho, W.F. and Granéli, E. 2010. Contribution of phagotrophy versus autotrophy to *Prymnesium parvum* growth under nitrogen and phosphorus sufficiency and deficiency. *Harmful Algae* 9, pp. 105–115.
- CEN 2004. Water quality – Guidance standard for the routine analysis of phytoplankton abundance and composition using inverted microscopy (Utermöhl technique) CEN TC 230/WG 2/TG 3/N83.
- Chang, F.H. and K.G. Ryan. 1985. *Prymnesium calathiferum* sp. nov. (Prymnesiophyceae), a new species isolated from Northland, New Zealand. *Phycologia* 24, pp. 191-198.
- Cosquer, A., Pichereau, V., Pocard, J. A., Minet, J., Cormier, M. and Bernard, T. 1999. Nanomolar levels of dimethylsulfoniopropionate, dimethylsulfonioacetate, and glycine betaine are sufficient to confer osmoprotection to *Escherichia coli*. *Appl. Environ. Microbiol.* 65, pp. 3304–3311.
- Curson, A.R.J., Rogers, R., Todd, J.D., Brearley, C.A. and Johnston, A.W. 2008. Molecular genetic analysis of a dimethylsulfoniopropionate lyase that liberates the climate-changing gas dimethylsulfide in several marine alpha-proteobacteria and *Rhodobacter sphaeroides*. *Environ Microbiol.* 2008 Mar;10(3), pp. 757-67.
- Curson, A.R.J., Liu, J., Bermejo-Martínez, A., Green, R.T., Chan, Y., Carrión, O., Williams, B.T., Zhang, S.H., Yang, G.P., Bulman-Page, P.C., Zhang, X.H. and Todd, J.D. 2017. Dimethylsulfoniopropionate biosynthesis in marine bacteria and identification of the key gene in this process. *Nat. Microbiol.* 2, p. 17009.
- Curson, A.R.J., Williams, B.T., Pinchbeck, B.J., Sims, L.P., Bermejo-Martínez, A., Rivera, P.P.L., Kumaresan, D., Mercadé, E., Spurgin, L.G., Carrión, O., Moxon, S., Cattolico, R.A., Kuzhiumparambil, U., Guagliardo, P., Clode, P.L., Raina, J.B. and Todd, J.D. 2018. DSYB catalyses the key step of dimethylsulfoniopropionate biosynthesis in many phytoplankton. *Nat. Microbiol.* 3, pp. 430–439.
- Dafni, Z., Ulitzer, S., and Shilo, M. 1972. Influence of light and phosphate on toxin production and growth of *Prymnesium parvum*. *J. Gen. Microbiol.* 70, (2), 199-207.
- Daims, H., Brühl, A., Amann, R., Schleifer, K.-H., and Wagner M. 1999. The domain-specific probe EUB338 is insufficient for the detection of all Bacteria: development and evaluation of a more comprehensive probe set. *Sys. and App. Microbiol.* 22:3, pp. 434–444.
- Davies, A.W. 1977. Investigations into the eutrophication of the Norfolk Broads. Anglian Water Authority, Huntingdon. In George, M. 1977. The Decline in Broadland's Aquatic Fauna and Flora: A Review of the Present Position. Transactions of the Norfolk and Norwich Naturalists Society, 24, part 2.

- Dickschat, J.S., Rabe, P. and Citron, C.A., 2015. The chemical biology of dimethylsulfoniopropionate. *Organic & biomolecular chemistry*, 13(7), pp. 1954–1968.
- Dickson, D.M.J. and Kirst, G.O. 1986. The role of β -dimethylsulphonioacetate, glycine betaine and homarine in the osmoacclimation of *Platymonas subcordiformis*. *Planta*. 167, pp. 536–43.
- Dietrich, W. and Hesse, J. K. 1990. Local fish kill in a pond at the German North Sea coast associated with a mass development of *Prymnesium* sp. *Meeresforsch.* 33, pp. 104–106.
- Downie, J.A. et al. 1983. Cloned nodulation genes of *Rhizobium leguminosarum* determine host range specificity. *Mol. Gen. Genet.* 190, pp. 359–365.
- Drábková, M., Admiraal, W., Maršálek, B. 2007. Combined Exposure to Hydrogen Peroxide and Light Selective Effects on Cyanobacteria, Green Algae, and Diatoms. *Environ. Sci. Technol.* 41, pp. 309–314.
- Driscoll, W.W., Espinosa, N.J., Eldakar, O.T., Hackett, J.D. 2013. Allelopathy as an emergent, exploitable public good in the bloom-forming microalga *Prymnesium parvum*. *Evolution* 67(6), pp. 1582–1590.
- Edler, L. 1979. Phytoplankton succession in the Baltic Sea. *Acta Bot. Fenn.* 110, pp. 75–78.
- Edwardsen, B. and Paasche, E. 1998. Bloom dynamics and physiology of *Prymnesium* and *Chrysochromulina* in D.M. Anderson, A.D. Cembella, G.M. Hallegraeff (Eds.), *Physiological Ecology of Harmful Algal Blooms*, Springer-Verlag, Berlin. pp. 193–208.
- Edwardsen, B. and Imai, I. 2006. The Ecology of Harmful Flagellates Within Prymnesiophyceae and Raphidophyceae. In: Granéli E, Turner JT, editors. *Ecology of Harmful Algae*. Berlin, Heidelberg: Springer. pp. 67–79.
- Environmental Agency. 2015. From a phone call to a fish rescue [Internet], [cited 15th June 2020]. <https://environmentagency.blog.gov.uk/2015/06/09/from-a-phone-call-to-a-fish-rescue/>
- Errera, R.M. and Campbell, L. 2013. Osmotic stress does trigger brevetoxin production in the dinoflagellate *Karenia brevis*. *Proc Natl Acad Sci USA* 110: E2255.
- Evans, C., Malin, G., Wilson, W. H. and Liss, P. S. 2006. Infectious titers of *Emiliania huxleyi* virus 86 are reduced by exposure to millimolar dimethyl sulfide and acrylic acid. *Limnol. Oceanogr.* 51, pp. 2468–2471.
- Evans, C., Kadner, S.V., Darroch, L.J., Wilson, W.H., Liss, P.S. and Malin, G. 2007. The relative significance of viral lysis and microzooplankton grazing as pathways of

- dimethylsulfoniopropionate (DMSP) cleavage: an *Emiliana huxleyi* culture study. *Limnol Oceanogr* 52, pp. 1036–1045.
- Eyice, Ö., Myronova, N., Pol, A. et al. 2018. Bacterial SBP56 identified as a Cu-dependent methanethiol oxidase widely distributed in the biosphere. *ISME J* 12, pp. 145–160.
- Figurski, D.H. and Helinski, D.R. 1979. Replication of an origin-containing derivative of plasmid RK2 dependant on a plasmid function provided in trans. *Proc Natl Acad Sci USA* 76: pp. 1648– 1652.
- Fistarol et al .2003. Allelopathic Effect of *Prymnesium parvum* on a Natural Plankton Community *Marine Ecology Progress Series* 255, pp. 115-125.
- Frada, M., Probert, I., Allen, M.J., Wilson, W.H. and De Vargas, C. 2008. The ‘Cheshire Cat’ escape strategy of the coccolithophore *Emiliana huxleyi* in response to viral infection. *P Natl Acad Sci USA*. 105, pp. 15944–15949.
- Freitag, M.S., Beszteri, Vogel, H., and John, U. 2011. Effects of physiological shock treatments on toxicity and polyketide synthase gene expression in *Prymnesium parvum* (Prymnesiophyceae) *Eur. J. Phycol.*, 46 (2011), pp. 193-201.
- Gage, D.A. et al., 1997. A new route for synthesis of dimethylsulphonioipropionate in marine algae. *Letters to Nature*, 387, pp. 891–894.
- Galí, M., Devred, E., Levasseur, M., Royer S.-J. and Babin M. 2015. A remote sensing algorithm for planktonic dimethylsulfoniopropionate (DMSP) and an analysis of global patterns. *Remote Sens. Environ.* 171, pp. 171–184.
- Gallego, V., Sanchez-Porro, C., Garcia, M. T., and Ventosa, A. 2006. *Roseomonas aquatica* sp. nov., isolated from drinking water. *Int. J. Syst. Evol. Microbiol.*, 56, pp. 2291- 2295.
- Galluzzi, L., Bertozzini, E., Penna, A., Perini, F., Pigalarga, A, Graneli, E, et al. 2008. Detection and quantification of *Prymnesium parvum* (Haptophyceae) by real-time PCR. *Lett Appl Microbiol.* 46, pp. 261-266.
- GEOHAB, 2001. Global Ecology and Oceanography of Harmful Algal Blooms, Science Plan. Glibert, P., and G. Pitcher (eds.). SCOR and IOC, Baltimore and Paris. p. 87.
- Ghoul, M., Minet, J., Bernard, T., Dupray, E. and Cormier, M. 1995. Marine macroalgae as a source for osmoprotection for *Escherichia coli*. *Microb. Ecol.* 30, 171–181.
- Ginzburg, B., Chalifa, I., Gun, J., Dor, I., Hadas, O. and Lev, O. 1998. DMS formation by dimethylsulfoniopropionate route in freshwater. *Environ. Sci. Technol.* 32, p. 2130.
- Glöckner, F.O., Fuchs, B., and Amann, R. 1999. Bacterioplankton composition of lakes and oceans: a first comparison based on fluorescence *in situ* hybridization. *Appl. Environ. Microbiol* 65, pp. 3721– 3726.

- Glöckner, F.O., Zaichikov, E., Belkova, N., Denissova, L., Pernthaler, J., Pernthaler, A., and Amann, R. 2000. Comparative 16S rRNA analysis of lake bacterioplankton reveals globally distributed phylogenetic clusters including an abundant group of actinobacteria. *Appl Environ Microbiol* 66, pp. 5053– 5065.
- Gonzalez, J.M., Whitman, W.B., Hodson, R.E. and Moran, M.A. 1996. Identifying numerically abundant culturable bacteria from complex communities: An example from a lignin enrichment culture. *Appl. Environ. Microbiol.* 62, pp. 4433–4440.
- Granéli, E. and Hansen, P.J. 2006. Allelopathy in Harmful Algae: A Mechanism to Compete for Resources?. In: Granéli E., Turner J.T. (eds) *Ecology of Harmful Algae. Ecological Studies (Analysis and Synthesis)*, vol 189. Springer, Berlin, Heidelberg .
- Granéli, E., Weberg, M., and Salomon, P.S. 2008. Harmful algal blooms of allelopathic microalgal species: the role of eutrophication. *Harmful Algae*, 8, pp. 94-102.
- Granéli, E., Salomon, P.S., Fistarol, G.O. 2008. The Role of Allelopathy for Harmful Algae Bloom Formation. In: Evangelista V., Barsanti L., Frassanito A.M., Passarelli V., Gualtieri P. (eds) *Algal Toxins: Nature, Occurrence, Effect and Detection. NATO Science for Peace and Security Series A: Chemistry and Biology.* Springer, Dordrecht.
- Green, J.C., Hibberd, D.J., and Pienaar R.N. 1982. The taxonomy of *Prymnesium* (Prymnesiophyceae) including a description of a new cosmopolitan species, *P. patellifera* sp. nov., and further observations on *P. parvum* N. Carter. *Brit Phycol J.* 17 pp. 363–382.
- Green, J.C., and Leadbeater, B.S.C. 1994. *The Haptophyte algae.* (London: Published for the Systematics Association by Academic Press). Pp. 134, 149.
- Green, D.H., Echavarrri-Bravo, V., Brennan, D. and Hart, M.C. 2015. Bacterial Diversity Associated with the Coccolithophorid Algae *Emiliania huxleyi* and *Coccolithus pelagicus* f. *braarudii*. *BioMed Res. Int.* 15.
- Greene, R.C. 1962. Biosynthesis of dimethyl- β -propiothetin. *J Biol Chem* 237, pp. 2251–2254.
- Grossart, H.-P. 1999. Interactions between marine bacteria and axenic diatoms (*Cylindrotheca fusiformis*, *Nitzschia laevis*, and *Thalassiosira weissflogii*) incubated under various conditions in the lab. *Aquat. Microb. Ecol.* 19, 1–11. doi: 10.3354/ame019001
- Guillard, R.R.L. 1975. Culture of phytoplankton for feeding marine invertebrates. pp 26- 60. In Smith W.L. and Chanley M.H (Eds.) *Culture of Marine Invertebrate Animals.* Plenum Press, New York, USA.
- Guo, M., Harrison, P. J. and Taylor, F. J. R. 1996. Fish kills related to *Prymnesium parvum* N. Carter (Haptophyta) in the People's Republic of China. *J. Appl. Phycol.* 1996, 8, (2), pp. 111-117.

- Haas, B.J., Papanicolaou, A., Yassour, M., Grabherr, M., Blood, P.D., Bowden, J. et. al. 2013. De novo transcript sequence reconstruction from RNA-seq using the Trinity platform for reference generation and analysis. *Nat. Protoc.*, 8, p. 1494.
- Hahn, M.W. and Schauer M., 2007 '*Candidatus Aquirestis calciphila*' and '*Candidatus Haliscomenobacter calcifugiens*', filamentous, planktonic bacteria inhabiting natural lakes. *Int J Syst Evol Microbiol.* 57, pp. 936-940.
- Hallegraeff, GM. 1993. A review of harmful algal blooms and their apparent global increase. *Phycologia.* 32, pp. 79–99.
- Hanson, A.D., Rivoal, J., Paquet, L. and Cage, D. A. 1994. Biosynthesis of 3- dimethylsulfonio-propionate in *Wollastonia biflora* (L.) DC. Evidence that S- methylmethionine is an intermediate. *Plant Physiol.* 105, pp. 103–110.
- Hatton, A.D., and Wilson, S.T. 2007. Particulate dimethylsulphoxide and dimethylsulphonio-propionate in phytoplankton cultures and Scottish coastal waters. *Aquat Sci.* 69, pp. 330–40.
- Havill, D. C., Ingold, A. and Pearson, J. 1985. Sulphide tolerance in coastal halophytes. *Vegetatio* 62, pp. 279–285.
- Hehemann, J.H., Law, A., Redecke, L. and Boraston A.B. 2014. The Structure of RdDddP from *Roseobacter denitrificans* Reveals That DMSP Lyases in the DddP-Family Are Metalloenzymes. *PLOS ONE* 9(7): e103128.
- Hems, E.S., Wagstaff, B.A., Saalbach, G. and Field, R.A. 2018. CuAAC click chemistry for enhanced detection of novel alkyne-based natural product toxins. *Chem. Commun.*, 54, p. 12234.
- Hockin, N.L., Mock, T., Mulholland, F., Kopriva, S. and Malin, G. 2012. The response of diatom central carbon metabolism to nitrogen starvation is different from that of green algae and higher plants. *Plant Physiol.* 158, pp. 299–312.
- Holdway, P.A., Watson, R.A., and Moss, B. 1978. Aspects of the ecology of *Prymnesium parvum* (Haptophyta) and water chemistry in the Norfolk Broads, England. *Freshwater Biology.* 8 (4), pp. 295-311.
- Holdway, P.A. 1978. Influences exerted by salinity on a Norfolk Broads strain of *Prymnesium parvum* (Carter), *SIL Proceedings, 1922-2010, 20:4*, pp. 2336-2340.
- Holman, I.P. and Hiscock, K.M. 1993. Investigation of salinity in the River Thurne Catchment of North-East Norfolk. *Anglian Region Operational Investigation OI 535/1/A*.
- Howard, E.C., Henriksen, J. R., Buchan, A., Reisch, C. R., Bürgmann, H., Welsh, R., et al. 2006. Bacterial taxa that limit sulfur flux from the ocean. *Science* 314, pp. 649–652.

- Howard, E.C., Sun, S., Biers, E. J. and Moran, M. A. 2008. Abundant and diverse bacteria involved in DMSP degradation in marine surface waters. *Environ. Microbiol.* 10, pp. 2397–2410.
- Huisman, J., Matthijs, H.C.P., and Visser, P.M.. 2005. Harmful cyanobacteria. Springer, Dordrecht, Netherlands.
- Hunter, P.D., Tyler, A.N., Willby, N.J. and Gilvear, D.J. 2008. The spatial dynamics of vertical migration by *Microcystis aeruginosa* in a eutrophic shallow lake: A case study using high spatial resolution time-series airborne remote sensing *Limnol. Oceanogr.*, 53(6), 2008, pp. 2391–2406.
- Husband, J. D., Kiene, R. P., and Sherman, T. D. 2012. Oxidation of dimethylsulfoniopropionate (DMSP) in response to oxidative stress in *Spartina alterniflora* and protection of a non-DMSP producing grass by exogenous DMSP + acrylate. *Environ. Exp. Bot.* 79, pp. 44–48.
- Igarashi, T., Satake, M. and Yasumoto, T. 1996. Pymnesin-2: A potent ichthyotoxic and hemolytic glycoside isolated from the red tide alga *Prymnesium parvum*. *J. Am. Chem. Soc.* 118, (2), pp. 479-480.
- Igarashi, T, Satake, M, Yasumoto, T. 1999. Structures and partial stereochemical assignments for pymnesin-1 and pymnesin-2: Potent ichthyotoxic and hemolytic glycosides isolated from the red alga *Prymnesium parvum*. *J Am Chem Soc.* 121, pp. 8499–8511.
- Irvine, K., Moss, B., Bales, M., and Snook, D. 1993. The changing ecosystem of a shallow, brackish lake, Hickling Broad, Norfolk, UK I: Trophic relationships with special reference to the role of *Neomysis integer*. *Freshwater Biology*, 29, pp. 119– 139.
- James, F., Pacqut, L., Sparace, S. A., Gage, D. A. and Hanson, A. D. 1995. Evidence implicating dimethylsulfoniopropionaldehyde as an intermediate in dimethylsulfoniopropionate biosynthesis. *Plant Physiol.* 108, 1439–1448.
- Jiang, C-Y., Dai, X., Wang, B-J., Zhou, Y-G., and Liu, S-J. 2006. *Roseomonas lacus* sp. nov., isolated from freshwater lake sediment. *Int. J. Syst. Evol. Microbiol.*, 56, pp. 25- 28.
- Jiao, N.Z., Liu, C.Z., Hong H.S., Harada, S., Koshikawa H., and Watanabe, M. 2003. Dynamics of dimethylsulfide and dimethylsulfoniopropionate produced by phytoplankton in the Chinese seas — distribution patterns and affecting factors. *Acta Bot. Sin.*, 45(7), pp. 774–786.
- Johansson, N. and Granéli, E. 1999. Influence of different nutrient conditions on cell density, chemical composition and toxicity of *Prymnesium parvum* (Haptophyta) in semi-continuous cultures. *J. Exp. Mar. Biol. Ecol.* 239, (2), pp. 243-258.

- John, U., Beszteri, B., Derelle, E., Van de Peer, Y., Read, B., Moreau, H. and Cembella, A. 2008. Novel insights into evolution of protistan polyketide synthases through phylogenomic analyses. *Protist* 159, pp. 21–30
- Johnsen, G., Volent, Z., Tangen, K., and Sakshaug, E. 1997. Timeseries of harmful and benign phytoplankton blooms in the northwest European waters using the seawatch buoy system. In: Kahru M, Brown CW (eds) *Monitoring algal blooms: new techniques for detecting large-scales environmental change*. Landes Bioscience, Austin, TX. p 113 – 139.
- Johnston, A.W.B, Green, R.T. and Todd, J.D. 2016. Enzymatic breakage of dimethylsulfoniopropionate—a signature molecule for life at sea. *Curr Opin Chem Biol* 31, pp. 58–65.
- Johnston, A.W.B, Todd, J.D., Sun, L., Nikolaidou-Katsaridou, M.N., Curson, A.R.J. and Rogers, R. 2008. Molecular diversity of bacterial production of the climate-changing gas, dimethyl sulphide, a molecule that impinges on local and global symbioses, *J. of Exp. Botany*, Vol. 59: 5: pp. 1059–1067.
- Kaartvedt, S., Johnsen, T. M. Aksnes, D. L. Lie, U. and Svendsen, H. 1991. Occurrence of the toxic phytoflagellate *Prymnesium parvum* and associated fish mortality in a Norwegian fjord system. *Can. J. Fish. Aquat. Sci.* 48, (12), pp. 2316-2323.
- Kageyama, H., Tanaka, Y., Shibata, A., Waditee-Sirisattha, R. and Takabe, T. 2018. Dimethylsulfoniopropionate biosynthesis in a diatom *Thalassiosira pseudonana*: Identification of a gene encoding MTHB-methyltransferase. *Arch. Biochem. Biophys.* 645, pp. 100–106.
- Karsten, U., Kuck K., Vogt, C., and Kirst, G.O. 1996. “Dimethylsulphoniopropionate production in phototrophic organisms and its physiological function as a cryoprotectant,” in *Biological and Environmental Chemistry of DMSP and Related Sulphonium Compounds* eds Kiene R. P., Visscher P. T., Keller M. D., Kirst G. O. (New York, NY: Plenum Press) pp. 143–153.
- Keen, N. T., Tamaki, S., Kobayashi, D. and Trollinger, D. 1988. Improved broad-host-range plasmids for DNA cloning in Gram-negative bacteria. *Gene* 70, pp. 191–197.
- Keller, M.D., Bellows, W.K. and Guillard, R.R.L., 1989. Dimethyl Sulfide Production in Marine Phytoplankton. *Biogenic Sulfur in the Environment*, pp.167–182.
- Keller, M.D., Kiene R.P., Matrai P.A., and Bellows, W.K. 1999. Production of glycine betaine and dimethylsulfoniopropionate in marine phytoplankton. II. N-limited chemostat cultures. *Mar. Biol.* 135, pp. 249–257.

- Kettle, A.J. et al., 1999. A global data base of sea surface dimethyl sulfide (DMS) measurements and a simple model to predict sea surface DMS as a function of latitude, longitude, and month. *Global Biogeochem. Cycles*, 13(2), pp. 399–444.
- Kettle, A.J. and Andreae, M.O., 2000. Flux of dimethylsulfide from the oceans: A comparison of updated data sets and flux models. *Journal of Geophysical Research*, 105, p.26,793-26,808.
- Kettles, N.L., Kopriva, S., and Malin, G. 2014. Insights into the regulation of DMSP synthesis in the diatom *Thalassiosira pseudonana* through APR activity, proteomics and gene expression analyses on cells acclimating to changes in salinity, light and nitrogen. *PLoS One*.
- Khan, S.T., Fukunaga, Y., Nakagawa, Y., and Harayama, S. 2007. Emended descriptions of the genus *Lewinella* and of *Lewinella cohaerens*, *Lewinella nigricans* and *Lewinella persica*, and description of *Lewinella lutea* sp. nov. and *Lewinella marina* sp. nov. *Int J Syst Evol Microbiol.* 57, pp. 2946-51.
- Kiene, R.P. 1996. Production of methanethiol from dimethylsulfoniopropionate in marine surface waters, *Marine Chemistry*, Vol. 54, Issues 1–2, pp. 69-83.
- Kiene, R.P., Visscher, P.T., Keller, M.D., and Kirst, G.O. 1997. Biological and environmental chemistry of DMSP and related sulfonium compounds. Plenum Press.
- Kiene, R.P. and Linn, L.J. 2000. Distribution and turnover of dissolved DMSP and its relationship with bacterial production and dimethylsulfide in the Gulf of Mexico. *Limnol. Oceanogr.*, 45, pp. 849–861.
- Kiene, R.P. and Linn L.J. 2000. The fate of dissolved dimethylsulfoniopropionate (DMSP) in seawater: tracer studies using ³⁵S-DMSP. *Geochim. Cosmochim. Acta* 64, pp. 2797–2810.
- Kinsey, J. D., Kieber, D. J. and Neale, P. J. 2016. Effects of iron limitation and UV radiation on *Phaeocystis antarctica* growth and dimethylsulfoniopropionate, dimethylsulfoxide and acrylate concentrations, *Environ. Chem.*, 13, pp. 195–211.
- Kirst, G.O., Thiel, C., Wolff, H., Nothnagel, J., Wanzek, M. and Ulmke R. 1990. Dimethylsulfoniopropionate (DMSP) in ice algae and its possible biological role. *Mar. Chem.* 35, pp. 381–388.
- Kirkwood, M. et al., 2010. The dddP gene of *Roseovarius nubinhibens* encodes a novel lyase that cleaves dimethylsulfoniopropionate into acrylate plus dimethyl sulfide. *Microbiology*, 156(Pt 6), pp. 1900–6.

- Kocsis, M.G., Nolte, K. D., Rhodes, D., Shen, T. L., Gage, D. and Hanson, D. 1998. Dimethylsulfoniopropionate biosynthesis in *Spartina alterniflora*. Evidence that S-methylmethionine and dimethylsulfoniopropylamine are intermediates. *Plant Physiol.* 117, pp. 273–281.
- Kocsis, M.G. and Hanson, A.D. 2000. Biochemical evidence for two novel enzymes in the biosynthesis of 3-dimethylsulfoniopropionate in *Spartina alterniflora*. *Plant Physiol.* 123, pp. 1153–1161.
- Kodama, M., Doucette, G. and Green D. 2006. Relationships between bacteria and harmful algae. In: Granéli E, Turner JT, editors. *Ecology of Harmful Algae*. 1st Ed. Springer; Berlin: 2006. pp. 243–255.
- Kozakai, H., Oshima, Y. and Yasumoto, T. 1982. Isolation and structural elucidation of hemolysin from the phytoflagellate *Prymnesium parvum*. *Agric. Biol. Chem.* 46, pp. 233-236.
- Kumar, S.S., Chinchkar, U., Nair, S., Bharathi, P.A.L., and Chandramohan, D. 2009. Seasonal dimethylsulfoniopropionate (DMSP) variability in Dona Paula bay. *Estuar. Coast. Shelf Sci.*, 81, pp. 301–310.
- Lane, D. J. et al. 1985. Rapid determination of 16S ribosomal RNA sequences for phylogenetic analyses. *Proc. Natl Acad. Sci. USA* 82, pp. 6955–6959.
- Larsen, A. and Edvardsen, B. 1998. Relative ploidy levels in *Prymnesium parvum* and *P. patelliferum* (Haptophyta) analyzed by flow cytometry. *Phycologia*. 37, (6), pp. 412-424.
- Larsen, A. and Medlin, L. K. 1997. Inter- and intraspecific genetic variation in twelve *Prymnesium* (haptophyceae) clones. *J. Phycol.* 33, (6), pp. 1007-1015.
- Larsen, A., Eikrem, W. and Paasche, E. 1993. Growth and toxicity in *Prymnesium patelliferum* (Prymnesiophyceae) isolated from Norwegian waters. *Can. J. Bot.* 71, (10), pp. 1357-1362.
- Lau, S.S.S. and Lane, S.N. 2002. Biological and chemical factors influencing shallow lake eutrophication: a long-term study. *Sci. Total Environ.*, 288: pp. 167-181.
- Leah, R.T., Moss, B. and Forrest, D. E. 1978. Experiments with large enclosures in a fertile, shallow, brackish lake, Hickling Broad, Norfolk, United Kingdom. *Int. Rev. ges. Hydrobiol.*
- Lee, R. E. 1980. *Phycology*. Cambridge University Press, Cambridge. pp. 478.
- Legrand, C.N., Johansson, G., Johnsen, K.Y., Borsheim and Granéli, E. 2001. Phagotrophy and toxicity variation in the mixotrophic *Prymnesium patelliferum* (Haptophyceae) *Limnol. Oceanogr.*, 46, pp. 1208-1214.

- Levine, N. M., Varaljay, V. A., Toole, D. A., Dacey, J. W., Doney, S. C., and Moran, M. A. 2012. Environmental, biochemical and genetic drivers of DMSP degradation and DMS production in the Sargasso Sea, *Environ. Microbiol.*, 14, pp. 1210–1223.
- Liebert, F. and Deerns, W. M. 1920. Onderzoek naar de oorzaak van een vischsterfte in den Polder Workumer-Nieuwland. 1, 6.
- Lindehoff, E., Granéli, E. and Granéli, W. 2009. Effect of tertiary sewage effluent additions on *Prymnesium parvum* cell toxicity and stable isotope ratios, *Harmful Algae*, 8:2, pp. 247-253.
- Lindholm, T., Öhman, P., Kurki-Helasma, K., Kincaid, B., and Meriluoto, J. 1999. Toxic algae and fish mortality in a brackish-water lake in Åland, SW Finland. *Hydrobiologia*. 397, pp. 109-120.
- Litchman, E. 2010. Invisible invaders: Non-pathogenic invasive microbes in aquatic and terrestrial ecosystems. *Ecol Lett* 13(12), pp. 1560–1572.
- Living Lakes Partnership. 1998-2005. Global Nature fund
<https://www.globalnature.org/en/living-lakes/europe/broads>
- Liu Z., Koid A., Terrado R., Campbell V., Caron D., Heidelberg K. 2015. Changes in gene expression of *Prymnesium parvum* induced by nitrogen and phosphorus limitation. *Frontiers in Microbiology*. Vol. 6: 631.
- Lutz-Carrillo, D.J., Southard, G.M. and Fries, L.T.. 2010. Global genetic relationships among isolates of golden alga (*Prymnesium parvum*). *J Am Water Resour Assoc.* 46(1): pp. 24–32.
- Malmstrom, R.R., Kiene, R.P., Cotrell, M.T. and Kirchman, D.L. 2004. Contribution of SAR11 Bacteria to Dissolved Dimethylsulfoniopropionate and Amino Acid Uptake in the North Atlantic Ocean. *App. and Env. Micro.*, 70(7), pp.4129–4135.
- Malmstrom, R.R., Kiene, R.P., Vila, M., and Kirchman, D.M. 2005. Dimethylsulfoniopropionate (DMSP) assimilation by *Synechococcus* in the Gulf of Mexico and northwest Atlantic Ocean. *Limnology and Oceanography*, 50(6), pp.1924–1931.
- Manning, S.R. and La Claire, J.W. II. 2010. Prymnesins: Toxic Metabolites of the Golden Alga, *Prymnesium parvum* Carter (Haptophyta). *Mar. Drugs*. 8, pp. 678-704.
- Manning, S.R. and La Claire, J. W. 2013. Isolation of polyketides from *Prymnesium parvum* (Haptophyta) and their detection by liquid chromatography/mass spectrometry metabolic fingerprint analysis. *Anal. Biochem.* 442, (2), pp. 189-195.

- Manz, W., R. Amann, W. Ludwig, M. Wagner, K.-H. Schleifer. 1992. Phylogenetic oligodeoxynucleotide probes for the major subclasses of proteobacteria: problems and solutions. *Syst. Appl. Microbiol.*, 15 (1992), pp. 593-600
- Mardones, J.I., Shabala, L., Shabala, S., Dorantes-Aranda, J.J., Seger, A. & Hallegraeff, G.M. 2018. Fish gill damage by harmful microalgae newly explored by microelectrode ion flux estimation techniques. *Harmful Algae*, 80, pp. 55-63.
- Matthijs, H. C., Visser, P. M., Reeze, B., Meeuse, J., Slot, P. C., Wijn, G., Talens, R., Huisman, J. 2012. Selective suppression of harmful cyanobacteria in an entire lake with hydrogen peroxide. *Water Res.* 46, (5), pp. 1460-72.
- McLaughlin, J. J. A. 1958. Euryhaline Chrysomonads: nutrition and toxigenesis in *Prymnesium parvum*, with notes on *Isochrysis galbana* and *Monochrysis lutheri*. *J. Protozool.* 5, (1), 75-81.
- Meldahl A.S., Kvernstuen J., Grasbakken G.J., Edvardsen B., Fonnum F. 1995. Toxic Activity of *Prymnesium* spp. and *Chrysochromulina* spp. tested by different test methods. In: Lassus P., Arzul G., Erard-Le Denn E., Gentien P., Marcaillou-Le Baut C., editors. *Harmful Marine Algal Blooms: Proceedings of the Sixth International Conference on Toxic Marine Phytoplankton*; Nantes, France. October 1993; New York, NY, USA: Springer-Verlag; 1995. pp. 315–320.
- Michaloudi, E., Moustaka-Gouni, M., Gkelis, S. and Pantelidakis, K. 2009. Plankton community structure during an ecosystem disruptive algal bloom of *Prymnesium parvum*. *J. Plankton Res.* 31, (3), pp. 301-309.
- Moestrup, Ø., Akselman, R., Cronberg, G., Elbraechter, M., Fraga, S. et al. (Eds), 2009. IOC-UNESCO Taxonomic Reference. List of Harmful Micro Algae. <http://www.marinespecies.org/HAB>.
- Moss, B. 1978. The ecological history of a mediaeval man-made lake. Hickling Broad, Norfolk, United Kingdom. *Hydrobiologia* 60, pp. 23–32.
- Moss, B. 2001. *The Broads The People's Wetland*. The New Naturalist. Harper Collins Publishers, London.
- Moss, B., and Leah, R. T. 1982. Changes in the ecosystem of a guanotrophic and brackish shallow lake in eastern England: Potential problems in its restoration. *Internationale Revue der gesamten Hydrobiologie*, 67, pp. 625– 659.
- Nature Conservancy. 1965. Report on Broadland. London, HMSO.
- Newton, R.J., Jones S. E., Eiler, A., McMahon, K. D. and Bertilsson S. 2011. A guide to the natural history of freshwater lake bacteria. *Microbiol. Mol. Biol. Rev.* 75, 14–49.

- Nicholls, K.H. 2003. Haptophyte Algae. In: Wehr JD, Sheath RG, editors. *Freshwater Algae of North America*. Boston: Academic Press. pp. 511–521.
- Niki, T., Kunugi, M., and Otsuki, A. (2000). DMSP-lyase activity in five marine phytoplankton species: its potential importance in DMS production. *Mar. Biol.* 136, 759–764.
- Nygaard, K. And A. Tobiesen. 1993. Bacterivory in algae: A survival strategy during nutrient limitation. *Limnology and Oceanography* 38 (2), pp. 273-279.
- Paster, Z. K. 1973. Pharmacology and mode of action of prymnesin. Academic Press: NY. pp. 241-263.
- Paerl, H.W., Otten, T.G. and Kudela R. 2018. Mitigating the expansion of harmful algal blooms across the freshwater-to-marine continuum. *Environ. Sci. Technol.*, 52 (10), pp. 5519-5529.
- Phillips, G. and Jackson, R. 1990. The control of eutrophication in very shallow lakes, the Norfolk Broads, *SIL Proceedings, 1922-2010*, 24:1, pp. 573-575.
- Phillips, G., Kelly A., Pitt J.-A., Sanderson R. and Taylor E. 2005. The recovery of a very shallow eutrophic lake, 20 years after the control of effluent derived phosphorus. *Freshwater Biology*, 50.
- Pichereau, V., Pocard, J. A., Hamelin, J., Blanco, C. & Bernard, T. 1998. Differential effects of dimethylsulfoniopropionate, dimethylsulfonioacetate, and other S- methylated compounds on the growth of *Sinorhizobium meliloti* at low and high osmolarities. *Appl. Environ. Microbiol.* 64, 1420–1429.
- Place, A.R., Bowers, H.A., Bachvaroff, T.R., Adolf, J.E., Deeds, J.R. and Sheng, J. 2012. *Karlodinium veneficum* – the little dinoflagellate with a big bite. *Harmful Algae*, 14 (2012), pp. 179-195.
- Platt, U. and Le Bras, G. 1997. Influence of DMS on Ox-NO_y partitioning and the NO_x distribution in the marine background atmosphere. *Geophysical Res Letters* 24, pp.1935-1938.
- Porter, K.G. and Feig, Y.S. 1980. The use of DAPI for identifying and counting aquatic microflora. *Limnol. Oceanogr.* 25, pp. 943–948.
- Prescott, G. W. 1968. *The algae: A review*. Houghton Mifflin Co., Boston. pp. 436.
- Rahat, M. and Jahn, T.L. 1965. Growth of *Prymnesium parvum* in the dark: Note on ichthyotoxin formation. *J Protozool.* 12, pp. 246–250.
- Raina, J.-B. Tapiolas, D., Forêt, S. et al. 2013. DMSP biosynthesis by an animal and its role in coral thermal stress response. *Nature*, 502(7473), pp.677–80.

- Ramanan, R., Byung-Hyuk Kim, Dae-Hyun Cho, Hee-Mock Oh, Hee-Sik Kim, 2016. Algae–bacteria interactions: Evolution, ecology and emerging applications, *Biotechnology Advances*. Volume 34, Issue 1, pp. 14-29.
- Rashidan, K.K. and Bird, D.F. 2001. Role of predatory bacteria in the termination of a cyanobacterial bloom. *Microb. Ecol.* 41, pp. 97– 105.
- Rasmussen, S. A. Meier, S. Andersen, N. G. Blossom, H. E. Duus, J. Ø. Nielsen, K. F.; Hansen, P. J. Larsen, T.O. 2016. Chemodiversity of ladder-frame prymnesin polyethers in *Prymnesium parvum*. *J. Nat. Prod.* 2016, 79, (9), 2250-2256.
- Reisch, C.R., Stoudemayer, M.J., et al., 2011. Novel pathway for assimilation of dimethylsulphoniopropionate widespread in marine bacteria. *Nature*, 473(7346), pp.208–11.
- Reisch, C.R., Moran, M.A. and Whitman, W.B. 2011. Bacterial Catabolism of Dimethylsulfoniopropionate (DMSP). *Frontiers in microbiology*, 2(August), p.172.
- Rezayian, M., Niknam, V. and Ebrahimzadeh, H. 2019. Oxidative damage and antioxidative system in algae. *Toxicology Reports*. 6, pp. 1309-1313.
- Rhodes, D. et al., 1997. S-Methylmethionine Conversion to Dimethylsulfoniopropionate: Evidence for an Unusual Transamination Reaction. *Plant physiology*, 115, pp. 1541–1548.
- Rhodes, D., Gage, D., Cooper, A. and Hanson, D. 1997. S-Methylmethionine conversion to dimethylsulfoniopropionate: evidence for an unusual transamination reaction. *Plant Physiol.* 115, pp. 1541–1548.
- Riquelme, C.E., Fukami, K. and Ishida, Y. 1988. Effects of bacteria on the growth of a marine diatom, *Asterionella glacialis*. *Bull Jpn Soc Microb Ecol* 3, pp. 29–34
- Roberts, L.R., Sayer, C.D., Hoare, D., Tomlinson, M., Holmes, J.A., Horne, D.J., and Kelly, A. 2019. The role of monitoring, documentary and archival records for coastal shallow lake management. *Geo: Geography and Environment*. e00083.
- Roelke, D. L., Errera, R. M., Kiesling, R., Brooks, B. W., Grover, J. P., Schwierzke, L., Urena-Boeck, F., Baker, J. and Pinckney, J. L. 2007. Effects of nutrient enrichment on *Prymnesium parvum* population dynamics and toxicity: results from field experiments, Lake Possum Kingdom, USA. *Aquat. Microb. Ecol.* 46, (2), pp. 125-140.
- Roelke, D.L., Gable, G.M., Valenti, T. W., Grover, J.P., Brooks, B.W., and Pinckney, J.L. 2010. Hydraulic flushing as a *Prymnesium parvum* bloom-terminating mechanism in a subtropical lake. *Harmful Algae*, 9 (3), 323–332.

- Roelke, D.L., Barkoh, A., Brooks, B. W., Grover, J. P., Hambright, K. D., LaClaire, J. W. Moeller, P. D. R. and Patino, R. 2016. A chronicle of a killer alga in the west: ecology, assessment, and management of *Prymnesium parvum* blooms. *Hydrobiologia*. 764, (1), pp. 29-50.
- Rusch, D.B., Halpern, A.L., Sutton, G., Heidelberg, K.B., Williamson, S., et al. 2007. The Sorcerer II Global Ocean Sampling Expedition: Northwest Atlantic through Eastern Tropical Pacific. *PLoS Biol* 5: e77
- Sabour, B; Loudiki, LM; Oudra, B; Oubraim, S; Fawzi, B; Fadlaoui, S; Chlaida, M; Vasconcelos, V. Blooms of *Prymnesium parvum* associated with fish mortalities in a hyper eutrophic brackish lake in Morocco. In *Harmful Algae: An IOC Newsletter on Toxic Algae and Algal Blooms*; Wyatt, T, Ed.; IOC: Vigo, Spain, 21.
- Sambrook, J., Fritsch, E.F., Maniatis, T., and Nolan, C. 1989. *Molecular Cloning: A Laboratory Manual*. 3, Cold Spring Harbor Laboratory Press.
- Schoemann, V., Becquevort, S., Stefels, J., Rousseau, V. and Lancelot, C. 2005. *Phaeocystis* blooms in the global ocean and their controlling mechanisms: A review. *J. Sea Res.* 53, pp. 43-66.
- Schönhuber, W., Zarda, B., Eix, S., Rippka, R., Herdman, M., Ludwig, W. and Amann, R. 1999. *In situ* identification of Cyanobacteria with horseradish peroxidase-labeled, rRNA-targeted oligonucleotide probes. *Applied and Environmental Microbiology*. 65, pp. 1259–1267.
- Schreiber, U., Schliwa, U. and Bilger, W. 1986. Continuous recording of photochemical and non-photochemical chlorophyll fluorescence quenching with a new type of modulation fluorometer. *Photosynth Res.* 10 (1-2), pp. 51-62.
- Seibold, A., Wichels, A. and Schutt, C. 2001. Diversity of endocytic bacteria in the dinoflagellate *Noctiluca scintillans*. *Aquatic Microbial Ecology* 25, pp. 229-235.
- Seger, A., Dorantes-Aranda, J.J., Müller, M.N., Body, A., Peristyy, A., Place, A.R., Park, T.G., and Hallegraeff, G. 2015. Mitigating Fish-Killing *Prymnesium parvum* Algal Blooms in Aquaculture Ponds with Clay: The Importance of pH and Clay Type. *J. Mar. Sci. Eng.* 2015, 3, pp. 154-174.
- Sela-Adler, M., Said-Ahmad, W., Sivan, O., Eckert, W., Kiene, R.P. and Amrani, A. 2016. Isotopic evidence for the origin of dimethylsulfide and dimethylsulfoniopropionate-like compounds in a warm, monomictic freshwater lake. *Environ Chem* 13, pp. 340–351.
- Serfling, R. E. 1949. Quantitative estimates of plankton from small samples of Sedgwick-Rafter cell mounts of concentrate samples. *Trans. Am. Microsc. Soc.* 68, pp. 185–199.

- Seymour, J. R., Simó, R., Ahmed, T. and Stocker, R. 2010. Chemoattraction to dimethylsulfonio-propionate throughout the marine microbial food web. *Science* 329, pp. 342–346.
- Seymour, J. R. 2014. A sea of microbes: the diversity and activity of marine microorganisms. *Microbiology Australia* 35, pp. 183-187.
- Seymour, J. R., Amin, S. A., Raina, J. B. and Stocker, R. 2015. Zooming in on the phycosphere: the ecological interface for phytoplankton–bacteria relationships. *Nat. Microbiol.* 2, p. 17065.
- Sherr, E.B., and Sherr, B.F. 1993. Preservation and storage of samples for enumeration of heterotrophic protists, p. 207-212. In P. F. Kemp, B. F. Sherr, E. B. Sherr, and J. J. Cole (ed.), *Handbook of methods in aquatic microbial ecology*. Lewis Publishers, London, United Kingdom.
- Shilo, M. 1967. Formation and mode of action of algal toxins. *Bacteriol Rev.* 31, pp. 180–193.
- Shilo, M. and Aschner, M. 1953. Factors governing the toxicity of cultures containing the phytoflagellate *Prymnesium parvum* Carter. *J. Gen. Microbiol.* 8, (3), pp. 333-343.
- Sievert, S.M., Kiene, R. P. and Schulz-Vogt, H. N. 2007. The sulfur cycle. *Oceanography* 20(2), pp. 117–123.
- Šimek, K., Hornak, J., Jezbera, J., Nedoma, P. Znachor, J., Hejzlar, J. and Seda, J. 2008. Spatio-temporal patterns of bacterioplankton production and community composition related to phytoplankton composition and protistan bacterivory in a dam reservoir. *Aquat. Microb. Ecol.* 51, pp. 249–262.
- Simó, R. 2001. Production of atmospheric sulfur by oceanic plankton: Biogeochemical, ecological and evolutionary links, *Trends Ecol. Evol.*, 16, pp. 287– 294.
- Simó, R. et al., 2009. Annual DMSP contribution to S and C fluxes through phytoplankton and bacterioplankton in a NW Mediterranean coastal site. *Aquatic Microbial Ecology*, 57, pp. 43–55.
- Skovgaard, A. and Hansen, P.J. 2003. Food uptake in the harmful alga *Prymnesium parvum* mediated by excreted toxins. *Limnol. Oceanogr.*, 48, pp. 1161-1166
- Slezak, D.M., Puskaric, S. & Herndl, G.J., 1994. Potential role of acrylic acid in bacterioplankton communities in the sea. *Marine Ecology Progress Series*, 105(1–2), pp.191–198.
- Smayda, T.J. 1997. Harmful algal blooms: Their ecophysiology and general relevance to phytoplankton blooms in the sea. *Limnology and Oceanography*, 42(5), pp. 1137– 1153.
- Smayda, T.J. 2008. Complexity in the eutrophication-harmful algal bloom relationship, with comment on the importance of grazing. *Harmful Algae* 8, pp. 140-151

- Stefels, J. and van Boekel, W. H. M. 1993. Production of DMS from dissolved DMSP in axenic cultures of the marine phytoplankton species *Phaeocystis* sp. *Mar Ecol Prog Ser* 97, pp. 11-18.
- Stefels, J. 2000. Physiological aspects of the production and conversion of DMSP in marine algae and higher plants *J. Sea Res.*, 43 (3), pp. 183-197
- Stefels, J., Steinke, M., Turner, S., Malin, G. and Belviso, S. 2007. Environmental constraints on the production and removal of the climatically active gas dimethylsulphide (DMS) and implications for ecosystem modeling. *Biogeochem.*, 83, pp. 245–275.
- Strom, S. et al., 2003. Chemical defense in the microplankton I: Feeding and growth rates of heterotrophic protists on the DMS-producing phytoplankton *Emiliania huxleyi*. *Limnology and Oceanography*, 48(1), pp.217–229.
- Spielmeier, A. and Pohnert, G. 2012. Influence of temperature and elevated carbon dioxide on the production of dimethylsulfoniopropionate and glycine betaine by marine phytoplankton. *Mar Environ Res* 73, pp. 62–69.
- Suikkanen, S., Kremp, A., Hautala, H. and Krock, B. 2013. Paralytic shellfish toxins or spirolides? The role of environmental and genetic factors in toxin production of the *Alexandrium ostenfeldii* complex. *Harmful Algae*, 26, pp. 52-59.
- Summers, P.S. et al., 1998. Identification and Stereospecificity of the First Three Enzymes of 3-Dimethylsulfoniopropionate Biosynthesis in a Chlorophyte Alga 1. In *Plant Physiology*. pp. 369–378.
- Sun, H., Zhang, Y., Tan, S., Zheng, Y., Zhou, S., Ma, Q., Yang, G.-P., Todd, J.D. and Zhang, X-H. 2020. DMSP-Producing Bacteria Are More Abundant in the Surface Microlayer than Subsurface Seawater of the East China Sea. *Microbial Ecology*.
- Sun, L., Curson, A. R. J., Todd, J. D. and Johnston, A. W. B. 2012. Diversity of DMSP transport in marine bacteria, revealed by genetic analyses. *Biogeochemistry* 110, pp. 121–130.
- Sun J., Todd J.D., Thrash J.C., Qian Y., Qian M.C., Temperton B., Guo J., Fowler E.K., Aldrich J.T., Nicora C.D., Lipton M.S., Smith R.D., De Leenheer P., Payne S.H., Johnston A.W., Davie-Martin C.L., Halsey K.H., Giovannoni S.J. 2016. The abundant marine bacterium *Pelagibacter* simultaneously catabolizes dimethylsulfoniopropionate to the gases dimethyl sulfide and methanethiol. *Nat Microbiol* 1, p. 16065.
- Sunda, W., Kieber, D. J., Kiene, R.P., and Huntsman, S. 2002. An antioxidant function for DMSP and DMS in marine algae. *Nature*. 418, pp. 317–320.

- Sunda, W.G., Hardison, R., Kiene, R.P., Bucciarelli, E., and Harada, H. 2007. The effect of nitrogen limitation on cellular DMSP and DMS release in marine phytoplankton: climate feedback implications. *Aquat Sci* 69, pp. 341-351.
- Svenssen, D.K., Binzer, S.B., Medić, N., Hansen, P.J., Larsen, T.O. and Varga, E. 2019. Development of an Indirect Quantitation Method to Assess Ichthyotoxic B-Type Pymnesins from *Pymnesium parvum*. *Toxins*. 11, p. 251.
- Tett, A. J., Rudder, S. J., Bourdes, A., Karunakaran, R. and Poole, P. S. 2012. Regulatable vectors for environmental gene expression in Alphaproteobacteria. *Appl. Environ. Microbiol.* 78, pp. 7137–7140.
- Tillmann, U. 2004. Interactions between planktonic microalgae and protozoan grazers. *J. Eukaryot. Microbiol.* 2004, 51, (2), pp. 156-68.
- Tillmann, U. 2003. Kill and eat your predator: A winning strategy of the planktonic flagellate *Pymnesium parvum*. *Aquat Microb Ecol.* 32, pp. 73–84.
- Thierstein, H.R. and Young, J.R. 2004. Coccolithophores-from molecular processes to global impact. (Berlin: Springer). pp. 127-141.
- Thronsdon, J. 1978. Preservation and storage. In A. Sournia (ed.), *Phytoplankton manual*. UNESCO, Paris, France. pp. 69-74.
- Thume, K., Gebser B., Chen, L., Meyer, N., Kieber, D.J., Pohnert, G. 2018. The metabolite dimethylsulfoxonium propionate extends the marine organosulfur cycle. *Nature*. 563(7731), pp. 412-415.
- Todd, J.D., Curson, A.R.J., Dupont, C.L., Nicholson, P., Johnston, A.W.B. 2009. The dddP gene, encoding a novel enzyme that converts dimethylsulfoniopropionate into dimethyl sulfide, is widespread in ocean metagenomes and marine bacteria and also occurs in some Ascomycete fungi. *Environ Microbiol* 11, pp. 1376–1385.
- Todd, J.D. et al., 2007. Structural and regulatory genes required to make the gas dimethyl sulfide in bacteria. *Science (New York, N.Y.)*, 315(5812), pp.666–9.
- Tripp, H.J. et al., 2008. SAR11 marine bacteria require exogenous reduced sulphur for growth. *Nature*, 452(7188), pp.741–744.
- Uchida, A., Ooguri, T., Ishida, T., Kitaguchi, H. and Ishida, Y. 1996. Biosynthesis of dimethylsulfoniopropionate in *Cryptocodinium cohnii* (Dinophyceae). in Kiene, R.P., Visscher, P.T., Keller, M.D., Kirst, G.O. (Eds.). *Biological and Environmental Chemistry of DMSP and Related Sulfonium Compounds*, Plenum Press, New York, pp. 97–107.

- Ulf Karsten, G.O. and Kirst, C. 1992. Dimethylsulphoniopropionate (DMSP) accumulation in green macroalgae from polar to temperate regions: interactive effects of light versus salinity and light versus temperature. *Polar Biol.*, 12 (6–7), pp. 603-607.
- Ulitzur, S. and Shilo, M. 1964. A sensitive assay system for determination of the ichthyotoxicity of *Prymnesium parvum*. *J. Gen. Microbiol.* 36, (2), 161-169.
- UNESCO 2011. Understanding Harmful Algal Bloom Phenomena and Mitigating Risk. Tenth Session of the IOC Intergovernmental Panel on Harmful Algal Blooms, IOC, UNESCO, Paris, 12-14 April 2011 (accessed online unesco.org).
- Utermöhl, H. 1958. Zur Vervollkommnung der quantitativen Phytoplankton-Methodik. *Mitteilungen Internationale Vereinigung Theoretische und Angewandte Limnologie* 9, pp. 1–38.
- Vairavamurthy, A., Andreae, M.O. and Iverson, R.L. 1985. Biosynthesis of dimethylsulfide and dimethylpropiothetin by *hymenomonas carterae* in relation to sulfur source and salinity variations. *Limnol. Oceanogr.*, 30, pp. 1 59-70.
- Vallina, S.M. and Simó, R. 2007. Strong relationship between DMS and the solar radiation dose over the global surface ocean. *Science*. 315(5811), pp. 506-508.
- Van Hannen, E.J., Zwart, G., Van Agterveld, M.P., Gons, H.J., Ebert, J., and Laanbroek, H.J. 1999. Changes in bacterial and eukaryotic community structure after mass lysis of filamentous cyanobacteria associated with viruses. *Appl Environ Microbiol* 65, pp. 795–801.
- Van Rijssel, M. and Buma, A.G.J. 2002. UV radiation induced stress does not affect DMSP synthesis in the marine prymnesiophyte *Emiliana huxleyi*. *Aquat Microbial Ecology* 28, pp. 167-174.
- Van Rijssel, M. and Gieskes, W.W.C. 2002. Temperature, light, and the dimethylsulfonylpropionate (DMSP) content of *Emiliana huxleyi* (Prymnesiophyceae). *Journal of Sea Research* 48, pp. 17–27.
- Varaljay, V.A. et al., 2015. Single-taxon field measurements of bacterial gene regulation controlling DMSP fate. *The ISME Journal*, 10.1038/is, pp.1–10.
- Varaljay, V.A. et al., 2010. Deep sequencing of a dimethylsulfonylpropionate-degrading gene (*dmdA*) by using PCR primer pairs designed on the basis of marine metagenomic data. *Applied and Environmental Microbiology*, 76(2), pp. 609–617.
- Vila-Costa, M., Simó R., Harada, H., Gasol, J.M., Slezak, D., Kiene, R.P. 2006. Dimethylsulfonylpropionate uptake by marine phytoplankton. *Science*. 314(5799), pp. 652-654.

- Wagner-Döbler, I. and Biebl, H. 2006. Environmental biology of the marine Roseobacter lineage. *Annu Rev Microbiol.* 60, pp. 255-80.
- Wagstaff, B.A., Vladu, J.C., Barclay, J.E., Schroeder, D., Malin, G., and Field, R.A. 2017. Isolation and Characterization of a Double Stranded DNA Megavirus Infecting the Toxin-Producing Haptophyte *Prymnesium parvum*. *Viruses.* 9(3), p. 40.
- Wagstaff, B.A., Hems, E.S., Rejzek, M., Pratscher, J., Brooks, E., Kuhadomlarp, S., O'Neill, E.C., Donaldson, M.I., Lane, S., Currie, J., Hindes, A.H., Malin, G., Murrell, J.C. and Field, R.A. 2018 Insights into toxic *Prymnesium parvum* blooms: the role of sugars and algal viruses. *Biochem Soc Trans;* 46 (2), pp. 413–421.
- Wallner, G., Amann, R. and Beisker, W. 1993. Optimizing fluorescent in situ hybridization with rRNA-targeted oligonucleotide probes for flow cytometric identification of microorganisms. *Cytometry* 14, pp. 136– 143.
- Wang, Y. and Wang, Y. 1992. Biology and classification of *Prymnesium saltans*. *Acta Hydrobiol. Sin.* 16, pp. 193-199.
- Watson, S. 2001. Literature Review of the Microalga *Prymnesium Parvum* and its Associated Toxicity. Texas Parks and Wildlife Department, Report T3200-1158 (2001, August).
- Williams, B.T., Cowles, K., Bermejo-Martínez, A., Curson, A.R.J., Zheng, Y., Liu, J., Newton-Payne, S., Hind, A.J., Li, C.Y., Rivera, P.P.L., Carrión, O., Liu, J., Spurgin, L.G., Brearley, C.A., Mackenzie, B.W., Pinchbeck, B.J., Peng, M., Pratscher, J., Zhang, XH., Zhang, YZ., Murrell, J.C., and Todd, J.D. 2019. Bacteria are important dimethylsulfoniopropionate producers in coastal sediments. *Nature Microbiology*, 4(11), pp. 1815-1825.
- Wolfe, G. V. and Steinke M. 1997. Grazing-activated chemical defense in a unicellular marine alga. *Nature* 387, pp. 894–897.
- Xavier, M. 2018. Editorial: Metabolic Interactions Between Bacteria and Phytoplankton. *Frontiers in Microbiology.* Vol 9. p. 727.
- Yang, G., Li, C. and Sun, J. 2011. Influence of salinity and nitrogen content on production of dimethylsulfoniopropionate (DMSP) and dimethylsulfide (DMS) by *Skeletonema costatum*. *Chinese J. Oceanol. Limnol.* 29, pp. 378–386.
- Yariv, J. and Hestrin, S. 1961. Toxicity of the extracellular phase of *Prymnesium parvum* cultures. *J. Gen. Microbiol.* 24, (2), pp. 165-175.
- Yasumoto, T. and Murata, M. 1993. Marine toxins. *Chem. Rev.* 93, (5), pp. 1897-1909.
- Yoch, D.C., 2002. Dimethylsulfoniopropionate: Its Sources, Role in the Marine Food Web, and Biological Degradation to Dimethylsulfide. *Applied And Environmental Microbiology*, 68(12), pp. 5804–5815.

- Zamor, R.M., Glenn, K.L., Hambright, K.D. 2012. Incorporating molecular tools into routine HAB monitoring programs: Using qPCR to track invasive *Prymnesium*. *Harmful Algae*.
- Zwart, G., Crump, B.C., Kamst-van Agterveld, M., Hagen, F., and Han, S.-K. 2002. Typical freshwater bacteria: an analysis of available 16S rRNA gene sequences from plankton of lakes and rivers. *Aquat Microb Ecol* 28, pp. 141– 155.
- Zwart, G., Van Hannen, E.J., Kamst-van Agterfeld, M.P., Van der Gucht, K., Lindström, E.S., Van Wichelen, J., et al. 2003. Rapid screening of freshwater bacterial groups by using reverse line blot hybridization. *Appl Environ Microbiol* 69, pp. 5875– 5883.
- Zhang, X. H., Liu, J., Liu, J., Yang, G., Xue, C. X., and Curson, A. R. 2019. Biogenic production of DMSP and its degradation to DMS—their roles in the global sulfur cycle. *Sci. China Life Sci.* 62, pp. 1296–1319.
- Zheng, Y., Wang, J., Zhou, S. et al. 2020. Bacteria are important dimethylsulfoniopropionate producers in marine aphotic and high-pressure environments. *Nat Commun* 11, 4658.
- Zhuang, G., Yang, G., Yu, J. et al. 2011. Production of DMS and DMSP in different physiological stages and salinity conditions in two marine algae. *Chin. J. Ocean. Limnol.* 29, 369–377.
- Zubkov, M.V., Fuchs, B.M., Archer, S.D., Kiene, R.P., Amann, R., and Burkill, P.H. 2001. Linking the composition of bacterioplankton to rapid turnover of dissolved dimethylsulphoniopropionate in an algal bloom in the North Sea. *Environ Microbiol* 3, pp. 304–311.

RESEARCH ARTICLES

During the duration of this research study, I contributed towards the following publications:

Assessing the Toxicity and Mitigating the Impact of Harmful *Prymnesium* Blooms in Eutrophic Waters of the Norfolk Broads. Ben A. Wagstaff, Jennifer Pratscher, Peter Paolo L. Rivera, Edward S. Hems, Elliot Brooks, Martin Rejzek, Jonathan D. Todd, J. Colin Murrell, and Robert A. Field. *Environmental Science & Technology* 2021 55 (24), 16538-16551. DOI: 10.1021/acs.est.1c04742 (2021).

Dissecting the toxicity and mitigating the impact of harmful *Prymnesium* blooms in the UK waters of the Norfolk Broads. Ben A. Wagstaff, Jennifer Pratscher, Peter Paolo L. Rivera, Edward S. Hems, Elliot Brooks, Martin Rejzek, Jonathan D. Todd, J. Colin Murrell, and Robert A. Field. *BioRxiv Online Preprint*. <https://doi.org/10.1101/2020.03.26.010066>. Submitted to *Microbiome*. (2020).

Bacteria are important dimethylsulfoniopropionate producers in coastal sediments. Beth T. Williams, Kasha Cowles, Ana Bermejo Martínez, Andrew R. J. Curson, Yanfen Zheng, Jingli Liu, Simone Newton-Payne, Andrew J. Hind, Chun-Yang Li, **Peter Paolo L. Rivera**, Ornella Carrión, Ji Liu¹, Lewis G. Spurgin, Charles A. Brearley, Brett Wagner Mackenzie, Benjamin J. Pinchbeck, Ming Peng, Jennifer Pratscher, Xiao-Hua Zhang, Yu-Zhong Zhang, J. Colin Murrell and Jonathan D. Todd. *Nature Microbiology*, p1-11 (2019)

Author Correction: DSYB catalyses the key step of dimethylsulfoniopropionate biosynthesis in many phytoplankton. Andrew R. J. Curson, Beth T. Williams, Benjamin J. Pinchbeck, Leanne P. Sims, Ana Bermejo Martínez, **Peter Paolo L. Rivera**, Deepak Kumaresan, Elena Mercadé, Lewis G. Spurgin, Ornella Carrión, Simon Moxon, Rose Ann Cattolico, Unnikrishnan Kuzhiumparambil, Paul Guagliardo, Peta L. Clode, Jean-Baptiste Raina & Jonathan D. Todd. *Nature Microbiology*, vol 4, p540–542 (2019)

DSYB catalyses the key step of dimethylsulfoniopropionate biosynthesis in many phytoplankton. Andrew R. J. Curson, Beth T. Williams, Benjamin J. Pinchbeck, Leanne P. Sims, Ana Bermejo Martínez, **Peter Paolo L. Rivera**, Deepak Kumaresan, Elena Mercadé, Lewis G. Spurgin, Ornella Carrión, Simon Moxon, Rose Ann Cattolico, Unnikrishnan Kuzhiumparambil,

Paul Guagliardo, Peta L. Clode, Jean-Baptiste Raina & Jonathan D. Todd. *Nature Microbiology*, vol 3, p430–439 (2018)